To the Graduate Council:

I am submitting herewith a dissertation written by Oscar Edward Gilbert, Jr., entitled "Paleozoic Evolution of the Valley and Ridge Thrust Belt in Alabama." I have examined the final copy of this dissertation for form and content and recommend that it be accepted in partial fulfillment of the requirements for the degree of Doctor of Philosophy, with a major in Geology.

Dietrich Roeder, Major Professor

We have read this dissertation
and recommend its acceptance:

Kenneth R. Walker

Kula C. Misra

John B. Rehder

Accepted for the Council:

L. Evans Reed

Vice Chancellor
Graduate Studies and Research

PALEOZOIC EVOLUTION OF THE VALLEY AND RIDGE THRUST BELT IN ALABAMA

A Dissertation

Presented for the

Doctor of Philosophy

Degree

The University of Tennessee, Knoxville

Oscar Edward Gilbert, Jr.

December 1981

3055617

Copyright by Oscar Edward Gilbert, Jr. 1981
All Rights Reserved

ACKNOWLEDGMENTS

Field expenses, laboratory facilities, and technical assistance for this study were provided in part by the Department of Geology, Auburn University. U.S. Steel Corporation (Leeds Division) provided free access to certain properties and quarries in the study area. Exxon Production Research provided typing, photographic, and reproduction services.

A number of individuals contributed to this study by providing both assistance and support in formulating the interpretations presented in this study, but any errors of interpretation are wholly mine. These individuals include F. C. Breland and F. B. Keller (University of Tennessee, Knoxville), S. W. Shannon (Alabama Highway Department), J. A. Drahovzal (Gulf Research, Pittsburgh), D. N. Bearce (University of Alabama, Birmingham), J. W. Sears, T. J. Carrington, R. S. Taylor, and R. A. Gastaldo (Auburn University), and P. R. Vail (Exxon Production Research). T. L. Neathery, J. T. Kidd, C. W. Copeland, Jr., and K. E. Richter provided access to data gathered during investigations by the Geological Survey of Alabama.

Dietrich Roeder, K. R. Walker, K. C. Misra, and J. B. Rehder (University of Tennessee, Knoxville) served as faculty committee and provided guidance for and critical review of this study.

Field assistance was provided in part by R. W. Gilbert, and by my wife, Catherine, who also edited the manuscript and tolerated my eccentric activities during the course of this study.

ABSTRACT

The Valley and Ridge province in Alabama is part of a thin-skinned foreland thrust belt, formed by imbrication of the Paleozoic cratonic cover. The sedimentary sequence and structural configuration provide a record of regional tectonism over a period of 270 my. Basic data consist of stratigraphic and structural observations obtained from a geotraverse across the thrust belt.

Subsidence curves, compiled for each structural/stratigraphic belt of the foreland and palinspastically restored to their prethrust positions, depict the changing basement configuration through time. Changes in basement configuration indicate four historical phases: (1) a miogeoclinal phase (Early Cambrian-Early Ordovician) characterized by linear subsidence and development of a southeast-facing carbonate shelf, complicated by abortive local rifting (Middle Cambrian); (2) subsidence of the southeastern part of the shelf associated with development of a Middle Ordovician foredeep; (3) an epeiric phase (Silurian-Early Mississippian) characterized by minimal subsidence and differential uplift of the eastern Valley and Ridge; and (4) extreme subsidence of the entire basin to form an Early Mississippian-Early Pennsylvanian foredeep. Simultaneous initiation of subsidence throughout the latter foredeep, and differential uplift during the epeiric phase, indicate that the lithosphere behaved as an elastic material over short periods of stress application (< 14 my), and viscoelastically over longer periods (> 30 my).

Gross structure of the thrust belt is atypical, in that the dominant features are overthrusts discordant to structure in both the upper and lower plates. Mesoscopic fabric data and map relationships indicate that these faults represent the terminal phase of a thrust-fold-thrust kinematic cycle which migrated toward the foreland. Recognized sequences are of two types: (1) development of northwest vergent faults, followed by decapitation by northwest vergent faults soling rearward of the first faults; and (2) development of southeast vergent listric thrusts, later decapitated by northwest vergent thrusts. In both cases major transport is accomplished by the later, discordant, thrusts. Local thinning of stratigraphic units in the Early Pennsylvanian foredeep fill indicates that thrusting was penecontemporaneous with sedimentation. Sequential cross-sections, based on regional and local kinematic relationships, illustrate the sequence of Late Paleozoic thrusting.

TABLE OF CONTENTS

CHAPTER		PAGE
I.	INTRODUCTION	1
	Regional Geology	3
	Regional stratigraphy	5
	Regional structure	7
	Purposes and Methods of Investigation	11
II.	REGIONAL STRATIGRAPHY, DEPOSITIONAL ENVIRONMENTS, AND FACIES RELATIONSHIPS OF THE PALEOZOIC ROCKS, VALLEY AND RIDGE THRUST BELT AND CUMBERLAND PLATEAU, ALABAMA	13
	Methods of Study	17
	The Miogeoclinal Tectosome	21
	The Foredeep Periphery Tectosome	35
	The Epeiric Sea Tectosome	47
	The Foredeep Tectosome	57
III.	PALEOZOIC CRUSTAL SUBSIDENCE IN THE SOUTHERN APPALACHIAN VALLEY AND RIDGE OF ALABAMA	83
	Data Sources and Methods of Study	84
	Correction Factors in Determination of Crustal Subsidence	85
	Paleobathymetry	86
	Eustatic changes	90
	Sediment compaction	99
	Sediment loading	103
	Regional correlation	108
	Summary of factors	113
	Results and Interpretation	114
	Conclusions	125
IV.	STRUCTURAL MAPPING OF A DEEPLY WEATHERED CARBONATE TERRANE, SHELBY AND TALLADEGA COUNTIES, ALABAMA	127
	Geologic Analysis of Apollo 9 Imagery	131
	Geologic Analysis of LANDSAT Imagery	132
	Geologic Analysis of High-Altitide Color Infrared Imagery	134
	Geologic Data	137
	Conclusions	139

CHAPTER PAGE

V. GEOLOGIC STRUCTURE AND EVOLUTION OF THE VALLEY AND RIDGE THRUST BELT IN ALABAMA 142

Previous Research 143
Methods of Study 143
Basement configuration 144
Balanced cross-section 155
Local kinematic sequences 155
Regional kinematic relationships 158
Preorogenic Deformation 164
Structural Evolution 167
Implications for Hypotheses of Thrust Mechanics 175

VI. SUMMARY AND CONCLUSIONS 179

BIBLIOGRAPHY 183

APPENDICES 204

Appendix A 205
Appendix B 268

VITA 295

LIST OF TABLES

TABLE		PAGE
II-1.	Sources of Basic Data on Regional Paleozoic Stratigraphy of Alabama	18
II-2.	Lithologies, Regional Thicknesses, and Published Faunal Lists, Miogeoclinal Tectosome	22
II-3.	Lithologies, Regional Thicknesses, and Published Faunal Lists, Foredeep Periphery Tectosome	36
II-4.	Lithologies, Regional Thicknesses, and Faunal Lists, Epeiric Tectosome	49
II-5.	Lithologies, Regional Thicknesses, and Faunal/Floral Lists, Foredeep Tectosome	60
III-1.	Ranges of Paleobathymetric Indicators in Paleozoic Sequences	89

LIST OF FIGURES

FIGURE		PAGE
I-1.	Location of Study Area	4
I-2.	Regional Stratigraphy of the Paleozoic Rocks in Alabama	6
I-3.	Major Structural Elements of the Valley and Ridge Thrust Belt in Alabama	9
II-1.	Control of Sediment Body Geometry by Subsidence and Sediment Accumulation Rates, Appalachian Foreland in Alabama	15
II-2.	Location of Study Area in the Southern Appalachian Thrust Belt, Alabama	19
II-3.	Formation Names, Lithologies, Paleobathymetry, and Environmental Indicators in Selected Measured Sections of the Miogeoclinal Tectosome	24
II-4.	Regional Lithofacies Relationships in the Lower Cambrian Conasauga Group in Alabama	29
II-5.	Lithostratigraphic and Biostratigraphic Zonation in the Cambrian-Lower Ordovician of Alabama	31
II-6.	Middle and Upper Ordovician Stratigraphy of Alabama	38
II-7.	Middle and Upper Ordovician Regional Facies Patterns Plotted on Palinspastic Base	39
II-8.	Formation Names, Lithologies, Paleobathymetry, and Environmental Indicators in Selected Measured Sections of the Foredeep Periphery Tectosome	41
II-9.	Formation Names, Lithologies, Paleobathymetry, and Environmental Indicators in Selected Measured Sections of the Epeiric Sea Tectosome	50
II-10.	Facies Relationships in the Lower and Upper Mississippian, North Alabama and Northwest Georgia	58

FIGURE		PAGE
II-11.	Formation Names, Lithologies, Paleobathymetry, and Environmental Indicators in Selected Measured Sections of the Foredeep Tectosome	61
II-12.	Distribution of Linear Sand Facies in the Pride Mountain Formation, North Alabama	75
II-13.	Regional Lithofacies During mid-Chester and Late-Chester/Early Springer Time	76
II-14.	Schematic Illustration of Mississippian-Pennsylvanian Facies Relationships, Northern Alabama	80
II-15.	Progressive Filling of Late Paleozoic Foredeep	82
III-1.	Relative Paleozoic Coastal Onlap, Assuming Sea Level at the Cambrian-Ordovician Boundary as Zero	91
III-2.	Diagrammatic Representation of Unconformity Types, Stratal Patterns and Facies Relationships Used by Vail and Todd to Infer Relative Rates of Sea Level Change	93
III-3.	Determination of Long-Term Eustatic Change	94
III-4.	Diagrammatic Illustration of Inference of Eustatic Curve from Onlap, Unconformity Type, and Long-Term Eustatic Change	95
III-5.	Comparison of Coastal Onlap and Inferred Eustatic Sea Level Curves for the Upper Triassic to Lower Cretaceous, North Sea	97
III-6.	Inferred Paleozoic Eustatic Changes	98
III-7.	Carbonate Compaction by Solution of Grains	102
III-8.	Carbonate Compaction by Development of Stylonodular Structure	104
III-9.	Vertical Deflection of the Lithosphere Under Distributed Loading	106
III-10.	Stratigraphic and Absolute Time Scales, and Isochrons Used for Correlation	110

FIGURE		PAGE
III-11.	Corrected Finite Subsidence Curves for Pre-Paleozoic Basement Top in Selected Areas, Paleozoic Foreland, Alabama	116
III-12.	Configuration of the Paleozoic Foreland Basement	117
III-13.	Schematic History of Paleozoic Tectonism, Based on Subsidence History	120
IV-1.	Regional Geology of the Pell City Thrust Sheet, East Central Alabama	128
IV-2.	Structural Features Observed in LANDSAT Band 7 Infrared Imagery, Talladega County, Alabama	133
IV-3.	Structural Features Visible in Infrared Imagery, Logan Martin Dam Area	136
IV-4.	Geologic Map of Part of the Pell City Thrust Sheet	138
V-1.	Loading of a Semi-Infinite Lithospheric Plate in the Himalayan Collisional Orogenic Belt, and the Mechanical Analogy of Point-Loading of the Extremity of a Finite Beam	147
V-2.	Comparison of Lower Plate Deflections Predicted by Various Models	148
V-3.	Configuration of the Southern Appalachian Crystalline Overthrust	151
V-4.	Mechanical Analogies of Mathematical Models Proposed by Hetenyi Including Point Loading of Infinite and Finite Beams, and Distributed Loading of Infinite and Finite Beams	153
V-5.	Mesoscopic Fabric Elements, Coosa Deformed Belt	157
V-6.	T_1-F-T_2 Kinematic Sequence, Glover Mountain, Shelby County	159
V-7.	T_1-T_2 Kinematic Sequence, Kelly Creek, Shelby County	160
V-8.	Three-Dimensional Relationships of Mesoscopic Fabric Elements, Glover Mountain	161

FIGURE PAGE

V-9. T_1-T_2 Kinematic Sequence, Rocky Row, Jefferson County 162

V-10. Three-Dimensional Relationships of Mesoscopic Fabric Elements, Rocky Row 163

V-11. Orientation of Prethrust Growth Faults, Birmingham Anticlinorium 166

V-12. Comparison of Elliot and Chapple Hypotheses of Thrust Mechanics 176

B-1. Sedimentary and Diagenetic Features of the Weisner Formation and Shady Dolomite 269

B-2. Sedimentary Features of the Rome Formation and Conasauga Group 271

B-3. Sedimentary Features of the Copper Ridge Dolomite 273

B-4. Sedimentary and Diagenetic Features of the Chepultepec Dolomite and Newala Limestone 275

B-5. Sedimentary Features of the Columbiana Formation and Little Oak Limestone 277

B-6. Sedimentary Features of the Greensport Formation and Colvin Mountain Sandstone 279

B-7. Sedimentary Features of the Stones River, Nashville, and Sequatchie Formations, Birmingham, Jefferson County 281

B-8. Sedimentary Features of the Red Mountain Formation, Frog Mountain Sandstone and Chattanooga Shale 283

B-9. Sedimentary and Diagenetic Features of the Fort Payne Chert and Tuscumbia Limestone 285

B-10. Sedimentary Features of the Pride Mountain Formation and Hartselle Sandstone, Jefferson County 287

B-11. Sedimentary Features of the Floyd Shale, Leeds, Jefferson County 289

B-12. Sedimentary Features of the Floyd Shale and Parkwood Formation 291

FIGURE PAGE

B-13. Sedimentary Features of the Pottsville Formation 293

LIST OF PLATES

PLATE

I. Major Structural Features of the Valley and Ridge Thrust Belt in Alabama . . . . . In Pocket

II. Sequential Cross-Sections Illustrating Late Paleozoic Thrusting . . . . . In Pocket

CHAPTER I

INTRODUCTION

The Valley and Ridge province of the southern Appalachians is one of the most intensively studied fold and thrust belts in the world, and is the region where many modern concepts of thrust belt geology were developed (for example, Rich, 1934; Rodgers, 1949). Yet despite this intensive study, many aspects of the evolution of the Valley and Ridge remain unknown.

In the past ten years, several conceptual models dealing with the structural evolution of the Valley and Ridge thrust belt have been proposed. Most have concentrated on tectonic mechanisms responsible for late Paleozoic deformation, including gravity sliding (Dennison, 1976; Milici, 1975; Bearce, 1978), gravity spreading (Roeder, Gilbert, and Witherspoon, 1978), lateral compression (Hatcher, 1972, 1978) and basement uplift (Thomas and Drahovzal, 1974). These and other studies have also addressed the problems of the sequence of deformational events and the migration of deformation across the thrust belt (Milici, 1975; Roeder, Yust, and Little, 1978; Perry, 1978).

Other studies have concentrated on crustal subsidence as indicated by changes in bathymetry and sediment deposition patterns (Briggs and Roeder, 1975; Benedict and Walker, 1978; Shanmugam and Walker, 1978, 1980), or on facies and sediment distribution patterns as evidence of tectonism (Thomas, 1972a, 1972b).

One synthesis (Roeder, Gilbert, and Witherspoon, 1978) attempted to integrate crustal subsidence, sedimentation, and structural style into a developmental model for the Valley and Ridge of Tennessee and Virginia. This synthesis suffered from several disadvantages, including (1) lack of paleobathymetric control throughout the stratigraphic sequence, (2) reliance upon published stratigraphic and structural data of variable quality, and (3) kinematic interpretations based on the work of several individuals working in isolated areas.

The overall goal of the present study was, therefore, to integrate the methods of sedimentology and structural geology in order to formulate a comprehensive tectonic history of the thrust belt in Alabama. In addition to contributing to knowledge of the evolution of thrust belts in general, the results of this study provide additional information on several regional geologic problems. Additional evidence pertinent to the question of Taconic (Ordovician) tectonism in the Valley and Ridge belt (Denson and Waage, 1966; Shaw, 1973; Keller, 1977; Roeder, Yust, and Little, 1978; Perry, 1978) is provided. Analysis of crustal subsidence and changing patterns of sedimentation provide indirect evidence of tectonic events outside the depositional basin (Benedict and Walker, 1978), thus helping to relate Valley and Ridge tectonism to events in the crystalline belts.

A comprehensive study of the evolution of an entire thrust belt is beyond the scope of a limited project. A more feasible approach is that of selecting a corridor across the thrust belt, and considering the limited area as representative of the thrust belt as a whole. Such a multidisciplinary study of a selected area is termed a geotraverse

(Gary et al., 1972), and is a method effectively utilized in other orogenic belts (Bögel and Closs, 1976; Rast and Stringer, 1980).

The area selected for this geotraverse lies near the southwestern terminus of the exposed thrust belt in central Alabama (Fig. I-1). This area was selected because it includes a number of major structural and stratigraphic belts, including regional lithofacies zonations which persisted from Middle Ordovician through Pennsylvanian time in the southern Appalachians (Butts, 1926; Drahovzal and Neathery, 1971; Thomas, 1972a). More important, selection of this area was critical to the study of preorogenic subsidence, since it is the only area where a complete Cambrian through Pennsylvanian stratigraphic sequence is preserved in the interior of the thrust belt.

The line of the geotraverse extends from the vicinity of Birmingham, southeast to the metamorphic front (Fig. I-1). However, not all exposures examined for structural and stratigraphic data are located within this narrow corridor, so that the actual study area was larger (Fig. I-1).

I. REGIONAL GEOLOGY

The Valley and Ridge of the southern Appalachians is typical of thin-skinned foreland fold and thrust belts. It consists of an eroded crystalline basement terrane of Precambrian age, overlain by a Cambrian-Ordovician clastic and carbonate miogeoclinal sequence. During the Middle Ordovician, a problematical northeasterly clastic source developed, and persisted through the Silurian. During the Mississippian and Pennsylvanian, the depositional basin was filled by a massive influx

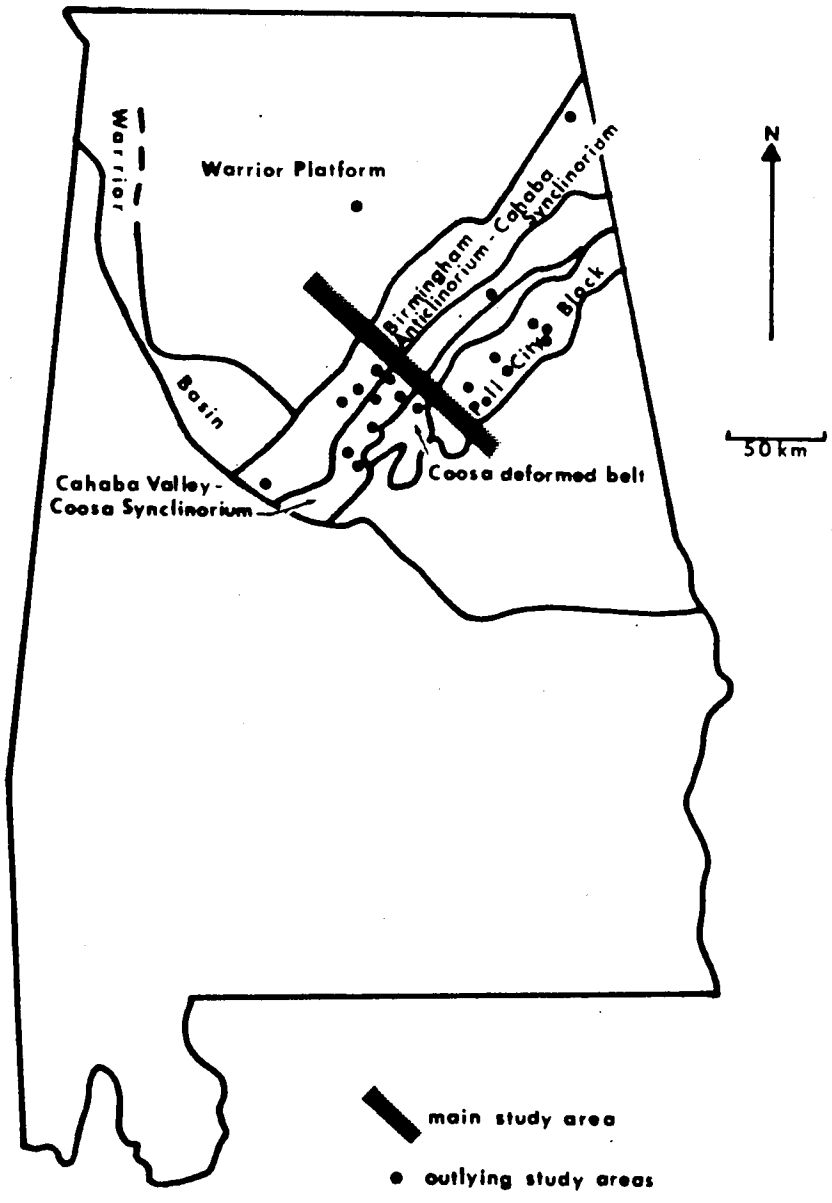

Figure I-1. Location of study area. Southern terminus of the Paleozoic thrust belt, Alabama.

of southeasterly derived clastics, and subsequently disrupted by west vergent sled-runner thrusting. Available evidence suggests that late Paleozoic deformation affected only the Paleozoic sedimentary cover, leaving the Precambrian crystalline rocks as an east-dipping uninvolved structural basement (Rodgers, 1949).

Regional Stratigraphy

The Paleozoic strata of Alabama represent an almost complete stratigraphic sequence, ranging in age from Early Cambrian to Early Pennsylvanian, interrupted by several lacunae of both depositional and erosional origin. For purposes of description, the Paleozoic outcrop area can be subdivided into six broad geological subregions (Fig. I-1).

The lithostratigraphic column (Fig. I-2) can be subdivided into four tectosomes. The oldest is the miogeoclinal tectosome, a Lower Cambrian-Lower Ordovician sequence which represents the gradual encroachment of the Early Paleozoic proto-Atlantic onto the subsiding miogeoclinal shelf of eastern North America. This tectosome is characterized by a thick sequence of peritidal strata, the basal members of which young progressively onto the craton (Fig. I-2).

Above a major lacuna (the post-Knox unconformity) is a Middle to Upper Ordovician foredeep-periphery tectosome, which contains only shelf and starved basin deposits. Coarse-grained Taconic clastic foredeep sediments similar to those of Tennessee (Shanmugam and Walker, 1978) and Virginia (Markello et al., 1979) are absent. The western facies consists of platform peritidal deposits, and the eastern facies of slope, shelf reentrant, and starved basin deposits. The first development of an

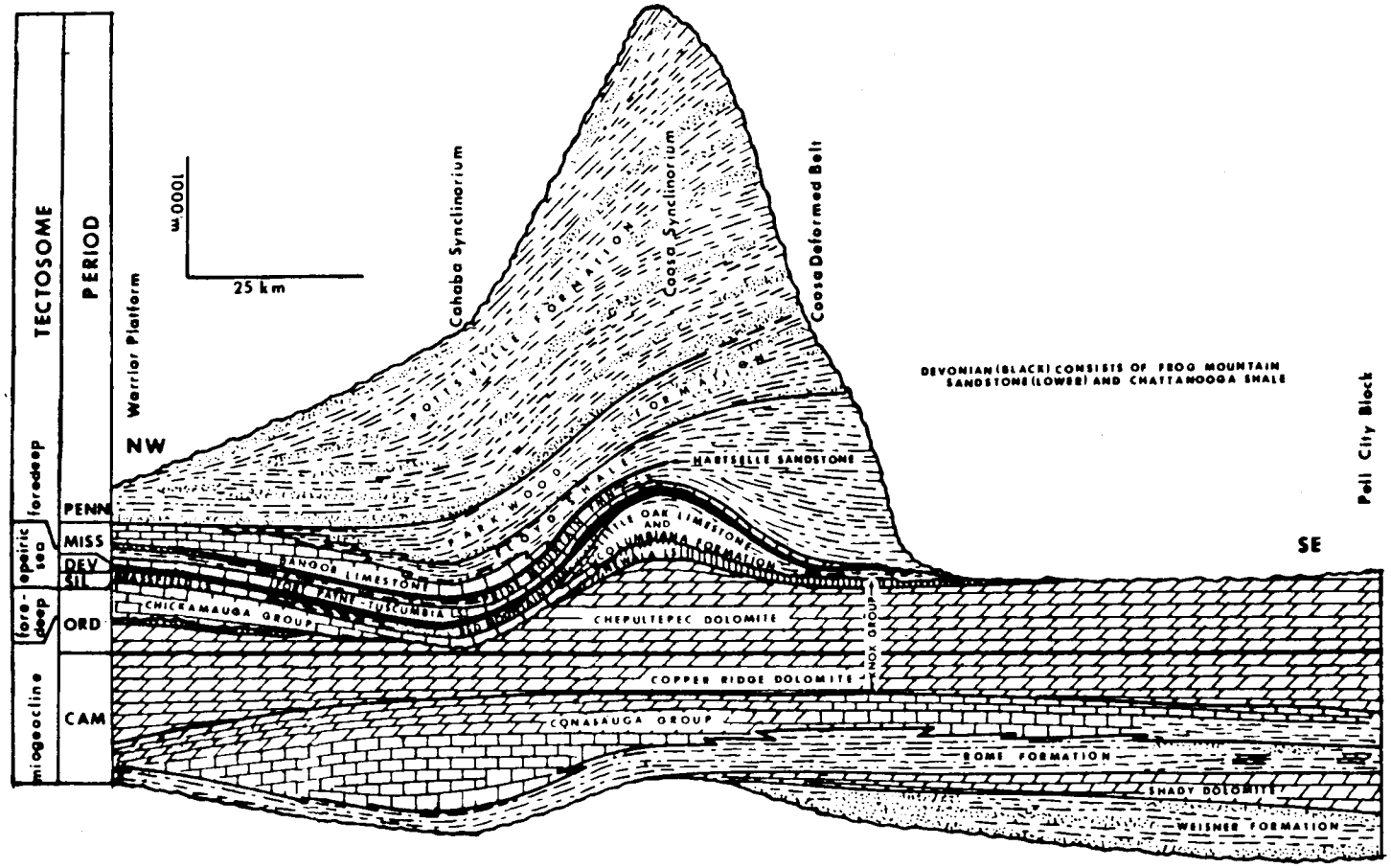

Figure I-2. Regional stratigraphy of the Paleozoic rocks in Alabama. Symbols represent regional lithotype only, and not relative abundance of lithologies within formations. Thickness and palinspastic base from this study.

"Appalachian" clastic source is indicated by the occurrence of thin and areally-restricted northeasterly clastic facies, which occur in the northeastern part of the study area.

The Silurian, Devonian, and lowermost Mississippian strata comprise an epicontinental sea tectosome characterized by a northwesterly shallow water carbonate facies in the Warrior platform-Warrior basin area, and a southeasterly clastic facies in the Valley and Ridge. All the formations in this tectosome pinch out to the southeast in a series of depositional hiata and degradational vacuities, indicating periodic subaerial exposure of the eastern Valley and Ridge.

Finally, the Lower Mississippian through Lower Pennsylvanian strata represent an Alleghenian foredeep and foreland shelf tectosome. Thick sequences of prodeltaic and deltaic clastics in the Valley and Ridge record extremely rapid subsidence and influx of clastics from southeasterly and easterly sources. The Warrior platform survived as a stable, slowly subsiding foreland shelf with dominantly carbonate sedimentation, until, in the Early Pennsylvanian, prodeltaic and deltaic clastics flooded over the Warrior platform. During and after deposition of the deltaic deposits, the entire Paleozoic sequence was involved in foreland thrusting, and the depositional basin destroyed.

Regional Structure

The study area includes the entire width of the Appalachian Valley and Ridge thrust belt, from the Sequatchie anticline (technically a part of the Plateau province) southeast to the Talladega fault, along which metamorphic rocks have been thrust over the Valley and Ridge. It

therefore includes five major structural belts (Fig. I-3). Details of structures within these major subdivisions are shown in Plate I.

The Warrior platform belt consists of strata of Cambrian to Pennsylvanian age, warped into a series of broad, open folds. The major structural feature is the Sequatchie anticline, a northwest vergent asymmetric fold. Although no subsurface data are available, the Sequatchie is the surface manifestation of movement over a décollement at depth, since along strike to the northeast the northwest-vergent Browns Valley and Sequatchie thrust faults are exposed in the core of the anticline. The Sequatchie anticline is flanked to the northwest and southeast by the Arkadelphia and Coalburg synclines, respectively, which are areas of flat-lying strata.

The northwest edge of the thrust belt is defined by the Birmingham and Murphrees Valley anticlinoria (Fig. I-3). The boundary between the Plateau and these anticlinoria is complex, consisting of a northwest-facing, locally overturned anticlinal limb, locally complicated by northwest vergent thrust faults, or one of several southeast vergent thrust faults (backthrusts). The Murphrees Valley anticline is a surficial brow fold resulting from transport on the underlying Straight Mountain backthrust. The Birmingham anticlinorium is a multi-crested fold, complicated by several small thrusts and backthrusts within the exposed core. These faults sole at various stratigraphic levels, including the Cambrian, Silurian, and Mississippian. The Birmingham anticlinorium and Cahaba synclinorium are features within an areally extensive thrust sheet above the Opossum Valley fault (Fig. I-3).

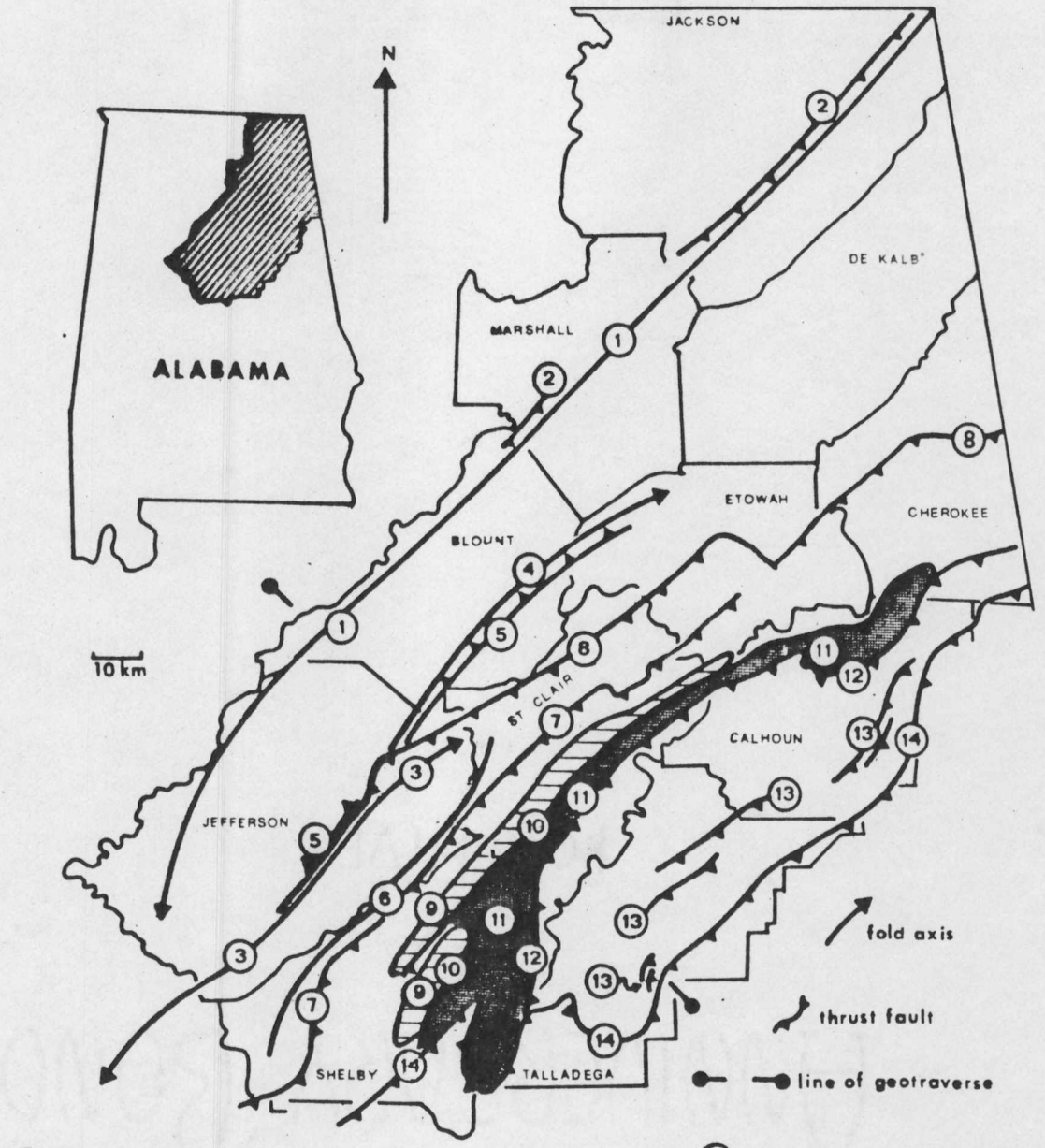

(1) Sequatchie Anticline
(2) Browns Valley/Sequatchie Fault
(3) Birmingham Anticlinorium
(4) Murphrees Valley Anticlinorium
(5) backthrusts
(6) Cahaba Synclinorium
(7) Helena Fault
(8) Opossum Valley/Rome Fault
(9) Coosa coal field
(10) Coal City/Yellow Leaf Faults
(11) Coosa deformed belt
(12) Pell City Fault
(13) sheets/klippen of Lower Cambrian strata
(14) Talladega/metamorphic front faults

Figure I-3. Major structural elements of the Valley and Ridge thrust belt in Alabama. Talladega/metamorphic front faults mark southeast edge of nonmetamorphosed rocks. Simplified map after Self et al., 1975; extension of Opossum Valley fault system into St. Clair and Etoway Counties by author.

The Helena fault, which forms the Cahaba synclinorium-Coosa synclinorium boundary, is a major structural unit in the Valley and Ridge, separating the relatively simple outer Valley and Ridge from the more complex belts to the southeast. The Coosa synclinorium is the exposed updip end of the thrust sheet overlying the Helena fault. The synclinorial nature of the Coosa and subsidiary Yellow Leaf coal fields (Fig. I-3) is superficial, and is a manifestation of thrusting and folding which involves only the surficial Carboniferous sequence rather than the entire Paleozoic section (Gilbert, 1977b). The southeastern boundaries of the surficial synclinoria are marked by the east-dipping Coal City and Yellow Leaf faults, which have juxtaposed Mississippian against Pennsylvanian strata.

Southeast of the Coal City and Yellow Leaf faults is a belt of complexly folded, thrust-faulted, and pervasively sheared Middle to Upper Mississippian clastics called the Coosa deformed belt (Thomas and Drahovzal, 1974). Embedded within this terrain are a number of thin (less than 300 m), elongate (up to 16 km), east-dipping imbricate thrust sheets of Lower Ordovician through Lower Mississippian strata.

The structures of the Coosa deformed belt are truncated upward by the low angle (3 degrees), fold discordant Pell City fault (Fig. I-3). The overthrust sheet consists of a broad area of internally deformed Lower Cambrian through Lower Ordovician strata which extends 30 km to the southeast. The flat, thin nature of the upper sheet is demonstrated by the occurrence of erosional windows up to 15 km southeast of the main fault trace. This broad thrust sheet is in turn broken by a series of imbricate thrusts which have displaced lowermost Cambrian clastics onto

Upper Cambrian-Lower Ordovician carbonates as a series of rooted thrust sheets and klippen (Bearce, 1977; Gilbert, 1977a) (Fig. I-3).

II. PURPOSES AND METHODS OF INVESTIGATION

The overall goal of this study was to describe in detail the tectonic history of the southernmost Appalachian foreland. This history consisted of two parts, an early phase characterized by vertical movement of the crystalline basement and sedimentary cover, and a second phase characterized by rapid subsidence and deformation of the cover. In Alabama, neither phase has previously been quantitatively described.

Study of the deformation of the sedimentary cover utilized methods employed in the study of other foreland thrust belts. A balanced cross-section was constructed from surface geologic data, using geometric principles described by Dahlstrom (1969) and Roeder, Gilbert, and Witherspoon (1978). Mesoscopic fabric data and crosscutting relationships of structures were analyzed to determine the relative chronology of deformation. The kinematic sequence data and balanced cross-section were used to generate a stepwise palinspastic restoration of the sedimentary cover prior to deformation.

Interpretation of regional geology was based primarily on previous mapping. In areas where surface geologic exposures are sparse, satellite and high-altitude aircraft imagery were used to interpret areal geology.

The preorogenic diastrophic history of the region was analyzed indirectly using sedimentological data to determine the history of vertical crustal movement. The method utilized is "geohistory analysis" as described by Van Hinte (1978), and utilized in studies of several

sedimentary basins (see Sweeney, 1976). However, this study differed from most previous studies in several significant details.

Many previous studies have used simplified techniques which do not account for such factors as eustatic sea level change, paleobathymetry, or sediment compaction. In this study, I have attempted to account for these factors where possible. A major difference in technique is that most studies have used a simplified (Airy) model of lithosphere response to sediment loading; in this study, I have utilized, where appropriate, mathematical models which approximate a more complex (viscoelastic) response of the lithosphere.

The most significant difference is that this study represents an analysis of the preorogenic subsidence behavior of a highly deformed region. Previous studies have utilized the technique only in undeformed basins or sedimentary basins formed by rifting.

The subsidence and kinematic histories of the thrust belt have been used to formulate a preliminary tectonic history of the region. Although it is not entirely satisfactory to attempt an interpretation of regional tectonism from the subsidence history of the foreland, it is a useful technique in this region, where the age and nature of tectonic episodes in the orogenic core are unknown or controversial.

It should be emphasized that geotraverses are essentially reconnaissance studies, and that future investigations will, in all likelihood, alter or invalidate some conclusions reached during this study. However, the present approach does represent an integrated tectonic history of the southern Appalachian thrust belt which is much more comprehensive and realistic than previous interpretations.

CHAPTER II

REGIONAL STRATIGRAPHY, DEPOSITIONAL ENVIRONMENTS, AND FACIES RELATIONSHIPS OF THE PALEOZOIC ROCKS, VALLEY AND RIDGE THRUST BELT AND CUMBERLAND PLATEAU, ALABAMA

Butts (1926) compiled the first comprehensive summary of the Paleozoic stratigraphy of Alabama, based both on his own work and that of others (McCalley, 1896, 1897; Prouty, 1916; unpublished work by Eugene Allen Smith). Butts recognized that the Paleozoic strata represent the record of long-term subsidence punctuated by periods of uplift and erosion, but recognized neither the full significance of regional lithofacies nor the volumes of strata removed by erosion. He postulated that various units were deposited in isolated depositional basins (Butts, 1926, plates 71-76).

Most subsequent investigators followed Butts' terminology and concepts until the 1960's, when regional lithofacies relationships were recognized and described. Lithofacies relationships within the Middle and Upper Ordovician were inferred from biostratigraphic correlations (Drahovzal and Neathery, 1971; Bergstrom and Drahovzal, 1972; Raymond, 1973), and areal facies changes in the Mississippian from lithostratigraphic correlations (Thomas, 1972a). Regional facies changes have also been described from the Cambrian (Thomas and Drahovzal, 1973; Gilbert, 1974; Bearce, 1977), Silurian (Sheldon, 1964, 1970), and Devonian (Kiefer, 1970; Bearce, 1977).

Most regional studies of Paleozoic stratigraphy in Alabama have considered depositional environments only superficially. Kolter and Vest (1953), Taylor (1971, 1973), Thompson (1971), Wilson (1971), and Yeager (1971) described depositional environments of geographically restricted parts of the Middle and Upper Ordovician strata, and Drahovzal and Neathery (1971) compiled an interpretation of regional lithofacies and inferred depositional environments. Welch (1958, 1959), Smith (1967), Dinnean (1974), White (1976), Handford (1977), and Beavers (1977) described depositional environments in areally and stratigraphically restricted parts of the Mississippian, and Thomas (1972a) interpreted regional facies relationships and depositional environments in the Mississippian. Less detailed work has been conducted on the Cambrian (McKinney, 1977; Mack, 1980), Silurian (Bensko, 1953; Sheldon, 1964, 1970), Devonian (Conant and Swanson, 1961; Kelley, 1969), and Pennsylvanian (Schlee, 1963; Ferm et al., 1967; Breland, 1972; Hobday, 1974; Gilbert, 1976; Murrie et al., 1976; Horsey, 1979).

One of the goals of this study was to determine the preorogenic diastrophic history of the foreland from regional stratigraphy. The sediment types and two-dimensional sediment body geometries within the Paleozoic stratigraphic sequence (Fig. I-2, page 6) were used as a basis for preliminary subdivision and interpretation.

The two-dimensional sediment body geometries of the time-restricted sedimentary sequences reflect differential crustal subsidence and sediment supply, the interaction of these factors controlling not only cross-sectional geometries but regional bathymetry and lithofacies (Fig. II-1). In similar fashion, areal distribution of lithofacies and

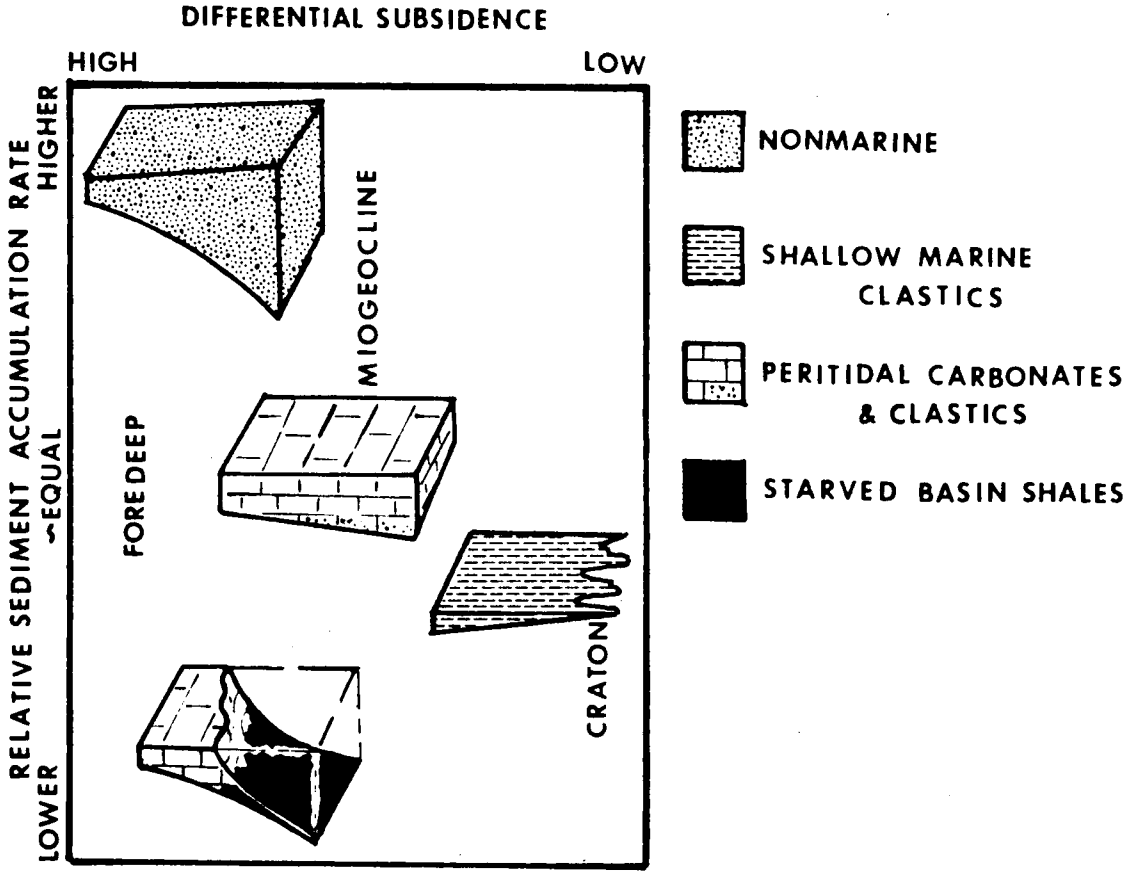

Figure II-1. Control of sediment body geometry by subsidence and sediment accumulation rates, Appalachian foreland in Alabama. Differential subsidence is regional variation in subsidence rates during a time interval. Sediment accumulation rates are considered relative to subsidence rates.

three-dimensional sediment body geometry may be used to infer areal variations in subsidence and sediment supply.

The relative abundance of terrigenous clastics is indicative of the presence or absence of a source terrane, and relative rates of uplift, erosion, and weathering in the source terrane (Krumbein et al., 1949).

On the basis of sediment body geometries and sediment types, the Paleozoic strata of the Valley and Ridge foreland can be subdivided into four major associations related to the tectonic history of the region. These major subdivisions are sequential in time, but each includes several formations or groups of the traditional stratigraphy. Sloss (1958, p. 625) used the term tectosome to describe a sequence of strata indicative of uniform tectonic conditions. In this study the term is used to denote stratigraphic subdivisions of greater than group or formation rank in which the strata were deposited in a similar tectonic setting such as a subsiding passive shelf, orogenic foredeep, or stable cratonic platform. This usage differs from that of Sloss (1958) in that tectonic conditions are not of necessity stable, as subsidence rates may change or local orogenic activity occur within the time span represented by any particular tectosome.

The four major subdivisions of foreland Paleozoic strata are the miogeoclinal, foredeep periphery, epeiric sea, and foredeep tectosomes described in Chapter I. In the following description of regional stratigraphy, these tectosomes are the major basis of classification, and traditional lithostratigraphic units are included as subdivisions of the tectosomes. Formations and groups have no chronologic significance, and

are the result of the interaction of crustal subsidence, sediment supply, eustatic change, and biological, tidal, wave, and current activity.

I. METHODS OF STUDY

The broad regional lithofacies relationships of the Paleozoic rocks in Alabama are fairly well known as the result of previous studies, and the traditional stratigraphic framework (Fig. I-2, page 6) was used as a starting point for this study. In addition, data on regional isopachous relationships, chronostratigraphy, and biostratigraphy were derived largely from the literature and unpublished research, field-checked by the author where feasible. The data sources are summarized in Table II-1.

The entire Paleozoic stratigraphic sequence was subdivided into large-scale facies intervals, generally equivalent to groups or formations. Where a single such interval crops out in several structural-stratigraphic belts, one or more reference sections were selected and measured in detail (Fig. II-2). Data obtained from individual outcrops or measured sections in other structural-stratigraphic belts were compared to these reference sections (Appendix A) for environmental and paleobathymetric analysis. In time-stratigraphic intervals where regional lithofacies variations exist, measured sections exhibiting the variations were compiled for each interval.

Each measured section was subdivided into units, or groups of beds with common characteristics. Characteristics, including bed form and thickness, mesoscopic sedimentary and biogenic structures, fossils, color, and lithologic characteristics such as grain size, were recorded in the field. Samples or groups of lithologic samples representative of

TABLE II-1

SOURCES OF BASIC DATA ON REGIONAL PALEOZOIC STRATIGRAPHY OF ALABAMA

Formation Name	Named by	Type Locality	Nomenclature Revisions	Primary Sources of Isopach, Lithofacies, and Biostratigraphic Data Used in This Study
Weisner Formation	Smith, 1890	Weisner Mtn., Cherokee Co.	Mack, 1980 (proposed)	Butts, 1926; Reed, 1949; Bearce, 1977; Mack, 1980
Shady Dolomite	Keith, 1903	Johnson Co., Tenn.		McCalley, 1897; Butts, 1926; Warman and Causey, 1962; Cloud, 1967; Bearce and McKinney, 1977; McKinney, 1977
Rome Formation	Smith, 1890	Rome, Georgia		Butts, 1926; Kidd, 1975; Bearce, 1978
Conasauga Formation	Hayes, 1891	Conasauga Valley, Ga.	Group status by Rodgers, 1953; not subdivided in Alabama	Butts, 1926; Thomas and Drahovzal, 1973; Kidd, 1975
Copper Ridge Dolomite	Ulrich, 1911	Knox Co., Tenn.		Butts, 1926, 1927a, 1940; Kidd, 1975
Chepultepec Dolomite	Ulrich, 1911	Chepultepec, Blount Co.		Butts, 1926, 1927a, 1940; Cummings, 1960; Kidd, 1975
Newala Limestone	Butts, 1926	Newala, Shelby Co.		Butts, 1926, 1927a, 1940; Yeager, 1971; Taylor, 1971
Lenoir Limestone	Safford and Killebrew, 1876	Lenoir City, Tenn.		Butts, 1926; Drahovzal and Neathery, 1971
Columbiana Formation*	Cooper, 1956	Calera, Shelby Co.		Butts, 1926, 1940; Drahovzal and Neathery, 1971
Little Oak Limestone	Butts, 1926	Little Oak Mtn., Shelby Co.		Butts, 1926; Drahovzal and Neathery, 1971; Taylor, 1971; Thomas and Drahovzal, 1974
Greensport Formation+	Drahovzal and Neathery, 1971	Greensport Gap, Etowah Co.		Drahovzal and Neathery, 1971
Colvin Mountain Sandstone+	Drahovzal and Neathery, 1971	Colvin Mtn., Calhoun Co.		Drahovzal and Neathery, 1971
Sequatchie Formation	Ulrich, 1912	Sequatchie Valley, Tenn.		Drahovzal and Neathery, 1971; Thompson, 1971
Stones River Group	Safford, 1851	Nashville, Tenn.	Formation status in Alabama, Drahovzal and Neathery, 1971	Kolter and Vest, 1953; Drahovzal and Neathery, 1971; Wilson, 1971; Kidd, 1975
Nashville Group	Safford, 1851	Nashville, Tenn.	Formation status in Alabama, Drahovzal and Neathery, 1971	Drahovzal and Neathery, 1971; Kidd, 1975
Inman Formation	Wilson, 1949	Marion Co., Tenn.		Drahovzal and Neathery, 1971
Leipers Formation	Hayes and Ulrich, 1903	Maury Co., Tenn.		Drahovzal and Neathery, 1971
Red Mountain Formation	Smith, 1876	Red Mtn., Jefferson Co.		Butts, 1926; Burchard and Andrews, 1947; Sheldon, 1964, 1970; Lundin and Newton, 1970
Brassfield Limestone	Foerste, 1905	Madison Co., Ky.	Wilson, 1949	Jewell, 1967; Lundin and Newton, 1970
Wayne Group	Drake, 1914	Wayne Co., Tenn.	Wilson, 1949	Jewell, 1969; Lundin and Newton, 1970; Kidd, 1975
Frog Mountain Sandstone	Hayes, 1894b	Frog Mtn., Cherokee Co.	Extended to include all pre-Chattanooga, Kiefer, 1970	Butts, 1926; Kiefer, 1970
Chattanooga Shale	Hayes, 1894a	Chattanooga, Tenn.	New standard section, Hass, 1956	Glover, 1959; Conant and Swanson, 1961
Fort Payne Chert	Smith, 1890	Fort Payne, DeKalb Co.		Butts, 1926; Drahovzal, 1967
Tuscumbia Limestone	Smith, 1894	Tuscumbia, Colbert Co.		Butts, 1926; Thomas, 1972a; Ruppel, 1979
Pride Mountain Formation	Welch, 1958	Pride Mtn., Colbert Co.	Thomas, 1972a	Thomas, 1972a
Hartselle Sandstone	Smith, 1894	Hartselle, Morgan Co.	Redefined by Butts, 1926, and Welch, 1958	Thomas, 1972a; Beavers, 1977; Thomas et al., 1980
Bangor Limestone	Smith, 1890	Bangor, Morgan Co.	Redefined by Butts, 1926	Drahovzal, 1967; Thomas, 1972a
Floyd Shale	Hayes, 1891	Floyd Co., Ga.		Butts, 1926; Thomas, 1972a
Parkwood Formation	Butts, 1910	Parkwood, Jefferson Co.	Culbertson, 1963	Thomas, 1972a
Pottsville Formation	Lesley, 1876	Pottsville, Penn.		Butts, 1926, 1940; Rothrock, 1949; Gilbert, 1976

*Athens Shale of Alabama Geol. Survey usage; the "Athens" of Alabama is lithologically dissimilar to that at the type locality, and the proposed Columbiana Formation is used in this report.

+Unofficial terms, not recognized by U.S. Geological Survey.

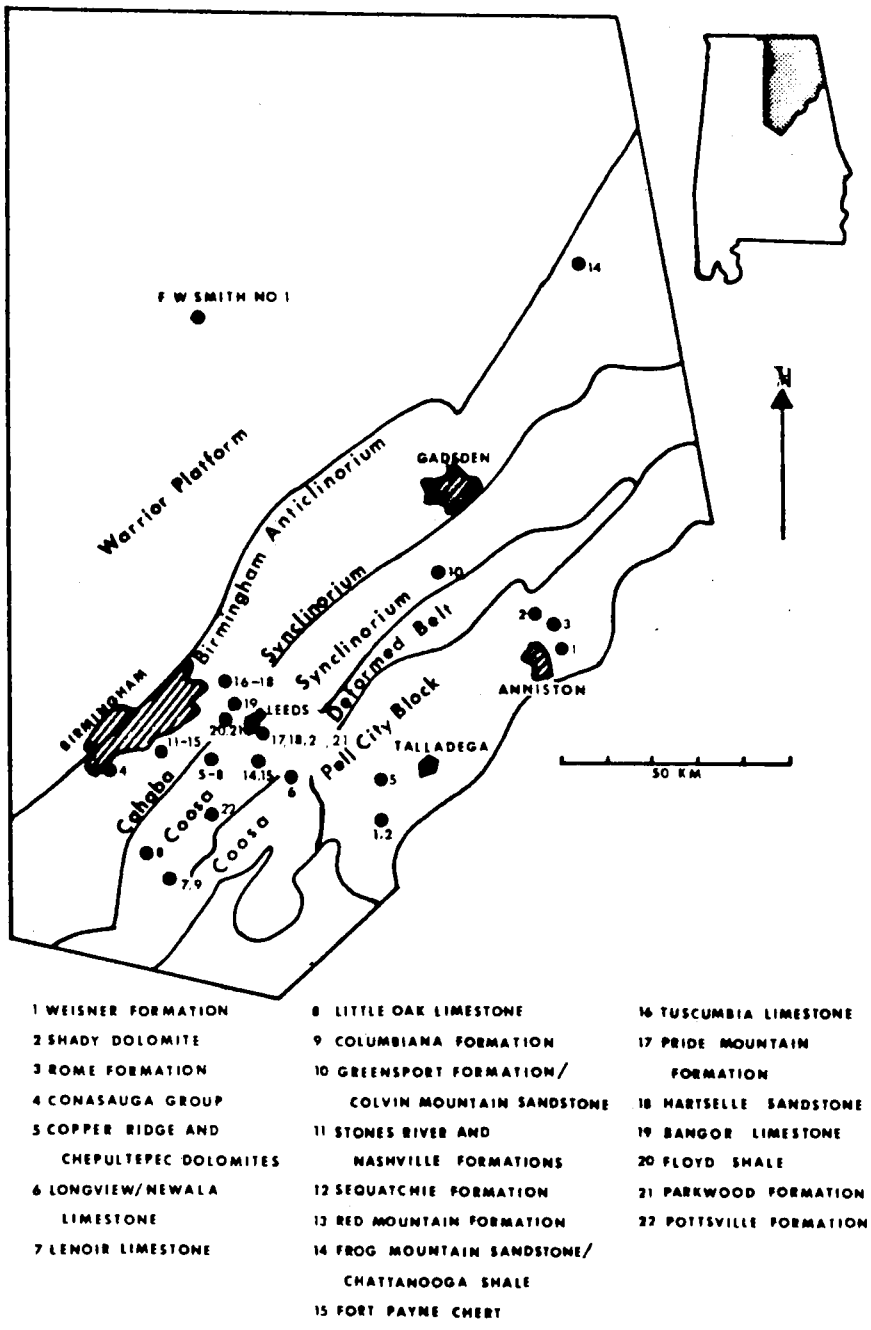

Figure II-2. Location of study area in the southern Appalachian thrust belt, Alabama. Numbered localities are sites of reference sections as described in text and Appendix A. F. W. Smith No. 1 is the only basement test well in the Paleozoic region of Alabama.

each unit were obtained for laboratory analysis. Thin-sections (264), polished slabs (35), and acetate peels (8) of selected samples were examined for small-scale mesoscopic and microscopic structure not observable in the field, particularly small-scale physical and biogenic structures and identity of fossil fragments.

Suites of characteristics, including physical and biogenic sedimentary structures, paleobathymetric indicators, sediment transport direction criteria, and biota, were compiled for each unit (Appendices A and B). Determination of probable depositional environment was made by comparison with characteristics of both modern and ancient environments, summarized by Selley (1978) and Reading (1978). Determination of specific environments was based on consideration of units, with intervals considered as aggregates of subenvironments. Relationship of the individual formation or section to the regional stratigraphic framework was also considered in final determination of depositional environment and paleobathymetry. Methods used in determination of paleobathymetry are described in more detail in Chapter III. The depositional environment and general range of paleobathymetric values associated with a particular lithofacies unit have been assumed to apply to that lithofacies throughout its geographic extent for purposes of regional interpretation, although actual data are limited to a few measured sections (Fig. II-2).

Unless otherwise indicated, the following description of regional stratigraphy includes interpretations of depositional environments, paleobathymetry, and sediment transport directions based on results of this study.

II. THE MIOGEOCLINAL TECTOSOME

The miogeoclinal tectosome comprises the lower part of the Paleozoic sequence, and consists of Cambrian and Lower Ordovician clastics and carbonates (Table II-2). The base of the tectosome, the major unconformity which separates the sedimentary cover from the crystalline basement, is diachronous. In the southeastern Valley and Ridge, Early Cambrian fossils (McKinney, 1977) occur 450 m above the base of the tectosome. The F. W. Smith No. 1 well (Fig. II-2) penetrated Cambrian clastics overlying the basement, but the lowermost fossils, of Franconian (mid-Late Cambrian) age, occur 230 m above the basal contact (Kidd and Neathery, 1976). Further onto the craton in Giles County, Tennessee, uppermost Middle Cambrian (Bolaspis zone) strata rest directly upon the basement (Lochman-Balk, 1971). The strata immediately overlying the basement are, therefore, progressively younger toward the northwest, indicating long-term (55 my) marine onlap onto the craton.

In general, time-equivalent units within the tectosome exhibit neither clear-cut differentiation into definite shelf and basinal environments, nor major paleogeographic variations. The major change is temporal, with a change from predominantly clastic sedimentation during the Early and Middle Cambrian to predominantly carbonate sedimentation during the Late Cambrian and Early Ordovician.

Outcrops of the oldest unit of the tectosome, the Weisner Formation, are restricted to the southeasternmost part of the thrust belt. Lithofacies in the Weisner are highly variable (Bearce, 1977), and Mack (1980) proposed that the unit be termed the Chilhowee Group, and subdivided

TABLE II-2

LITHOLOGIES, REGIONAL THICKNESSES, AND PUBLISHED FAUNAL LISTS, MIOGEOCLINAL TECTOSOME

Formation	Lithology	Thickness (m) Warrior Platform	Cahaba Synclinorium	Coosa Synclinorium	Pell City Block	Faunal Lists
Weisner Formation	dark yellow to light brown siltstone; dark gray to very dark gray arenaceous, micaceous shale or slate; fine- to coarse-grained white or light gray sandstone; white to light gray and pale pink orthoquartzite; coarse-grained conglomeratic, poorly sorted, locally ferruginous sandstone	---	---	0 to 300	± 416	Butts (1926)
Shady Dolomite	white to very pale gray to medium gray; very thin-bedded to massive finely crystalline siliceous dolostone; locally with alternating thin beds of dolostone and dolomitic siltstone or shale	---	---	undetermined	± 350	McCalley (1897); McKinney (1977)
Rome Formation	red, purplish-red, buff, and green laminated to thin-bedded micaceous shale and siltstone; dark brown, yellow, white, and light pink, thin- to thick-bedded, fine-grained calcareous quartzite; medium-bedded, fine-grained, light gray cherty dolostone	88	undetermined	4300 to 500	± 380	Butts (1926, 1940), Kidd and Neathery (1976)
Conasauga Group	medium gray, slightly silty or bioclastic dolostone; thin-bedded gray, black, or red shale; very thin-bedded to massive medium gray argillaceous micrite, dismicrite, biomicrite, biosparite and intrasparite; very light-gray siliceous coarsely crystalline dolostone (Ketona, Bibb and Brierfield Dolomites)	660	950	380	260	Butts (1926), Howell (1944), Bell (1978); Crepicephalus texanus (?) occurs near base of exposed Conasauga in Birmingham Valley (this study)
Copper Ridge Dolomite	thin-bedded to massive light-gray to very dark gray, fine- to medium-grained laminated and/or cross-bedded crystalline dolostone	770	± 400	340	+ 500	Butts (1926)
Chepultepec Dolomite	thin-bedded to massive, light gray to dark gray, fine- to medium-grained crystalline dolostone; medium- to dark-gray intrasparite; thin- to thick-bedded, sub-rounded, fine- to medium-grained orthoquartzite	230	0 to 50?	± 750	+ 600	Butts (1926, 1940)
Newala Limestone	very thin-bedded to massive light gray, cross-bedded locally dolomitic intrasparite and biosparite; medium gray "birdseye" micrite	undetermined	0?	± 150	undetermined	Butts (1926)

Zero indicates absence probably due to erosion, hyphen indicates absence probably due to nondeposition or lithofacies change, undetermined indicates formation present but thickness indeterminate due to poor data or exposure.

into the Cochran, Nichols, Wilson Ridge, and Weisner Formations. In the study area proper, only the slate and fine-grained sandstone lithofacies (Nichols Formation of Mack, 1980) is exposed.

The lower part of the Weisner south of Talladega (Fig. II-2) is dominated by evenly laminated slate, with thin, planar interbeds and lenses of fine-grained sandstone (Appendix B). The sequence coarsens upward, and the upper 10 m contains alternating cross-bedded sandstones and slates, with poorly-sorted conglomeratic quartzite at the top (Fig. II-3).

The dominance of fine-grained, evenly laminated sediments in the lower part of the section suggests deeper subtidal water depths, grading upward into a shallow subtidal environment (Fig. II-3). The presence of scour channels, lenticular sand lenses, interbed sorting, and cross-bedding suggests a pronounced tidal influence (Wunderlich, 1970; Reineck and Wunderlich, 1968); other structures, such as vertical burrows, suggest shallow water depths for the upper part of the section (Fig. II-3). The most probable depositional environment of the Weisner southwest of Talladega was a nearshore marine shelf environment into which coarser sediment was introduced by storm action and reworked by tidal currents. Several poorly-defined coarsening upward cycles are represented, with a general shallowing upward trend (Fig. II-3).

Another important depositional environment is represented by the thick-bedded to massive orthoquartzites of the Weisner in Calhoun and Cleburne Counties (Bearce, 1977). The sequence of coarsening upward cycles, sedimentologically mature quartzites, and planar cross-beds

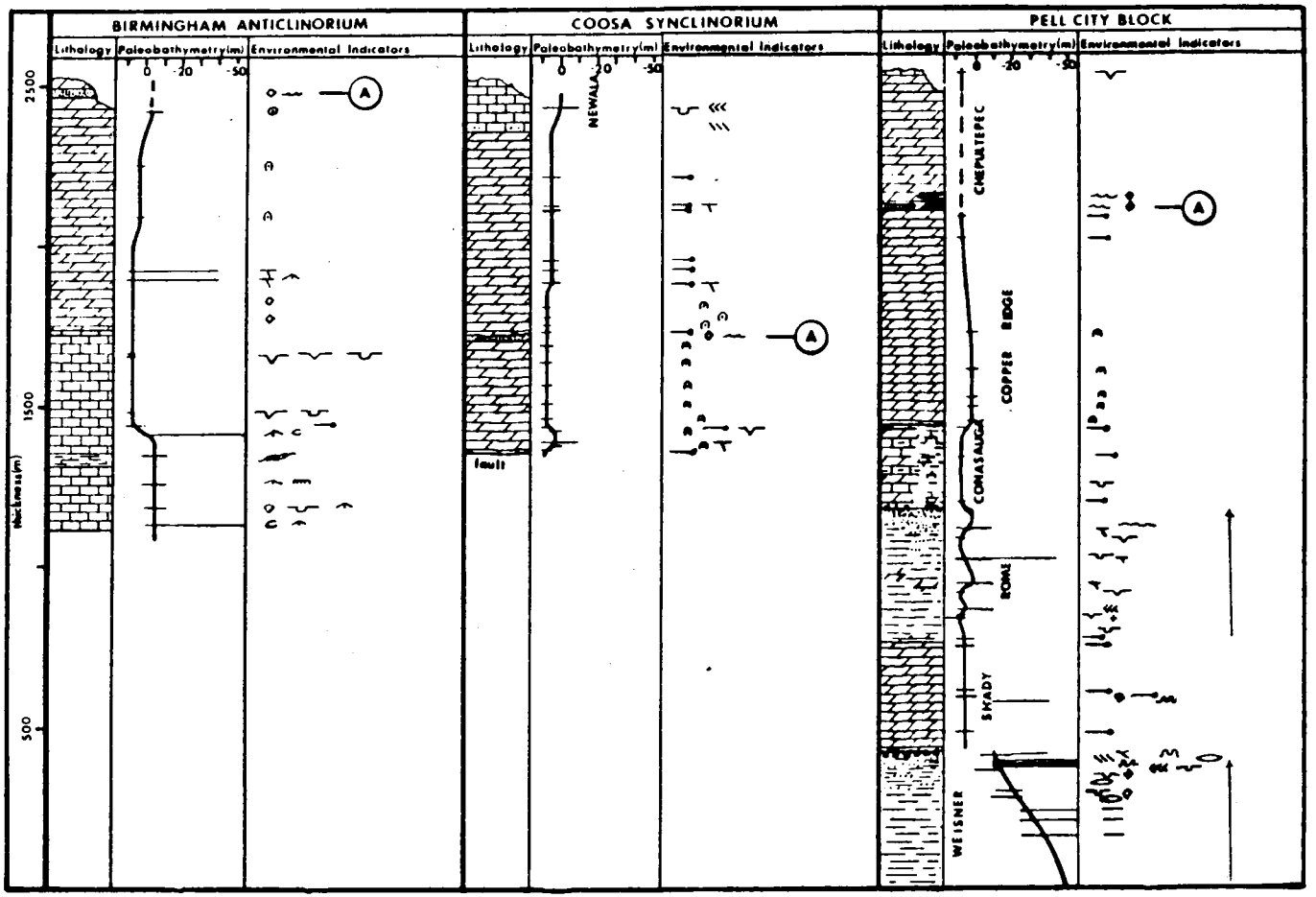

Figure II-3. Formation names, lithologies, paleobathymetry, and environmental indicators in selected measured sections of the miogeoclinal tectosome. Horizontal bars under "paleobathymetry" are maximum possible ranges of paleobathymetry as determined from environmental indicators.

Physical

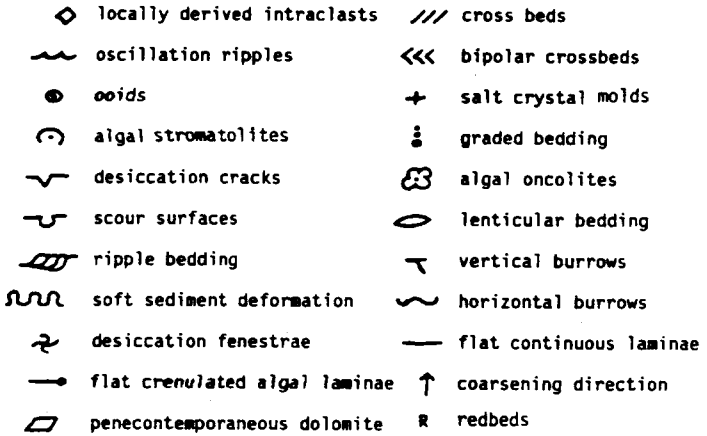

Biological

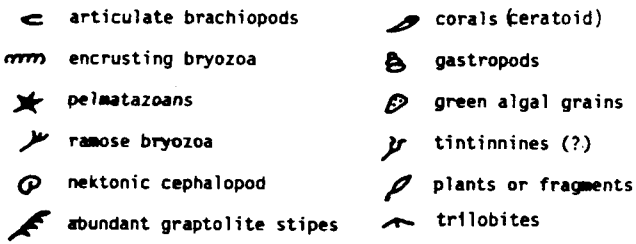

Other Symbols

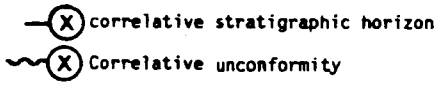

Figure II-3 (continued).

dipping gently south or southeast (Appendix B) represent a south or southeast-facing beach or barrier island complex (Mack, 1980).

The contact of the Weisner with the overlying dolostone unit (Shady Dolomite) has been described both as an unconformity (Cloud, 1967) and as a comformable contact. South of Talladega the contact is irregular, with up to 3 m of relief, is marked by a zone of sedimentary breccia containing poorly sorted quartzite blocks, and represents abrupt transition from subtidal clastic to supratidal carbonate lithologies (Fig. II-3), all of which suggest an unconformity associated with a relative drop in sea level. A similar, apparently unconformable, Shady-Weisner contact extends throughout the eastern Valley and Ridge, indicating that the dolostone facies is everywhere younger than the clastic facies.

The Shady carbonates in the immediate area of the geotraverse have been completely altered to coarse-grained replacement dolostone, and most sedimentary structures obliterated; the only preserved structures are problematical algal sediment laminae, and rounded interclasts up to 3 cm in diameter (Fig. II-3; Appendix B). The uppermost Shady in central Calhoun County (Fig. II-2, page 19) exhibits flat crenulated, algal, sediment laminae and thin beds of intramicrite (Appendix B). While quality of exposure is too poor to formulate an adequate model, the dominant environment of the Shady was apparently high intertidal to supratidal (Fig. II-3).

McKinney (1977) proposed that a part of the Shady near the city of Talladega (Fig. II-2) was deposited in an open marine environment at water depths of 30-50 m, based on the inferred paleoecology of

archaeocyathids from these exposures. It is thus probable that the Shady dolostone facies represents a number of environments from supratidal to deeper subtidal, although the slope and basin facies described in Virginia (Pfeil and Read, 1980) are absent.

Exposures near Anniston, Calhoun County (Fig. II-2, page 19), indicate that the Shady is gradational into an overlying red shale-sandstone-dolostone unit (Rome Formation). The Rome is lithologically distinctive and has been mapped throughout most of the foreland.

Harris and Milici (1977) postulated that the Shady and Rome were time-equivalent, representing an offshore carbonate bank and nearshore intertidal zone, respectively. Although the Shady and Rome appear to be vertically gradational, available biostratigraphic evidence suggests that they are not time-equivalent in Alabama. All known Shady in Alabama belongs to the Lower Olenellus zone while the Rome belongs to the Upper Olenellus to Bathyuriscus/Elrathia zones.

Within the study area proper, the Rome is too poorly exposed to compile a complete measure section. Typical exposures consist of 1 to 2 m of saprolite. The most complete exposures observed during this study are located west of Fourmile in Calhoun County (Fig. II-2), where the Rome consists of mixed micaceous shales and siltstones, sands, and carbonates. Sedimentary structures and lithologic associations (Fig. II-3; Appendix B) indicate that the exposures near Fourmile represent equivalents of the supratidal, mud flat, mixed flat, and sand flat intertidal environments described from the Rome of Tennessee by Samman (1975). Further, the occurrence of both upward-coarsening and upward-fining cycles suggests

vertical juxtaposition of high intertidal (mud flat) and low intertidal (sand flat) subfacies by transgressive/regressive cycles.

The Rome grades upward into the Conasauga Group, but the contact is so ill-defined that the Rome and Conasauga are not differentiated by some investigators (Bearce, 1978). The lithologic character of the Conasauga is highly variable, with pronounced regional lithofacies changes (Fig. II-4).

Physical and biogenic sedimentary structures (Fig. II-3; Appendix B) indicate an intertidal to shallow subtidal environment for the entire thickness of the Conasauga exposed in the Birmingham outcrop belt, and similar features in lithologies exposed east of the Pell City fault indicate intertidal environments. Oolitic cherts and limestones reported by Kidd (1975) from the Plateau region indicate very shallow (1 to 2 m) water depths during deposition of the Conasauga in that region.

Rocks mapped as Conasauga Group in Alabama contain a shaly facies in parts of Calhoun, St. Clair and Etowah Counties (Fig. II-4) similar to the Pumpkin Valley-Rogersville-Nolichucky Shales sequence described from Tennessee (Milici et al., 1973). Depositional environment of the shaly facies was not determined as part of this study, but Markello et al. (1979) considered similar Conasauga Group shales in Virginia to represent a deeper subtidal shelf embayment facies.

In the Cahaba Valley, Birmingham anticlinorium, and Warrior plateau outcrop belts (Fig. I-1, page 4), the uppermost units in the Conasauga are chemically pure dolostones, the Bibb, Brierfield, and Ketona Dolomites. Depositional environments of these units cannot be adequately determined, since replacement dolomite has obliterated most sedimentary

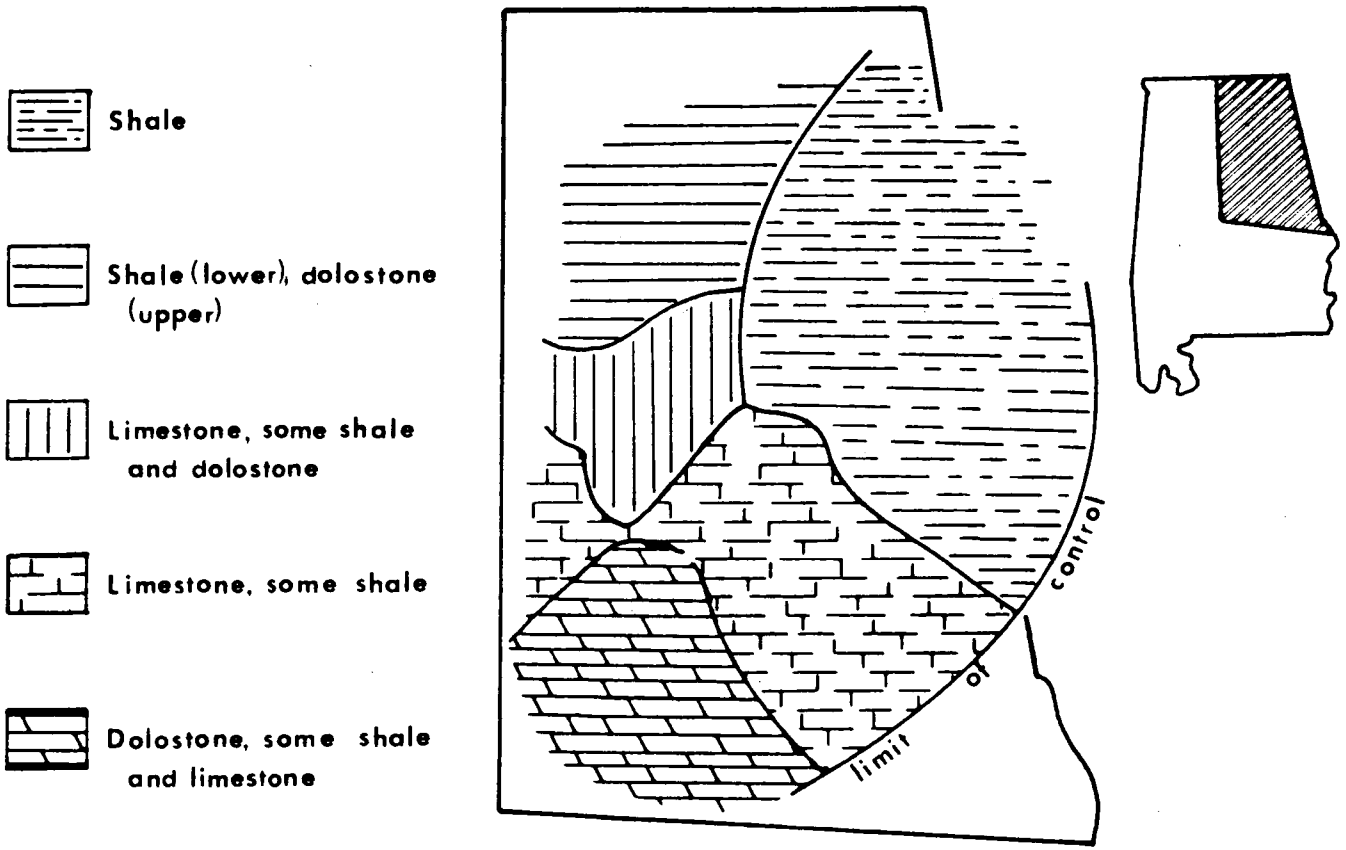

Figure II-4. Regional lithofacies relationships in the Lower Cambrian Conasauga Group in Alabama. Palinspastic base from this study and Dietrich Roeder, unpublished cross sections. Lithologic data from Thomas and Drahovzal (1973), Gilbert (1974), and Kidd (1975).

features (Appendix B), but where remnants of original lithotypes can be observed, they are similar to those in the underlying Conasauga. The basal contact of these units is not isochronous, but crosscuts three trilobite biostratigraphic zones along strike, as determined from paleontological work by Bell (1978) and mapping by Kidd and Shannon (1977) and the present author. It is probable that the Ketona represents a highly dolomitized upper member of the Conasauga as suggested by Howell et al. (1944).

Correlations based on trilobite assemblages indicate that the Rome and the Conasauga are in part time-equivalent. Figure II-5 portrays a combination of formation correlations based on lithotype, compared to trilobite zone boundaries. The trilobite zones are those of Lochman-Balk and Wilson (1958) and Lochman-Balk (1971), supplemented by faunal zone associations of Howell et al. (1944). Faunal elements from published literature (McCalley, 1897; Butts, 1926, 1940; Howell and Mason, 1938; Resser, 1938; Palmer, 1962; McKinney, 1977; Bearce and McKinney, 1977; and Bell, 1978), unpublished collections (D. N. Bearce, Gordon Bell, and J. T. Kidd, personal communications, 1979), and collections made during this study, were plotted in their stratigraphic position, and assigned to a trilobite zone (Fig. II-5). Where possible, multiple genera were used to assign a stratigraphic horizon to a zone, but in some cases only a single genus could be used.

The lack of correlation between lithostratigraphic and biostratigraphic subdivisions suggests that the Rome, Conasauga, and Bibb, Brierfield, and Ketona dolostones represent contemporaneous clastic and carbonate facies, and that additional work will be required to

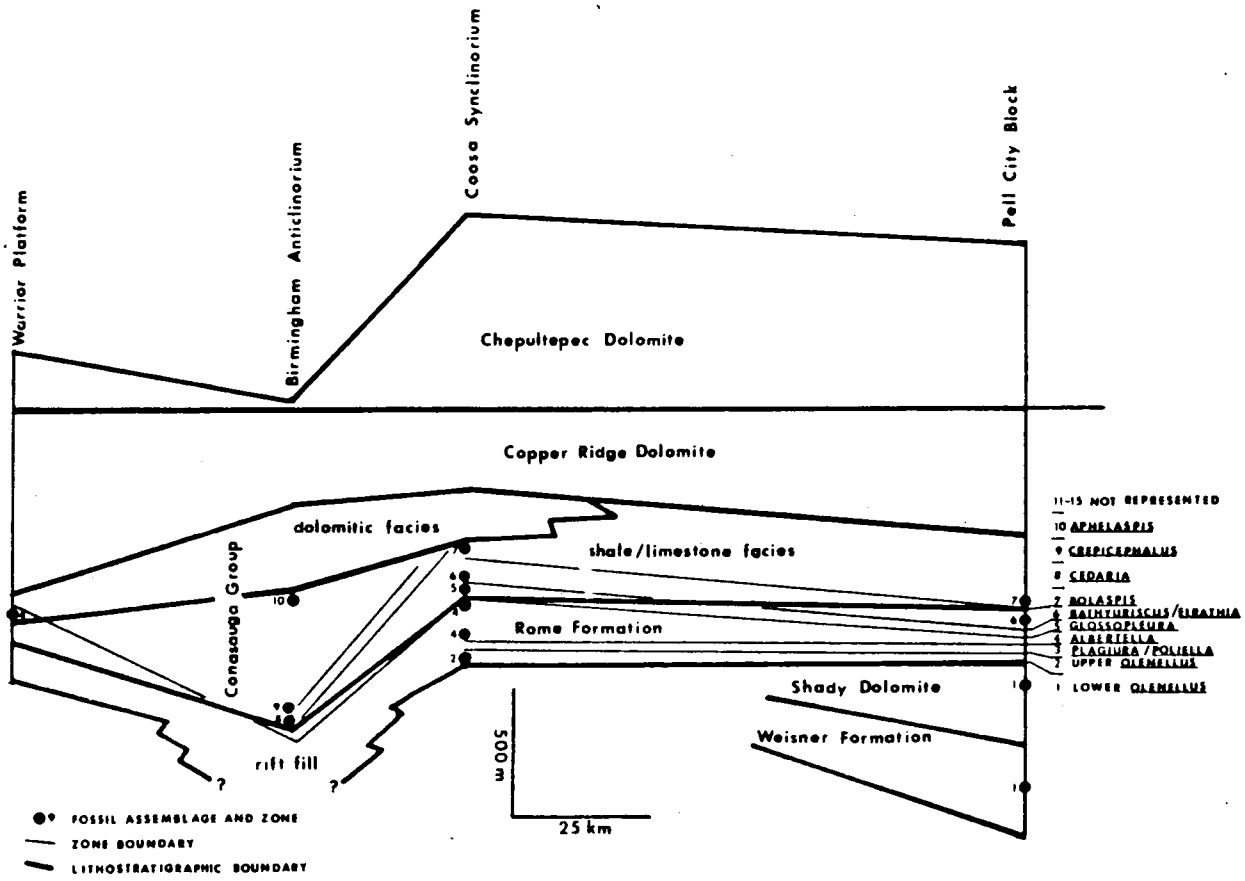

Figure II-5. Lithostratigraphic and biostratigraphic zonation in the Cambrian-Lower Ordovician of Alabama. Trilobite zones after Lochman-Balk and Wilson (1958), Lochman-Balk (1971), and Howell et al. (1944). Note that formation boundaries as presently defined are diachronous to inferred biostratigraphic zone boundaries.

determine true age relationships within this Middle to Upper Cambrian interval. An alternative possibility is that depositional environment rather than time succession exerted the dominant control over the observed faunal associations. Markello et al. (1979), in discussing trilobite zones in the Conasauga of Virginia, noted that since the individual zones are assemblage zones, they are likely to show some degree of environmental control. Research by Palmer and Campbell (1976) indicates that major problems are encountered in shelf to basin correlations, but that correlations between shelf areas (Fig. II-5) are generally more reliable. Additional problems are that collections are inadequate and some identifications of genera may be suspect, but solutions of these problems are beyond the scope of this study. Alternative lithostratigraphic correlations would require an unusually complex regional subsidence history (Chapter III), suggesting that the proposed biostratigraphic correlations are correct in general, if not in detail.

Although not observed in the present study, the contact of the Conasauga with the overlying Copper Ridge Dolomite is reported to be gradational (Cummings, 1960). The Copper Ridge was deposited in intertidal and supratidal environments. In the Cahaba Valley section, the basal 60 m of the Copper Ridge represents a high intertidal to supratidal environment (Fig. II-3, page 24). The overlying 28 m represent a transition to a high intertidal environment with discrete algal stromatolites (Appendix B) separated by shallow (less than 10 cm) scoured channels filled with cross-bedded dolostones, in turn overlain by 255 m of high intertidal deposits characterized by discoidal and algal stromatolites. Examination of selected outcrops in the Birmingham

anticlinorium and east of the Pell City fault indicate similar environments of deposition.

The upper contact of the Copper Ridge is conformable except in the Birmingham anticlinorium, where the overlying Chepultepec is reportedly missing through erosion or nondeposition (Butts, 1926). Butts (1926) placed the boundary between the Copper Ridge and the overlying Chepultepec at the point where "mealy" or "worm-eaten" chert and fossil gastropods become relatively abundant. This placement is imprecise, since both types of chert occur in the residuum overlying each formation. In this study, the contact is placed at the first appearance of bedded orthoquartzites, following the practice of Rodgers (1953) and Cummings (1960) in Tennessee.

Lithologies of the Chepultepec are, on the whole, similar to those in the Copper Ridge, but the Chepultepec also contains numerous beds of fine-grained intrasparite and crystalline dolostone. Algal stromatolites are rare but disruption by both vertical burrows and horizontal trails is common.

Several beds of orthoquartzite 2 to 30 cm in thickness (Appendix B) occur near the base of the Chepultepec. These units consist of subrounded, fine- to medium-grained, frosted quartz sand. Individual beds contain angular voids left by weathering of carbonate pebbles. The quartzite beds are laterally discontinuous, with planar basal contacts, and upper surfaces marked by oscillatory ripples (Gilbert, 1974). East of the Helena fault, the basal Chepultepec locally contains a clastic sequence of variable thickness (0 to 76 m), consisting of medium-grained

chert sand, gray to purple cross-laminated silty clays, and lenticular beds of quartz and chert pebble conglomerates (Self et al., 1974).

Depositional environments are inferred to have been a series of intertidal-supratidal cycles (Fig. II-3, page 24) characterized by a severely limited gastropod fauna, vertical burrows, and scour surfaces overlain by "tidal veneers" (Brown and Woods, 1974) of intrasparite and biosparite. Scattered interbeds of dolomitized micrite with a high density of random trails apparently represent tidal ponds in which gastropods were trapped at low tide. The formation consists of stromatolitic intertidal deposits in the basal 115 m, grading upward into dominantly high intertidal to supratidal deposits.

Butts (1926) subdivided the Lower Ordovician limestones overlying the Chepultepec into two formations, with the distinction in the field based on the presence or absence of chert. Most subsequent workers have found the subdivision impractical. In this report, the entire sequence is referred to as the Newala.

The Newala is absent in the Birmingham anticlinorium, apparently as the result of pre-Middle Ordovician erosion. Examination of sections in the Cahaba Valley and Coosa deformed belts indicates that the lower Newala was deposited in low to high intertidal environment, and the upper Newala in a supratidal environment (Fig. II-3, page 24; Appendix B). Yeager (1971) also concluded that the Newala was primarily intertidal, with limited subtidal and supratidal deposits.

The upper contact is a major pre-Middle Ordovician unconformity which extends throughout the study area, and represents the upper boundary of the miogeoclinal tectosome.

Sediment types and sediment body geometries indicate that the miogeoclinal tectosome represents the gradual subsidence of the North American craton, and progressive onlap of the proto-Atlantic Ocean from southeast to northwest. The sediment body thickens from northwest to southeast, but sedimentation kept pace with subsidence, so that no major regional bathymetric differentiation occurred. The upper and lower boundaries of the tectosome are defined by major unconformities, but significant unconformities within the tectosome, with the exception of the Weisner-Shady contact, cannot be demonstrated from available data. The dominant source of clastic sediment was the exposed North American craton (Bearce, 1977; Mack, 1980).

III. THE FOREDEEP PERIPHERY TECTOSOME

The foredeep periphery tectosome includes strata of Middle and Late Ordovician age (Table II-3). Sediment types and sediment body geometries suggest similarities to the Taconic orogenic foredeep of the Tennessee and Virginia Appalachians (Shanmugam and Walker, 1980), although coarse clastic foredeep deposits are absent. This interval marked the first development of a distinct east-west facies zonation in the Valley and Ridge of Alabama. The most pronounced facies change occurs across the Helena fault (Fig. I-1, page 4), which has juxtaposed southeastern (clastic) and northwestern (carbonate) facies. Numerous formation names, with accompanying correlations, have been proposed, the most recent of which are those of Drahovzal and Neathery (1971), based on established conodont and graptolite biostratigraphies (Berry, 1960; Bergstrom, 1970; Sweet et al., 1970; preliminary work of Raymond, 1973) and tentative

TABLE II-3

LITHOLOGIES, REGIONAL THICKNESSES, AND PUBLISHED FAUNAL LISTS, FOREDEEP PERIPHERY TECTOSOME

Formation	Lithology	Thickness (m) Warrior Platform	Cahaba Synclinorium	Coosa Synclinorium	Coosa Deformed Belt	Faunal Lists
Lenoir Limestone	thick-bedded medium-gray micrite; medium- to thick-bedded medium gray to very dark gray biosparite; locally intramicrite	---	---	50 to 250	---	Drahovzal and Neathery (1971)
Columbiana Formation	thinly laminated to thin-bedded, locally pyritic, locally silty, black shale; thin beds of very dark gray to black argillaceous biosparite; bentonite	---	---	- to 94	0 to 62	Drahovzal and Neathery (1971; Bergstrom and Drahovzal (1972; NOTE: extensive limestone or graptolite and conodont fauna summarized
Little Oak Limestone	thick-bedded, dark-gray argillaceous, burrow mottled biomicrite, locally cherty or silty; bentonite	---	---	- to 78	---	Drahovzal and Neathery (1971)
Greensport Formation	medium- to thick-bedded, maroon to dark-gray argillaceous micrite; maroon to yellow calcareous to noncalcareous siltstone	---	---	- to 50	---	Drahovzal and Neathery (1971)
Colvin Mountain Sandstone	thin-bedded to massive, light gray to white, cross-bedded, fine- to coarse-grained orthoquartzite, lenses of shale and conglomerate	---	---	- to 23	---	no fossils known
Sequatchie Formation	maroon to olive, very thin- to thin-bedded shale and fine-grained sandstone; gray, dark gray and gray-green siltstone and dolostone; medium- to yellowish-gray silty biosparite	0 to 60	0 to 2	undetermined	undetermined	Drahovzal and Neathery (1971)
Stones River Formation	medium- to dark-gray, very thin-bedded to massive, locally pyritic micrite, biomicrite, biosparite, and oolitic biosparite; interbedded thin beds of laminated greenish-gray calcareous shale and argillaceous micrite; bentonite; chert pebble conglomerate locally at base, with chert sand or maroon clay	undetermined[a]	+ 60	---	---	Drahovzal and Neathery (1971)[b]; Kolter and Vest (1953)
Nashville	same as Stones River	undetermined[a]	± 20	---	---	Drahovzal and Neathery (1971)[b]

[a]Not subdivided in subsurface.

[b]Summarized all previous lists.

Zero indicates absence probably due to erosion, hyphen indicates absence probably due to nondeposition or lithofacies change, undetermined indicates formation present but thickness indeterminate due to poor data or exposure.

correlation of bentonite beds (Smith et al., 1971). The Middle and Upper Ordovician rock-stratigraphic terminology and time-stratigraphic correlations used in this study (Fig. II-6) are adapted from Drahovzal and Neathery (1971) and Stig Bergstrom (personal communication, 1979).

The strata of this tectosome can be geographically differentiated into northwestern (carbonate), southeastern (black shale-carbonate) and northeastern (carbonate-clastic) subdivisions (Fig. II-7).

Locally the basal unit of both the southeastern and northeastern subdivisions is a peritidal carbonate unit, the Lenoir Limestone (Drahovzal and Neathery, 1971) (Appendix A). To the southeast this unit is absent, probably as the result of a facies change into the time-equivalent Columbiana Formation, and to the northwest the facies change into equivalent carbonates is obscured by tectonic shortening along the Helena fault. In the southeastern subarea, the Lenoir is comformably overlain by the Columbiana Formation (Cooper, 1956).

The dominant and most characteristic lithology of the Columbiana is a fissile, thinly-laminated to thin-bedded, locally pyritic black shale and silty shale, with thin laminae of crystalline calcite (Appendix B), thin beds of very-dark-gray to black argillaceous fine-grained biosparite at the base, and one or more beds of bentonite (Butts, 1926; Drahovzal and Neathery, 1971). The laminae and thin beds in the Columbiana are continuous over long distances, and exhibit no evidence of subaerial exposure or shallow water depths. Turbidites are absent, and calcite-rich laminae indicate depths above the carbonate compensation depth. The fauna is limited to graptolite stipes and rare trilobites with hyperdeveloped or diminutive eyes (Butts, 1926).

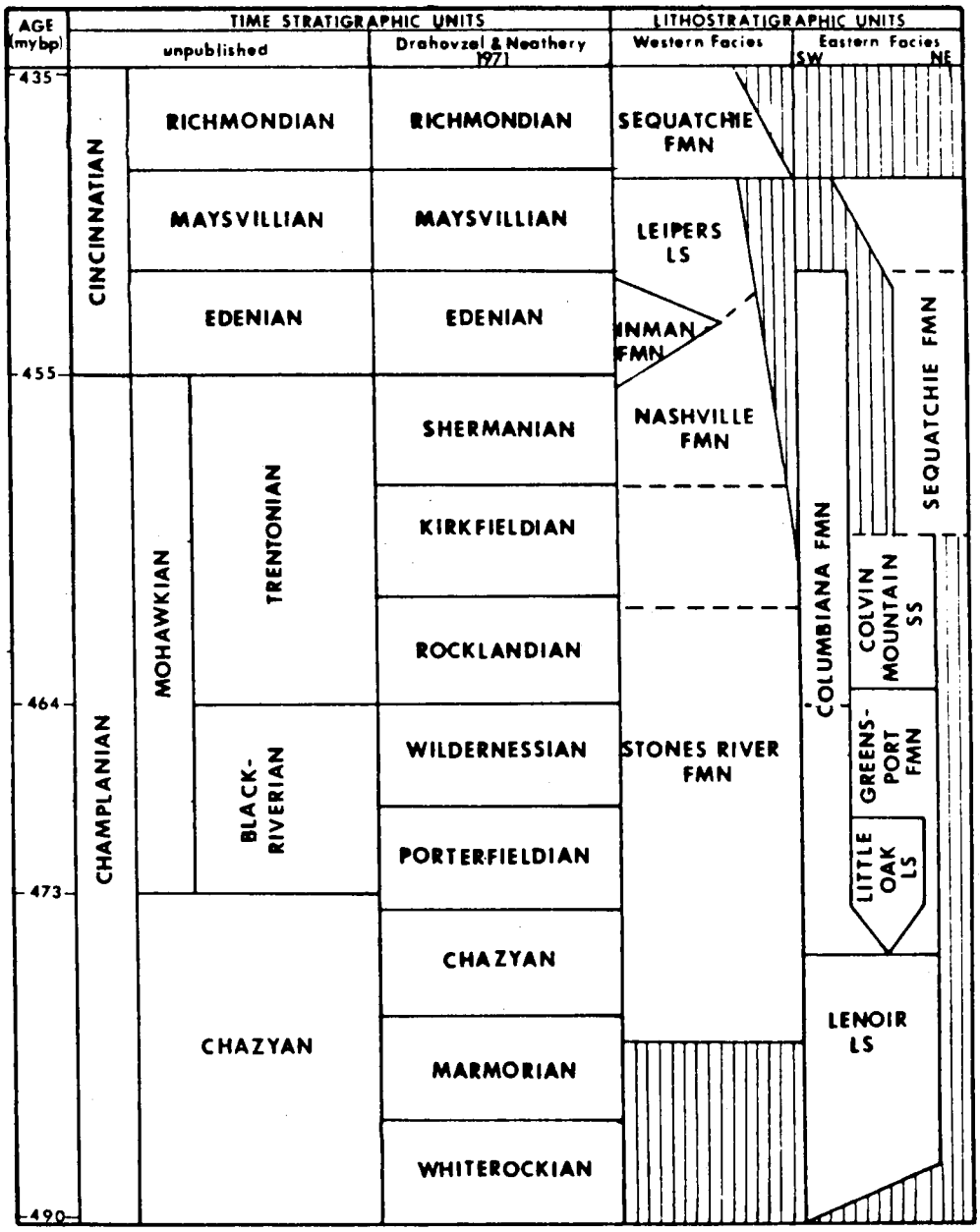

Figure II-6. Middle and Upper Ordovician stratigraphy of Alabama. Modified from Drahovzal and Neathery (1971). Stage names of Drahovzal and Neathery (1971) are correlated to stage names and chronostratigraphic zones from unpublished sources. Vertical ruling denotes intervals not represented in stratigraphic record.

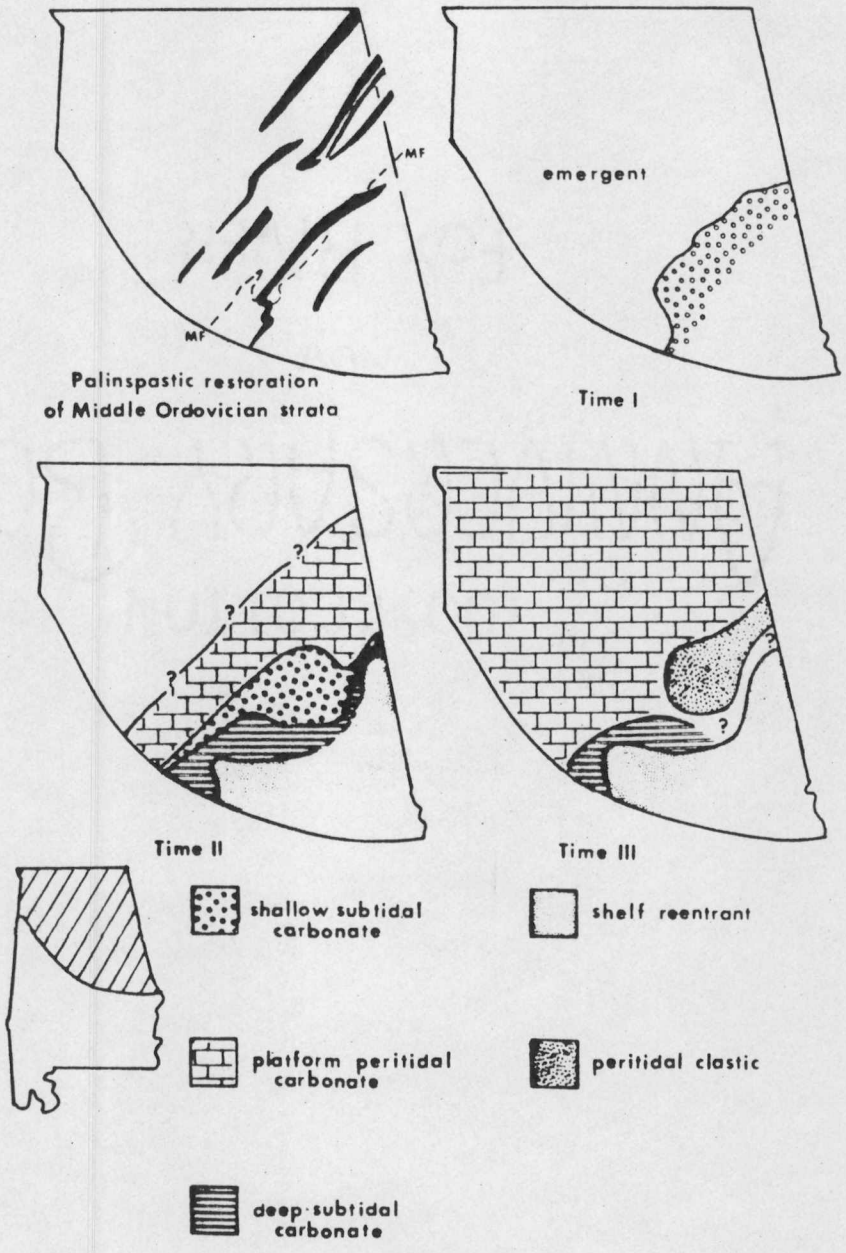

Figure II-7. Middle and Upper Ordovician regional facies patterns plotted on palinspastic base. MF denotes present eastern limit of exposed Valley and Ridge thrust belt. Time I—Upper Whiterockian; Time II—Porterfieldian; Time III—Rocklandian. Basic data from Drahovzal and Neathery (1971), and this study.

The limited bathymetric indicators suggest that the probable depth of Columbiana deposition was deep subtidal with a probable toxic bottom environment (Fig. II-8). Since these sediments are time-equivalent to shallow water shelf carbonates along and across strike, the most probable depositional environment was a starved basin and shelf embayments with limited water circulation at depth, but supporting a nonbenthic biota. The absolute paleobathymetry of the Columbiana is difficult to determine, as paleobathymetric indicators present in this unit have broad ranges (see Chapter III), which allow a possible paleobathymetric range of 50 to over 1000 m. The paleobathymetry of the Columbiana in the Cahaba Valley belt is constrained by its relationship to the carbonate shelf slope. The absence of carbonate debris flows in the Columbiana suggests a low shelf slope of less than 3°, the inclination of modern stable coasts (Shepard, 1973). This slope, together with the paleogeographic separation of the Columbiana basin and the sites of contemporaneous peritidal carbonate sedimentation (Fig. II-7), indicates possible water depths of 600 m or less. Application of the same assumptions to the deeper southeastern parts of the basin would indicate water depths as great as 1300 m, or as little as 600-700 m if a flat basin floor is assumed. The great discrepancy of apparent subsidence (sediment thickness plus paleobathymetry) between the Birmingham anticlinorium and Coosa synclinorium sections would seem to imply an eastward sloping basin floor.

Throughout the southeastern subarea, and the eastern part of the northeastern subarea, the Columbiana comprises the entire preserved Middle and Upper Ordovician sequence (Figs. II-6, II-7). The upper contact is erosional, with the Columbiana overlain by Devonian or Mississippian rocks.

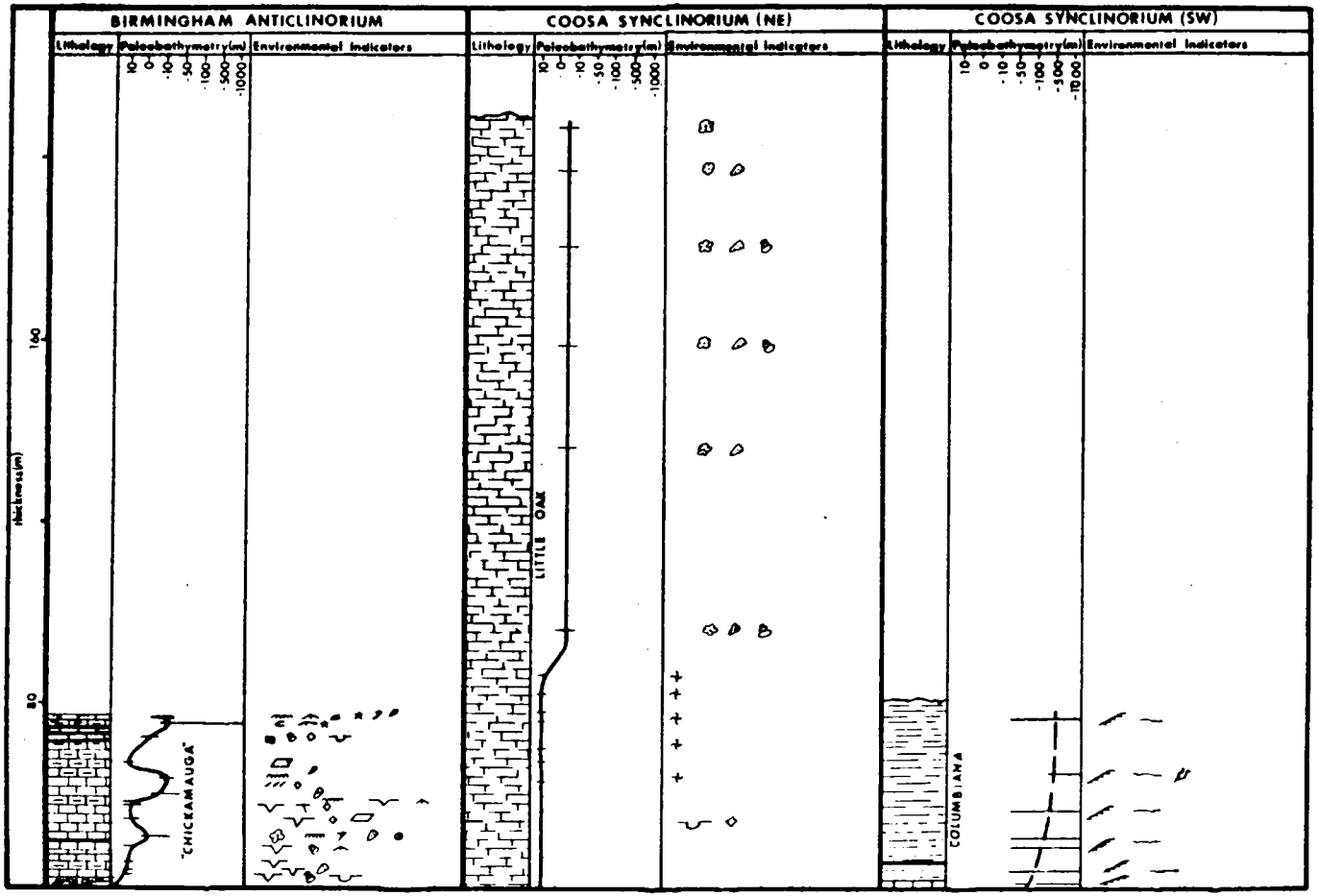

Figure II-8. Formation names, lithologies, paleobathymetry, and environmental indicators in selected measured sections of the foredeep periphery tectosome. Explanation of symbols in Figure II-3, page 24.

To the northeast the Columbiana is laterally gradational into the Little Oak Limestone, an argillaceous biomicrite. Taylor (1971) interpreted the Little Oak as a sub-wave base shelf edge deposit, transitional between the deeper water Columbiana Formation and shallow water carbonates to the west. Examination of two sections in Shelby County (Fig. II-2, page 19) indicates that the Little Oak facies represents a slope transition from peritidal to deeper subtidal environments.

In northern Shelby County (Fig. II-2) the Little Oak is a biomicrite with features indicative of a shallow subtidal environment (Fig. II-8; Appendix B). Near the type locality in central Shelby County (Fig. II-2) the upper 80 m consists of burrowed and disrupted biomicrite with a diverse biota indicative of deeper subtidal conditions within the photic zone (Fig. II-8). Thus, while the basal Little Oak was everywhere deposited in peritidal water depths, by late Little Oak time sedimentation in the southwestern area had not kept pace with increasing water depths, and environments had become differentiated into peritidal shelf edge and shelf edge slope (Little Oak) and deep subtidal shelf reentrant (Columbiana) environments (Fig. II-7).

In the transitional region between the southeastern and northeastern subareas (Fig. II-7), the Lenoir and Little Oak comprise the entire preserved Middle Ordovician, but much of the sequence has been removed by erosion. To the northeast the Little Oak grades laterally into the dominantly clastic Lenoir Limestone-Greensport Formation-Colvin Mountain Sandstone-Sequatchie Formation sequence (Fig. II-7).

The Greensport consists of argillaceous micrite, changing abruptly upward into calcareous to noncalcareous siltstones and fine-grained

sandstone. The suite of lithologies and associated sedimentary structures (Appendix B) indicate that the Greensport consists of cyclic low intertidal sand-facies and high intertidal clay-facies deposits.

The basal contact of the Greensport is not exposed, but is probably gradational into the underlying Lenoir Limestone. It grades upward into the Colvin Mountain Sandstone, a sequence of fine- to coarse-grained orthoquartzites (Table II-3). The conformable relationship of the Colvin Mountain to peritidal clastics above and below (Drahovzal and Neathery, 1971; Thompson, 1971), and sedimentary structures suggest that the Colvin Mountain represents a sequence of peritidal sands (Appendix B) exposed to wave action, and probable strong tidal influence (Wunderlich, 1970). The Colvin Mountain is inferred to represent a beach or nearshore environment, with interbedded intertidal deposits.

The Colvin Mountain is conformably overlain by the Sequatchie Formation, a sequence of shale and fine-grained sandstone, grading upward into siltstone and dolostone. This unit was not examined during this study, but eastern facies of the Sequatchie are red terrigenous-carbonate (intertidal to supratidal), gray terrigenous-carbonate (shallow subtidal), micrite (shallow subtidal) and calcarenite (shallow subtidal with strong tidal currents), all associated with a west-facing shoreline (Thompson, 1971). The Sequatchie is unconformably overlain by Silurian or Devonian sediments. The Greensport, Colvin Mountain, and Sequatchie are absent in the study area proper as the result of pre-Devonian erosion.

Butts (1926) assigned all the Middle and Upper Ordovician carbonate rocks of the northwestern subarea (Fig. II-7) to the Chickamauga

Limestone. Drahovzal and Neathery (1971) elevated the Chickamauga to group status, with the Stones River and Nashville Formations included, and established the separate Inman Formation, Leipers Limestone, and Sequatchie Formation. However, the formations proposed by Drahovzal and Neathery (1971) were established on the basis of gross lithologic similarities, and are not directly correlative with the type localities of those formations. In the study area the Stones River consists of micrite, biomicrite, biosparite, oolitic biosparite, calcareous shale and argillaceous micrite, and the basal Attalla Chert Conglomerate Member (Table II-3).

Wilson (1971) studied exposures in northeastern Alabama, and concluded that the Stones River was deposited in peritidal environments. Wilson (1971) assigned the lower one-third of the section to a shallow subtidal to sub-wave base bathymetric range, grading upward into intertidal and supratidal ranges. Kolter and Vest (1953) and Stock and Benson (1981) described small (less than 1.5 m high) bioherms, with a diverse biota, from the Birmingham area.

Detailed study of the section at Birmingham (Fig. II-2, page 19) supports the conclusion that the Stones River was deposited in peritidal environments. The basal Attalla member is localized in topographic lows developed on the underlying Knox Group and the discontinuity, coarse clastics, and oxidized conglomeratic shales suggest a probable origin as subaerial or supratidal sinkhole fillings. The Stones River carbonates immediately above the Attalla exhibit features indicative of supratidal or high intertidal environments (Appendix B). The bulk of the Stones River at Birmingham does not exhibit a consistent shallowing or deepening

trend, but represents a series of vertically alternating bathymetric zones ranging from shallow subtidal to supratidal (Fig. II-8).

The Stones River is gradational into the overlying Nashville Formation to which it is lithologically similar (Table II-3). The thin sequence of Nashville preserved in the study area was deposited in shallow subtidal environments (Fig. II-8; Appendix B) and represents a continuation of the environmental conditions which prevailed during deposition of the Stones River.

Drahovzal and Neathery (1971) concluded that regional thinning was the result of pre-Upper Ordovician erosion of the Nashville, but no evidence of such an erosional surface has been observed. Given the geographic extent of the area over which thinning occurs, the small magnitude of the missing section, and the peritidal conditions, it is probable that areas where the Nashville is unusually thin may represent nondeposition or slow deposition on bathymetric highs.

The Inman-Leipers sequence (Table II-3) is missing in the study area, either through post-Middle Ordovician erosion or nondeposition.

The western facies of the Sequatchie consists of calcareous shales and fossiliferous limestones (Table II-3). The Sequatchie is laterally gradational from a shaly sequence in the east to a thinner carbonate sequence in the west, and is represented in the study area by less than 1 m of intrabiosparite of shallow subtidal origin (Fig. II-8; Appendix B).

The upper boundary of the tectosome is an erosional unconformity which increases in magnitude toward the southeast; most of the tectosome is preserved in the Birmingham anticlinorium, but in parts of the Coosa deformed belt the entire tectosome is absent.

The Middle and Upper Ordovician of Alabama contains no coarse clastic basinal facies similar to those of Virginia and Tennessee. However, chronologic and facies relationships indicate that the evolution of the Middle and Upper Ordovician shelf and basin margin was similar to that described from Tennessee (Benedict and Walker, 1978) and Virginia (Markello et al., 1979). The Lenoir and the basal beds of the Stones River represent supratidal to shallow subtidal sediments deposited on a pre-Middle Ordovician erosional surface. Age relationships within the Lenoir-Stones River (Drahovzal and Neathery, 1971) indicate that the Middle Ordovician sea encroached upon the land surface from the south and east (Fig. II-7, Time I). By the Upper Chazyan-Porterfieldian (Fig. II-7, Time II), the shelf had differentiated into several environmental zones. To the west the Stones River and Nashville accumulated in a mosaic of supratidal to shallow subtidal environments formed on a slowly subsiding shelf. The eastern margin of the shelf was irregular, with shallow subtidal carbonates (Little Oak) gradational into deeper subtidal shelf-edge reentrant and starved basin deposits (Columbiana). At present no shelf-edge grainstone banks or ooid shoals similar to those in the Tennessee section (Benedict and Walker, 1978; Clayton Breland, personal communication, 1979) have been observed.

With continued subsidence, the deeper subtidal deposition of the Columbiana gradually encroached upon the shelf (Fig. II-7, Time III), as the basal Columbiana is time transgressive (Drahovzal and Neathery, 1971; Stig Bergstrom, personal communication, 1979). At the same time, carbonate sedimentation in the shallow northeastern end of the

depositional basin was being superseded by intertidal clastics from a northeasterly source. During the uppermost Ordovician or Early Silurian, the easterly areas were uplifted, causing preferential erosion of the easterly facies.

IV. THE EPEIRIC SEA TECTOSOME

The epeiric sea tectosome includes the thin assemblage of Silurian through lowermost Mississippian strata which were deposited in a shallow epicontinental sea adjoining a northwest facing shoreline. During this interval of geologic time, the basin polarity was reversed from that of the other tectosomes; i.e., basinward was toward the northwest, and the southeastern part of the foreland was uplifted and periodically emergent.

The lower boundary of the tectosome is a major unconformity throughout the study area, and the Lower Silurian is absent (Lundin and Newton, 1970). The major stratigraphic units internal to the tectosome are separated by major unconformities which increase in magnitude toward the southeast, so that the three lower units within the tectosome thin and pinch out southeastward, and are bounded above and below by erosional unconformities.

The lowermost unit of the tectosome is the Silurian sequence which consists of a thin offshore shale carbonate sequence (the Brassfield Limestone and Wayne Group) in the Warrior platform area, and a time-restricted nearshore clastic sequence (the Red Mountain Formation) in the Valley and Ridge.

Neither the Brassfield nor the overlying Wayne Group crop out in the study area, and no direct determination of depositional environment

was feasible. Butts (1926) described Favosites and Halysites, the only faunal elements (except ostracodes) thus far described from the western facies of the Silurian. Lecompte (1956) has concluded that these organisms generally lived in the open marine shallow to deeper subtidal zone, in water depths of 5 to 50 m.

Lundin and Newton (1970) interpreted the upper contact of the Brassfield as a short depositional hiatus, followed by deposition of the Wayne Group, which they described as the Silurian unit A-unit B sequence.

The nature of the upper contact of the Wayne Group with the overlying Devonian is uncertain. A zone with no diagnostic fossil species occurs between the rocks bearing Late Silurian species and those bearing Early Devonian species, and it is not possible to determine whether any depositional hiatus exists; Lundin and Newton (1970) suggested that no lacuna exists.

The western shale-carbonate facies represents an essentially complete Middle and Upper Silurian sequence. The Red Mountain Formation (Table II-4) represents a time-restricted part of the early Niagaran (Lundin and Newton, 1970; Berry and Boucot, 1970; Chaiffetz, 1974). The basal Red Mountain is transgressive toward the southeast, as indicated by relative ages of the basal Brassfield and Red Mountain (Lundin and Newton, 1970; Berry and Boucot, 1970). The lithologies of the Red Mountain are a mixture of calcareous or silty sandstones, shales, biosparite, ferruginous sandstone, oolitic sandstone, and intraformational conglomerates (Table II-4). To the northwest the Red Mountain becomes more shaly and interfingers with a carbonate facies. In the subsurface to the southeast

TABLE II-4

LITHOLOGIES, REGIONAL THICKNESSES, AND FAUNAL LISTS, EPEIRIC TECTOSOME

Formation	Lithology	Thickness (m) Warrior Platform	Cahaba Synclinorium	Coosa Synclinorium	Coosa Deformed Belt	Faunal Lists
Red Mountain Formation	light-gray, red-gray and gray-brown, fine- to medium-grained, thin-bedded to massive calcareous or silty sandstone; medium- to dark-gray laminated to thin-bedded calcareous shale; medium-gray thin-bedded biosparite thick-bedded, dark red, medium- to coarse-grained poorly sorted ferruginous sandstone and oolitic fossiliferous sandstone; intraformational conglomerate	---	± 70	- to 30	---	Butts (1926); Berry and Coucot (1970; Astrospongia, Favosites, and Codeacian and Dasycladacean algae noted in this study.
Brassfield Limestone	greenish-gray, medium-gray to grownish-gray, locally cherty, argillaceous, dolostone, siliceous, sandy and glauconitic limestone	---	---	---	---	Lundin and Newton (1970); Butts (1926)
Wayne Group	red and green shale; red, gray, or green silty limestone; gray and green sparry limestone	---	---	---	---	Lundin and Newton (1970)
Frog Mountain Sandstone	varicolored fine- to coarse-grained locally conglomeratic, ferruginous or calcareous sandstone; laminated black to gray siltstone and shale; medium dark-gray to reddish brown biomicrite and biosparite	undetermined	0 to 7	0 to 5	0 to 12	Butts (1926, 1927); Kiefer (1970)
Chattanooga Shale	dark-gray to black laminated to thinly-laminated pyritic bituminous shale; interbeds of poorly sorted fine- to coarse-grained sandstone near base	undetermined	0 to 6	-?	-?	Glover (1959); Kelley (1969)
Fort Payne Chert	buff, light brown and yellowish gray thin- to medium-bedded fossiliferous chert; laminated brown plastic clay; oolitic in east	undetermined	± 30	± 30	0 to 20	Butts (1926)

Zero indicates absence probably due to erosion, hyphen indicates absence probably due to nondeposition or lithofacies change, undetermined indicates formation present but thickness indeterminate due to poor data or exposure.

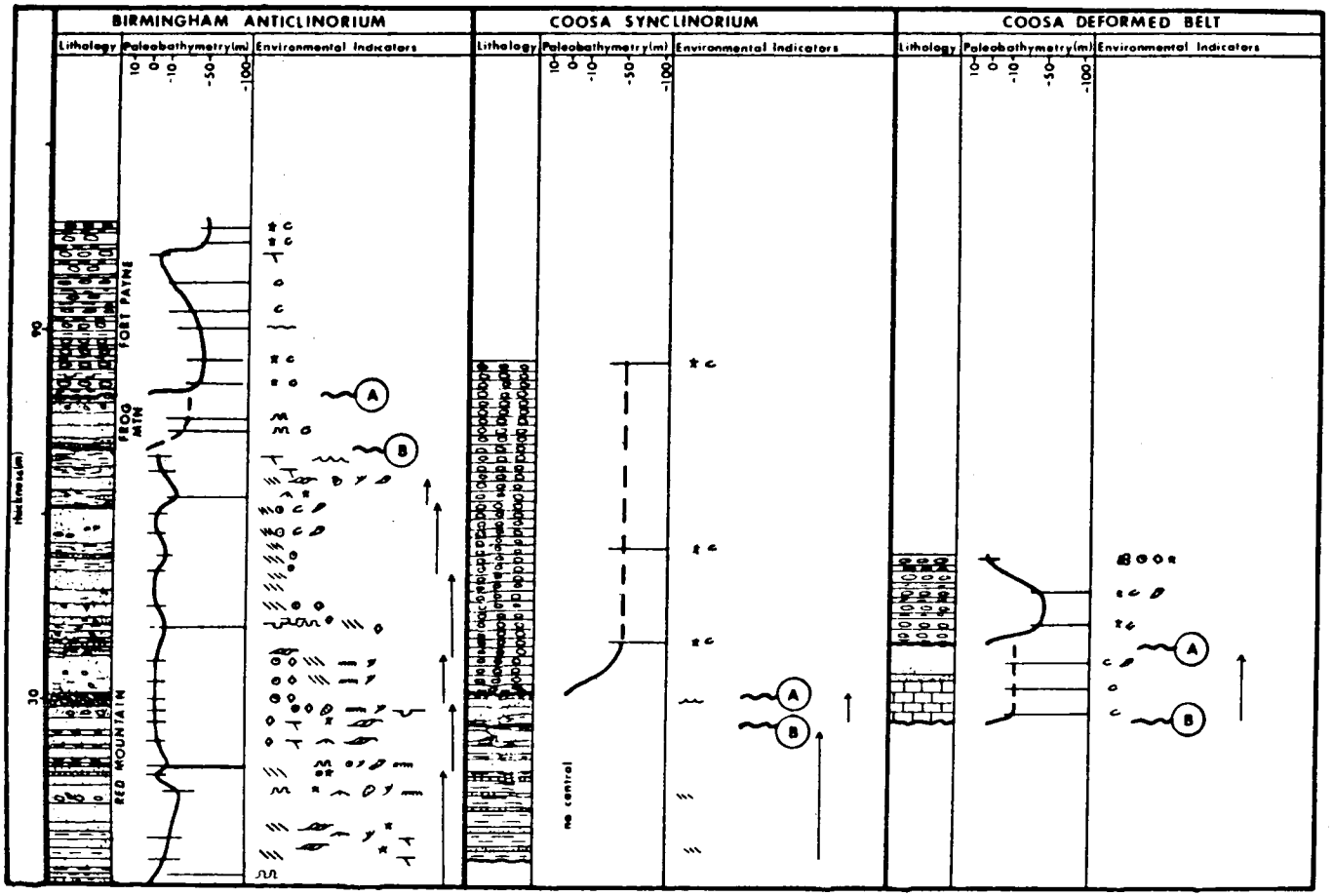

Figure II-9. Formation names, lithologies, paleobathymetry, and environmental indicators in selected measured sections of the epeiric sea tectosome. Explanation of symbols in Figure II-3, page 24.

the Red Mountain locally grades into a dark gray lagoonal shale facies (Sheldon, 1964, 1970).

Exposures of the Red Mountain near Birmingham (Fig. II-2, page 19) exhibit lithologic associations indicative of a mosaic of shallow subtidal environments (Fig. II-9; Appendix B). The hematitic ore beds of the formation (Appendix B) represent a cross-bedded to massive, rounded to subangular fossiliferous sand and/or ooid shoal subfacies (Fig. II-9). The shoal subfacies is laterally and vertically gradational into a shaly subfacies which exhibits random trails and both vertical and horizontal burrows, but body fossil species diversity is low. The low species diversity, shallow water depths, association with oolitic subfacies rocks, and lack of strong tidal or wave influence suggest that these strata represent semi-protected lagoonal areas behind or among the sand/ooid shoals. A third subenvironment is represented by a subtidal mixed sand/shale subfacies with high species diversity (Fig. II-9). The subtidal sand/shale subfacies is volumetrically more important in the more westerly exposures of the Red Mountain. The upper boundary of the Silurian is a major erosional unconformity in the Valley and Ridge, and a nondepositional hiatus in the Warrior platform region (Lundin and Newton, 1970).

The Early to Middle Devonian is characterized by an easterly sand/shale facies, and an unnamed limestone and chert facies in the Warrior basin (Kidd, 1975). Early to Middle Devonian strata are missing from the Plateau region of north central Alabama and unit thicknesses vary widely in the Valley and Ridge as the result of pre-Late Devonian erosion (Kiefer, 1970). The Late Devonian is represented by the

widespread Chattanooga Shale, which thins to the north and southeast as the result of erosion.

Kidd (1975) summarized available information on the nonclastic facies. The only clue to possible depositional environments is the presence of glauconite, indicative of subtidal conditions. This unit does not occur in the study area, but is restricted to west Alabama and Mississippi. Thomas (1972b) speculated that the equivalent "Arkansas Novaculite" and siliceous micrite represent the entire Devonian system in the subsurface of Mississippi.

The Frog Mountain Sandstone as described here includes all the pre-Chattanooga Devonian clastic rocks in the Alabama Valley and Ridge (Butts, 1926; Kiefer, 1970). Lithologically the Frog Mountain consists of sandstones, calcareous siltstone and shale, chert, and brown limestones (Table II-4). In the Birmingham Valley the grain size distribution and lithologic similarity of the sediments suggest that most of the Frog Mountain was derived by reworking of the underlying Red Mountain sands (Kiefer, 1970; D. N. Bearce, personal communication, 1972). The diverse fauna and physical sedimentary structures (Appendix B) suggest that the Frog Mountain was deposited in shallow subtidal water depths in areas not strongly affected by tidal flow (Fig. II-9).

In the Coosa deformed belt the Frog Mountain consists primarily of sandstones with local zones of shale pebbles, siltstones (typically at the base of the section) and, in some exposures, sparry limestone with no remnant of original textures (Table II-4). Butts (1926, 1927) and Kiefer (1970) reported a diverse biota from shales at some localities

(Table II-4). The extremely diverse biota suggests an open marine environment, with some current activity but below wave base (Fig. II-9).

Extreme variation in thickness results from pre-Upper Devonian erosion, as indicated by outliers in northeastern Alabama and the hiatus between the Frog Mountain and the overlying Chattanooga Shale (Kiefer, 1970). The basal Frog Mountain rests on strata of Lower Ordovician to Silurian age, but on the outcrop scale bedding in the Frog Mountain is parallel to that in underlying units. In view of the large geographic area involved, it is not likely that the regional angularity is the result of any significant pre-Devonian deformation. Age of the basal Frog Mountain is progressively younger toward the southeast, indicating that the Frog Mountain was transgressive. The pre-Frog Mountain hiatus is progressively greater toward the southeast, and the youngest basal Frog Mountain rests upon the oldest underlying strata (Lower Ordovician), suggesting broad uplift of the eastern Valley and Ridge during the Silurian-Devonian.

The upper contact of the Frog Mountain is an erosional unconformity resulting in isolated erosional outliers of Frog Mountain. The majority of the overlying Chattanooga Shale in Alabama belongs to the Gassaway member as defined by Glover (1959), who also concluded that the more southeasterly outcrop belts contain a higher percentage of sand. The conglomeratic basal sands of the Chattanooga are locally cross-bedded, with oscillation ripple marks and containing clasts derived from the underlying units (Glover, 1959; Kelley, 1969), but the bulk of the formation consists of finely laminated bituminous shale (Appendix B). Conant and Swanson (1961) provided a particularly complete summary of the

evidence for both deep and shallow water deposition, and proposed a shallow-water origin, but features truly diagnostic of a shallow water origin are lacking.

Recent work (Duff, 1975; Hallam and Bradshaw, 1979) on similar bituminous shales in the Jurassic of Europe suggest that they were deposited during intervals of rapidly rising relative sea-level, under conditions of low terrigenous clastic input and conditions unfavorable to carbonate sedimentation. In this model local stagnation resulting from bottom topography resulted in deposition of shales in an anaerobic environment. This model would suggest that the basal beds of Chattanooga are of shallow subtidal origin, but basin filling did not keep pace with relative sea-level rise and the overlying shales were deposited under conditions of ever-deepening water. However, absolute paleobathymetry cannot be determined, since such sequences can be deposited in a wide bathymetric range. The great areal extent of the Chattanooga and its equivalents would suggest either a rapid sea-level rise in the Late Devonian not described by Vail et al. (1977), or relative subsidence of much of the North American continent. In either case, little or no differential subsidence within the Chattanooga basin is implied. The upper contact of the Chattanooga is an erosional unconformity, as indicated by the occurrence of erosional outliers (Kelley, 1969).

The Lower Mississippian Fort Payne Chert consists of fossiliferous chert and laminated clay (Table II-4). In a very few outcrops where the original lithotype is preserved, the chert was observed to be a replacement of medium- to dark-gray biomicrite (Appendix B), biosparite and, in the easternmost outcrop belts, beds of oolite with symmetrical algal

oncolites and intraclasts (Appendix B). The diverse biota, relative abundance of unabraded pelmatozoan ossicles and articulate brachiopods, and the micritic substrate indicate an open marine, sub-wave base environment (Fig. II-9). A gradual shoaling toward the southeast is suggested by the occurrence of lenses and beds of oolitic chert, and eastward thinning of the section. In the western belts the Fort Payne is gradational upward into the Tuscumbia Limestone and thence into the Pride Mountain Formation (Fig. I-2, page 6). In the southeast (Coosa deformed belt) the Fort Payne thins to zero, and the basal Floyd Shale (Tuscumbia-Pride Mountain equivalent) rests directly upon the Devonian. The southeastward thinning of the Fort Payne is probably due in part to depositional pinchout, as indicated by the southeastward shoaling; however, the upper contact is an unconformity with erosional outliers.

Precise lateral time and facies relationships among the Fort Payne, Pride Mountain, and basal Floyd are unknown, but apparently complex. The previously described relationships indicate that deposition of the Fort Payne-Tuscumbia-Pride Mountain was continuous in the northwest. In the absence of an adequate basis for correlation, it can only be assumed that the Fort Payne-basal Floyd unconformity extends laterally into a conformable surface within the Fort Payne-Tuscumbia-Pride Mountain sequence. Because the clastics of the Floyd-Pride Mountain were derived from the south or southeast (see Foredeep Tectosome, this chapter) and prograded northwestward over the Tuscumbia carbonates, it has been assumed, for purposes of this study, that the Fort Payne-Floyd unconformity is approximately correlative with the Fort Payne-Tuscumbia boundary in the

northwest. This correlation is in agreement with correlations proposed by Thomas (1972a).

The epeiric sea tectosome is relatively thin, was deposited with no major geographic variation in bathymetry, and is interrupted by several lacunae of variable duration. All these criteria suggest minor subsidence and deposition in marginal to a shallow epeiric sea which persisted for nearly 100 my.

Nearshore-offshore facies relationships in the Silurian system indicate that the sea was bordered on the southeast by a low-lying land mass which contributed no significant amounts of clastic sediment. After development of a major lacuna resulting from a sea level lowstand at the Ordovician-Silurian boundary (Vail et al., 1977), the sea encroached from northwest to the southeast during the Niagaran. In western Alabama shallow to deeper subtidal conditions persisted through the remainder of the Silurian and into the Devonian, but post-early Niagaran strata are absent in the Valley and Ridge. This lacuna may be attributed to relative uplift of the Valley and Ridge, or to a later subaerial erosion. Since the Silurian highstand was achieved during the late Niagaran (Vail et al., 1977), erosion during the major Early Devonian (Deerparkian) lowstand is likely, particularly since the upper part of the Silurian section is locally missing (eroded?) in northwest Alabama (Lundin and Newton, 1970). Some uplift of the eastern Valley and Ridge during the Silurian-Early Devonian is implied by the manner in which the pre-Frog Mountain unconformity bevels into progressively older strata in a southeastward direction (Kiefer, 1970).

Following the Deerparkian lowstand, the sea once more onlapped from the northwest, as suggested by the relatively younger age of the basal Frog Mountain in the southeastern belts (Butts, 1926, 1927a, 1927b). Sediments of the Frog Mountain consist of both reworked local sediments, and transported clastics from central Tennessee (Kiefer, 1970; D. N. Bearce, personal communication, 1977).

Following development of an unconformity related to a late Middle Devonian (Erian) sea level fall (Vail et al., 1977), the Chattanooga Shale was deposited over an erosional surface which locally exposed units as old as Early Ordovician (Kelley, 1969). Deposition of the Chattanooga apparently spans the Devonian-Mississippian systemic boundary in Tennessee (Hass, 1956), but age relationships are poorly known in Alabama. The uppermost unit of the tectosome (Fort Payne) represents a period of marine onlap with resumption of shallow to deep subtidal carbonate sedimentation.

V. THE FOREDEEP TECTOSOME

The foredeep tectosome, including the associated foreland shelf, consists of Lower Mississippian through Lower Pennsylvanian strata which exhibit complex areal lithofacies zonation (Fig. II-10) and a strongly asymmetric sediment body geometry (Fig. I-2, page 6). The northwestern lithofacies is dominantly carbonate, gradational laterally and vertically into a northwestward prograding coarsening upward clastic lithofacies (Fig. I-2; Fig. II-10). The three-dimensional relationships of the component lithofacies units within the tectosome are sufficiently complex that they cannot be conveniently separated into regional or temporal

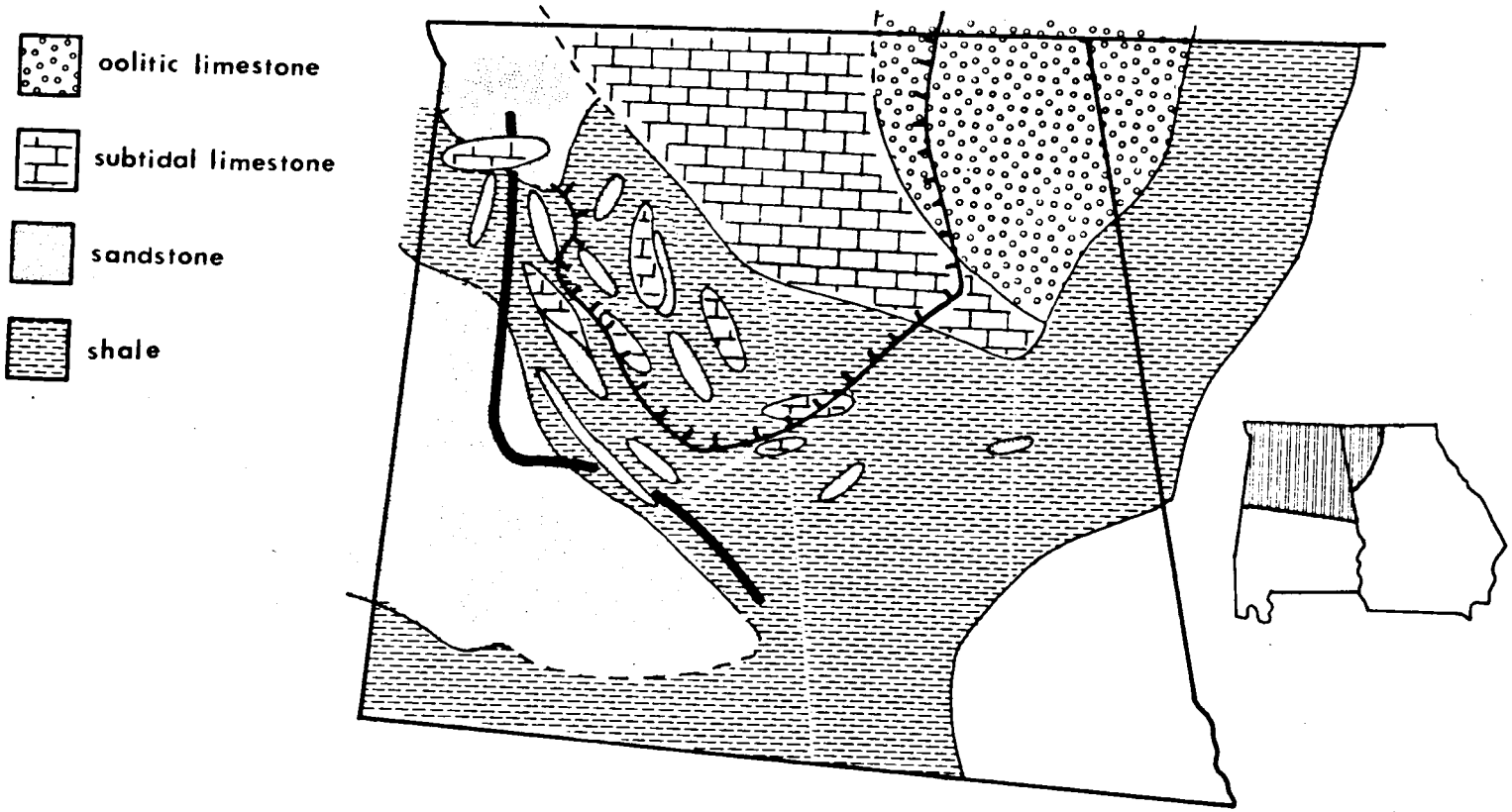

Figure II-10. Facies relationships in the Lower and Upper Mississippian, north Alabama and northwest Georgia. Patterns represent facies in Early Mississippian time. Hachured line denotes main facies boundary in Upper Mississippian, with shallow subtidal carbonate hachured side of line, surrounded by prodelta shales and sandstones. Heavy line represents edge of Warrior platform. Lithofacies data from Thomas (1972a), and Smith (1967), and this study.

grouping for description. Therefore, units will be discussed separately, and their interrelationships summarized.

The basal contact relationships of the tectosome are complex. In the Birmingham anticlinorium and Warrior platform region the basal unit of the tectosome, the Tuscumbia Limestone, is gradational into the underlying Fort Payne Chert, and the tectosome boundary is extrapolated from other areas. In the Coosa synclinorium the clastic lithofacies equivalent of the Tuscumbia, the Pride Mountain Formation, apparently rests comformably on the Fort Payne (Fig. I-2, page 6). Further southeast the basal lithofacies unit, the lower Floyd Shale (Fig. I-2) rests unconformably on Middle Ordovician strata. These relationships indicate that the Fort Payne was deposited in a northwestward-deepening basin, but in Early Mississippian time the southeastern foreland underwent rapid subsidence, inundating the southeastern landmass and changing the slope polarity of the depositional basin. At the same time, clastics of southeasterly source prograded over the Fort Payne, grading northwestward into the Tuscumbia. The basin polarity change and clastic influx define the base of the tectosome, which was extrapolated into the northwestern carbonate sequence.

The Tuscumbia (Table II-5) crops out in the study area only in the Birmingham anticlinorium. Physical and biological paleobathymetric indicators (Appendix B) distributed throughout the section indicate shallow subtidal to sub-wave base water depths (Fig. II-11). The entire section exhibits a general shallowing upward trend, with sub-wave base micrites dominant near the base, eventually grading upward into very shallow subtidal oolitic biosparites (Fig. II-11). Petrographic

TABLE II-5

LITHOLOGIES, REGIONAL THICKNESSES, AND FAUNAL/FLORAL LISTS, FOREDEEP TECTOSOME

Formation	Lithology	Thickness (m) Warrior Platform	Cahaba Synclinorium	Coosa Synclinorium	Faunal/Floral Lists
Tuscumbia Limestone	massive silty biomicrite and biosparite; lenses of well-sorted cross-bedded palmatazoan grainstones; oolitic biosparite and oolite	28 to 36	- to 30	---	Drahovzal (1967)
Pride Mountain Formation	laminated dark gray to very dark gray clay shale; nodules and beds of siderite or pyrite	15 to 70	30 to 120	30 to 90	Butts (1926)
Hartselle Sandstone	gray to white, very fine- to fine-grained, thin- to thick-bedded, well sorted, locally cross-bedded conglomeratic quartz sandstone and ortho-quartzite; silty calcareous shale; locally oolitic wacke-stone; dark-gray very fine-grained argillaceous sandstone	3 to 30	- to 14	- to 35	
Bangor Limestone	medium to dark gray argillaceous biomicrite; calcareous clay shale; oolite; thick-bedded to massive pelmatazoan grainstone	125 to 170	- to 160	---	Butts (1926)
Floyd Shale	laminated to very thin-bedded, dark to very dark gray carbonaceous micaceous shale; nodules of siderite; massive calcareous shale; thin beds dark gray to black argillaceous intrasparite	---	100 to 280	230 to 550	Butts (1926)
Parkwood Formation	dark- to very dark-gray; laminated to massive micaceous, carbonaceous shale and silt-stone; very fine to fine-grained light to medium gray argil-laceous micaceous sandstone; medium to coarse-grained light gray orthoquartzite toward top	- to 30	380 to 550	150 to 560	Culbertson (1967)
Pottsville Formation	thin-bedded to massive light gray, fine- to coarse-grained cross-bedded orthoquartzite, locally conglomeratic; laminated dark gray carbonaceous shale; laminated to massive dark brown to gray shale and siltstone; thin- to thick-bedded silty micaceous subgraywacke sandstone	± 180	± 3200	± 3200	Wanless (1975; Reed and Mamey (1964); Rothrock (1949)

Zero indicates absence probably due to erosion, hyphen indicates absence probably due to nondeposition or lithofacies change, undetermined indicates formation present but thickness indeterminate due to poor data or exposure.

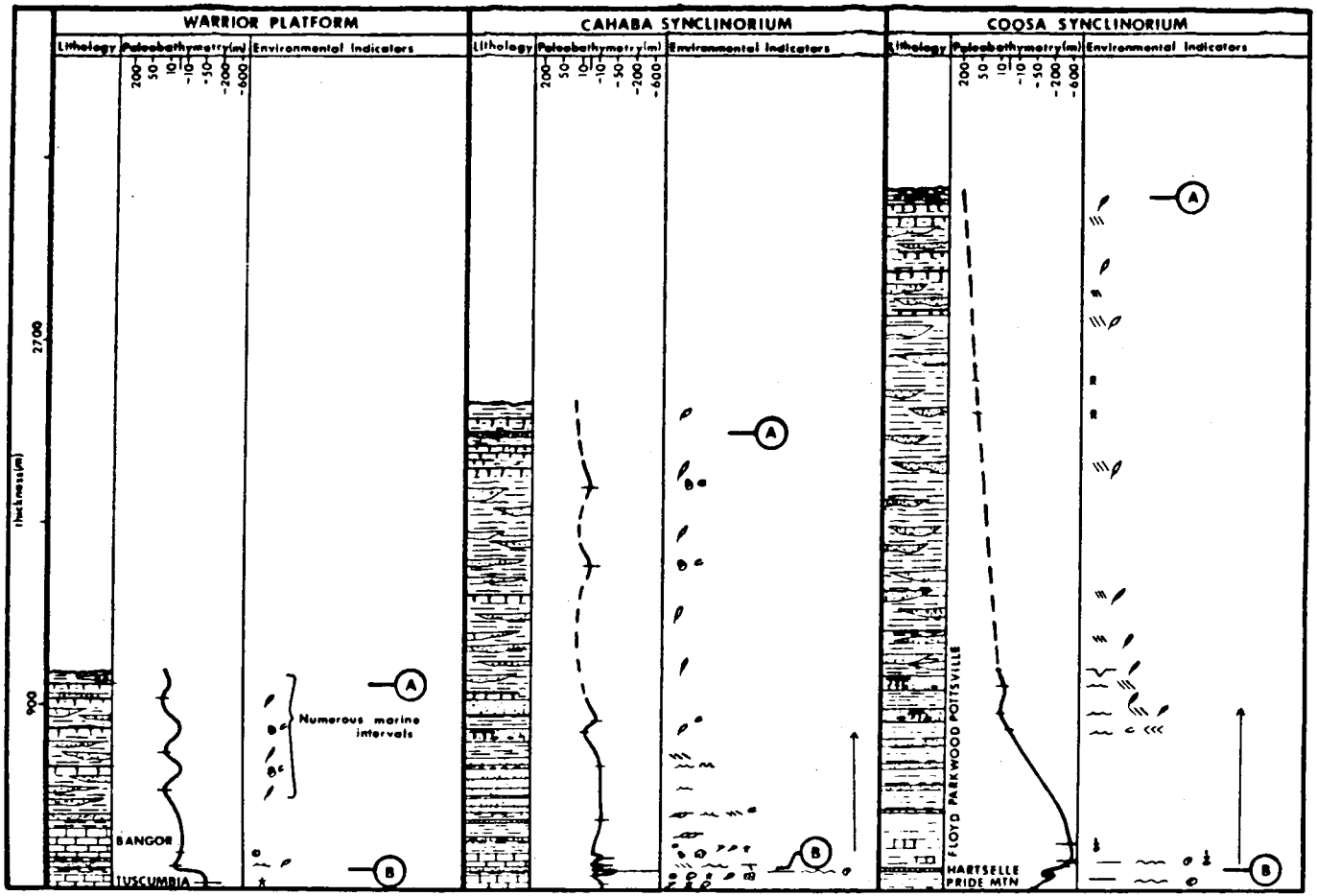

Figure II-11. Formation names, lithologies, paleobathymetry, and environmental indicators in selected measured sections of the foredeep tectosome. Explanation of symbols in Figure II-3b, page 24.

descriptions of the Tuscumbia by Smith (1967) indicate the same shallow subtidal depositional environment and shallowing upward sequence in the Tuscumbia of the Tennessee Valley.

The Pride Mountain consists primarily of clay shale, with thin beds and nodular layers of siderite and rare pyrite (Table II-5; Appendix B). Horizontal burrows are locally common, and the basal few meters are sparsely fossiliferous, although the formation is generally nonfossiliferous with rare goniatites and finely comminuted plant material. Thomas (1972a, 1977) summarized facies relationships outside the study area proper, describing a central clay shale facies in the Warrior platform area, grading northeastward into carbonate, and southwestward into a sandy facies characterized by northwest-southeast trending linear sand members. He postulated that the Pride Mountain-carbonate relationship represented evidence for a southwesterly clastic source for the Carboniferous clastics of the southern Appalachians. However, since the westerly and southwesterly equivalents (palinspastically restored Ouachita facies) of the Pride Mountain are the abyssal turbidites of the Stanley, Jackfork, and Johns Valley Groups (Briggs, 1974; Morris, 1974; Thomas, 1972b), it is probable that the sand facies represents a subtidal, tidally influenced shelf edge sand. Such a sand facies may have been produced by wave-induced winnowing of clastics, with sand concentrated along the shelf margin, and argillaceous sediment worked into the Ouachita flysch basin.

Depositional environments and paleobathymetry of the Pride Mountain in the study area proper are difficult to establish. The lack of criteria suggestive of shallow depths suggest a below wave-base environment (Fig. II-11). Open marine conditions are suggested by the relative

abundance of the nektonic cephalopods. At the base, however, the Pride Mountain overlies and interfingers with oolitic limestones of the Tuscumbia (Table II-5). The Pride Mountain is in conformable contact with the overlying Hartselle Sandstone, of shallow subtidal origin, but the Hartselle was deposited during an interval of greatly lowered sea level (Vail et al., 1977; John M. Dennison, personal communication, 1979), further suggesting a deeper subtidal origin for the Pride Mountain.

Two depositional environments are possible—subtidal open marine or lagoonal ("back-barrier marine" of Thomas, 1972a). The Pride Mountain thickens and is laterally gradational into the basinal Floyd Shale to the southeast, south, and southwest, and gradational into peritidal carbonates on the northeast. These regional relationships also suggest that the Pride Mountain represents a deeper subtidal clastic foredeep fill.

The Hartselle Sandstone is characterized by light colored orthoquartzites, grading laterally into carbonaceous sandstone on the south, southeast, and southwest. In all areas contacts with the overlying Floyd Shale and the underlying Pride Mountain are conformable. The Hartselle is restricted primarily to the Warrior platform region, with a thin tongue extending into the Valley and Ridge (Fig. I-2, page 6). Features observed near Birmingham (Fig. II-11; Appendix B) suggest a shallow water, possible barrier bar or barrier island environment for the Hartselle. This is in accord with Beavers (1977), who concluded that the Hartselle in northwest Alabama was deposited on a broad, stable, tidally dominated shelf, with subtidal and intertidal subenvironments, and characterized by linear subtidal sand bodies developed in response to northwest-southeast tidal flow. Thomas (1972a, p. 44) also suggested

". . . barrier face sands . . ." and ". . . partly forested subaerial barrier flats."

The Hartselle in the Warrior platform and Birmingham anticlinorium is conformably overlain by the Bangor Limestone (Table II-5). Thomas (1972a) described a regional facies zonation of the Bangor on the Warrior platform, consisting of an oolitic belt, and areas southwest and northeast of this belt. The oolitic belt roughly coincides with the limestone isolith maximum and edge of the Warrior platform, and consists predominantly of biosparite, massive oolitic limestone, and calcareous shale (Thomas, 1972b). To the west and southwest the Bangor interfingers with the much thicker clastic sequences of the Floyd Shale and Parkwood Formation in the Warrior basin (Thomas, 1972a, 1972b). In this area the Bangor interval consists of medium- to dark-gray, argillaceous, fine-grained biomicrite, calcareous clay shale, some oolitic limestone, maroon and green mudstone, and cherty limestone (Thomas, 1972b). To the north east the dominant lithology is light- to medium-gray biomicrite, with proportionately lesser amounts of oolitic limestones, rare calcareous shales, and rare maroon and green mudstones near the top (Thomas, 1972b). In northeastern Alabama this facies grades into the shallow water clastics of the Pennington Formation (Thomas, 1972b).

In the study area proper, the eastward extension of the oolitic facies grades laterally into the Floyd Shale. Physical and biogenic structures (Appendix B) indicate shallow subtidal environments of variable paleobathymetry (Fig. II-11). In map pattern, the Bangor grades laterally (within 1.6 km along strike) into tidally influenced clastics of the Floyd Shale, suggesting proximity to the edge of the carbonate

platform. Further southeast the Bangor is absent, but the corresponding Floyd interval contains scattered horizons of argillaceous limestone which represent carbonate debris flows originating on the Bangor carbonate platform (see description of Floyd Shale).

The Bangor is conformably overlain by the Floyd Shale, which is lithologically indistinguishable from the Pride Mountain, and where the Hartselle is absent, the Floyd includes Pride Mountain equivalents (Thomas, 1972a). Throughout most of the Valley and Ridge the Floyd consists of very carbonaceous and micaceous clay shale with clay ironstone or siderite (Table II-5).

In the eastern Valley and Ridge, the basal Floyd contains beds of biogenic allochems and clay shale intraclasts in a clay matrix (Appendix B), usually described as "argillaceous" limestones (Butts, 1926; Thomas, 1972a). These units are typically pyritic and cupriferous. Associated with these carbonates are ill-defined horizons of medium-bedded highly calcareous shale, generally distinguishable from the associated shales by lack of internal lamination. The Floyd represents the basal part of a coarsening-upward sequence, and the upper Floyd contains thin-bedded fine-grained "dirty" sandstones like those in the overlying Parkwood Formation; however, since the Floyd-Parkwood boundary is by convention defined as the transition to sandy sediments, some workers (for example, Thomas, 1972a) include these sands in the Parkwood.

Depositional environments and paleobathymetry of the Floyd are problematical and variable both geographically and chronologically. The fine clastics which comprise the bulk of the sequence east of the Helena fault exhibit neither evidence of subaerial exposure, nor characteristics

of tidally influenced sediments. Individual beds are laterally continuous over great distances, and the orientation of mica grains and finely-divided plant debris parallel to lamination (Appendix B) suggestive of low agitation. Silty laminae rarely exhibit low-angle cross-bedding indicative of weak bottom currents as well as poorly developed grading, but scour surfaces and turbidites and microturbidites are absent. Rapid sedimentation is indicated by development of microfaults and piercement dewatering structures (Appendix B).

The shales and silts are locally disrupted by the burrows of deposit feeders (Fig. II-11), so that the degree of bioturbation ranges from absent to intense, but body fossils of an identifiable infauna are absent. The fauna is similar to the deep water "Namurian Goniatite Community" (Ramsbottom, 1978) and that of the Caney Shale, the slope deposits on the north flank of the Ouachita flysch basin (Hammes, 1965). The calcareous shales also contain few body fossils, the extremely rare crinoid columnals and strophomenid brachiopods constitute an association similar to Ramsbottom's (1978) "Basinal Benthic Community."

The limestone units near the base of the Floyd contain a diverse biota as well as irregular shale intraclasts and aggregate grains (Fig. II-11). However, several factors suggest that the carbonates may have been transported. Some faunal elements, such as the corals and bryozoa, while able to tolerate limited water turbidity (Duncan, 1957), would not have been likely to colonize a soft mud substrate, or survive under the conditions of low current activity and high sedimentation rate implied by the enveloping shales. Likewise the local abundance of algal oncolites is incompatible with the absence of wave-generated structures

in the enveloping shales. The source of the individual grains was apparently diverse, as evidenced by the shale intraclasts and by the mixture of elements which are bathymetrically incompatible, such as crinoids and symmetrical algal oncolites.

Rapid deposition of the carbonate units is indicated by abrupt basal contacts (Appendix B), allochems indenting and deforming fine laminations in the underlying shale, and by irregular flame and load structures at the basal contacts. Upper contacts are abrupt, with an irregular top with protruding grains immediately overlain by thinly-laminated shales (Appendix B).

Although this evidence suggests that the limestones represent shallow-water material transported into a deeper basin, a transport mechanism is problematical. Storm-agitated water would be unlikely to transport large (up to 5 cm) clay intraclasts any great distance laterally, nor do the beds exhibit unequivocal characteristics typical of mass flow processes. The observed bed characteristics, including absence of basal scours, grooves, flutes or tool marks, as well as the poor-sorting, random fabric, and irregular top conform most closely to those of debris flow (Middleton and Hampton, 1976).

The various indicators suggest the basal Floyd east of the Helena fault was deposited in relatively deep water, below the zone of wave and tidal current activity, with weak bottom currents and periodic influxes of silt and carbonate debris from adjacent shallow areas. However, no unequivocal criteria are available for determination of paleobathymetry. The limited biota and sediment characteristics correspond to the lower part of the shelf-mud facies of Reineck and Singh (1973), deposited in

50-100 m depths, and the mica content further suggests depths of 50-150 m (Doyle et al., 1968).

The probable water depth can be more closely approximated using a method described by Shanmugam and Walker (1980). Absence of submarine slump features in the Floyd suggest a paleoslope of 3° or less, based on observation of modern stable slopes (Shepard, 1973). However, the presence of debris flow deposits implies a slope approaching unstable conditions; for this reason I have assumed a paleoslope of 2.5° to 3° along the western margin of the Floyd basin. Palinspastic restoration of the eastern Floyd basin and the edge of the contemporaneous carbonate platform indicates a map-distance separation of some 30 km. This separation, and the assumed paleoslope, indicate a probable bathymetric range of 500 to 600 m below MLW (Fig. II-11). The eastern part of the Floyd shallows upward, and is transitional into the shallow subtidal Parkwood Formation.

Northwest of the Helena fault the Floyd was deposited at shallow subtidal depths, as indicated by the presence of "wavy-bedded" and ripple-bedded silts and sands, and by the lateral gradation into the shallow subtidal Bangor.

The Floyd is gradational upward into the Parkwood Formation, but because the boundary is placed at the first appearance of significant sandstones the boundary is somewhat arbitrary.

The dominant lithologies in the Parkwood are shales, siltstones, and clay shales similar to those of the Floyd, are typically micaceous and/or carbonaceous, and only locally calcareous (Table II-5). Intervals of shale are frequently interlaminated or interbedded with siltstone or

very fine- to fine-grained, light to medium gray micaceous argillaceous sandstone, with clay drapes and ripple-bedded structure (Appendix B). Major sandstone units commonly contain fossil plant debris ranging from finely divided leaf fragments to limbs and trunks up to 60 cm in length. The sandstones are coarser grained, thicker bedded, more numerous, and less argillaceous toward the top of the Parkwood, so that in general the entire sequence coarsens upward.

With rare exceptions, the sediments of the Parkwood do not exhibit criteria suggestive of subaerial exposure, and physical structures and marine invertebrates suggest a marine environment. Examination of a section along the Cahaba River near Birmingham, and other exposures along the same strike belt, suggest lateral and vertical juxtaposition of several subenvironments (Fig. II-11). The basal Parkwood in general consists of marine shales, siltstones and fine-grained sandstones with features indicative of sub-wave base sedimentation in an area influenced by strong tidal flow and rapid subsidence (Wunderlich, 1970).

Higher in the section, thicker sandstones locally exhibit features indicative of near-wave base sedimentation, and locally derived clay chips resulting from reworking of semi-consolidated clays (Fig. II-11). The upper part of the section is characterized by cross-bedded sandstones with features indicative of sorting by high wave activity. The coarser sandstones typically exhibit large scale, multidirectional, planar, tabular cross-bedding probably formed in migrating sand shoals (Appendix B). The entire Parkwood thus represents a shallowing upward, tidally influenced clastic marine sequence.

The contact of the Parkwood with the overlying Pottsville Formation is locally conformable and locally an erosional surface with the Pottsville filling channels eroded into the Parkwood (Appendix B). The channels have led some investigators to describe the contact as an erosional unconformity, but the channels are more likely of tidal origin, as they occur at a subtidal (Parkwood)-beach or barrier island (basal Pottsville) contact .

Internal stratigraphy of the Pottsville is consistent throughout the region. Butts (1926) subdivided the Pottsville into upper and lower subdivisions, and later gave member status to some sandstone units (Butts, 1927a, 1940). The Pottsville in the Coosa synclinorium has been subdivided into four "sequences," the Narrows, Straight Ridge, Yellowleaf, and Wattsville in order of decreasing age (Gilbert, 1976). This subdivision was based on gross lithologic associations, and is also applicable to the Pottsville outside the Coosa synclinorium.

The Narrows sequence consists of the Shades Sandstone, "interconglomerate measures," and Pine Ridge Sandstone of Butts (1927a) (Table II-5, page 60). Prominent characteristics of the Shades are large scale, low angle tubular cross-bedding, and erosional channels in both the Shades and the underlying Parkwood, filled with steeply dipping trough cross-bedded sandstones (Appendix B). Exposures within the thrust belt are relatively small, but exhibit the same features which led Hobday (1974) to conclude that the equivalent Boyles Sandstone of northwest Alabama and Georgia represents beach or barrier island complexes (Fig. II-11, page 61).

The Pine Ridge Sandstone (Table II-5, page 60) is similar to the Shades, but is generally more conglomeratic, less shaly, and is generally thicker. Because of the similarity to the Shades, the Pine Ridge is also assumed to represent a beach or barrier island complex.

The intervening "interconglomerate measures" (Table II-5) consist of a variable thickness (30 to 94 m) of carbonaceous shale, sandstone, and thin coal beds. Sand bodies typically have tabular basal contacts with ripple-marked upper surfaces, and represent migrating bodies of fine sand on a cohesive mud bottom. Body fossils are absent, but bedding surface trails, deposit feeder burrows, and finely divided plant debris are locally abundant. The absence of body fossils and criteria suggesting subaerial exposure, and the association with barrier sand complexes suggests that the interconglomerate measures were deposited in brackish lagoons protected from strong wave and current activity, but subject to periodic influxes of coarser clastic material reworked by weak bottom currents (Fig. II-11, page 61).

The Pine Ridge Sandstone is overlain by the Straight Ridge sequence (Table II-5) of interbedded shale, siltstone, and sandstone. Finely divided plant debris (Calamites) and desiccation cracks are locally common. Laminated to massive shale and siltstone with very thin, tabular beds and lenses of fine-grained sandstone comprise approximately 60 percent of the sequence. The balance of the sequence consists of sandstone, which exhibits marked lateral variations over small distances. Observed variations include thick-bedded, medium-grained, well-sorted angular, light- to yellowish-gray, carbonaceous, feldspathic, locally conglomeratic cross-bedded sandstone, with scour channels; thick-bedded to massive,

fine-grained, locally silty, white sandstone; massive-grained, olive-brown carbonaceous subgraywacke; and thick-bedded, fine- to medium-grained poorly-sorted carbonaceous subgraywacke (Gilbert, 1976). Minor sandstone units are discontinuous, grading laterally into shales and siltstones. Lithologically the Straight Ridge sands exhibit characteristics of both the underlying Narrows (barrier/beach) and overlying Yellowleaf (fluvial) sands. The mud/silt subfacies exhibits evidence of variable current activity, and periodic subaerial exposure (Fig. II-11, page 61). On the basis of these criteria, the Straight Ridge is tentatively interpreted as representing deposits formed in an estuarine environment, with tidally influenced river mouths and interdistributary tidal flats.

The Yellowleaf and Wattsville sequences are similar in overall lithology both consisting primarily of siltstone, shale and clay (seat-rock) (Table II-5, page 60). These fine clastics are generally nonfossiliferous, and are not obviously bioturbated, although some massive units may be attributable to disruption of lamination by root systems.

Sandstones in both sequences are typically thin-bedded to massive, trough cross-bedded, channel-filling, fine- to very fine-grained, poorly sorted carbonaceous subfeldspathic lithic wacke. Quartz pebble and intraformational conglomerates, and sand-filled stem-molds of Calamites occur as lag deposits in channels filled with tabular and trough cross-bedded and cross-laminated sands (Appendix B). In map pattern sand units grade laterally into the shales/siltstone units.

Lithologic relationships and sedimentary structures (Table II-5, Fig. II-11) indicate that the Yellowleaf and Wattsville sequences represent

fluvial deposits formed in meandering stream channels (sand subfacies) and interchannel flood plains (silt/shale subfacies). The major sand units are of considerable lateral extent (up to 33 km along strike) suggesting that the stream complexes meandered over a broad fluvial plain.

The Yellowleaf sequence locally contains extensive irregular lenses of reddish-brown siltstone and shale "redbeds" (Appendix B), which represent early diagenetic oxidation of interchannel deposits uplifted above the water table (Gilbert, 1976). The Wattsville is distinguished from the Yellowleaf by the presence of laterally persistent coal beds indicative of vegetated flood plain, and by both a higher density and greater diversity of terrestrial plants (see references in Table II-5, page 60).

The Pottsville exhibits greater regional variation in thickness than any other stratigraphic unit in the study area, and in general thickens dramatically toward the southeast. Since the entire Pottsville was deposited in fluvial environments within a limited range of sea level, the extreme variations in thickness represent major late Paleozoic downwarping of the southeastern Valley and Ridge.

The pronounced temporal and areal facies changes in this tectosome demonstrate a geologically sudden transition from a shallow epeiric seaway to an orogenic foredeep that reached its maximum development during the Early Pennsylvanian. The transition involved development of a southeasterly clastic source in the rising Appalachians, from which westward and northwestward flowing stream systems transported sediment into the foredeep. Sediment input was such that sediment accumulation exceeded the rate of subsidence, eventually filling the foredeep, so that in the

latter stages clastics prograded westward onto the edge of the stable craton in northwest Alabama.

Strata of the previous (epeiric) tectosome were deposited in a shallow sea, bordering on a low-lying landmass to the southeast. During the Early Mississippian the eastern valley and Ridge began to subside, so that the eastern landmass was inundated. By Meramecian time, asymmetry of the depositional basin was reversed, and bathymetric differences of several hundred meters were developed between the southeastern and northwestern areas. The deep subtidal clastics of the Pride Mountain Formation were deposited in the deep southeasterly trough, while the carbonates of the Tuscumbia Limestone were deposited in shallower water on the Warrior platform. Prior to the mid-Chester, a combination of crustal subsidence, rising eustatic sea level, and increasing influx of clastics resulted in the Pride Mountain clastic sequence prograding onto the Warrior platform. During this phase a major sand facies of the Pride Mountain developed along the southwest margin of the Warrior platform (Fig. II-12). Although this sand facies was not examined in detail as part of this study, lithologies and geographic position between shallow subtidal clastics of the Pride Mountain on the Warrior platform and the deep basinal turbidites of the Ouachitas suggest that it represents shelf edge sand bodies developed as a result of greater wave action along the margin of the deeper Ouachita flysch basin. (This possibility will be discussed in greater detail with regard to the Hartselle and Bangor.)

A major drop in sea level during mid-Chester time is associated with development of a shelf edge sand body, the Hartselle Sandstone, along the southwest margin of the Warrior platform (Fig. II-13). The Hartselle

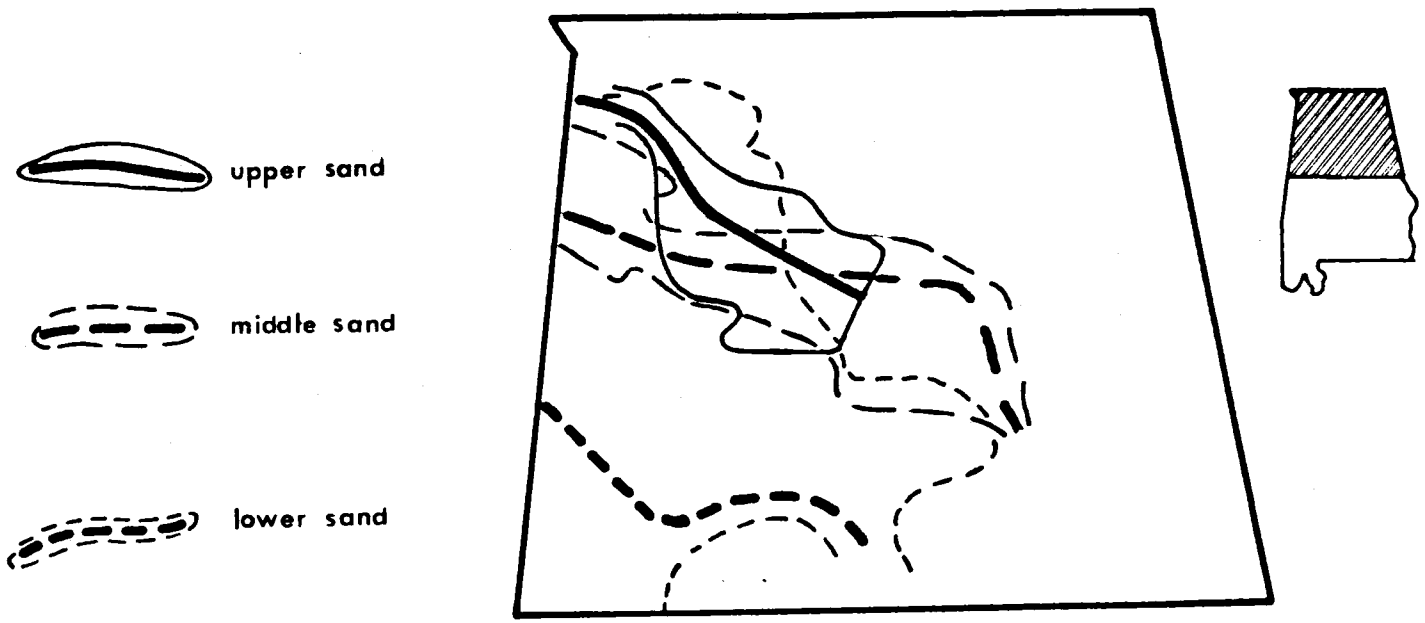

Figure II-12. Distribution of linear sand facies in the Pride Mountain Formation, north Alabama. Narrow lines denote outer margins of sand bodies, wide lines denote isopach maxima. Note parallelism of isopach maxima to edge of Warrior platform (Fig. II-17). Adjacent facies are peritidal carbonate (northeast) and deep subtidal shales (southeast, southwest). Lithostratigraphic data from Thomas (1972a).

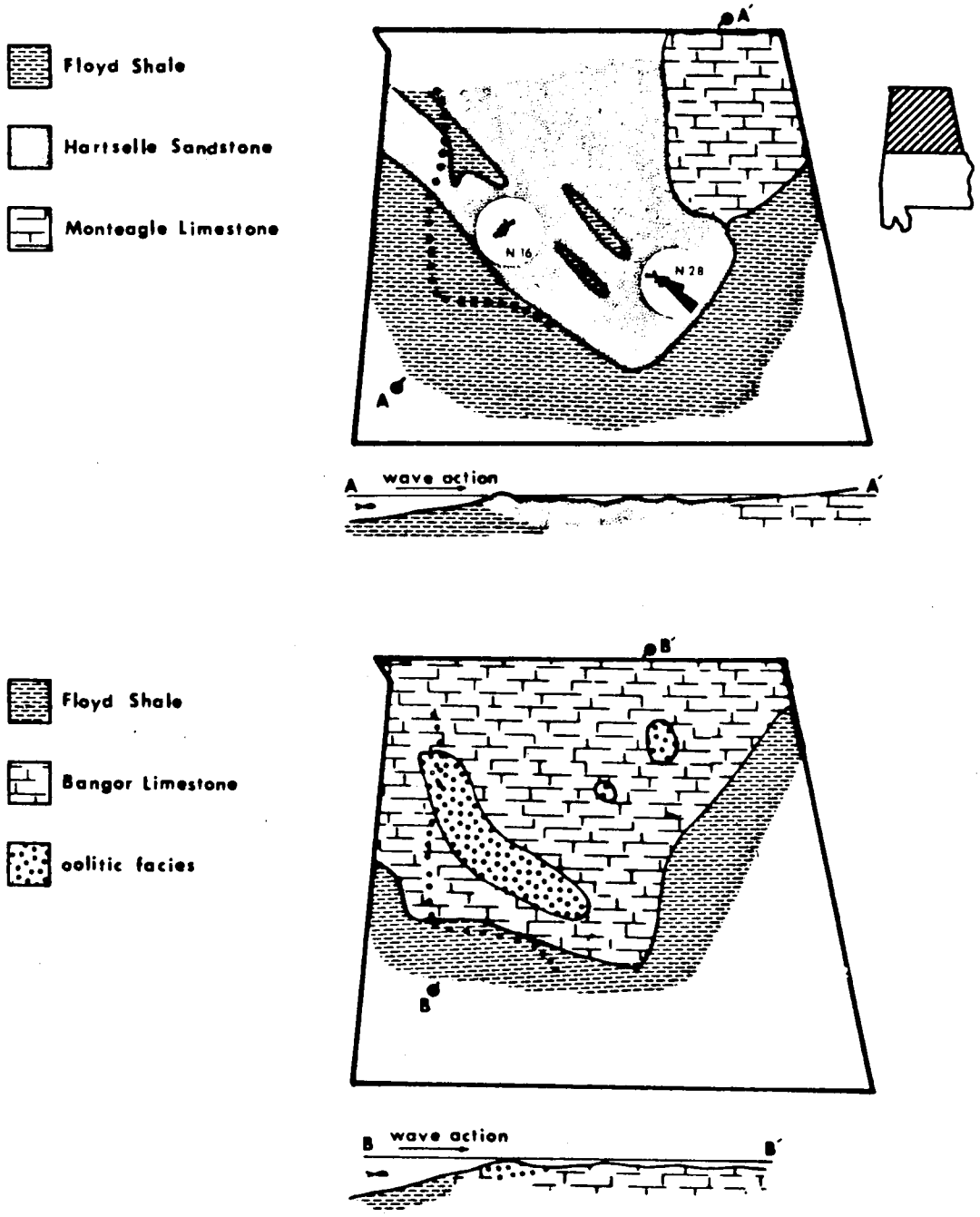

Figure II-13. Regional lithofacies during mid-Chester (upper) and late-Chester/early-Springer (?) time (lower). Note alignment of high-energy sand and ooid facies subparallel to margin of Warrior platform (dotted line), and dip of tabular cross-beds (rosettes) of barrier island facies toward margin of platform. Lithofacies patterns from Thomas (1972a) and this study; cross-bed data from this study; cross-section interpretation from this study.

was deposited in peritidal environments restricted to the Warrior platform, grading southwestward and southeastward into the deeper subtidal Pride Mountain-Floyd sequence, and northeastward into peritidal carbonates. Several previous authors, notably Thomas (1972a) and Thomas et al. (1980) have interpreted the northwesterly alignment of isopach trends, and cross-bed orientations to represent a northeast-facing barrier island complex, bounded by offshore carbonates to the northeast and lagoonal Pride Mountain-Floyd shales to the southwest. However, since the Pride Mountain-Floyd southeast of the Warrior platform represents a basinal clastic facies, it is probable that the lithologically similar shales of the Floyd southwest of the Warrior platform (Fig. II-13) are also deep subtidal marine. (The Floyd southwest of the Warrior platform occurs only in the subsurface, and well cuttings are not adequate for determination of depositional environment.) Furthermore, cross-bedding attitudes in Hartselle outcrops suggest that the Hartselle barrier islands or bars faced oceanic basins to the southeast and southwest, according to criteria defined by Klein (1967), Selley (1978), Davies et al. (1971), and summarized by Elliott (1978). The most diagnostic-facing criterion is the polarity of seaward-dipping beach face laminae; orientations of these laminae in the Hartselle are depicted in Figure II-13. Thus, both bathymetric relationships and facing of the Hartselle barrier complexes suggest that the Warrior platform during mid-Chester time was a bathymetric high, bordered on the southeast and southwest by deeper subtidal clastic basins. The preferential development of the Hartselle barrier facies along the southwestern margin of the Warrior platform may have resulted from the presence of a broad oceanic basin to

the southwest, resulting in greater wave energy concentrated against the exposed margin of the platform. Wave-sorting along the high energy margin may have resulted in concentration of coarser sediment in the barrier complex, while finer sediment was worked offshore and eventually into the contemporaneous Ouachita flysch basin to the west. It was at this time that an easterly, rather than a southerly, clastic source came to dominate flysch sedimentation in the Ouachita trough, as indicated by paleocurrent directions (Briggs, 1974; Morris, 1974). Palinspastic restoration of the Ouachita facies, using cross-sections provided by Briggs and Roeder (1975), Wickman (1977) and Viele (1979), places it west and southwest of the autochthonous Warrior platform, further supporting this hypothesis. Graham et al. (1975) previously proposed a somewhat similar model for origin of the Ouachita flysch, using the Himalayan trough-Bengal fan as a modern analog.

During the subsequent sea level rise, the subtidal Bangor Limestone prograded southwestward and southeastward over the Hartselle. Like the Hartselle, the Bangor contains a shallow-water high energy reef and ooid shoal facies (Settle, 1954; Thomas, 1972a) with isolith trends oriented parallel to the southwest margin of the Warrior platform, and interfingering to the southwest and southeast with the Floyd Shale (Fig. II-13). To the northeast, the Bangor consists of shallow subtidal biosparite and biomicrite grading northeastward into dolostones and peritidal clastics of the Pennington Formation (Thomas, 1972a).

The southeasterly Pride Mountain-Floyd basin was sufficiently deep that it was not affected by the mid-Chester sea level drop, and deposition of the basinal facies was continuous. As previously noted, lithologic

similarities suggest that this basinal facies extends around the southwest margin of the Warrior platform. Clastic sediments deposited in the deeper basins were apparently derived from the southeast or south. No transport direction indicators were observed in the Pride Mountain-Floyd, but those in the overlying Parkwood-Pottsville sequence indicate a southerly or southeasterly source. Continuity of bedding over great distances and limited cross-bedding indicate that most of the sediment was introduced by settling from suspension, with limited reworking by weak bottom currents. Absence of turbidites or other mass transport features indicates a very low (< 2°) topographic slope on the eastern margin of the basin. Limited volumes of exotic carbonate sediment were introduced into the basin by debris flows moving down the steeper (2 to 4°) western slope of the basin.

During the Late Mississippian and Early Pennsylvanian the rate of sediment accumulation exceeded that of subsidence, resulting in filling of the basin. This filling resulted in northwestward progradation of a shallow marine (Parkwood) and fluvial (Pottsville) sedimentary sequence into the subsiding basin. A schematic illustration of the various facies relationships is provided in Figure II-14.

The general fining upward sequence and lithologic association has led most previous workers to interpret the Pottsville and related sediments as a deltaic complex. However, several lines of evidence suggest that the typical delta model is not directly applicable. In both areal extent ($\sim$ 1.5 million km^2) and tectonic setting (prograding into an epicontinental foredeep) the Pottsville has no modern analog in any delta or complex of deltas. In addition, the general stratigraphic sequence

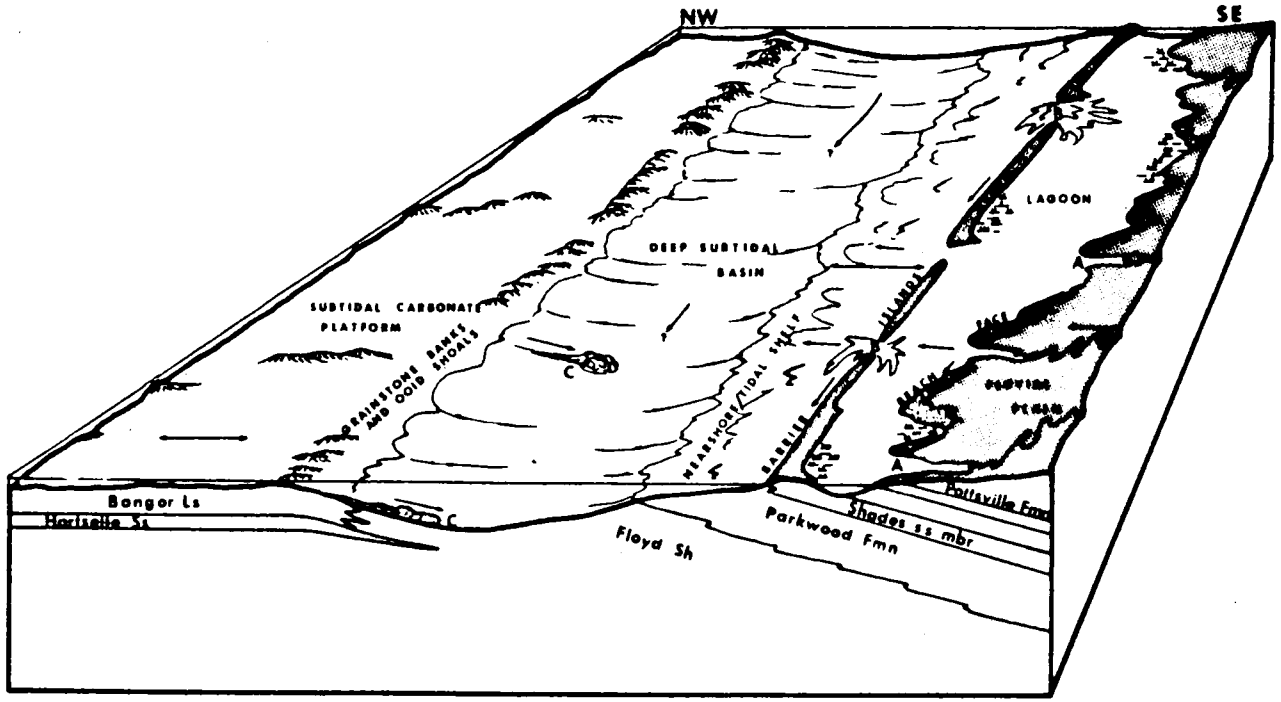

Figure II-14. Schematic illustration of Mississippian-Pennsylvanian facies relationships, northern Alabama. Arrows indicate direction of sediment transport; double-headed arrows indicate tidal sediment transport directions. Terrigenous sediment is introduced by streams flowing across the fluvial plain toward estuarine river mouths (A). Some sediment is winnowed to produce coarse-grained beach face deposits landward of the lagoon, and fine-grained lagoonal sediments. Sediment bypassed through tidal passes (B), or through channels bypassing the lagoon, is winnowed to generate coarse-grained barrier islands. Finer-grained material is progressively worked offshore, with clay and fine silt introduced into the basin floor. Shallow-water carbonate detritus is introduced into the basin by debris flows (C). Transport within the deep basin is problematical.

observed in the Pottsville of the Valley and Ridge conforms to none of the modern deltaic sequences described by Coleman (1976). Instead, the base of the Pottsville, corresponding to the front of the prograding complex, is everywhere marked by a complex of barrier island or beach sands more typical of linear wave-dominated shoreline. Further, the fluvial sands of the Pottsville do not consist of linear bar finger sands, but of areally extensive channel sand complexes deposited by streams which meandered over broad areas.

The preferred interpretation of the Pottsville depositional environment is a broad fluvial plain dominated by meandering streams, and bounded on the northwest by a wave-dominated shoreline. Sediment sorting along this high-energy coast line resulted in development of several distinct facies zones, including the fluvial plain (Pottsville), wave-dominated linear coast line (basal Pottsville), shallow subtidal tidally influenced offshore (Parkwood), and a deeper subtidal basin (Pride Mountain-Floyd) into which fine clastics were introduced from suspension. These zones and their relationships are depicted schematically in Figure II-14.

Deposition in the fluvial plain was maintained by the balance between sediment input and subsidence. The excess of sediment input during the Late Mississippian and Early Pennsylvanian resulted in northwestward progradation of the clastic shoreline, and infilling of the basin (Fig. II-15).

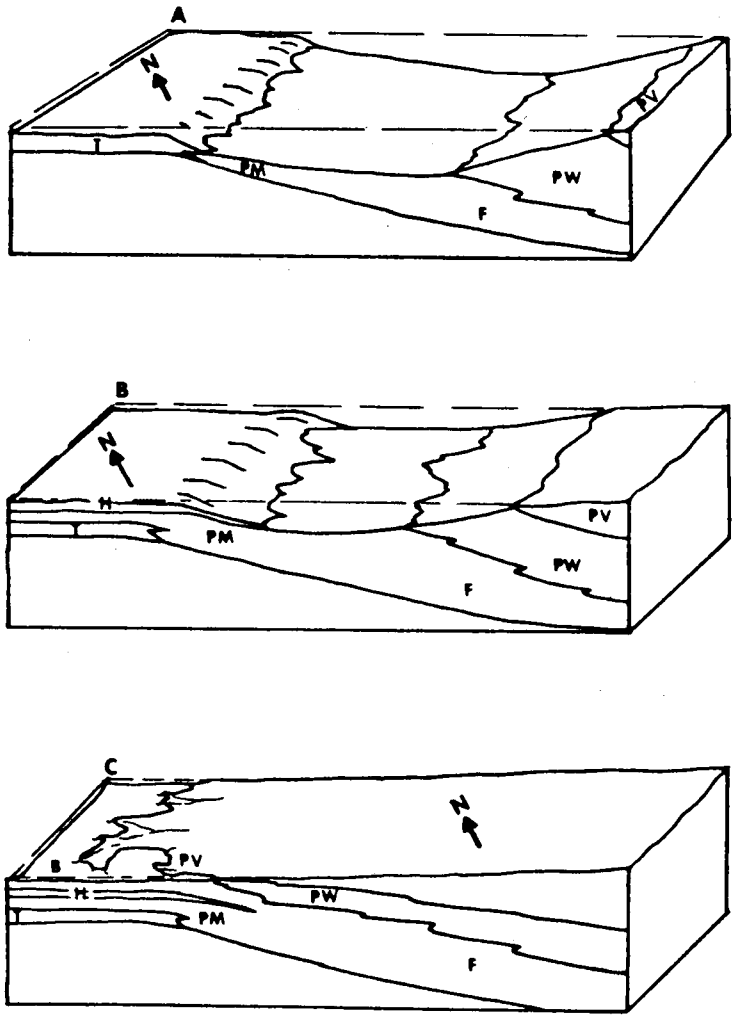

Figure II-15. Progressive filling of late Paleozoic foredeep. In stage A (Early Mississippian) subsidence exceeds sediment input, creating a deep shale basin (PM-Pride Mountain, F-Floyd), bounded by stable carbonate platform (T-Tuscumbia) and nearshore and fluvial deposits (PW-Parkwood, PV-Pottsville) derived from erosion of tectonic highlands. By stage B (Late Mississippian) the advancing deltas have partially filled the basin; platform covered by sand unit (H-Hartselle). During stage C (Early Pennsylvanian), sediment influx exceeds subsidence, the foredeep is filled, and fluvial sediments spill over the carbonate platform (B-Bangor). North arrow indicates present-day north.

CHAPTER III

PALEOZOIC CRUSTAL SUBSIDENCE IN THE SOUTHERN APPALACHIAN VALLEY AND RIDGE OF ALABAMA

Rates of sedimentation, sediment type, and basin and sediment body geometries represent clues to the tectonic setting and history of a sedimentary basin. James Hall, in unpublished lectures, discussed the significance of sediment type and sediment body geometry as an essential element of what eventually became the geosynclinal theory (Dana, 1866), and with the advent of plate tectonics theory, certain rock assemblages and sediment body geometries came to be recognized as indicators of specific sedimentary and tectonic environments.

In contrast, quantitative studies of crustal subsidence have been rare. In 1911, Lemoine summarized the Mesozoic-Cenozoic stratigraphy of the Paris basin, with crustal subsidence described as changes in elevation of the basement through time (van Hinte, 1978). Barrell (1917), Bailey (1936), and Lee (1954) discussed the relationship between tectonism and accumulation of sedimentary sequences, both in theory and application. Kay (1955) summarized sedimentation rates and implied subsidence rates for 85 sedimentary basins, and related these rates to geosynclinal setting. Later studies demonstrated that rates and geometric relationships of crustal subsidence are criteria for recognition of tectonic events in and contiguous to the basin (Briggs and Roeder, 1975; Sleep, 1976; Shanmugam and Walker, 1978; van Hinte, 1978).

One of the goals of this study was to determine rates and regional patterns of crustal subsidence in the southernmost Appalachian foreland, and from them to determine the preorogenic tectonic history of the foreland. In addition, the subsidence history of the foreland is useful in determining the history of the entire orogen by relating timing of tectonic events in the foreland to causative events in the orogenic core.

I. DATA SOURCES AND METHODS OF STUDY

Central Alabama was selected as a study area because a more complete easterly (interior) Paleozoic sequence is represented here than in any other part of the southern Appalachian foreland. Published stratigraphic sections and sections measured during this study were used to compile composite sections for the undeformed plateau and each exposed thrust sheet (Fig. II-2, page 19). The strata in each belt were examined, both in the field and by laboratory techniques, to determine paleobathymetry, depositional environment, and relationship to the regional stratigraphic framework. The results were used to construct a corrected subsidence curve, or "geohistory diagram," for each outcrop belt, using an absolute time versus elevation of basement system described by Sweeney (1976) and van Hinte (1978). In this system, changes in elevation of the basement through time are plotted as a curve on a scale of time (abscissa) and elevation relative to a datum (ordinate).

A balanced cross-section (Chapter V) was used to restore stratigraphic sections measured in the Valley and Ridge thrust belt to their preorogenic positions (Plate I). Restored to their relative positions, the configuration of the Precambrian basement top, surface of sedimentation,

and sediment body were determined for various times during the Paleozoic history of the basin.

II. CORRECTION FACTORS IN DETERMINATION OF CRUSTAL SUBSIDENCE

Kay (1955) first summarized the difficulties involved in determination of crustal subsidence. These included: (1) determination of stratigraphic thickness; (2) paleobathymetry; (3) effects of eustatic changes; (4) accurate determination of sediment body geometry; (5) relationship of geologic time to absolute time; (6) recognition of lacunae; and (7) correlation of local stratigraphy to standard sections.

Because adequate data are typically not available, Kay and subsequent workers (for example, Keen and Keen, 1973; Sweeney, 1976, 1977) attempted to eliminate or minimize the significance of one or more factors. Sweeney's (1976, 1977) studies of the subsidence history of the Sverdrup Basin indicate the number of simplifying assumptions which are frequently invoked. Sweeney's assumptions included: (1) no subsidence as a result of sediment compaction; (2) relief on the depositional surface approached zero, with no significant geographic bathymetric variation; (3) sedimentation rate was equal to subsidence rate; (4) no eustatic variations; (5) continuous sediment accumulation; and (6) subsidence rates were constant over intervals longer than 50 my. While certain of these assumptions were necessitated by a limited data base, they represented significant sources of error in calculation of the subsidence history.

van Hinte (1978) described a method of "geohistory analysis" in which the effects of paleobathymetry and sediment compaction can be

accounted for, and biostratigraphic zones accurately related to an absolute time scale. The method described by van Hinte is based on the use of Foraminifera as paleobathymetric indicators and for correlating biostratigraphic zones to an absolute time scale, and is applicable only to the post-Triassic geologic record.

Quantitative studies of Paleozoic crustal subsidence are also hampered by factors not recognized by Kay (1955), including determination of sediment compaction, correlation across facies boundaries, and discrimination between subsidence resulting from sediment loading as opposed to tectonic subsidence. Although it is not possible to eliminate these problems, their effects can be minimized or estimated as potential sources of error.

Paleobathymetry

The simplest method of estimating subsidence is to assume that all sediment accumulated at or near sea level (for example, Briggs and Roeder, 1975; Sweeney, 1976, 1977) and use net stratigraphic thickness as an estimate of subsidence. However, studies based only on stratigraphic thickness fail to detect short-term changes in subsidence rate, since deposition does not necessarily keep pace with subsidence (Kay, 1955; Benedict and Walker, 1978). Alternatively, under conditions of high sediment input and nonmarine sedimentation, sediment thickness may exceed subsidence.

A more precise method involves the determination of paleobathymetry, so that variations in water depth can be used to indicate accumulation. Benedict and Walker (1978) and Shanmugam and Walker (1980) described a

method of paleobathymetric analysis for pre-Mesozoic sequences utilizing depth-restricted faunal elements, physical sediment structures, and chemical parameters considered within an ecostratigraphic and regional stratigraphic framework. This technique, in modified form, was used in this study. The basic data for paleobathymetric analysis were derived from several sources, primarily direct observations made during the course of this study. Other sources included published faunal lists and published interpretations of depositional environment (see Chapter II).

In each outcrop belt of the study area, formations were subdivided into units, each unit representing one or more beds with similar characteristics which distinguish them from beds above and below. Unit characteristics, including bed thickness and form, mesoscopic sedimentary and biogenic structures, fossils, color, and lithology were recorded in the field. Individual units were sampled, and multiple samples taken where vertical or lateral gradations were observed; in thick units with no discernible gradation, one or more samples were taken at random. Oriented samples were used to prepare thin sections (264), polished slabs (35), and acetate peels (8), which were examined for physical and biogenic bathymetric indicators. During examination of prepared samples, the carbonate samples were classified by rock type, types and relative abundance of faunal elements described, and the presence of bathymetric indicators noted. Thin sections were less extensively utilized in the study of the terrigenous clastic sediments, paleobathymetric determinations instead being based on sedimentological structures observed in the field.

Paleozoic water depths were approximated by comparison of bathymetric indicators observed in outcrop and in laboratory examination with the probable ranges of these indicators (Table III-1). Benedict and Walker (1978) and Shanmugam and Walker (1978) provided discussions of the application of the bathymetric indicators, as well as potential sources of error in their use.

In application, Table III-1 provides only a probable range of ancient water depths. Determination of this range is made by comparison of observed physical and biological indicators with their probable ranges; if several indicators are present the probable depth range can be further restricted to the zone of range overlap. In actuality, it is difficult to determine paleobathymetric values because of the broad overlap of some indicators, the possibility that some indicators may have been transported out of their original environment, and the variable reliability of some indicators. In some units indicators are lacking and the probable bathymetric range is assumed to lie within the range defined by overlying and underlying units. Paleobathymetric estimates developed from the criteria in Table III-1 are most precise in the peritidal zone (within ± 10 m of mean low water), with precision decreasing rapidly into deeper bathymetric zones. Paleobathymetric estimates were refined by consideration of the location of the unit within the regional stratigraphic framework. This method is described by Shanmugam and Walker (1980), and applications in this study are described in Chapter II.

TABLE III-1

RANGES OF PALEOBATHYMETRIC INDICATORS IN PALEOZOIC SEQUENCES *

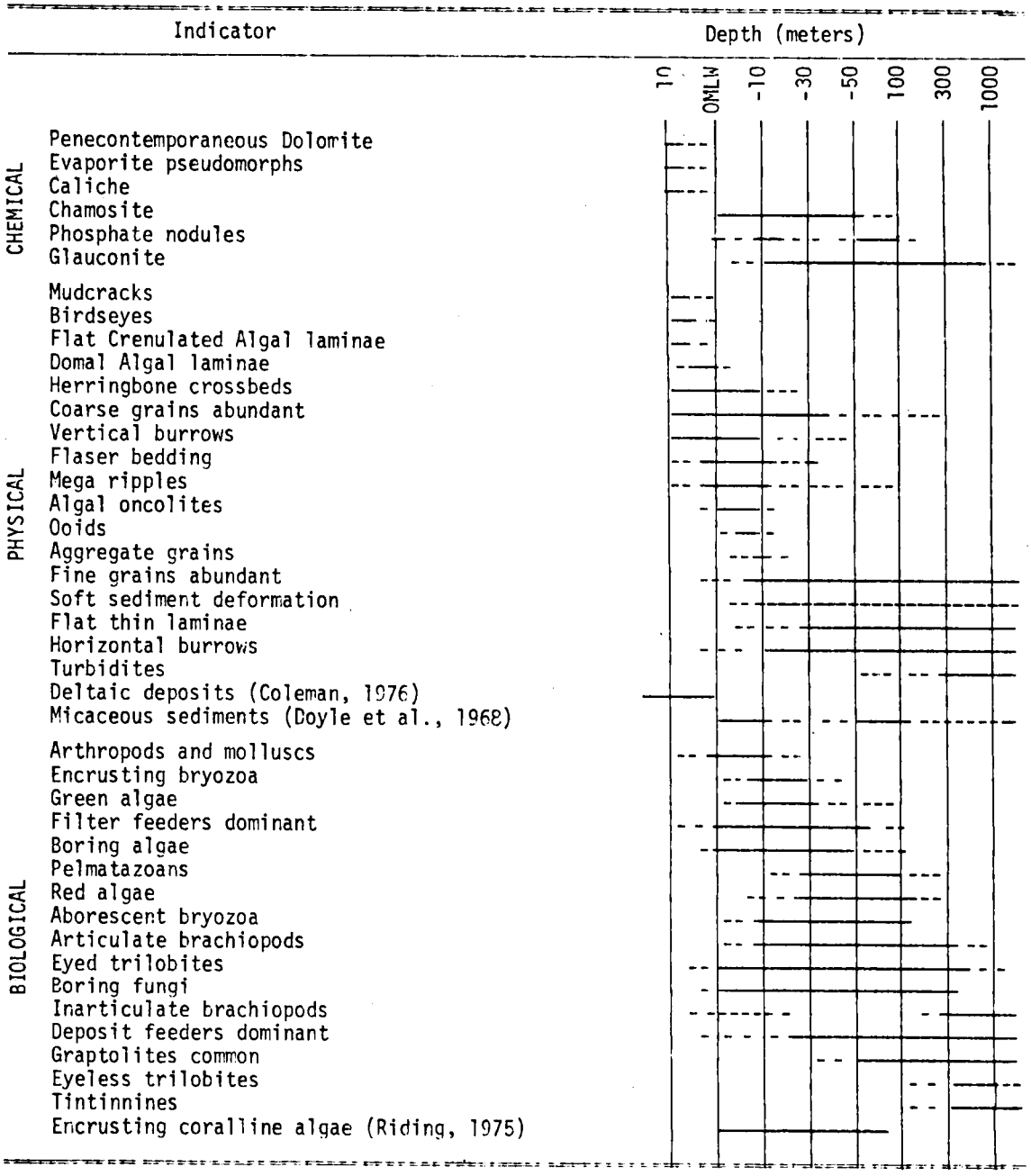

*Modified after Benedict and Walker (1978) by deletion of some indicators not used in this study. Solid bar indicates most common range; dashed bar less common range. References for indicators are given in Benedict and Walker (1978); indicators with references are those not listed by Benedict and Walker.

Eustatic Changes

Despite Kay's (1955) early recognition of their significance, most studies (for example, Sweeney, 1976; Benedict and Walker, 1978) have not accounted for eustatic changes. The potential margin of error which can be introduced by failure to account for eustatic changes is discussed by Vail et al. (1977). They noted net fluctuations of up to 550 m over a period of 40 my (Cretaceous to Miocene), with short-term (less than 5 my) changes of up to 400 m.

Vail et al. (1977) described relative changes of Paleozoic sea level in arbitrary onlap-offlap units, based on seismic-stratigraphic studies of selected areas. They described a large-scale (first order) cycle of sea level change of approximately 350 million years duration, with a relative highstand near the Cambrian-Ordovician boundary (500 mybp), and lowstands during the Precambrian and Triassic. Superimposed on this curve were shorter (second order) cycles of 10 to 80 my duration. The first and second order cycles described by Vail et al. (1977) are in general agreement with changes in Paleozoic sea level described by Schuchert (1955), Hallam (1977), and Dennison (personal communication, 1980).

In an attempt to partially account for the effects of eustatic changes, I have utilized data presented by Vail et al. (1977) in modified form. The chart of "relative sea level" presented by Vail et al. (1977) is actually a chart of relative coastal onlap. This type of chart depicts only the relative geographic onlap of sedimentary sequences (Fig. III-1), which results from interaction of eustatic change and crustal subsidence. Quantitative estimates of actual eustatic change are made using short-term

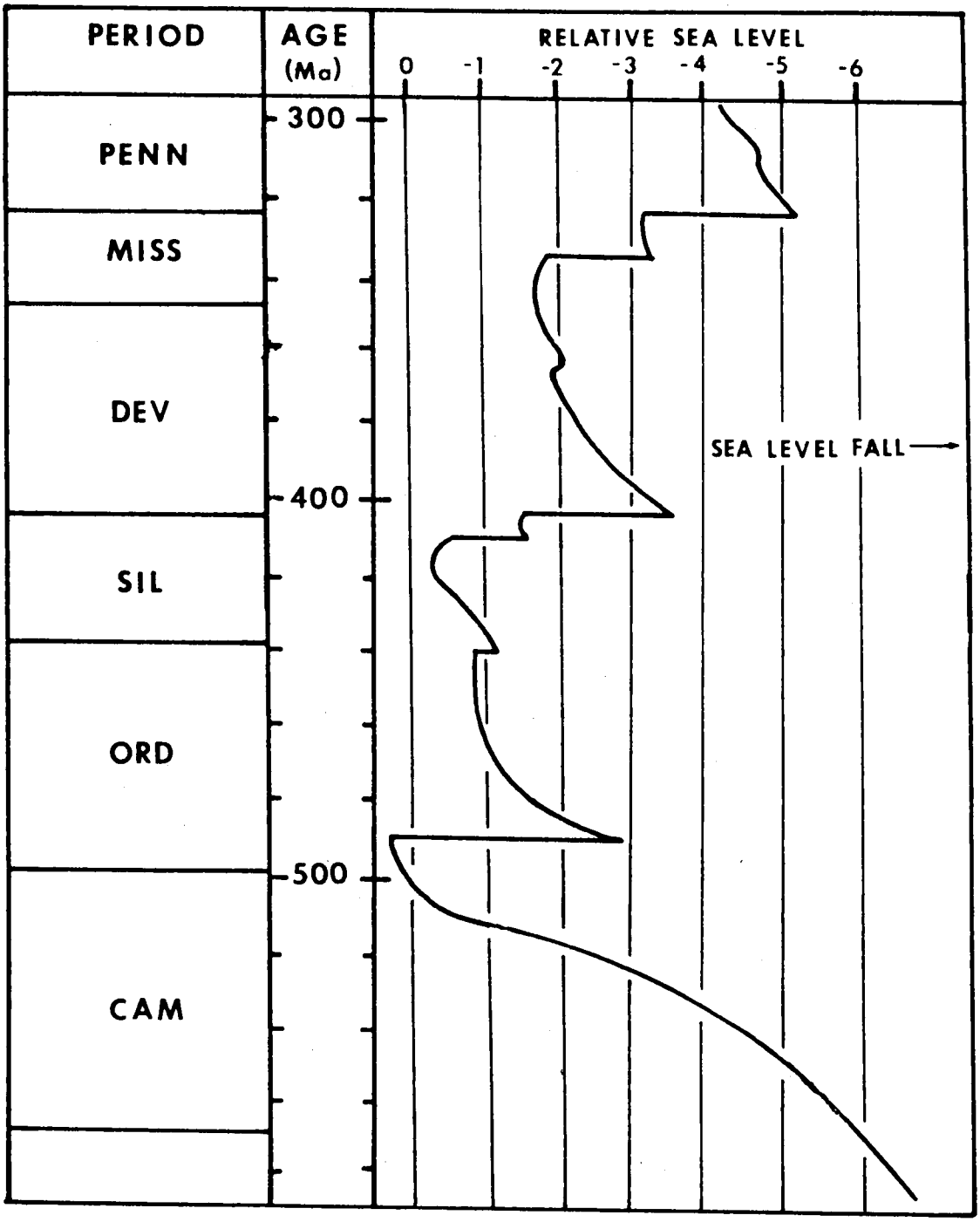

Figure III-1. Relative Paleozoic coastal onlap, assuming sea level at the Cambrian-Ordovician boundary as zero. Modified from Vail et al. (1977)

trends and relative rates of eustatic change determined from facies patterns and unconformity types, and long-term eustatic changes determined from long-term subsidence behavior (Vail and Todd, in press).

Unconformity characteristics and facies relationships used to determine rates and nature of short-term eustatic changes are illustrated in Figure III-2. Long-term eustatic changes can be determined only on quiescent margins characterized by low rates of subsidence. Paleobathymetry and sediment thickness data for a number of points of established age are plotted on an assumed lithogenetic subsidence curve which has been corrected for sediment loading (Fig. III-3). Elevation changes of the water column top relative to the basement top are assumed to represent long-term fluctuations of sea level (Fig. III-3); these are the "first order cycles" of Vail et al. (1977). Similar elevation changes occurring simultaneously in geologically separate areas are assumed to represent worldwide eustatic cycles; all other, nonsimultaneous, changes are assumed to be the result of perturbations in local subsidence behavior. Use of curves derived from separate areas is necessary, since subsidence seldom approximates the ideal behavior shown in Figure III-3. In the final step the coastal onlap curve and unconformity types are justified to the long-term eustatic curve, producing the eustatic curve (Fig. III-4). At present the data base is inadequate to construct eustatic curves for the Paleozoic, and estimates used in this study were based on relative onlap charts.

If regional onlap or offlap occurs on a shelf with low slope and little relief relative to the width of the shelf, magnitude of onlap or offlap is approximately proportional to the magnitude of the causal

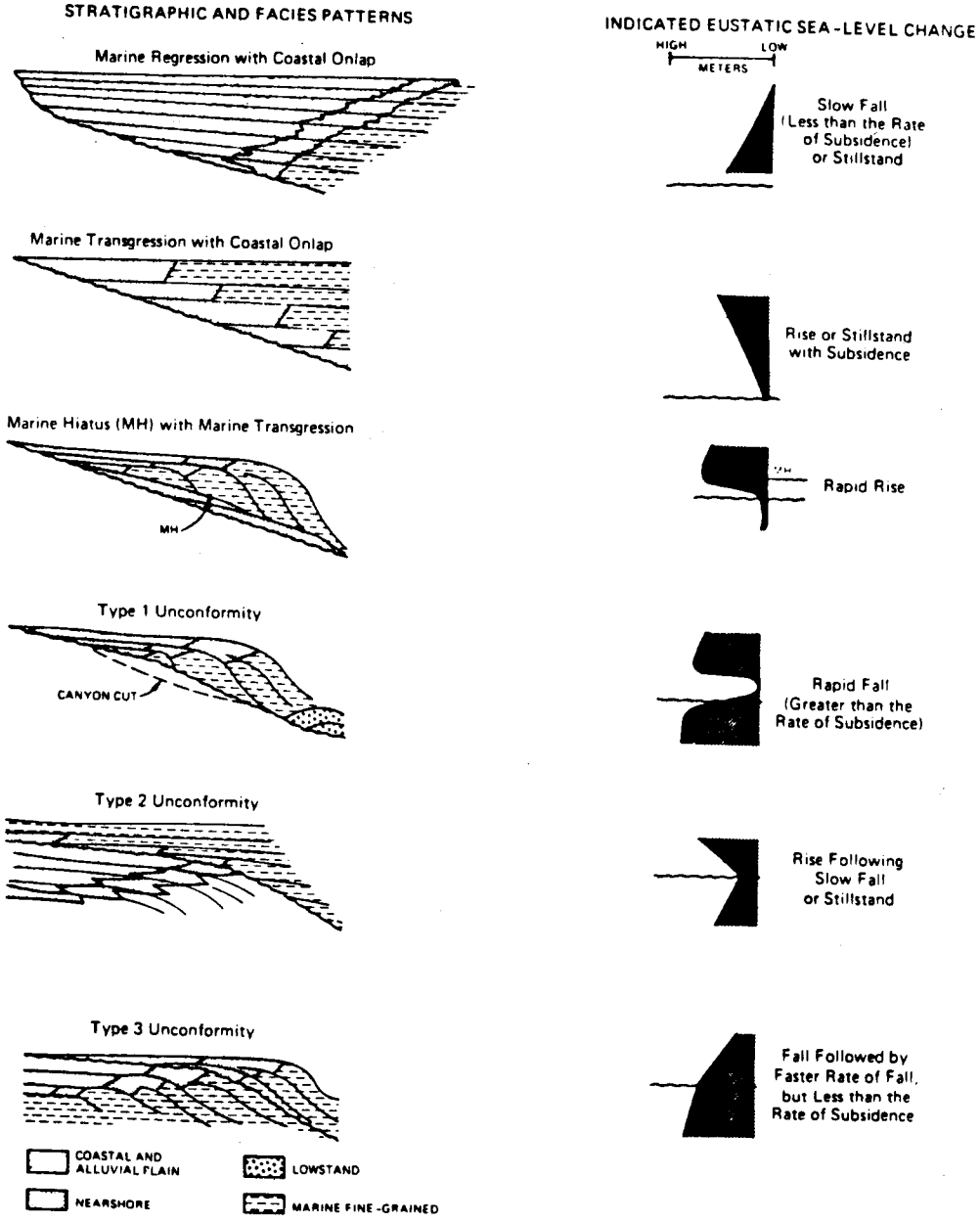

Figure III-2. Diagrammatic representation of unconformity types, stratal patterns and facies relationships used by Vail and Todd (in press) to infer relative rates of sea level change. Absence of alluvial deposits suggests that most of the recognized unconformities in the Paleozoic foreland are Type 1. Juxtaposition of fine-grained (deep water) marine and nearshore (shallow water) deposits in Rapid Rise case is similar to relationships observed in the Columbiana Formation and Chattanooga Shale (Chapter II). Figure from Vail and Todd (in press).

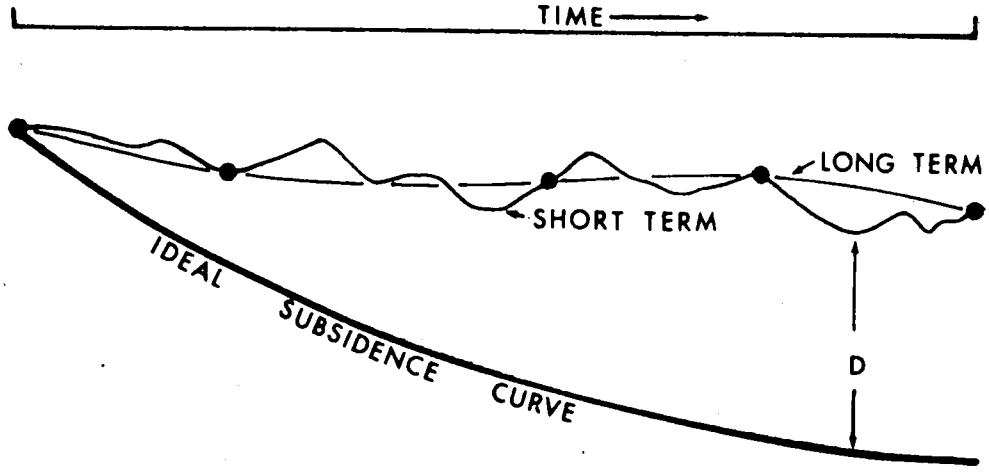

Figure III-3. Determination of long-term eustatic change. Ideal subsidence curve is assumed exponentially decreasing subsidence rate of passive margin (Sleep and Snell, 1976; Jarvis and McKenzie, 1980). D is basement to sea level interval, corrected for crustal loading, paleobathymetry, and sediment compaction. Black discs are control points of precisely known age. Long-term eustatic change is assumed to be the best fit curve to control points. Short-term eustatic changes are imprecisely dated perturbations from the long-term curve. In actual application, long-term curves for several distinct basins should be averaged, as crustal subsidence seldom follows an "ideal" curve.

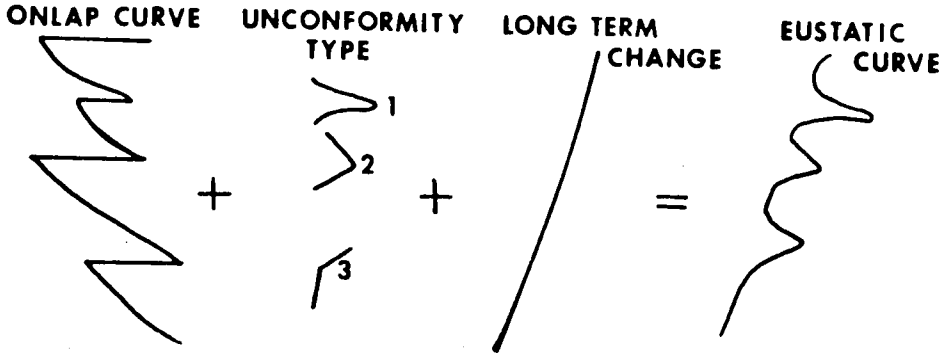

Figure III-4. Diagrammatic illustration of inference of eustatic curve from onlap, unconformity type, and long-term eustatic change. Process is applicable only to interpretation of one area; construction of global eustatic curves is iterative, requiring interpretation of more than one data set.

eustatic change. Comparison of relative onlap and eustatic curves for a specific stratigraphic interval should therefore exhibit similar trends and magnitude, for both short- and long-term eustatic changes (Fig. III-5).

In this study, relative rates of short-term eustatic changes have been inferred from the nature of unconformities and internal stratigraphy of sequences using the characteristics described by Vail and Todd (in press). Magnitude of changes are inferred from the relative onlap chart by assuming that (1) the magnitudes of Paleozoic eustatic variations were similar to those of the Mesozoic and Cenozoic, and (2) relative onlap/offlap and magnitude of eustatic rise/fall are proportional. Comparison of coastal onlap and eustatic sea level charts for the Jurassic of the North Sea (Vail and Todd, in press) suggests that the latter assumption is valid, except that major sea level declines produce disproportionately great offlap.

The approximate eustatic sea level chart thus constructed is shown in Figure III-6. The probable margin of error is ± 60 m. This margin of error is based on the assumption that short-term sea-level changes were neither detected nor accounted for in this study, and that the presumed eustatic values involve probable errors as great as the mean of the short-term (< 5 my) eustatic changes which occurred during the Jurassic (Vail and Todd, in press). Because modern sea level cannot be directly related to Paleozoic sequences (Vail et al., 1977), relative sea level at the Cambrian-Ordovician boundary has been assumed as a standard Paleozoic sea level.

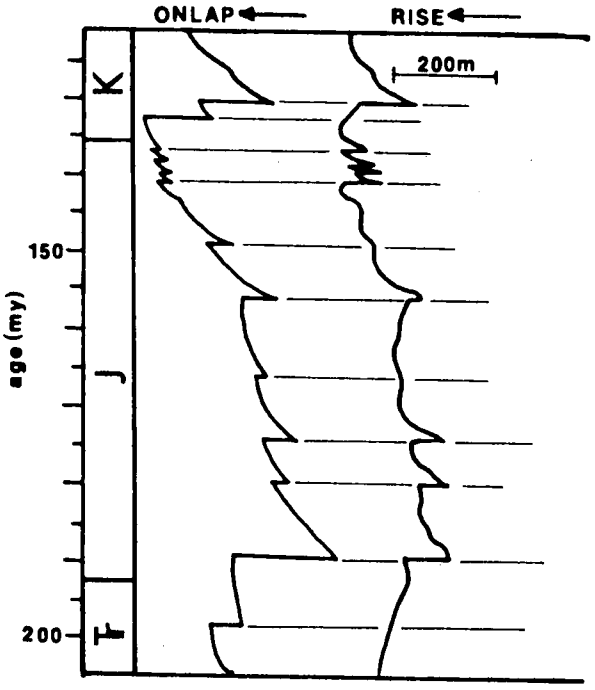

Figure III-5. Comparison of coastal onlap and inferred eustatic sea level curves for the Upper Triassic to Lower Cretaceous, North Sea. Data from Vail and Todd (in press). Note disproportionately great offlap produced by rapid fall (133 my and 189 my).

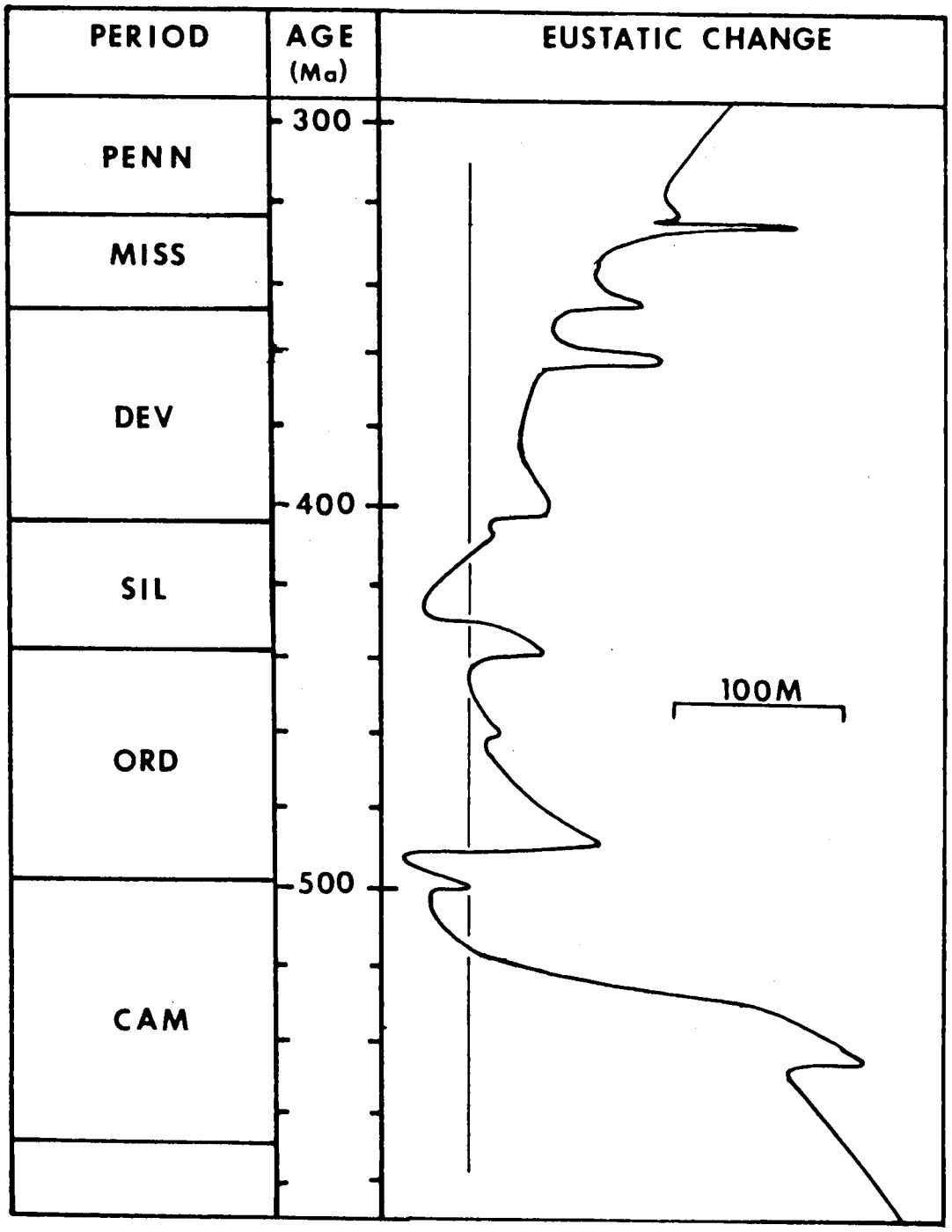

Figure III-6. Inferred Paleozoic eustatic changes. Constructed from worldwide long-term change (enveloping curve for onlap chart, Vail et al., 1977), probable magnitude of individual changes (Vail and Todd, in press; paleobathymetric data from this study), and unconformity types and facies relationships (this study). Arbitrary zone datum (vertical line) is probable sea level at Cambrian-Ordovician boundary.

Sediment Compaction

Of the factors involved in subsidence, the contribution of compaction is the least understood. While it is generally accepted that clays and shales undergo considerable reductions in volume, results of studies of sandstone and carbonate compaction have been equivocal and frequently contradictory.

Hedberg (1936) discussed the general theories of clay and shale compaction, and more recent authors, particularly Burst (1976), discussed mechanisms of clay compaction in detail. The most useful method for estimating shale compaction is the nomograph developed by Perrier and Quiblier (1974) to estimate original thickness as a function of observed thickness and depth of burial. Estimates of initial thickness made by alternative methods (for example, Gretener and Labute, 1969) may differ by as much as 20 percent, suggesting that accuracy of any available method is severely limited (van Hinte, 1978).

van Hinte (1978) suggested that, when possible, empirical data, such as estimation of compaction from deflection of bedding surfaces around presumably incompressible objects, should be used for refinement of estimates. Since suitable objects for measurement are rare, and frequently not amenable to unequivocal interpretation, this method was rarely used in this study.

Most recent studies of sandstone compaction (Perrier and Quiblier, 1974; Allen and Chilingarian, 1976; Wolf and Chilingarian, 1976) have concluded that sandstones are compressible to varying degrees, and that sorting, grain packing configuration, and vibration are important factors. Allen and Chilingarian (1976) also considered a number of other factors,

including composition, particle shape, and early cementation, but concluded that available data were insufficient to evaluate their influence. Based on observations by previous workers, Perrier and Quiblier (1974) concluded that sandstones do not compact significantly at burial depths less than 500 m, but undergo significant compaction at burial depths of 500 to 7000 m. Many of the sandstones examined petrographically during this study exhibited evidence of compaction, primarily indented grain boundaries and fractured grains. Because it is difficult to estimate compaction from such observations, the nomograph of decompaction number as a function of bed thickness and depth of burial (Perrier and Quiblier, 1974) was used to estimate sand compaction from present thickness.

The most controversial topic in the study of sediment compaction is that of carbonate compaction by nonstylolitic processes. Estimation of compaction is a particularly difficult problem in the case of mud-supported carbonates, where compaction would be effected through dewatering of the mud matrix, with relatively few grain interactions to reveal compaction. The controlling factor in compaction of carbonates is the stage of diagenesis at which cementation occurs (Bathurst, 1976; Meyers, 1980). It is not possible to determine absolute timing of cementation in Paleozoic carbonates, and even where features indicative of compaction are observed (Bathurst, 1966; Gocht, 1973; Coogan and Manus, 1975; Shinn et al., 1977), the observed features provide no means of making a quantitative estimate.

Coogan and Manus (1975) described compaction in terms of the Compaction Index, or percentage loss of original intergranular porosity in

grainstones. However, this method is difficult to apply in that it assumes certain ideal original porosities based on modern analogs. Meyers (1980) described the mechanism and timing of compaction in skeletal limestones, and concluded that most nonstylolitic compaction occurs at shallow depths (less than 200 m), and is complete under less than 1980 m of overburden.

During the course of this study, no evidence of nonstylolitic compaction was observed in mud-supported carbonates, and no compaction was assumed. Nonstylolitic compaction was only rarely observed in grain-supported carbonates. In grain-supported carbonates, compaction was estimated from truncation or interpenetration of grains (Fig. III-7), and assumed to have been essentially complete under overburden thicknesses of approximately 200 m. Considering the relatively small proportion of grain-supported carbonates in the regional stratigraphy, the shallow burial depths at which compaction is accomplished, and the poorly-known regional chronostratigraphy, the effects of nonstylolitic carbonate compaction are insignificant factors in the regional subsidence history.

A mechanism which results in significant volume loss in carbonate sequences is the development of throughgoing stylolites (Bathurst, 1976). Previous workers have either disregarded possible effects of stylolitization (Sweeney, 1977), or concluded that it contributed little to differential regional subsidence (Benedict and Walker, 1978). However, Dunnington (1967) demonstrated unit thickness variations of up to 16 percent resulting from stylolite development.

In general, stylolites are postcementation features (Bathurst, 1976), but the range of overburden pressures required to produce stylolites is

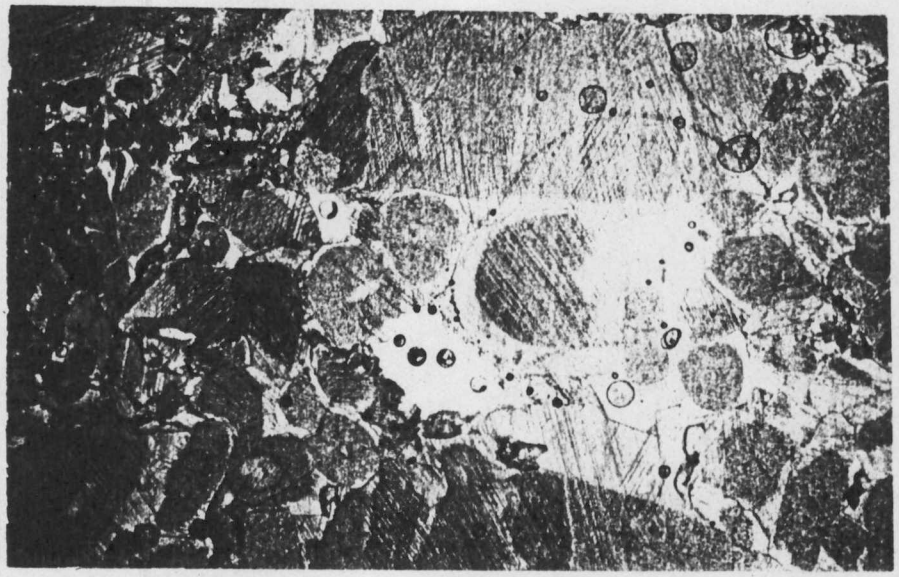

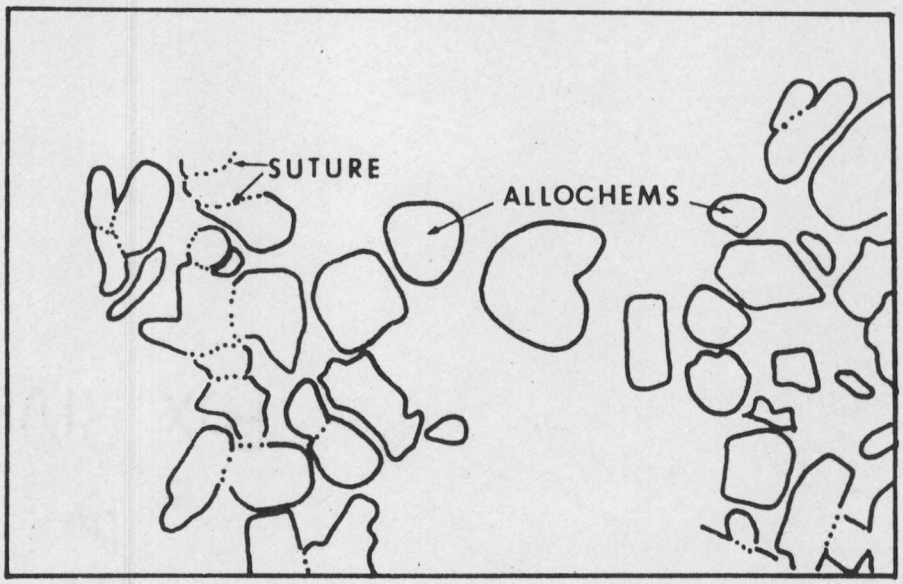

Figure III-7. Carbonate compaction by solution of grains. Some grain suturing predates cementation. Suturing at upper left postdates cementation, and represents development of stylolites. Tuscumbia Limestone, Trussville, Jefferson County. 16 X, unpolarized light.

problematical; minimum required burial depths of 600 m (Dunnington, 1967) to 1980 m (Meyers, 1980) have been proposed, but Schlanger (1964) reported micro-stylolites in limestones buried to depths of 90 m or less. Establishment of the "upper limit" of stylolite development is even more difficult. In the absence of any strictly applicable research, I have assumed that stylolites develop over geologically short time periods, and development is essentially completed at burial depths of less than 1100 m, the upper limit of the range proposed by Dunnington (1967).

Thickness reduction from stylolite development was estimated from interpenetration lengths of columnar and peaked stylolites (Bathurst, 1976). Volume loss per stylolite and density of stylolites were used to calculate thickness reduction for exposed parts of carbonate sections, and reduction for concealed parts of sections extrapolated from the result.

A greater problem is presented by lithologic units characterized by extensive stylolitization. The Middle Cambrian Conasauga Group and the Middle Ordovician Little Oak Limestone are characterized by stylobedded, stylomottled, and stylonodular structure (Fig. III-8), indicating considerable volume loss. In these units, volume loss by pressure solution cannot be accounted for, and represents a source of error in the subsidence history.

Sediment Loading

One of the major components of subsidence is the result of loading of the crust by sediment (Gunn, 1943; Walcott, 1972; Watts and Ryan, 1976; Sweeney, 1976, 1977), and this problem has been considered in many

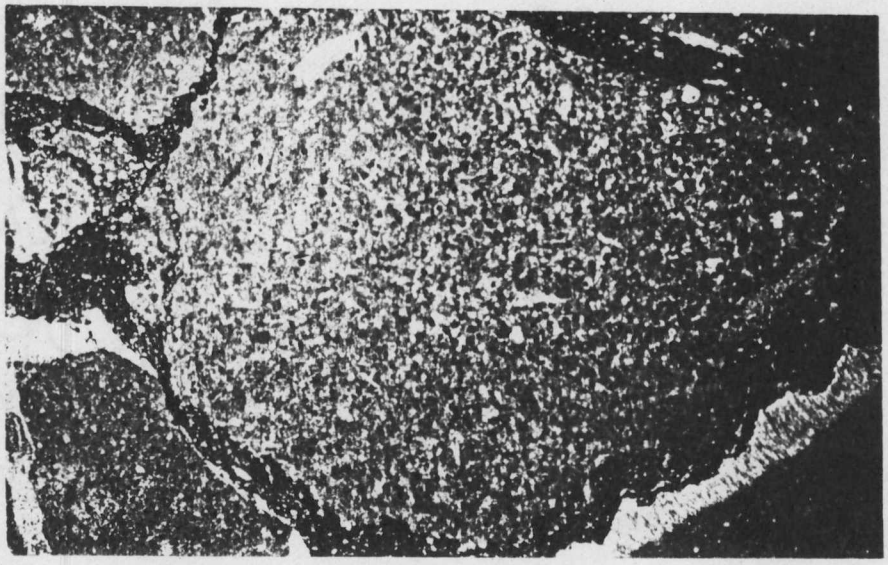

Figure III-8. Carbonate compaction by development of stylonodular structure. Little Oak Limestone, Pelham, Shelby County. 16 X, unpolarized light.

previous studies. Most studies of crustal behavior have been based on two end-member models of crustal behavior, the Airy isostasy model and the elastic beam model. In the Airy model, the crust is assumed to behave as a series of discrete vertical prisms which respond to surface loading by displacing a denser substrate. This model assumes that each prism responds individually, with no lateral transmission of bending stress, and is an approximation of a viscous crust. In this model, the depression of the crust caused by sediment loading at an individual prism can be represented mathematically as:

$$y = h \frac{\rho_m - \rho_s}{\rho_m - \rho_w}$$

where y = vertical deflection

h = thickness of sediment column

ρ_s = density of the sediment = 2.4 g/cm^3

ρ_w = density of seawater = 1.03 g/cm^3

ρ_m = density of the mantle = 3.4 g/cm^3

The other end-member is a two-dimensional elastic beam model (Hetenyi, 1946) based on the resistance to bending of a linearly elastic beam by a load applied at the extremity (Fig. III-9), while retaining the isostatic effects resulting from displacement of a plastic medium below the beam. This physical model is represented by:

$$y = h \frac{\rho_m - \rho_s}{\rho_m - \rho_w} (1 - \exp[\lambda a]\cos\lambda a)$$

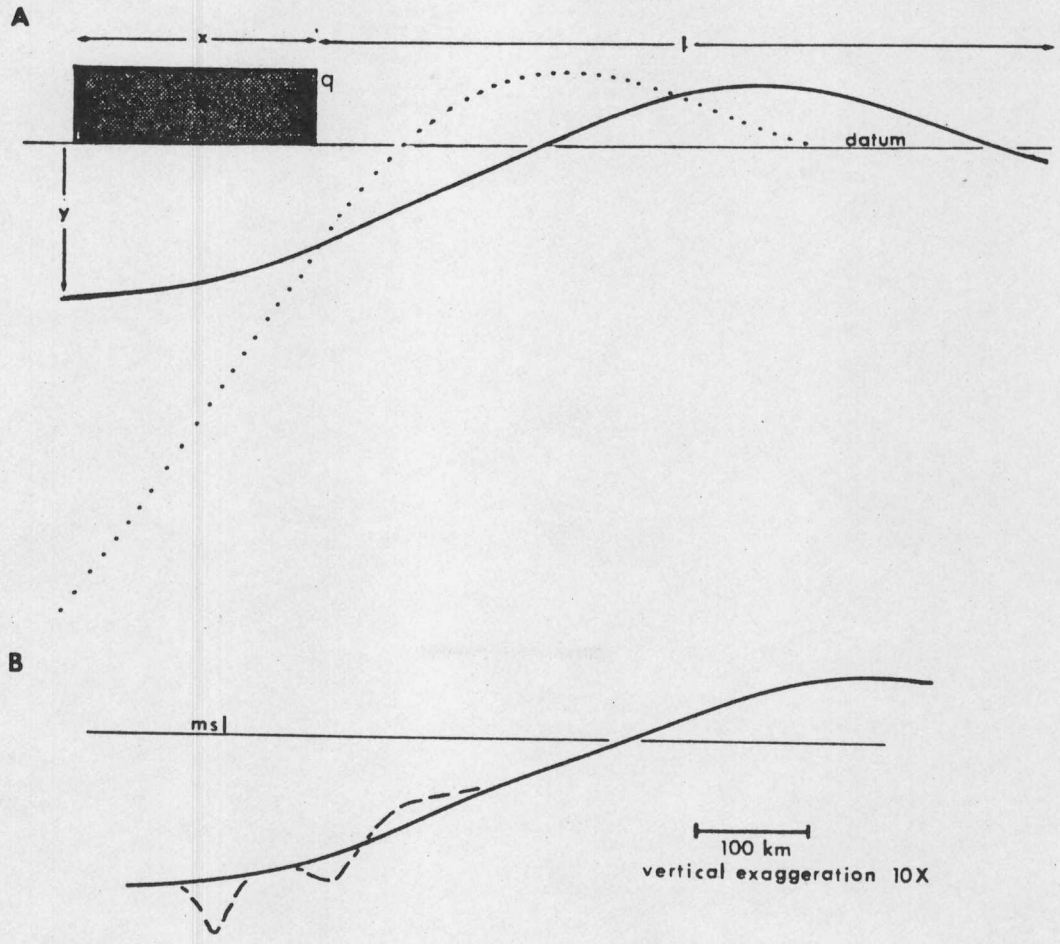

Figure III-9. Vertical deflection of the lithosphere under distributed loading. A. Vertical deflection (y) of a semi-infinite beam (solid line) under conditions of distributed loading, after Hetenyi (1946). q is the magnitude of the load, x the distance over which load is applied, ℓ the free surface of the beam over the distance (ℓ = wavelength - x). Comparison of theoretical deflection caused by distributed load model (solid line) and actual pre-Mesozoic basement top (dashed line), Blue Ridge to edge of continental shelf, North Carolina. Solid line only is shown where two lines are superimposed. Submarine data after Dillon et al. (1978).

where λ, or the characteristic of the system = $\sqrt[4]{g(\rho_m - \rho_w)/4D}$ = wavelength of flexure^{-1}

D = the flexural rigidity of the crust in Newton meters

g = acceleration of gravity

a = distance from free end of beam

This equation can also approximate behavior of materials between the end members of the continuum, since D and λ may vary. As $D \rightarrow \infty$ (a completely rigid beam), $\lambda \rightarrow 0$ and depression caused by surface loading approaches zero. If $D \rightarrow 0$ (no lateral transmission of bending stress), $\lambda \rightarrow \infty$, producing a situation of an infinitely weak beam approximating Airy behavior.

Watts and Ryan (1976) found that neither model accounts for the widths of continental shelves or subsidence rates which vary with time. The inability of the simple elastic beam model to account for shelf configuration is an inadequacy of a mathematical model which assumes no lateral or vertical variation in rigidity of the beam and end-loading rather than a distributed load (Hetenyi, 1946). The continental crust cannot be realistically modeled as a simple isotropic beam, since the mechanical properties vary laterally as the result of lateral changes in crustal structure and composition, and vertically as a function of temperature and confining pressure. In addition, Hetenyi (1946) demonstrated that this is not an adequate approximation of effects produced by a load distributed along the beam (Fig. III-9), and computer simulation of the two models indicates that assumption of a point load

model may lead to error of up to 16.9% in determining the elevation of the beam below a datum at a selected point.

A more accurate determination is given by Hetenyi (1946, p. 26) as:

$$y = q/2k\ [(1 + \exp(-\lambda\ell)\sin\lambda\ell - \exp(-\lambda\ell)(\cos\lambda\ell - \sin\lambda\ell))$$
$$(\exp(-\lambda\ell)(\cos\lambda x + \sin\lambda x)) - (1 + 2\exp(-\lambda\ell)\sin\lambda\ell -$$
$$\exp(-\lambda\ell(\cos\lambda\ell - \sin\lambda\ell))(\exp(-\lambda x)\sin\lambda x) + 2 - \exp(-\lambda x)$$
$$\cos\lambda x - \exp(\lambda(\ell-x)\cos\lambda(\ell-x))]$$

(Terms explained in Figure III-9.)

This model approximates deflection resulting from the load imposed by a body of approximately rectangular cross-section (Fig. III-9) on a semi-infinite beam. Potential sources of error in application of this method are in determination of the values of ℓ, x, and q, where $q = \rho_s hl$. This is a particular problem in the Valley and Ridge thrust belt, since the edge of the Paleozoic shelf is beneath the crystalline Appalachians and its location must be inferred from geophysical data.

This treatment represents downwarping associated with geologically instantaneous loading, and represents a situation where viscous behavior of the beam is insignificant. However, when loading occurs over periods in excess of 40 my or more and viscous effects may be significant (Walcott, 1972; Haxby et al., 1976; Murrell, 1976), the Airy model provides an adequate approximation.

Regional Correlation

The Paleozoic biostratigraphy of Alabama is, in general, poorly known, and previous regional stratigraphic studies have relied principally on lithostratigraphic correlation. In this study a limited number of

published biostratigraphic correlations, published faunal lists, and collections made during the course of this study were used to develop tentative correlations. Lithostratigraphic correlations were used where deposition of a stratigraphic unit could be related to a geologic event of presumably short duration.

None of the lithostratigraphic or biostratigraphic elements used in this study can be considered to be truly isochronous (sensu Hedberg, 1958), since they represent events, such as spread of a clastic facies unit or a change in faunal assemblages, which, although of geologically short duration, are nontheless demonstrably diachronous (Fischer, 1964). More problematical is the correlation between geologic and absolute time scales, a relationship which is particularly poorly defined for the Paleozoic. Given these factors, the "isochronal elements" used for correlation in this study represent time lines of variable accuracy and resolution, as indicated by time error bars on the subsidence history curves.

As a result of the general paucity of data, isochronal elements suitable for regional correlation are few and unevenly distributed through the Paleozoic stratigraphic sequence. Related to a scale of absolute time (Fig. III-10), the intervals between elements vary from 10 to 55 my, with an average duration of 26 my. Thus, subsidence curves developed for the region are finite curves (mean values of long period subsidence) rather than instantaneous values. This prevents recognition of some short-term subsidence events, but represents a problem which cannot be eliminated given the present data base.

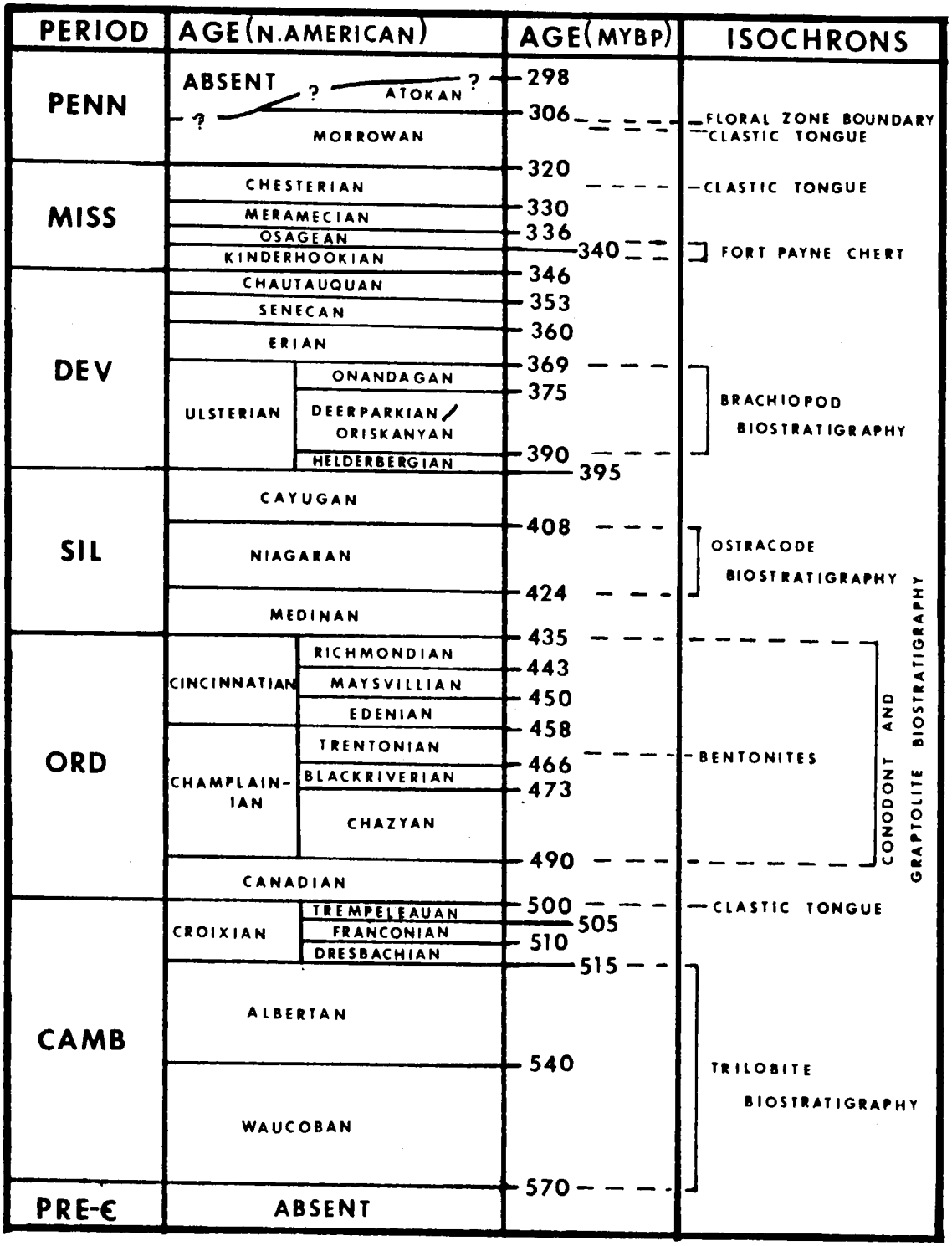

Figure III-10. Stratigraphic and absolute time scale, and isochrons used for correlation. Absolute time scale after van Eysinga (1975) and unpublished data. See text for description of isochrons.

Approximate correlations in the Cambrian and Lower Ordovician are based on trilobite biostratigraphy. Trilobite collections by Butts (1926, 1940), Palmer (1962), Kidd and Neathery (1976), Bell (1978), D. N. Bearce (personal communication, 1979), and the present author, as well as other faunal elements (McCalley, 1897; McKinney, 1977) were assigned to standard trilobite biostratigraphic zones (Howell et al., 1944; Lochman-Balk and Wilson, 1958), as shown in Figure II-5, page 31. Available collections are numerically inadequate and too sporadically distributed to construct correlative zone boundaries. However, the distribution of collections does indicate an anomalously thick Upper Cambrian sequence in the Birmingham anticlinorium (Fig. II-5).

The validity of even approximate correlations based on trilobite biostratigraphy may be disputed, since the effects of depositional environment on faunal zones is poorly known (Palmer and Campbell, 1976). However, alternative lithostratigraphic correlations would require a complex, and hence less likely, subsidence history with foreland crustal blocks rising and subsiding independently of adjoining blocks.

A beginning of clastic sedimentation in the Knox Group, marked by several beds of sand and minor quartz gravel (Self et al., 1974), is here used to define the approximate Cambrian-Ordovician boundary as suggested by Cummings (1960) for the Knox Group in Tennessee. Cummings (1960) believed that the sands were cratonic in origin, and resulted from a short-term drop in sea level. Gastropod collections by Butts (1926, 1940) and Self et al. (unpublished) indicate that the Cambrian-Ordovician systemic boundary is actually stratigraphically above the basal sand bed of this clastic facies, but the sandy facies has been used as a marker

horizon because it is readily identifiable over a large region. It is probable that onset of deposition of the sand facies was not strictly isochronous over the entire shelf, but that clastic sedimentation occurred over a span of several million years during the latest Cambrian.

Correlations in the Middle and Upper Ordovician are based on conodont and graptolite biostratigraphy (Drahovzal and Neathery, 1971; Bergstrom and Drahovzal, 1972; Raymond, 1973; J. A. Drahovzal, personal communications, 1971-1979; and Stig Bergstrom, personal communication, 1979), and widespread bentonite ash beds (Faul and Thomas, 1959; Smith et al., 1971; Drahovzal and Neathery, 1971).

Correlations within the Silurian and Devonian are poorly defined, based mainly on limited studies of ostracode (Lundin and Newton, 1970) and palynomorph (Chaiffetz, 1974) biostratigraphy in the Silurian, and brachiopod assemblages (Kiefer, 1970) in the pre-Chattanooga Shale Devonian. Biostratigraphic studies in the Chattanooga Shale of Alabama are inadequate to permit correlation.

Correlations within the Carboniferous are based on limited biostratigraphic data and prograding clastic tongues. The Hartselle Sandstone of middle Chester age (Drahovzal, 1967) was apparently derived from a northern source area (see Chapter II), probably as the result of subaerial exposure of the central Tennessee region resulting from a rapid drop in sea level (Vail et al., 1977; Dennison, 1978). Thus, the rapid spread of the Hartselle clastic "tongue" represents a short-term change in depositional regime useful as an isochronal element in regional correlation.

Correlations within the Pottsville Formation are based on both a change in depositional regime and on paleobotanical zones. Many of the Pottsville fluvial sandstones contain varying amounts of quartz gravels, but one stratigraphic horizon called the Fourth Conglomerate, Straven Conglomerate, or Wolf Creek Sandstone in the various coal basins, contains major amounts of rounded volcanic, metamorphic and Lower Paleozoic sedimentary clasts up to 15 cm in diameter (Rothrock, 1949; Gilbert, 1976; Squire, 1890; Jones, 1929; McCalley, 1900). This single influx of unusually coarse-grained and lithologically distinctive clastics into the Pottsville depositional basin apparently resulted from some geologically short-lived change in the capability of the Pottsville-age fluvial systems. Although useful for rough correlations, age of the conglomeratic horizon is unknown and precludes its direct use as an isochronal element. More useful is a floral zone boundary between the Westphalian "A" and Westphalian "B" of the European standard (Read and Mamay, 1964; unpublished data summarized by Wanless, 1975). As such, the boundary would represent an isochronal element about 310 mybp, but actual precision is probably poor, since European-North American floral zones are inadequately correlated (R. A. Gastaldo, personal communication, 1979).

Summary of Factors

In this study an attempt has been made to account for all possible sources of error in determining subsidence history. The effects of paleobathymetry, sediment compaction and sediment loading have been the subject of numerous studies, and their effects can be accounted for with

a high degree of probable accuracy, but the effects of eustatic changes cannot.

In the subsidence history curves for the study area, uncertainties in estimating effects of all factors are indicated by error bars. To evaluate effect of the most poorly understood factors (eustatic change, carbonate compaction), separate plots were prepared in which corrections for these factors were not attempted. Since these plots suggested no fundamental changes in the subsidence history, they are not presented. In one instance where difficulties in estimating a major factor were encountered (paleobathymetry of the Middle Ordovician shale basin), multiple subsidence history curves are presented.

III. RESULTS AND INTERPRETATION

Although lithofacies and unit thickness vary along the structural strike of the thrust belt, the greatest changes occur across the structural trend (Fig. I-2, page 6). This has resulted in a situation in which time-equivalent lithofacies are restricted to specific thrust sheets within the belt; for example, Middle Ordovician peritidal carbonates occur northwest of the Helena fault, while shelf edge reentrant and slope deposits occur southeast of the fault. This zonation reflects the fact that the Paleozoic margin of North America was essentially parallel to the present trend of the Appalachians. Tectonically induced subsidence and uplift of this free margin resulted in development of hinge lines subparallel to the continental margin, with pronounced differences in elevation of the basement top expressed as variations in unit thickness or paleobathymetry.

Figure III-11 represents corrected crustal subsidence curves for four areas along the line of the geotraverse illustrated in Figure I-1, page 4. These curves differ from previous published subsidence histories (for example, Sweeney, 1976, 1977; Briggs and Roeder, 1975) in that by accounting for paleobathymetric changes, episodes of rapid subsidence and uplift can be distinguished. In Figure III-12, the curves are plotted on a palinspastic base. This palinspastic restoration, with correlations at several approximately isochronous time lines of variable reliability, was used to generate a series of diagrams illustrating the elevation and configuration of the Precambrian basement top at intervals during the Paleozoic. Subsidence curves for local areas (Fig. III-11) and the changing configuration of the basement top (Fig. III-12) indicate several phases in the subsidence history of the foreland.

During an early miogeoclinal phase (~570 to 490 mybp) the area underwent moderate subsidence (mean rates 1.4 to 2.8 cm/1000 yr), with maximum subsidence near the shelf margin; as a result, marine sedimentation began near the shelf edge and migrated toward the craton. Subsidence during this phase was atypical in two respects. Evolving continental shelves typically exhibit subsidence rates which decrease exponentially with time (for example, Briggs and Roeder, 1975; Watts and Ryan, 1976; Sweeney, 1977; van Hinte, 1978), presumably as a result of lithospheric cooling (Sleep and Snell, 1976; Jarvis and McKenzie, 1980). However, during the early Paleozoic subsidence, rates in the study area did not decrease significantly over a period in excess of 60 my duration (Fig. III-11). Long-term linear subsidence resulting from periodic intermittent reactivation of an abortive rift system has been described

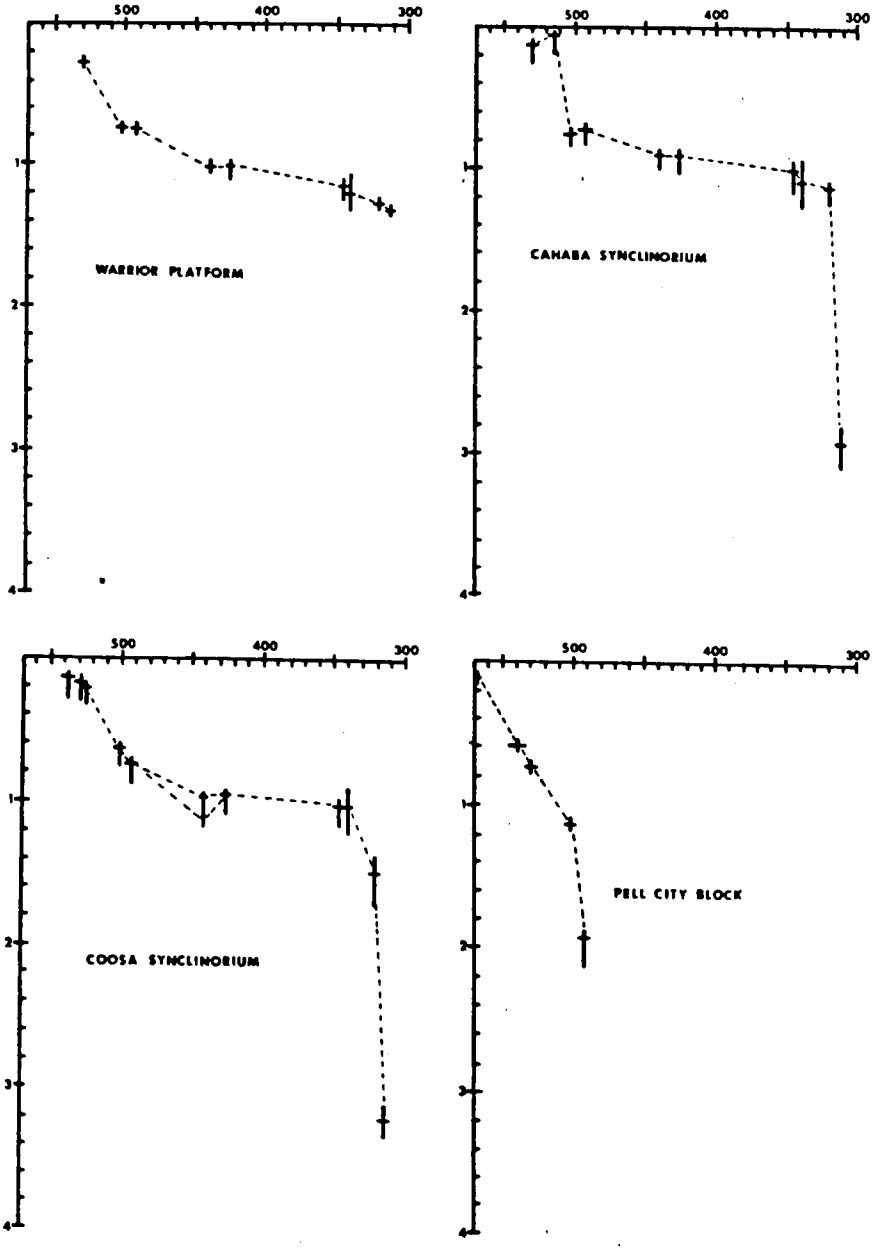

Figure III-11. Corrected finite subsidence curves for pre-Paleozoic basement top in selected areas, Paleozoic foreland, Alabama. Abcissa scale is in mybp; ordinate scale is in kilometers below sea level (taken as zero at the Cambrian-Ordovician boundary). Vertical arms of corsses represent cumulative elevation error from all sources; horizontal arms represent uncertainty in age determination. Divergent lines in Middle Ordovician ($\sim$ 450 my) represent alternative subsidence histories allowed by data, major Taconic subsidence (lower line), and minor subsidence (upper line).

Figure III-12. Configuration of the Paleozoic foreland basement. Numbers indicate mybp, letters denote major stratigraphic belts; WP-Warrior platform, CAH-Cahaba synclinorium, COO-Coosa synclinorium, PCB-Pell City Block. Top of polygon is a constant datum (sea level at the Cambrian-Ordovician boundary), bottom is basement top. Note differential subsidence in east (540-530), growth and collapse of the Birmingham crustal bulge (530-500), slight differential subsidence in the Middle Ordovician (440), Silurian-Devonian uplift (346), and the late Paleozoic asymmetric foredeep (320-312).

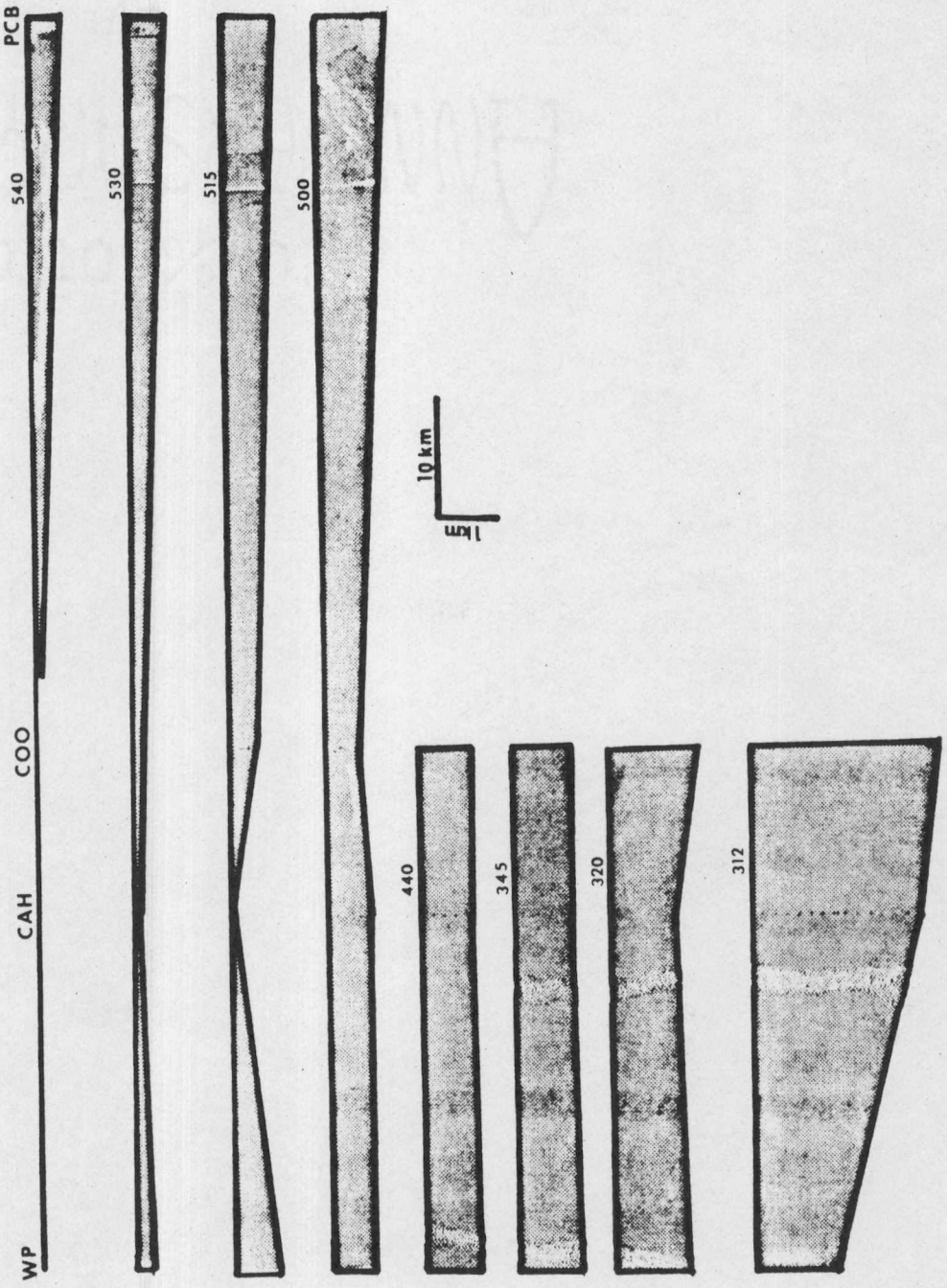

Figure III-12.

from the North Sea (Sclater and Christie, 1980); however, geophysical data (Woollard in Steinhart and Mayer, 1961) and regional stratigraphy preclude a similar explanation for long-term subsidence in the study area.

During the Middle and Late Cambrian the basement underneath the palinspastic position of the Birmingham anticlinorium-Cahaba synclinorium was uplifted relative to the adjacent regions, then collapsed to form a relative low (Figs. III-12, III-13). This type of uplift and collapse is typical of continental rifting, and may reflect abortive rifting associated with the contemporaneous rifting of the mid-continent Rome trough (Woodward, 1961; Black, 1979) and southern continental margin (King, 1959). The possibility of an aborted rift event is supported by the occurrence of a negative gravitational anomaly at the palinspastic position of the Birmingham anticlinorium (see Fig. 3 in King and Zietz, 1978).

The second, or "Taconic foredeep" phase, was characterized by abruptly reduced subsidence rates and by possible differential downwarping of the outer shelf east of the Cahaba synclinorium (Figs. III-11, III-12). In the northwestern foreland, low rates of subsidence can be documented by innundation of subaerial unconformity, followed by peritidal carbonate sedimentation (see Chapter II).

The southeastern foreland developed into a deep subtidal clastic basin with consequently less paleobathymetric control, and subsidence estimates are less precise (Fig. III-11). Observed paleobathymetric criteria and regional stratigraphic relationships of the basinal facies (Columbiana Formation) suggest a possible range of water depths from 50

Figure III-13. Schematic history of Paleozoic tectonism, based on subsidence history. Early miogeoclinal phase characterized by abortive rifting (A) and subsidence of cratonic margin (B); shelf edge (C) progrades seaward. During the foredeep periphery phase, oceanic basin is consumed by subduction beneath island arc (D); creating flysch basin in Tennessee (E), and shift of shelf edge (C) toward the craton. Collision in Alabama region may have been abortive, resulting in downwarp of shelf edge and creation of starved basin (F) without deformation of shelf margin (G); alternatively, shelf edge may have been involved in deformation (H), but evidence is inconclusive. During epeiric sea phase, downwarped shelf undergoes isostatic uplift (I), creating a west-facing shoreline and subaerial exposure of older shelf sediments (J). During final foredeep phase, collision with Africa (K) causes thrusting of Inner Piedmont island arc onto craton edge (L), resulting in development of asymmetric foredeep (M). Stippled areas represent North America shelf sediments; numbers in parentheses are dates in my before present for each phase; arrows represent motion of plate relative to sea level.

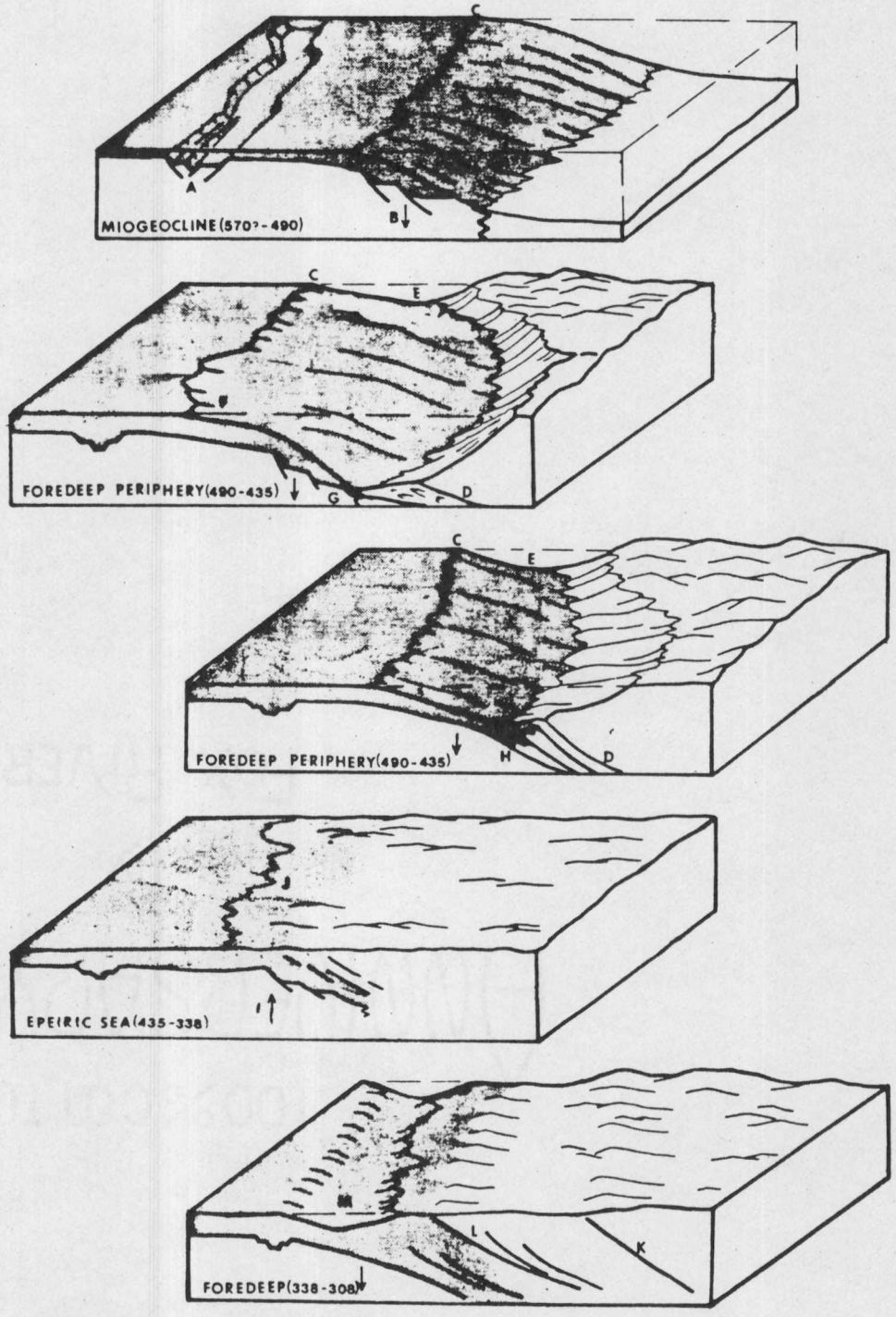

Figure III-13.

to over 1000 m (see Chapter II). Observed data do not allow an unequivocal interpretation of bathymetry or subsidence, and two possible alternatives are presented, in which the Columbiana basin may have represented either a starved basin peripheral to a Taconic foredeep or remnants of an eroded Taconic foredeep (Fig. III-13).

Several observations suggest low rates of regional Middle Ordovician subsidence. Turbidites of the type which characterize deeper (> 1000 m) Taconic foredeeps elsewhere in the southern Appalachians (for example, Shanmugam and Walker, 1978) are absent from the preserved Columbiana Formation. An uppermost Middle Ordovician graptolite fauna (Decker, 1952) from the southeastern part of the thrust belt indicates that most of the Columbiana is locally preserved, and that no Middle Ordovician turbidite sequence was ever deposited. The upper contact of the Columbiana is a pre-Middle Silurian subaerial unconformity, which could only have resulted from extremely rapid uplift (> 4 cm/1000 yr) of the southeastern foreland if the eastern basinal facies were deposited in 1000 m or more of water.

Several investigators (Shaw, 1970; Telle et al., 1979; Sears et al., ms. in prep.) have suggested that the basal Talladega Group of the Northern Piedmont represents a Taconic foredeep fill with debris derived from erosion of deformed pre-Middle Ordovician shelf rocks. This interpretation is, however, entirely speculative since the age of the basal Talladega is unknown.

No Taconic metamorphic or tectonic event has been documented in the Alabama-west Georgia Appalachians (Tull, 1978, p. 457), but Middle Ordovician foredeep fill in northwest Georgia was affected by Taconic

tectonism (Sears et al., ms. in prep.), suggesting the possibility of an unrecognized Taconic event in the region. The presence of volcanic ashfall deposits (Smith et al., 1971) in both basinal and shelf facies of the foreland suggest proximity to active centers of volcanism, and the sudden decrease in subsidence rates suggests a change in the tectonic setting of the foreland.

The absence of turbidites and Taconic metamorphism, and the low subsidence rates in the northwestern foreland could be explained by an aborted collision with an island arc which approached the shelf margin (Fig. III-13), supplying pyroclastics to the shelf and consuming the oceanic crust which contributed to lithogenetic subsidence of the shelf. In this conceptual model, the basinal Middle Ordovician deposits would represent a starved basin peripheral to the Taconic collision belt and foredeep in the Tennessee-north Georgia region. On the basis of both geological and geophysical data, Sears et al. (in prep.) have postulated that variations in style and intensity of Taconic tectonism resulted from irregularities of pre-Taconic North American shelf edge. The setting of the Columbiana peripheral basin in the Sears et al. model is illustrated schematically in Figure III-13.

An alternative hypothesis is that the Columbiana basin represents a less well-developed southwestward extension of the Taconic foredeep of east Tennessee. The apparent absence of a Taconic metamorphic event would suggest a collision with minor imbrication and downwarping of the shelf margin, producing a flysch basin (Talladega Group) separated from a southeast facing carbonate shelf by a shale basin (Columbiana). A modern analogue is the Timor Sea, where collision of a segment of the

Banda island arc complex with the irregular margin of the Australian continent has resulted in development of a linear foredeep which opens on the west into the Indian Ocean basin (Hinz et al., 1978). In this region the Australian shelf has been downwarped in the zone of actual collision, but not downwarped beyond the actual zone of collision. The setting of such a basin in the Sears et al. model is depicted as an alternative hypothesis in Figure III-13.

During the Silurian through earliest Mississippian subsidence rates were extremely low, approaching 0.007 cm/1000 yr. in the western belts. Subaerial erosional bevelling of the entire pre-Middle Silurian sequence in the southeastern Valley and Ridge requires significant pre-Silurian uplift of the eastern belts (Fig. I-2, page 6). Cessation of subsidence and differential uplift of the old shelf edge can be explained by isostatic recovery of tectonically downwarped continental crust over a period of 100 my (Fig. III-13).

During the Early Mississippian, rapid subsidence associated with the final foredeep phase began throughout the entire region and rates increased rapidly through the Early Pennsylvanian. Subsequent subsidence cannot be determined due to lack of preserved strata. The simultaneous initiation of subsidence throughout the region indicates a rigid continental crust exposed to extreme loading near the continental margin, an interpretation compatible with the concept of late Paleozoic orogenesis as the rapid thrusting of a crystalline nappe onto the continental margin (Fig. III-13).

IV. CONCLUSIONS

Quantitative interpretation of stratigraphic data, applied to the study of larger-scale crustal behavior, provides evidence of orogenic events both within and contiguous to the depositional basin. Results of this particular study have been used to formulate a Paleozoic tectonic history of the region, a major feature of which is the absence of a major Taconic tectonic event in the region. In addition, the data lead to the interpretation that the thinning of Paleozoic stratigraphic units over the Birmingham anticlinorium, frequently cited as evidence that foreland structures are basement-involved structures of great antiquity (for example, Thomas et al., 1970; Thomas, 1972a), instead may represent thinning over a peripheral bulge resulting from downwarping of the Paleozoic shelf (Fig. III-11), or isostatic uplift over an aborted rift (Fig. III-13).

Geodynamic observations of Paleozoic crustal behavior may also be applied to specific tectonic or sedimentological problems. Crustal flexure associated with subsidence and uplift of the Middle Ordovician Sevier basin of Tennessee apparently indicates viscous (Airy) behavior of the crust (G. Shanmugam, personal communication, 1978), an observation incompatible with the observed geodynamic behavior of a rigid craton (for example, Molnar et al., 1976). The Airy behavior observed by Shanmugam may indicate that the Taconic foredeep of Tennessee developed in part on weak, structurally disrupted crust. The differential subsidence and uplift of the eastern thrust belt of Alabama during the Middle Ordovician through Lower Mississippian indicates a strong component of

viscous behavior over long intervals (40 to 100 my). Similarly, widespread instantaneous initiation of late Paleozoic behavior indicates elastic behavior under short-term stress rates (< 18 my). These observations suggest that rates of plate convergence and imbrication, as well as crustal structure, may influence sediment basin geometry. Further investigation and quantification of subsidence data, particularly chronostratigraphic relationships, will aid in interpretation of ancient orogenic processes and rates.

CHAPTER IV

STRUCTURAL MAPPING OF A DEEPLY WEATHERED CARBONATE TERRANE, SHELBY AND TALLADEGA COUNTIES, ALABAMA

The easternmost part of the Valley and Ridge province in Alabama is geologically complex, and despite reconnaissance mapping, details of regional structure and stratigraphy are poorly known. One of the major problems is that of determining the geologic structure of the unusually broad area (4800 square km) underlain by weathered dolostones of the Upper Cambrian-Lower Ordovician Knox Group east of the Pell City fault (Fig. IV-1). As part of this study it was necessary to determine the internal structure and kinematic history of this area.

This belt is locally up to 20 km in width across the regional structural trend. Dips of bedding observed in rare exposures are gentle (less than 40 degrees), and toward both the southeast and northwest. This suggests the presence of northeast-striking open folds, further suggested by mapping of the northeastern extremity of the belt where stratigraphic units other than the Knox are exposed (Fig. IV-1). Regional outcrop patterns also indicate that the entire expanse of Knox Group carbonates are part of an areally extensive but thin thrust sheet, as Mississippian shales in the footwall of the Pell City fault are exposed in reentrants and windows up to 9 km southeast of the main fault trace (Fig. IV-1).

Butts (1926) and Causey (1965) did not attempt to define internal structure of the Pell City fault block. Shaw (1973, 1974, 1976) described

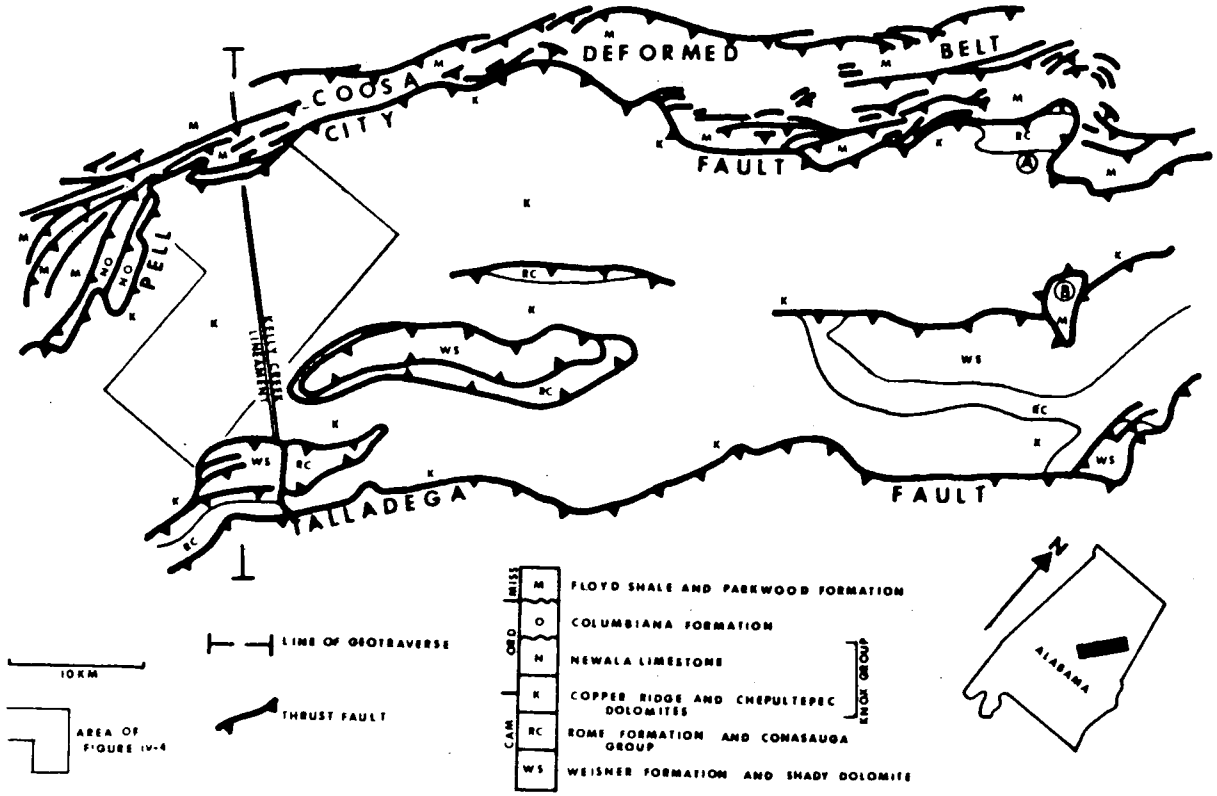

Figure IV-1. Regional geology of the Pell City thrust sheet, east central Alabama. Note the occurrence of Rome-Conasauga rocks in the upper sheet at (A), and the Fort McClellan window exposing Floyd Shale and Columbiana Formation strata of the lower sheet at (B). Geology based on Thomas and Drahovzal (1974), Bearce (1977), and Gilbert (1977), and this study.

the regional structure as a series of isoclinal recumbent folds, subsequently deformed by upright open folds. In his interpretation, the entire area of this study is underlain by an inverted stratigraphic sequence in the lower limb of a recumbent fold (Shaw, 1974). However, mapping by other investigators (Bearce, 1978, and unpublished map, 1974; Gilbert, 1977; and this study) has demonstrated that strata in the inverted limbs mapped by Shaw are in fact upright. Overturned isoclinal folds have been mapped (Thomas and Drahovzal, 1974), but they are not large-scale recumbent folds as described by Shaw.

The fundamental problems which have prevented adequate mapping of the region are the poor exposure and poorly-defined stratigraphy of the Knox Group. The Knox terrane is deeply weathered, with extensive karst development. The topography, however, is fairly rugged, with hills of up to 80 m relief supported by stony Knox residuum. Residual soil developed on the Knox Group is generally a yellowish orange to gray, locally sandy clay, with varying proportions of dark-gray blocky, angular, dense chert, or white to dark-gray vuggy chert cobbles and boulders. Many investigators have attempted to differentiate between the two major formations of the Knox on the residuum, with blocky dense chert in the lower Copper Ridge Dolomite, and vuggy ("worm-eaten") chert in the Chepultepec Dolomite (Fig. IV-1). This practice follows a suggestion by Butts (1926), but is not a reliable method of differentiation, since both types occur in the residuum overlying each formation.

Thickness of the residuum is variable, and exposures of unweathered dolostones are extremely rare. Throughout most of the area the residuum is at least 13 m in thickness, and test drilling at one construction site

disclosed a solution zone with residuum and cave fillings 206 m below the surface. One possible explanation for the extremely thick zone of weathering is the age of the surface, since Denson and Waage (1966) reported sinkhole fillings of Miocene age. As a result of the deep weathering, outcrops from which structural and stratigraphic data can be derived are few. In the 206 square km examined during this study, two exposures of unweathered Knox, and nine exposures of saprolite were observed. In some exposures a general facing direction can be determined from sedimentary and biogenic structures (primarily algal stromatolites and ripple marks), but no reliable dip can be determined because of slumping of the residuum.

Even in areas where it is better exposed, internal stratigraphy of the Knox is poorly known. Reconnaissance studies indicate that the entire Knox consists of peritidal carbonates, without distinctive stratigraphic units or biostratigraphic zones which can be correlated over broad areas or serve to define geologic structures. The only distinctive stratigraphic units are a series of thin-bedded orthoquartzites which occur below the Cambrian-Ordovician systemic boundary (Cummings, 1960; Self et al., 1974). In the study area these sand units occur as resistant units and serve as a stratigraphic marker zone as well as providing facing data and bedding attitudes.

Even estimates of the thickness of the Knox are conjectural. Based on average dip and width of outcrop data for one area where the structure is believed to be simple, thickness of the Knox Group is estimated to be 1100 m (Butts, 1926; Gilbert, 1974; Bearce, 1978). Gilbert and Nordstrom (unpublished ms.) estimated that the Copper Ridge is approximately 530 m

thick, and the Chepultepec over 550 m, although the top of the Chepultepec is missing through erosion and structural overlap along the Talladega fault (Fig. IV-1).

In order to circumvent the difficulties posed by poor exposure and absence of mappable rock units, remotely-sensed imagery was utilized as an interpretive tool. Three types of imagery were available: multispectral photographs from the Apollo 9 orbital mission, LANDSAT multispectral scanner imagery, and high altitude color infrared photographs.

I. GEOLOGIC ANALYSIS OF APOLLO 9 IMAGERY

As part of the S065 Multispectral Terrain Photography Experiment, multispectral photographic imagery (frame AS9-26-3790) was obtained for an area covering most of east-central Alabama, including the area of this study. Imagery included four bands: blue-green (BG), red (R), infrared (IR), and color infrared (CIR).

Preliminary analysis of the imagery by Powell et al. (1970) suggested the presence of a linear tonal anomaly (lineament) in part of the study area (Kelly Creek lineament in Fig. IV-1) visible on the BG, CIR and R band images. Later work (Drahovzal et al., 1973; Gilbert et al., 1976; Wielchowsky and Warren, unpublished ms.) demonstrated that the lineament represented a segment of a longer tonal anomaly which extends across much of the Valley and Ridge province. This and other lineaments have been variously interpreted as relatively recent (post-thrusting) "tensional fractures" (Powell et al., 1970), pervasive basement faults (Drahovzal et al., 1973), and zones of strike-slip faulting, associated with late Paleozoic thrusting (Gilbert et al., 1976). Although gross lithologic

and topographic changes could be recognized in the Valley and Ridge, no macroscopic structures were recognizable within the Knox terrane, probably as the result of the relatively poor resolution of 100 m.

II. GEOLOGIC ANALYSIS OF LANDSAT IMAGERY

Black and white prints of LANDSAT-I imagery (Bands 5 and 7) acquired on 14 January 1973, proved more useful than the Apollo 9 imagery. Band 5 imagery, in the 0.600-0.700 micrometer (μm, red) range, provided little useful data. Since band 5 is most useful in vegetation discrimination, the diverse land use patterns obscured most information of geological interest.

Band 7 (0.800-1.100 μm, infrared) imagery revealed the presence of numerous macroscopic structures not apparent in ground investigations. The low sun angle (elevation 28 degrees above horizon, at azimuth 147 degrees) served to shadow and accentuate topographic patterns resulting from differential weathering and erosion of stratigraphic units within the Knox. Particularly apparent are zig-zag ridge patterns indicative of plunging folds within the Knox (Fig. IV-2). Trends of the axial traces of these folds are variable, and are discordant to the trace of the fault along which the Lower and Middle Cambrian rocks, which comprise the Sleeping Giants complex, have been thrust over the Knox (Fig. IV-2). The fault trace, however, exhibits no evidence of folding. The discordance thus suggests that folding of the Knox predated emplacement of the Sleeping Giants complex.

The major thrust faults which comprise the boundaries of the area underlain by the Knox are readily distinguishable in the imagery.

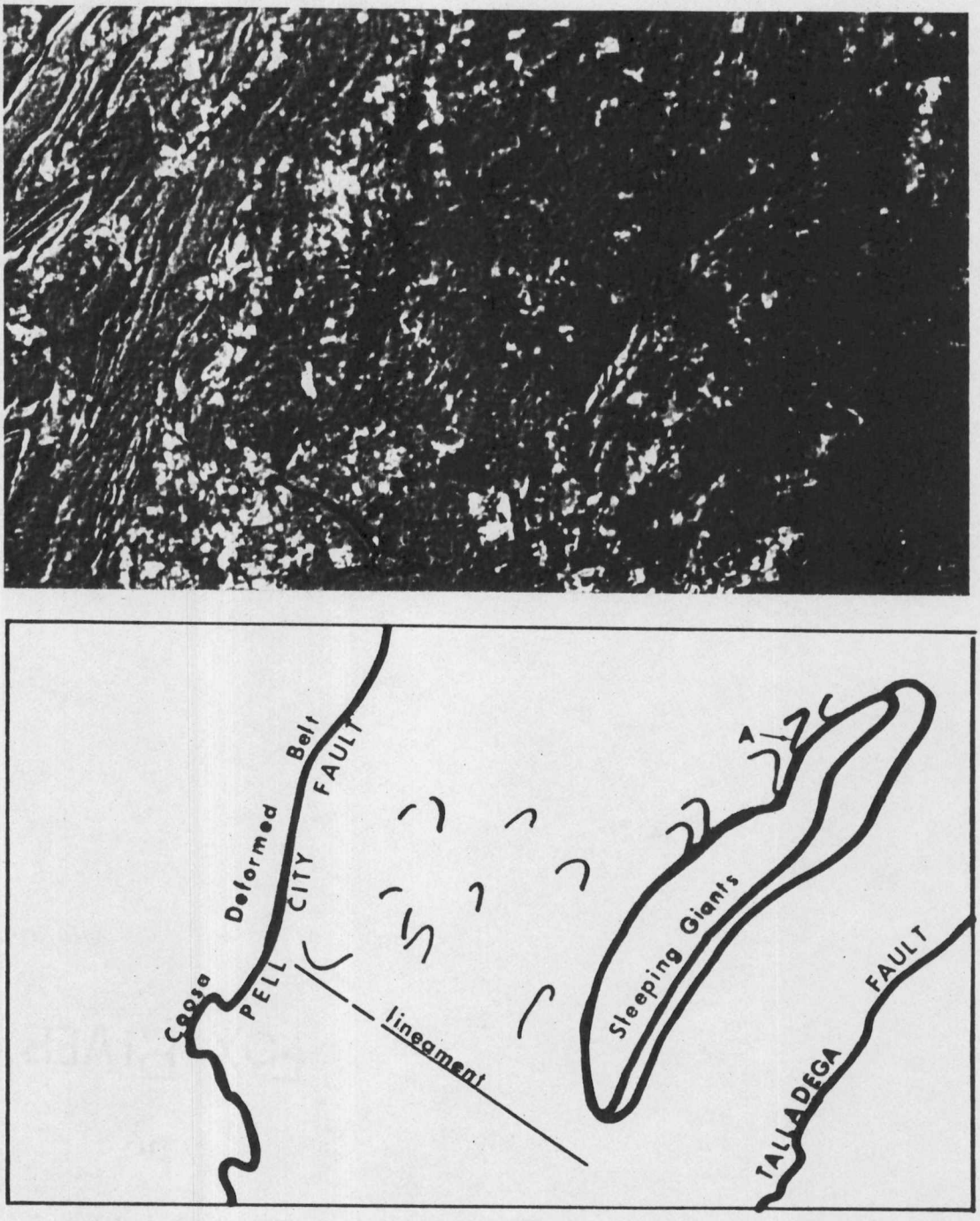

Figure IV-2. Structural features observed in LANDSAT band 7 infrared imagery, Talladega County, Alabama. Curved line segments are plunging folds expressed as ridges. Note discordance of fault bounding Sleeping Giants to folds in lower block at A.

Topography within the Knox terrane is generally subdued, with poorly defined ridges. The Coosa deformed belt to the northwest is characterized by pronounced northeast-trending en echelon ridges, and the boundary between the two topographic domains (the Pell City fault) is quite evident (Fig. IV-2). In band 7 imagery the Talladega fault is marked by an abrupt transition from the subdued Knox topography to uneven hills of high relief in the area underlain by metamorphic rocks of the Talladega Group. This boundary is also, but less precisely, marked by an abrupt change from mixed grazing-row cropping-forest (Knox) to mixed hardwood-coniferous forest (Talladega) land-use visible in band 5 imagery. Areas underlain by Lower and Middle Cambrian rocks thrust atop the Knox are characterized by high linear ridges visible in band 7 imagery, and by more heavily forested areas visible in band 5 imagery. However, these geologic boundaries are more readily and precisely defined by groundbased mapping (Bearce, 1977; Gilbert, 1977).

III. GEOLOGIC ANALYSIS OF HIGH-ALTITUDE COLOR INFRARED IMAGERY

On February 22, 1973, a U-2 aircraft operated by NASA photographed a large area of the Valley and Ridge from an altitude of 19,811 m using color infrared film. Square format 22.8 centimeter transparencies of appropriate frames were examined for this study, and proved to be the most useful imagery.

Because of the timing of imagery acquisition (mid-winter) and the effects of land-use pattern (mixed grazing, row cropping, pine-pulpwood growing, hardwood forest, and brush growth on clearcut tracts), regional

lithologic patterns could not be deduced from either vegetation associations or vegetation stress resulting from variations in soil moisture or type. Also because of mixed land-use and vegetation, variations in lithology could seldom be deduced from soil characteristics.

Certain elements useful in structural analysis were, however, visible in the imagery. The high altitude and large area available for synoptic viewing (892 square km per frame) served to accentuate topographic patterns not discernible on topographic maps. These topographic patterns are related to variations in the amount and nature of chert produced during weathering, and apparently represent lithologic units within the Knox. Particularly obvious are sinuous ridge patterns indicative of plunging folds (Fig. IV-3). These plunging fold patterns are also visible in LANDSAT imagery (Fig. IV-2).

Northeast-trending lineaments are defined by tonal anomalies, topographic linears, and linear stream patterns atypical of the region (Fig. IV-3). The trend of these lineaments parallel to regional strike, and their expressions as topographic lows indicative of less resistant rocks, suggest that these lineaments are the surface expression of northeast trending zones of intensive fracturing, probably faults. In some cultivated fields soil reflectance varies across these lineaments, probably as the result of soil moisture content due to differing subsurface drainage characteristics (Fig. IV-3). This further suggests the fault juxtaposition of rock units possessing different susceptibility to subsurface solution and weathering. Development of the inferred faults apparently postdates folding, since photolinears locally truncate topographic trends.

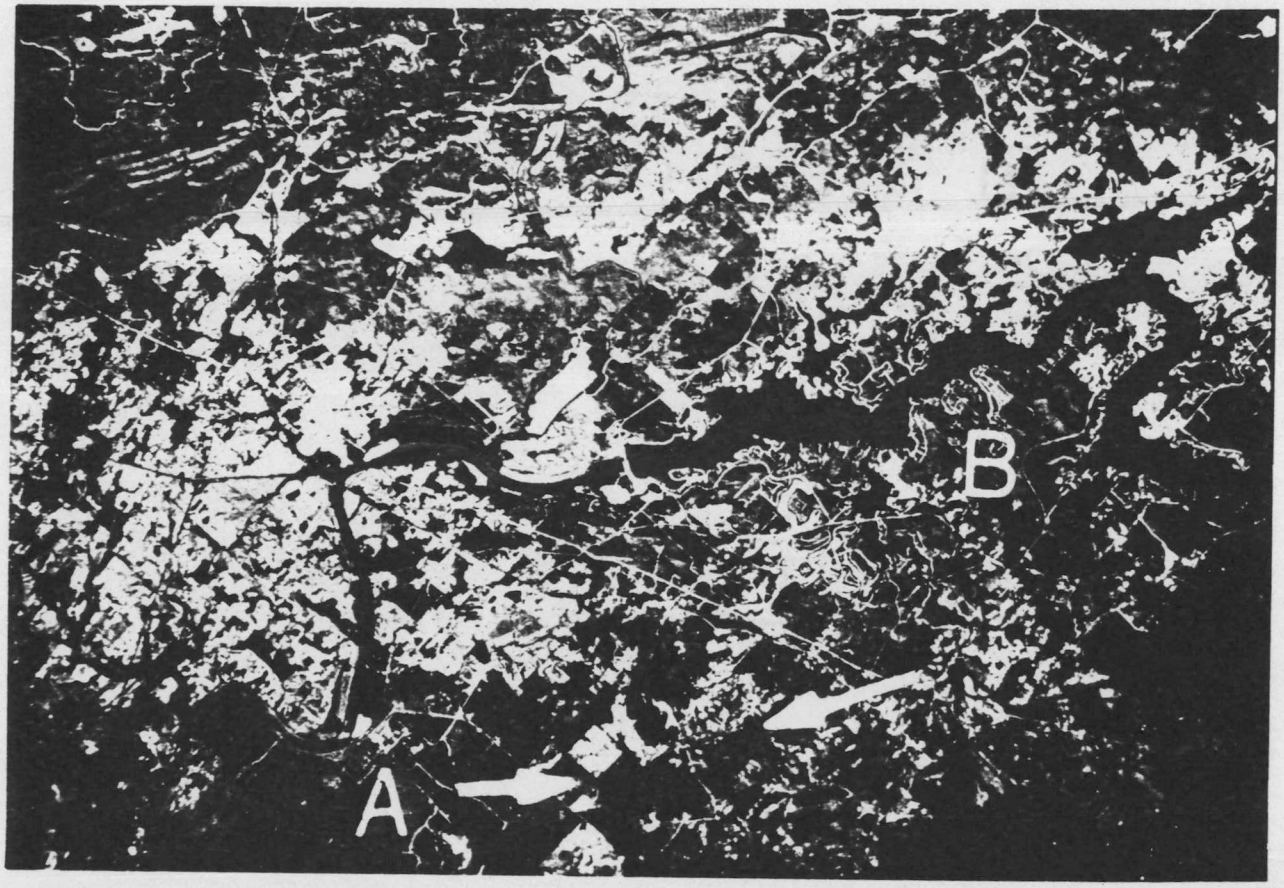

Figure IV-3. Structural features visible in infrared imagery, Logan Martin Dam area. Topographic and stream linears (A) are interpreted as fault traces; sinuous ridge to left and upper right of (B) define noses of plunging folds. Tonal anomalies not apparent in B & W imagery. North is to upper right; scale 1:184,000. NASA.

The distribution of elements, topographic patterns, lineaments, and changes in soil reflectance in part of the study area are depicted in Figure IV-4.

IV. GEOLOGIC DATA

Examination of limited available exposures provided data that, in general, supported conclusions reached from imagery interpretation. Mesoscopic fabric elements observed included bedding attitudes, mesoscopic fold axes, bedding telescopes (small-scale thrust faults), and solution cleavage.

Bedding attitudes observed in bedrock and saprolite exposures are consistent with strike directions of topographic trends observed in the imagery, supporting the assumption that these trends are the surface representation of lithologic layering. Facing criteria and bedding attitudes were used to determine the nature of folds expressed as sinuous ridges (i.e., beds dipping toward a fold axis indicate a syncline; beds dipping away an anticline) in Figure IV-4. The resulting interpretive map (Fig. IV-4) indicates a series of generally southwest-plunging folds, with some northeast-plunging folds.

Observed mesoscopic folds plunge both southwest and northeast, and axes have highly variable trends consistent with inferred macroscopic fold axes (Fig. IV-4). The observed deviation of fold axes may be the result of differential transport by later faulting, or of cross-folding. Cross-folding is suggested by the bimodal plunges of mesoscopic and inferred macroscopic folds, and the major change in structural trend to the southwest (Fig. IV-1). Symmetries of all mesoscopic folds are

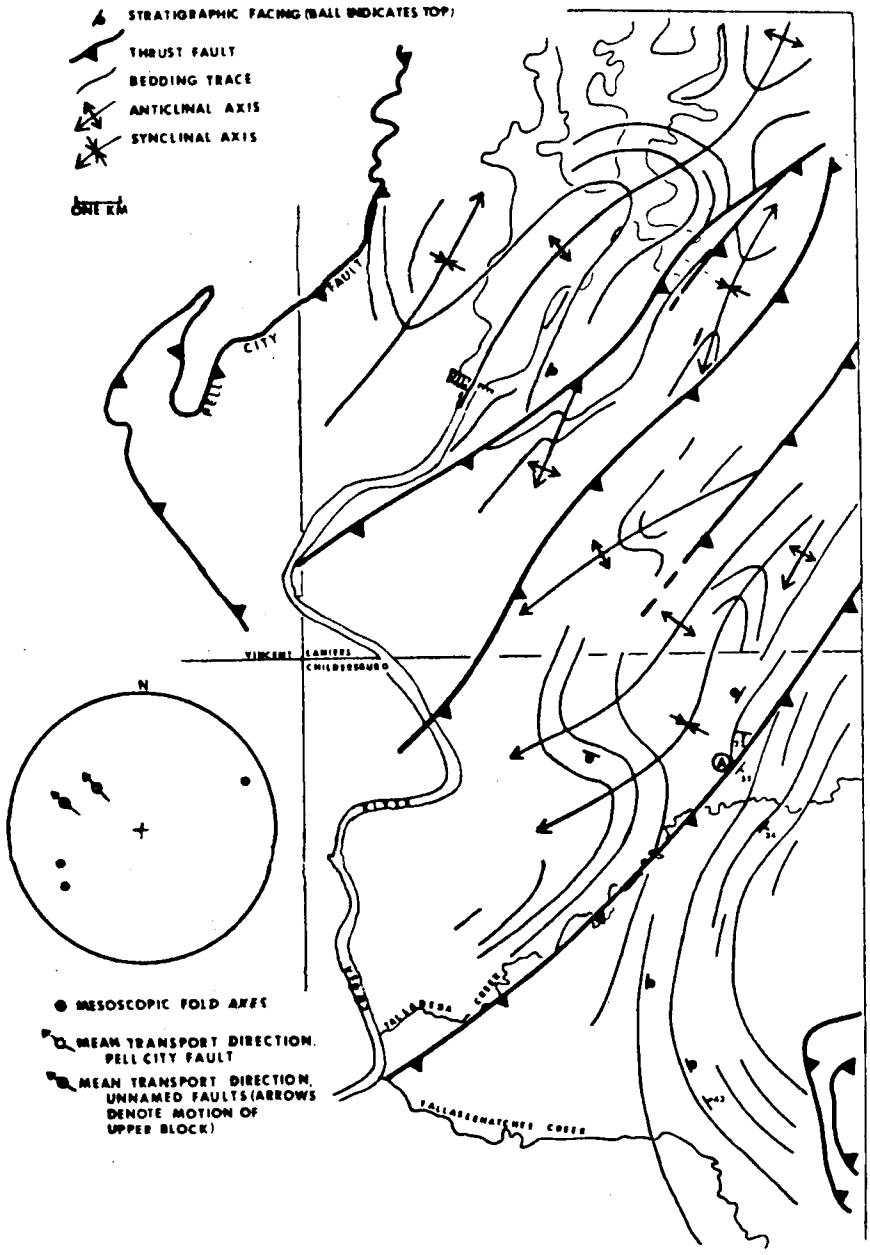

Figure IV-4. Geologic map of part of the Pell City thrust sheet. Childersburg, Laniers, and Vincent 7-1/2 minute quadrangles. Based on remotely-sensed data. Note discordance of bedding at (A). Anticline under dam verified by subsurface exploration. Pell City fault transport based on slickenside lineation in shales below fault. Transport direction on unnamed fault inferred from slickenside lineations of minor fractures of carbonates near faults. Fold plunge directions inferred from limited bed attitudes and facing criteria.

monoclinic, with steeper limbs facing northwest, indicating northwestward tectonic transport during the folding phase.

No faults could be unequivocally demonstrated because of poor exposure and general absence of marker beds. However, along one photolinear interpreted as a fault, bedding attitudes are strongly discordant across the boundary (Fig. IV-4). Bedding telescopes observed at one locality have b-kinematic axes parallel to surface traces of adjacent photolinears, and directions of tectonic transport consistent with interpretation of those photolinears as fault traces (Fig. IV-4). Kinematic axes and direction of transport are consistent with those of the Pell City fault to the northwest. As a further indication of the relative timing of tectonic events, bedding telescopes crosscut solution cleavage associated with folding.

V. CONCLUSIONS

Satellite and high-altitude aircraft imagery are useful in interpreting geologic structure of poorly exposed terranes. In areas where contrast between observable characteristics (spectral signature, residual soil type, vegetation cover) of lithologic units is low, utility of satellite imagery is greatly diminished. In these terranes, aircraft imagery is more desirable, since the greater resolution more readily permits nonquantitative intuitive interpretation. In addition, the scale of aircraft imagery more closely approximates the scale of macroscopic structures (less than 1 km square) likely to be of significance in local or regional structural interpretation.

As interpreted from imagery, mesoscopic fabric data, and regional outcrop patterns, the tectonic history of the Pell City fault block consisted of at least three, possibly four, phases. The first phase was a hypothetical event of thrust faulting (T_1). This phase is considered hypothetical because no mesoscopic fabric data have been found to demonstrate its existence, but in the Coosa deformed belt to the west, a thrusting phase antedates the first fold phase. The second phase (first demonstrable phase) consisted of development of monoclinic folds (F_1) vergent toward the northwest. The monoclinic symmetry and vergence suggest that these folds are superficial structures developed above a deeper transport zone (T_1?).

The third phase involved development of an extremely low angle (approximately 3° dip) thrust surface (T_2), the Pell City fault. Regional map patterns indicate that the Pell City thrust was discordant to both footwall and hanging wall structures, as it decapitates imbricate thrust sheets of the Coosa deformed belt in the footwall, and plunging fold structures in the hanging wall terminate downward against the fault surface (Fig. IV-4). Topographic and tonal anomalies (traces of inferred faults) within the Pell City block are discordant to fold structures, and bedding telescopes have the same orientation and sense of transport as shear surfaces associated with the Pell City fault (Fig. IV-4). The T_2 event is believed to consist of both major overthrusting along the master Pell City fault, and development of upward splays which dissected the folded hanging wall (Fig. IV-4).

Subsequent to T_2, both hanging wall and footwall structures were refolded about an east-plunging axis (F_2), expressed as an abrupt bend

in Coosa deformed belt structures, the trace of the Pell City fault, and folds within the Pell City block (Fig. IV-1, page 129). Regional outcrop patterns indicate that the Pell City fault has been folded above a subcropping thrust fault in the Wilsonville-Columbiana-Page Springs area (Fig. IV-1).

CHAPTER V

GEOLOGIC STRUCTURE AND EVOLUTION OF THE VALLEY AND RIDGE THRUST BELT IN ALABAMA

Foreland fold and thrust belts comprise the cratonic margin of most orogenic belts. In general, they are divisible into two classes: thick-skinned thrust belts, in which crystalline rocks and their sedimentary cover are deformed; and thin-skinned belts, in which only the sedimentary cover is affected (Rodgers, 1949). Published (Jacobeen and Kanes, 1974; Tegland, 1978; Cook et al., 1979b) and proprietary geophysical data support interpretation of the Appalachian Valley and Ridge as a thin-skinned belt.

Many of the early North American studies of thrust belt structure were conducted in the central and southern Appalachians. As early as 1843, H. D. Rogers and W. B. Rogers described the general features of the central Appalachian thrust belt (Rodgers, 1949). In subsequent years many of the concepts of the thin-skinned style were developed in the central and southern Appalachians, particularly underthrusting or back-thrusting (Gibson, 1893; Smith, 1893), ramping (Rich, 1934), and the general framework of the thrust belt (Rodgers, 1953).

The Canadian Rockies were intensively studied during the 1950s and 1960s, and the principles of thin-skinned thrusting conclusively demonstrated. Notable developments included the detailed description of thrust belt architecture from seismic data (Bally et al., 1966), and the

application of mesoscopic fabric studies to determine kinematic sequences (Roeder, 1960, 1967; Price, 1967).

In recent years interest in the structure of the Valley and Ridge of the southern Appalachians has increased. Most studies, however, have been of only local scope, with few areal syntheses (for example, Milici, 1975; Roeder, Gilbert and Witherspoon, 1978).

I. PREVIOUS RESEARCH

Most early studies of the geology of the Paleozoic rocks of Alabama were of local scope, although a preliminary geologic map was produced as early as 1894 (Smith, 1894). Butts (1926) compiled the first comprehensive study of the Paleozoic rocks of Alabama, and outlined the major structural and stratigraphic elements of the foreland. Most subsequent studies have merely refined or reinterpreted his work.

Simpson (1963) made the first quantitative study of Valley and Ridge structure by determining regional stress systems responsible for development of structures in the Birmingham iron district. Other workers have proposed developmental models for various geographic subareas of the thrust belt (Thomas and Drahovzal, 1974; Shaw, 1976; Gilbert, 1977b; Roeder and Witherspoon, 1977; Bearce, 1978).

II. METHODS OF STUDY

Surficial structure of the region can be subdivided into five major belts: the Warrior basin and platform, Birmingham anticlinorium-Cahaba synclinorium, Coosa synclinorium, Coosa deformed belt, and Pell City fault block (Fig. I-3, page 9). Smaller structures within each belt are

described in detail by Self et al. (1975). This study describes the structural evolution of the thrust belt by concentrating on the study of a single geotraverse (Fig. I-1, page 5).

Because geophysical data support the thin-skinned style, certain features have been assumed to be present, particularly an undeformed basement sloping gently toward the hinterland. Depth to crystalline basement is established only at one basement test well in Cullman County (Kidd and Neathery, 1976). This depth, together with established unit thicknesses and structure contour data from other wells, was used to establish probable depth to basement in the Warrior platform region. In the absence of suitable geophysical data, slope and elevation of the basement surface under the eastern Valley and Ridge was determined using modifications of a loaded elastic beam equation described by Hetenyi (1946). Downward projection of surface structure, compatible with known elements of the prevalent style (Rodgers, 1949; Bally et al., 1966; Roeder, 1967; Dahlstrom, 1970), was used to "fill" the resultant surface-to-basement-top void. Requirements imposed by geometric balancing (Dahlstrom, 1969; Hossack, 1979) were satisfied, although the total lack of deep subsurface data introduces probable errors. Local and regional kinematic sequences were developed from mesoscopic fabric data and cross-cutting relationships.

Basement Configuration

Balanced cross-sections are restricted by certain boundary conditions, particularly elevation and configuration of the lower boundary of deformation. The configuration of this boundary is of particular

significance in analyses of thin-skinned thrust belts, where the basal décollément represents a physical boundary below which deformation is absent (Rodgers, 1949). However, in most such terranes geophysical data adequate to define this boundary are unavailable or not within the public domain. Available geophysical data from other orogenic belts suggest that it is nonplanar, and that the slope is variable (Royse et al., 1975; R. A. Price, personal communication, 1980).

An alternative method is to formulate a mathematical model in which an elastic sheet (the lithosphere) overlying a plastic substrate (the aesthenosphere) is depressed by a load. Similar models have been successfully used to explain observed geometries of oceanic trench slopes (Watts and Talwani, 1974; Parsons and Molnar, 1976), orogenic foredeeps (Molnar et al., 1976), and Benioff zones (Karig et al., 1976). However, most such models have been based on simple mechanical and mathematical models.

The physical model for deflection of the lithosphere is analogous to several commonly encountered engineering applications, and the mathematical treatment of the model is well-established (Hetenyi, 1946; Nadai, 1963). The primary problems in application of a theoretical treatment to problems of crustal dynamics are the establishment of realistic boundary conditions and selection of an appropriate model. In application to trenches and orogenic foredeeps, calculations can be simplified by assumption of a two-dimensional model since these features are essentially linear rather than radially symmetric.

Parameters which affect choice of a model are configuration of the imposed load, and the extent of the loaded beam. Hetenyi (1946,

pp. 10-26) described the deflection of both infinite and finite beams under conditions of point-loading and under distributed loads of varying configuration. The majority of previous studies (Watts and Talwani, 1974; Parsons and Molnar, 1976; Molnar et al., 1976) have utilized the least complex model, which describes the deflection of a finite beam under point-loading of the extremity (Fig. V-1).

Molnar et al. (1976) successfully utilized this model to explain the configuration of the Ganga basin south of the Himalayas. In the Himalayas, overthrusting is localized along the Main Boundary Fault which soles near the base of the lithosphere (Fitch, 1970; Molnar et al., 1976). As a result of this discontinuity, the major part of the load is applied to the narrow zone of imbrication (~80 km) beneath the Lower Himalaya, approximating a point-load at the end of a finite beam (Fig. V-1). Similarly, Watts and Talwani (1974), and Parsons and Molnar (1976) used this model to explain the observed topography and geophysical characteristics of oceanic trenches and associated peripheral bulges.

However, two lines of evidence indicate that the applicability of this model is limited. Karig et al. (1976) compared and evaluated several models, including end-point-loading of a finite beam, and triangular-shaped distributed loads on both infinite and finite beams (Fig. V-2). Karig et al. (1976) concluded that all models are in close agreement near the periphery of the depression (area "X" of Fig. V-2). Calculations performed as part of this study indicated that a potential error of 16 percent results from use of an end-loading model. The results obtained by comparison of the distributed load models were in close agreement, particularly as the load was distributed over a greater length of the

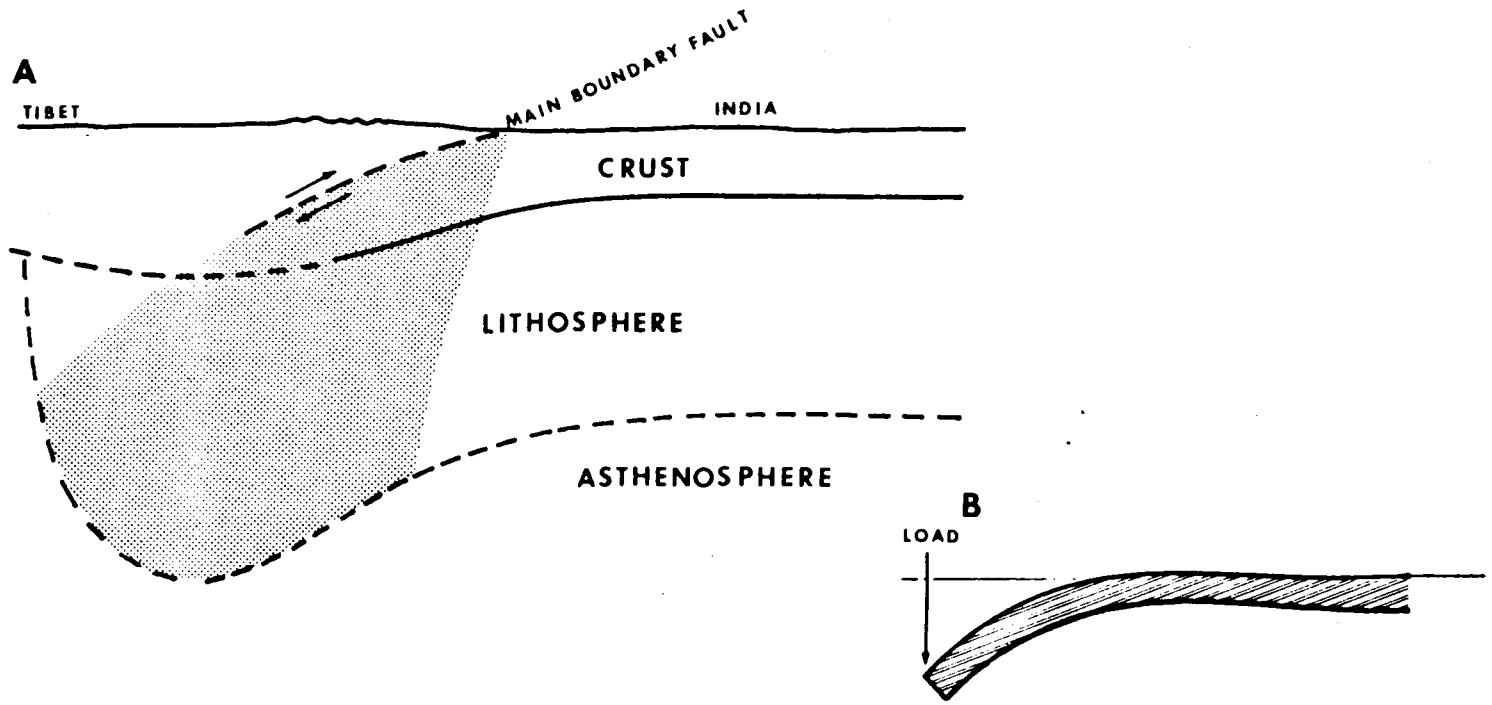

Figure V-1. Loading of a semi-infinite lithospheric plate in the Himalayan collisional orogenic belt (A), and the mechanical analogy of point-loading of the extremity of a finite beam (B). Note that as Tibet is thrust over the Indian subcontinent, the load is applied over a relatively small part of the beam (shaded area) relative to the beam thickness. Himalaya cross-section after Molnar et al. (1976); beam model after Hetenyi (1946).

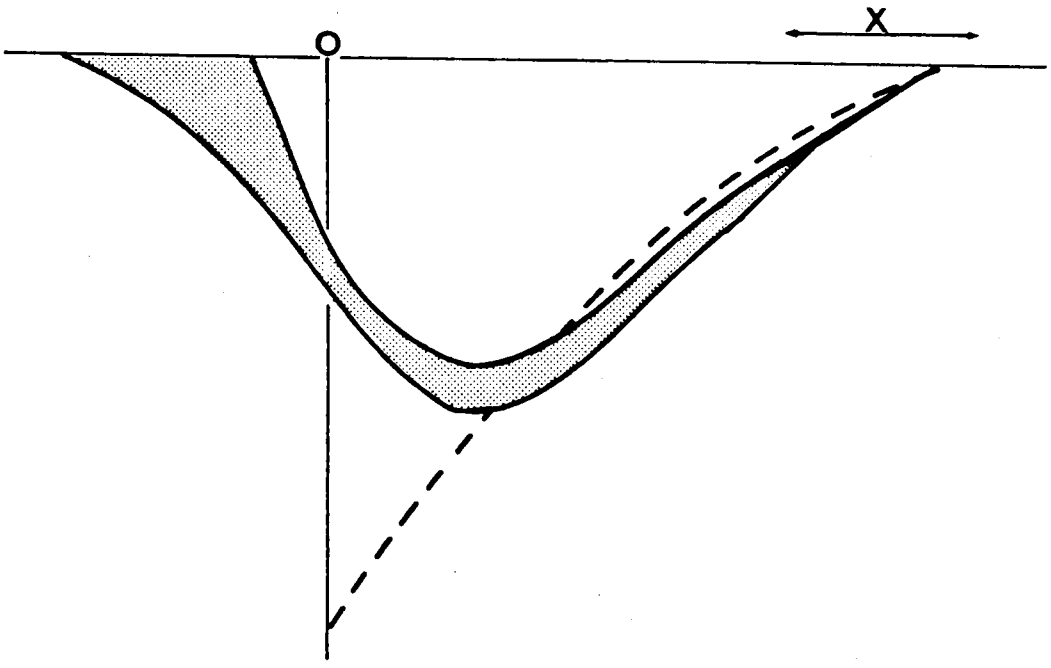

Figure V-2. Comparison of lower plate deflections predicted by various models. Configurations predicted by various distributed load models fall within the shaded area; configuration predicted by the end-loading model is shown as a dashed line. Note difference in the area of interest (X). Modified from Karig et al. (1976).

beam. However, the configuration of the loaded end of the finite beam was radically different for the point-load model (Fig. V-2). The increase in curvature of the point-loaded finite beam is at variance with geophysical observations of the lower plate configuration in various orogenic belts (for example, Fitch, 1970; Cook et al., 1979b). In this study the end-loading model was tested by simulation of the Grenville basement configuration under the southern Appalachians. Six depth-to-basement estimates from the plateau and exterior Valley and Ridge thrust belt were used to generate a theoretical basement-top curve. Based on the end-loading model, the upper surface of the Grenville basement beneath the Appalachian crystalline overthrust should be from 1360 to 1560 km below sea level, clearly an absurd result. Instead, the geophysical data (Cook et al., 1979b) place the boundary at an elevation of ∿15 km below sea level. Although the end-loading model is adequate to describe the lower plate configuration in the outer foreland of an orogen characterized by major overthrusting, the model is inapplicable to the interior of the belt.

A seismic reflection profile (COCORP) of the southern Appalachians exhibits a group of planar reflecting horizons which extend, albeit not continuously, from the subsurface of the Valley and Ridge beneath the crystalline Appalachians. This series of reflectors has been interpreted as the continuation of the Grenville cratonic basement and Paleozoic sedimentary cover underneath a major crystalline overthrust (Harris and Bayer, 1979; Cook et al., 1979b) (Fig. V-3). (Cook et al., 1979b, provided only a schematic cross-section; the section in Figure V-3 is from an unpublished interpretation by Dietrich Roeder.) This

interpretation is supported by the occurrence of windows exposing possible Paleozoic (Valley and Ridge equivalent) rocks in the interior of the crystalline belt (Jonas, 1929; Clarke, 1952; Sears et al., in press). The configuration of these reflectors suggests that the Grenville basement slopes gently ($\sim$1.5°) toward the hinterland under the exterior thrust belt, but flattens to a subhorizontal attitude under the interior crystalline belt (Fig. V-3). This configuration is similar to that produced by distributed loading of either an infinite or finite beam (Hetenyi, 1946; Nadai, 1963; Karig, et al., 1976), suggesting a greater applicability of distributed load models.

The choice of load configuration is of necessity arbitrary, but constrained within certain limits by available geophysical data. Seismic data (COCORP) suggests that the lower boundary of the crystalline overthrust (the load) dips gently east, flattening to near horizontal under the interior of the orogen (Fig. V-3). As a result, the upper plate can be described as a combination of simple geometric shapes (Fig. V-3). Several configurations, two of which are shown in Figure V-3, approximate a crustal structure model based on interpretation of gravity, heat flow and seismic velocity data from the southernmost Appalachians (Wielchowsky, ms.).

Several explanations for this configuration are possible; the most likely is that it is a result of isostatic adjustment in compensation for postorogenic uplift and erosion. In modern collision systems, the collision front progrades downward and into the lower plate, resulting in a wedge-shaped leading edge for the upper plate, bounded at the base by a thrust dipping steeply toward the hinterland (Fig. V-1). This results

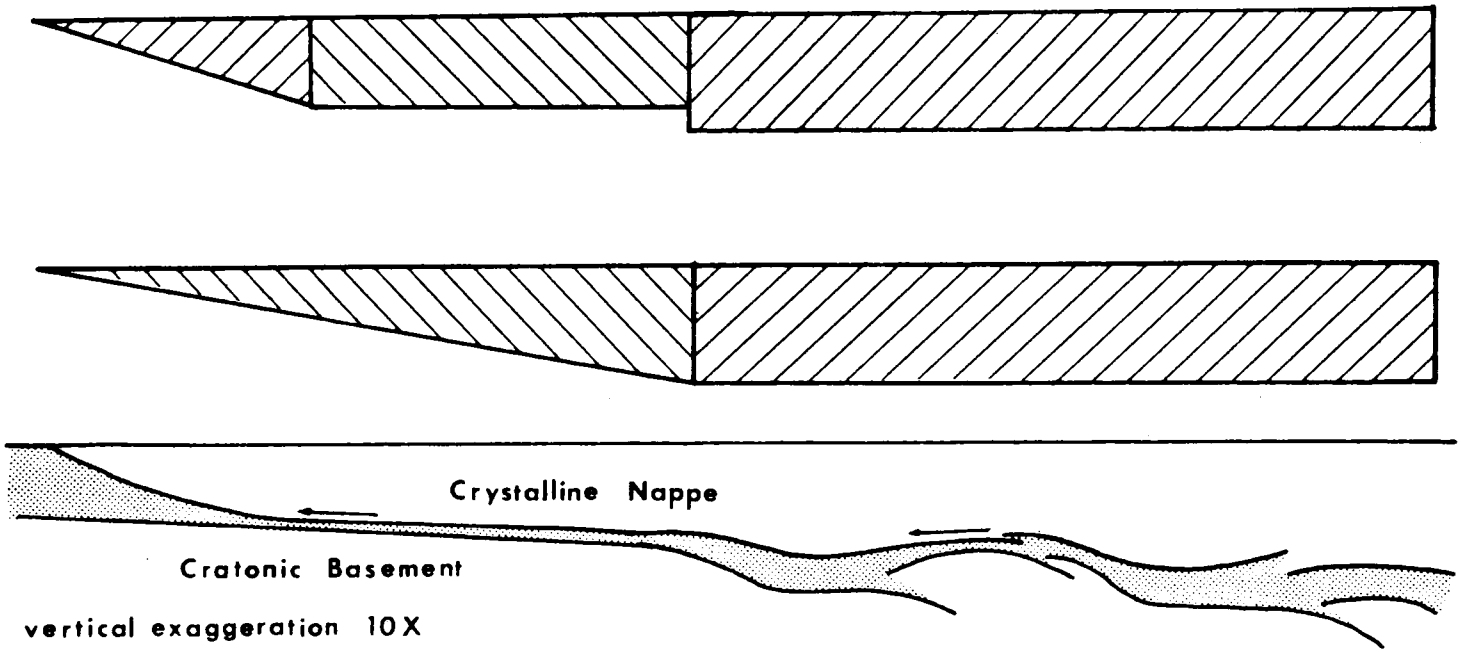

Figure V-3. Configuration of the southern Appalachian crystalline overthrust. The crystalline nappe has been thrust at least 260 kilometers over the cratonic basement along a transport zone in the Paleozoic cover of the craton (shaded). The load thus imposed upon the cratonic basement can be resolved as a combination of simple geometric shapes (top). (Uppermost configuration preferred in this study.) Cross-section modified from Dietrich Roeder (unpublished).

in large-scale overthrusting of lower-plate crystalline basement over the sedimentary cover of the foreland, as on the Main Central Thrust of the Himalayas (Gansser, 1964). Uplift resulting from translation along the basal fault maintains the topographic high against erosion. With cessation of uplift, the excess topography is removed by erosion, resulting in unloading of the beam. Uplift velocity resulting from bouyancy of the lithosphere is proportional to magnitude of the original load, with maximum rate of uplift occurring in the areas of maximum deflection (Nadai, 1963). The result of this differential uplift is the development of a flattened zone under the area of maximum loading (Lougee, 1953; Nadai, 1963). Differential uplift is still in progress underneath the southern Appalachians, as indicated by northeast-striking negative gravitational anomalies of up to 40 milligals underneath the central crystalline belt, decreasing toward the foreland (data by Woollard in Steinhart and Meyer, 1961).

Selection between an infinite and a finite plate model cannot be facilitated by inference from geophysical data, since the extent of the lower plate is undetermined, and both were considered in this study. If a finite plate model is utilized, the probable position of the distal end is marked by the regional gravity gradient beneath the crystalline rocks in Georgia. However, since the lower plate may consist, in part, of oceanic lithosphere extending beyond this point, infinite plate models were also evaluated.

Each of the models described by Hetenyi (1946) was evaluated, using both assumed and mathematically derived values for the various parameters (Fig. V-4). Analysis demonstrated that the best fit to observed

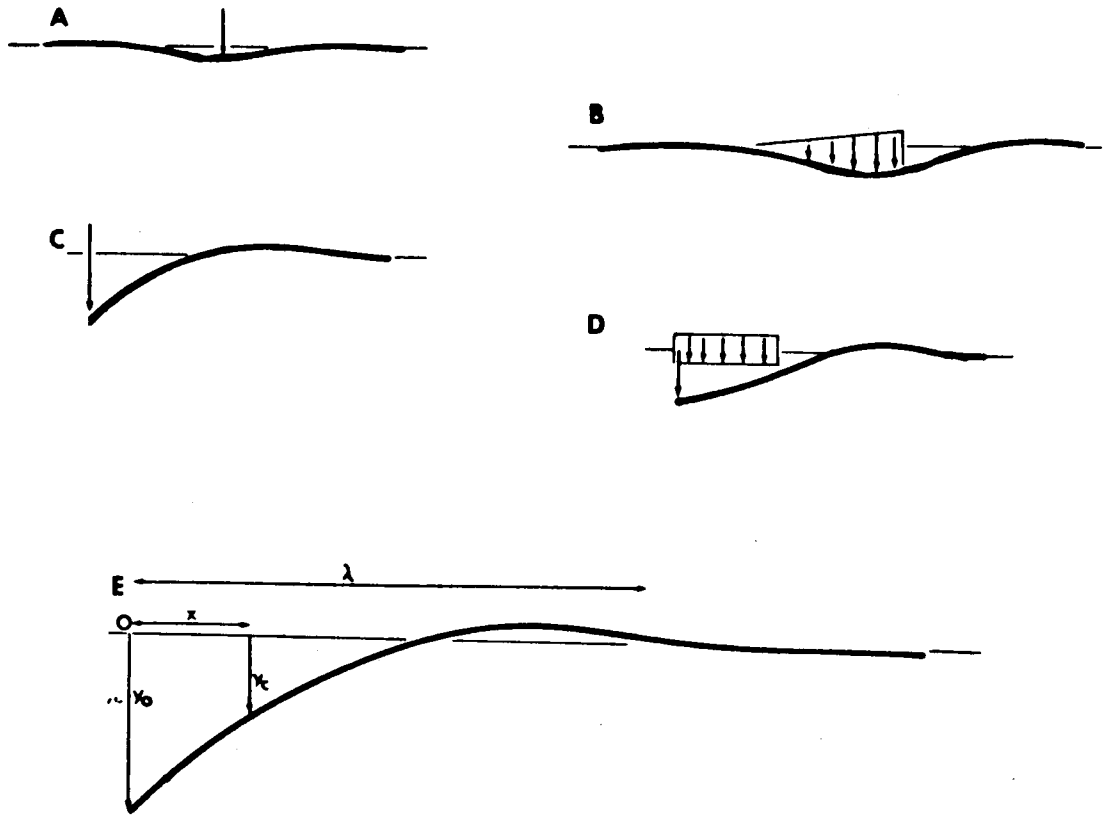

Figure V-4. A-D. Mechanical analogies of mathematical models proposed by Hetenyi (1946) including point loading of infinite (A) and finite (C) beams, and distributed loading of infinite (B) and finite (D) beams. E. Explanation of terms used in equations (1)-(4) in text: y_0 = vertical deflection at some distance (x) from origin; λ is the characteristic of the system, defined as λ = wavelength^{-1}, or λ^4 = k/4D, where k = (density of material below beam - density of material above), D is the flexural rigidity of the beam in Newton meters, P is mass of the load.

nonpenetrative nature of deformation and poor exposure the data base is poor. Mesoscopic fabric elements, useful in determining the sequence of events over limited areas, are of limited utility in determining relative or absolute chronology of regional kinematic events since the locus of deformation migrates with time. Regional correlation of kinematic sequences would necessitate the assumption that similar styles of deformation are of the same age, although they are demonstrably diachronous (Roeder, Gilbert and Witherspoon, 1978). In this study, mesoscopic fabrics were used to establish kinematic sequences only in local areas.

In areas where adequate mesoscopic fabric data are available, relationships indicate that the major regional thrusts represent the final phase of a local thrust-fold-thrust (T_1-F-T_2) or thrust-thrust (T_1-T_2) sequence. The T_1-T_2 sequences may contain a problematical folding phase not expressed by mesoscopic fabric elements.

The T_1-F-T_2 sequence is best illustrated by outcrops of the Coosa deformed belt adjacent to the Pell City fault, where the T_1 phase is expressed as distributive but nonpenetrative shearing. Shales in the Floyd-Parkwood are pervasively sheared, and shearing of thin beds and laminae of sandstone has resulted in development of boudins, mullions, and transposition folds (Fig. V-5A). Medium-bedded to massive sandstone sequences are not pervasively sheared, but are disrupted into lenticular boudins and mullions several meters to tens of meters across. Tectonic slices of pre-Floyd carbonates embedded within the deformed Floyd-Parkwood are continuous over long distances, but exhibit evidence of anisotropic penetrative shear in the form of deformed crinoid ossicles, brachiopods, ooids, and intraclasts (Fig. V-5B).

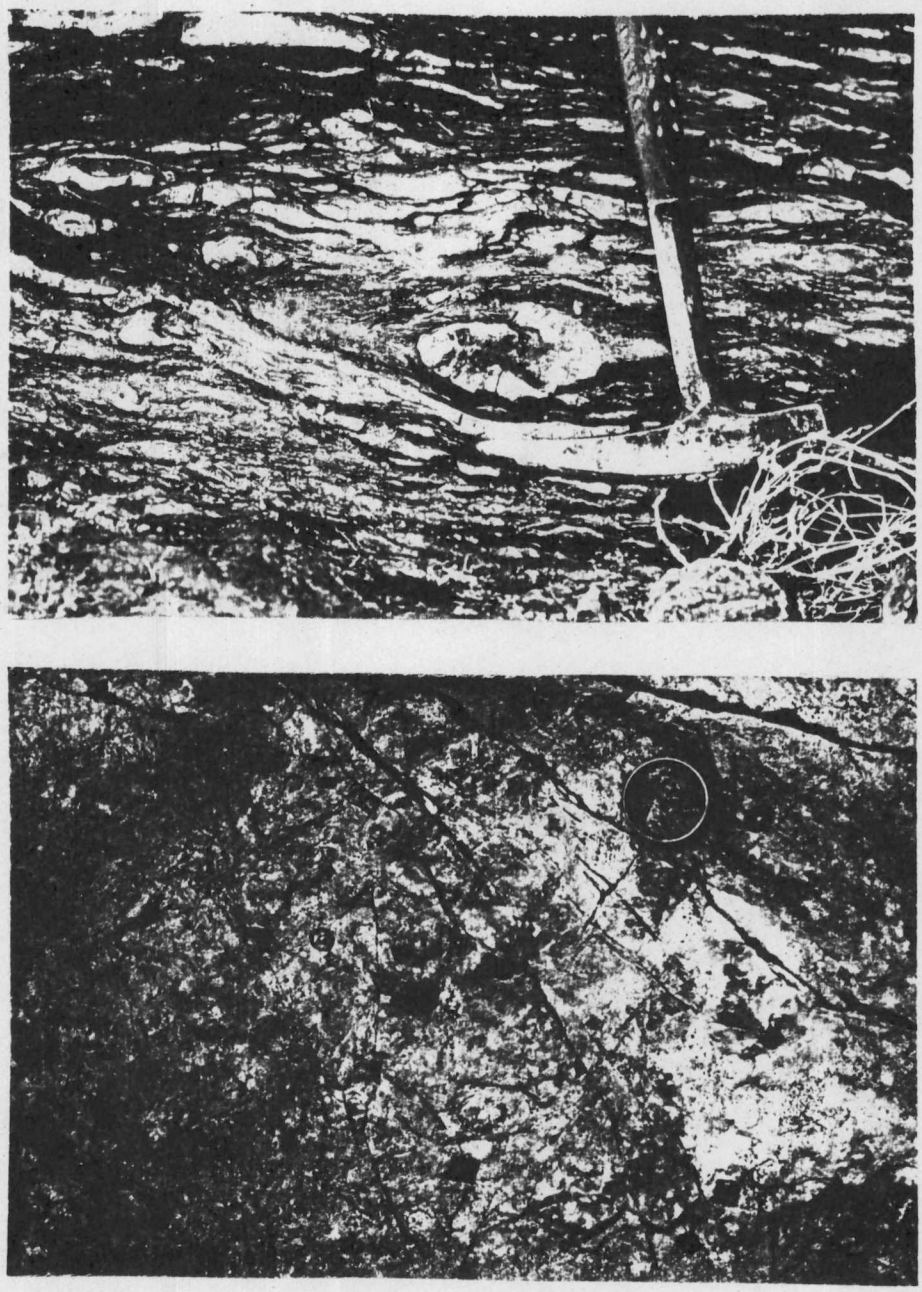

Figure V-5. Mesoscopic fabric elements, Coosa deformed belt. A. Apparent bedding in Mississippian shales of the Coosa deformed belt is boudins and mullions transposed by shearing. Nodule of sandstone above point of hammer has been rolled into a spiral by counterclockwise shearing. B. Competent units have been anisotropically sheared. Note transverse and longitudinal sections of crinoi ossicles exhibiting various degrees of strain. Fort Payne Chert, Shelby County. Coin is 1.8 cm in diameter.

T_1 shear fabrics are folded about northeast-trending doubly-plunging axes to produce small scale tight to isoclinal orthorhombic and monoclinic folds (Fig. V-6). An axial plane cleavage is locally developed in more calcareous units of the Floyd (Fig. V-6).

The final, T_2, phase is characterized by development of widely spaced subhorizontal faults of small displacements (Figs. V-6, V-7), which disrupt massive sandstone units, crosscut cleavage, and decapitate folds. These late faults are coplanar with the overlying Pell City fault, which decapitates major Coosa deformed belt structures. Three dimensional relationships of these fabric elements are illustrated in Figure V-8.

The T_1-T_2 sequence is best illustrated by fabrics in the footwall of the Opossum Valley fault north of Birmingham (Fig. V-9). Conjugate sets of bedding telescopes indicate initial southeastward (T_1) transport of Upper Cambrian Knox Group carbonates over Silurian Red Mountain clastics. These telescopes have in turn been rotated and folded by a group of gently east-dipping monoclinic folds associated with a splay off the northwest vergent (T_2) Opossum Valley fault (Fig. V-9). Three dimensional relationships are shown in Figure V-10.

Regional Kinematic Relationships

Determinations of regional kinematic relationships are based on observations of cross-cutting relationships of regional structures (Plate II). These observations indicate that in general the locus of active thrusting migrated toward the foreland by a process of downward shifting of the basal décollément in the stratigraphic pile. Although tectonic models have been proposed to suggest migration of deformation

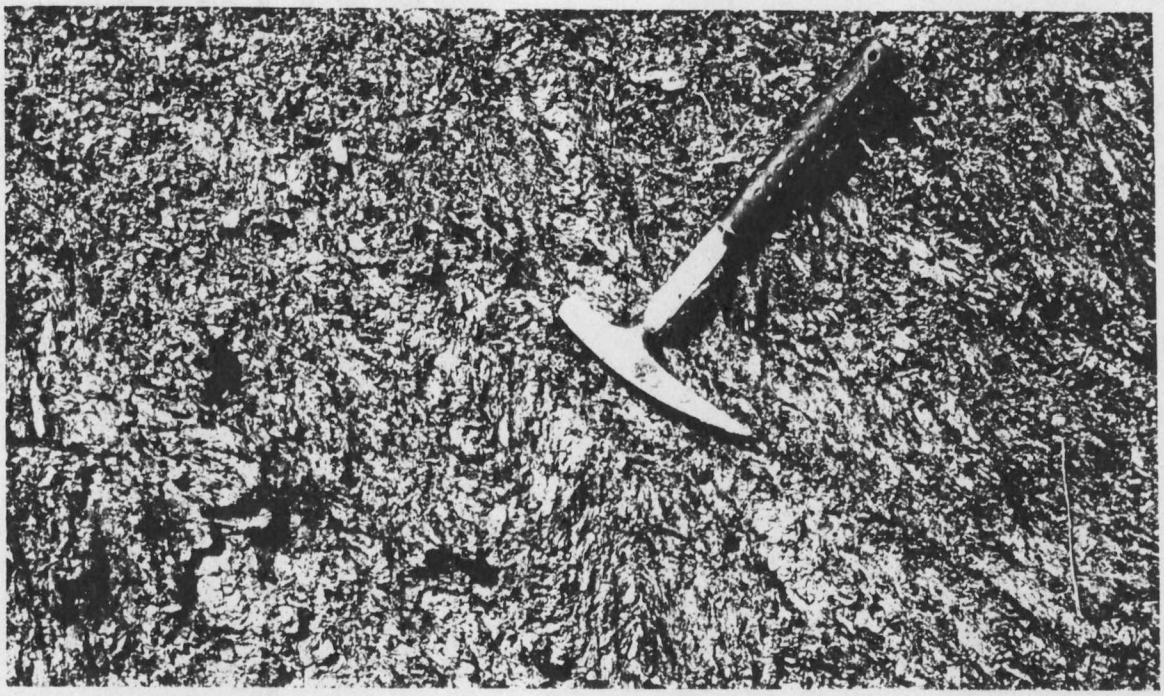

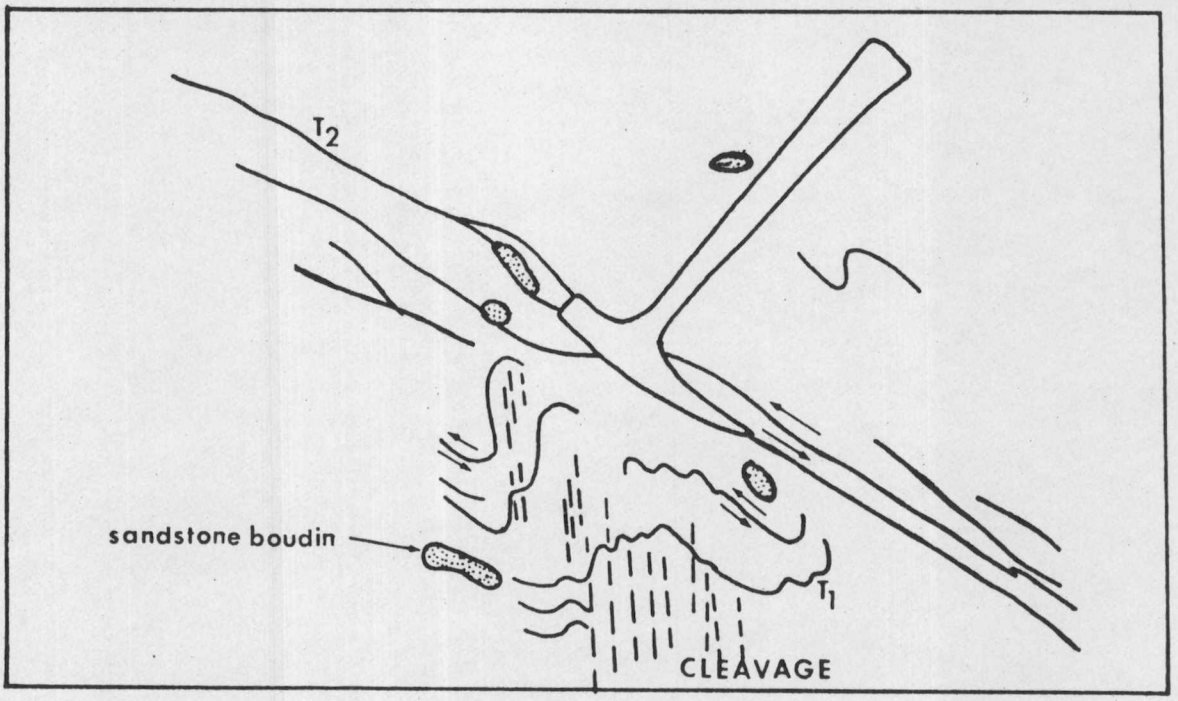

Figure V-6. T_1-F-T_2 kinematic sequence, Glover Mountain, Shelby County. Early shear surfaces (T_1) are folded and nonpenetrative cleavage developed. Folds and cleavage crosscut by T_2 surfaces coplanar to overlying Pell City fault.

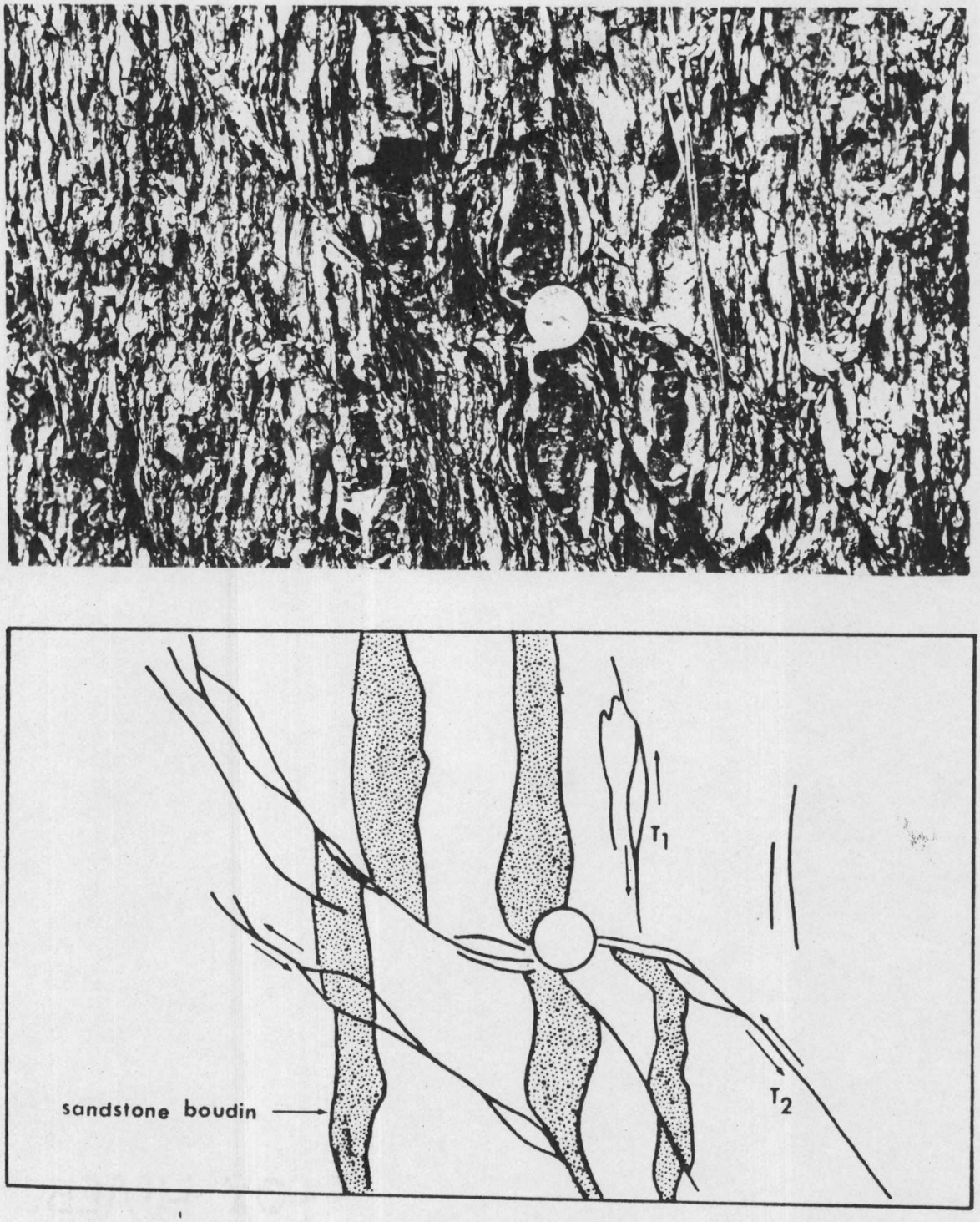

Figure V-7. T_1-T_2 kinematic sequence, Kelly Creek, Shelby County. Where T_1 planes are at a high angle to T_2 compression, orthorhombic and monoclinic folds are poorly developed or absent. T_2 disrupts sandstone bodies up to 2 m thick. Coin is 2.4 cm in diameter.

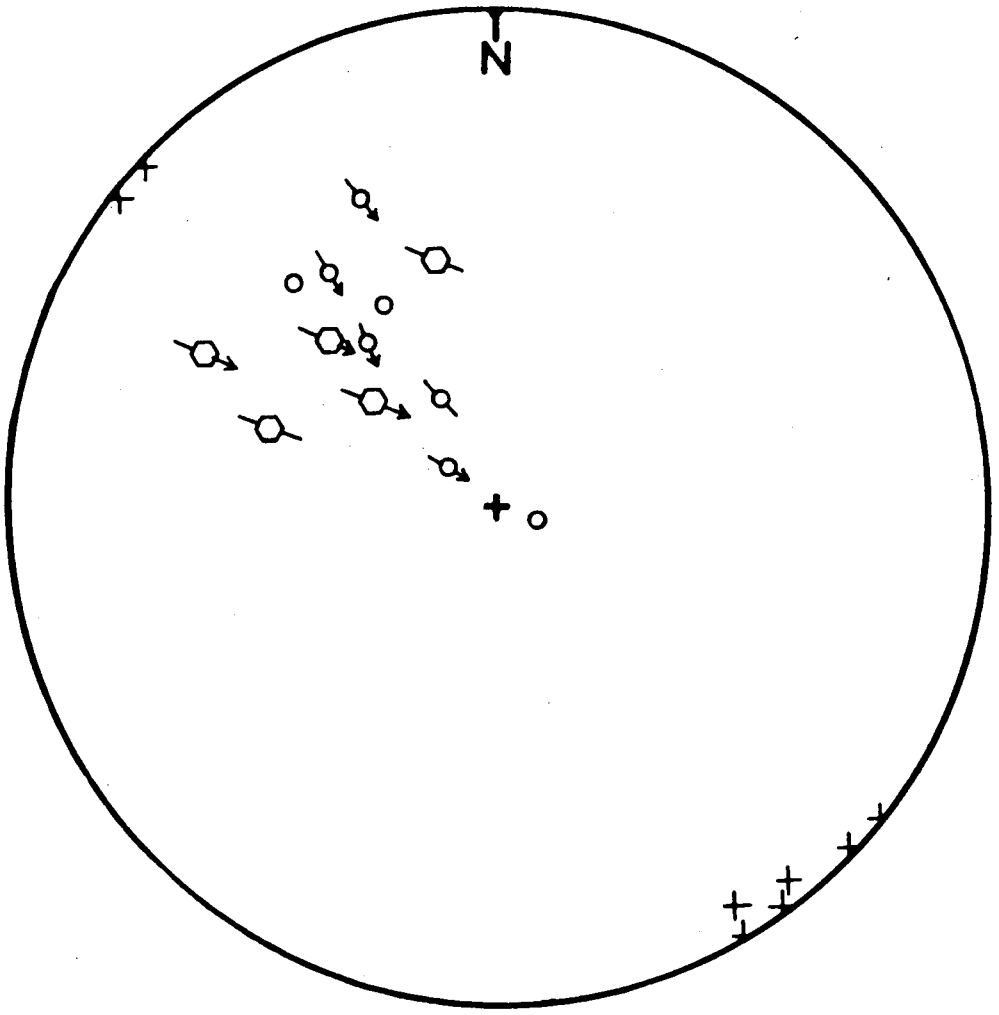

Figure V-8. Three-dimensional relationships of mesoscopic fabric elements, Glover Mountain. Circles-poles to S_1 shearing subfabrics; hexagons-poles to S_2 shearing subfabric; cross-poles to F_1 fold/ cleavage subfabric. Arrows represent relative motion of lower block.

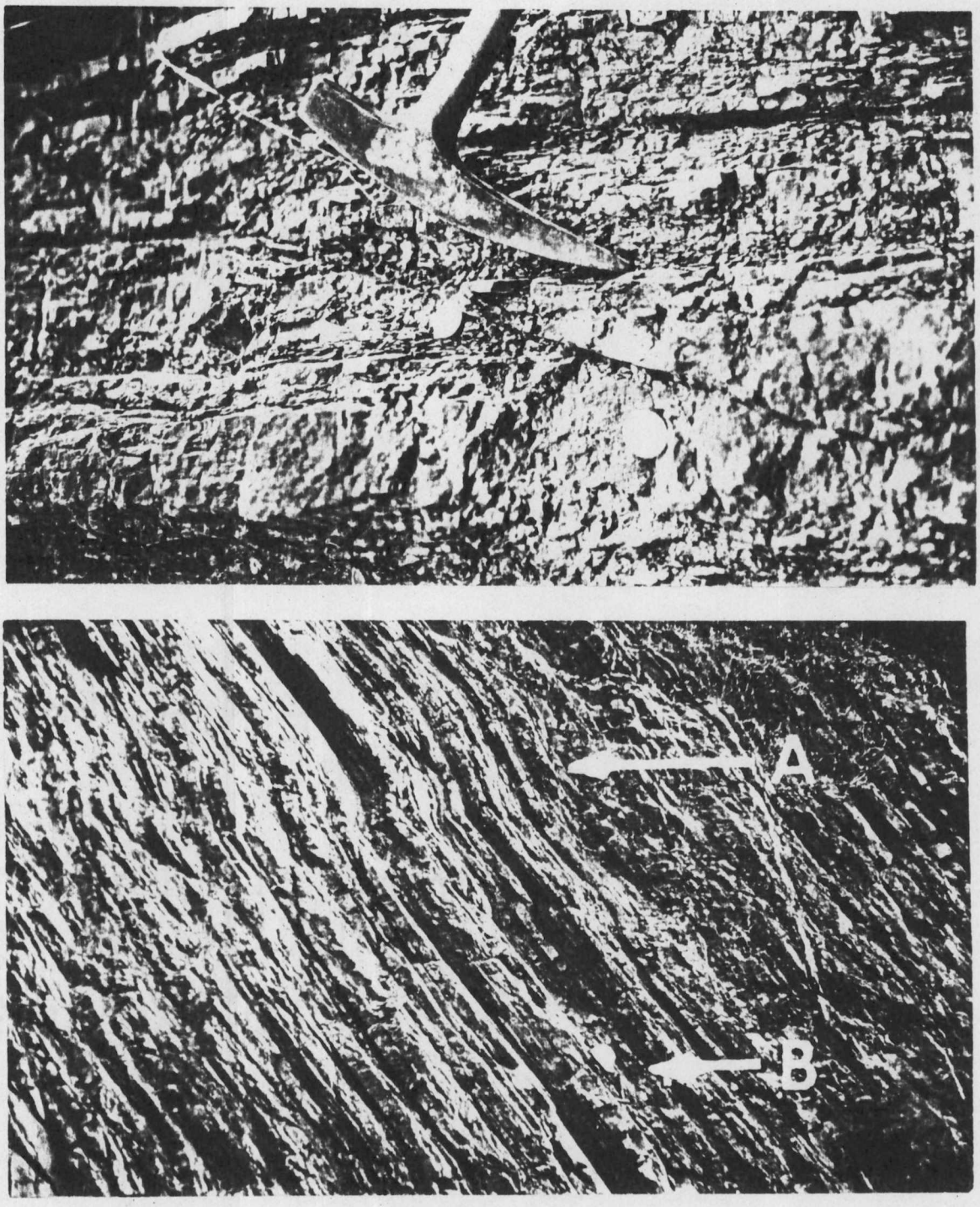

Figure V-9. T_1-T_2 kinematic sequence, Rocky Row, Jefferson County.
A. Bedding telescopes associated with early SE vergent thrusting.
B. T_1 bedding telescopes (A) are folded about NW vergent monoclinic folds developed by T_2 thrusting (Opossum Valley fault). Scale indicated by helmet and hammer (B).

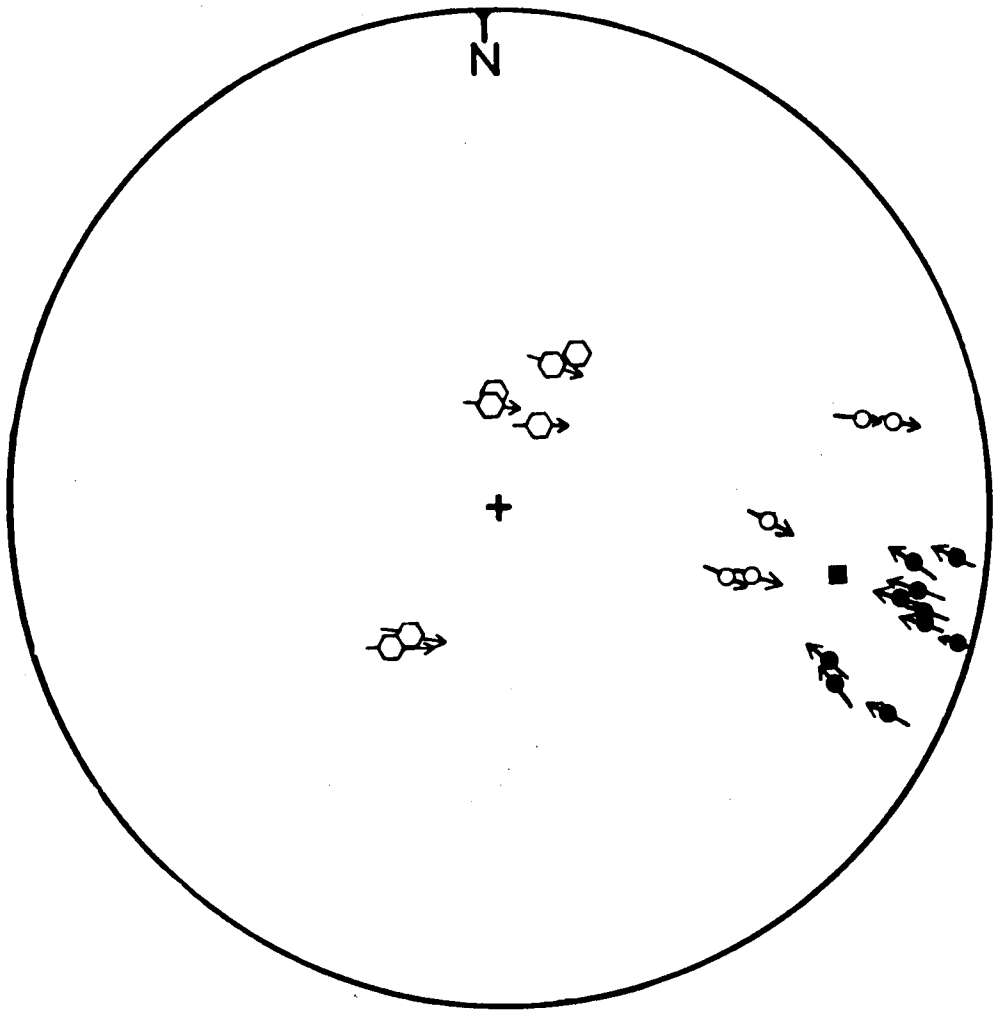

Figure V-10. Three-dimensional relationships of mesoscopic fabric elements, Rocky Row. Black discs-poles to T_1 (backthrust)-associated bedding telescopes; circles-poles to bedding telescopes conjugate to T_1; hexagons-poles to kink folds/faults associated with T_2 thrusting. Arrows represent relative motion of lower block. Square-mean bedding attitude.

of deformation toward the hinterland (Milici, 1975), the exterior progradation trend is compatible with observed structural relationships and with generally accepted models of thrust mechanics discussed in detail by Elliott (1976), Chapple (1978), and Roeder, Gilbert and Witherspoon (1978).

III. PREOROGENIC DEFORMATION

Some previous investigators have proposed that folding began in the Valley and Ridge during Middle Ordovician time and continued through the Pennsylvanian, based on regional variations in thickness of units preserved between unconformities (Thomas et al., 1970; Thomas et al., 1979), and penecontemporaneous faults of Devonian and Mississippian age dipping away from the crest of the Birmingham anticlinorium (Thomas, 1968; Thomas et al., 1970).

Variations in thickness of units between unconformities is a questionable criterion, since it may result from differential erosion below the upper unconformity, or relief on the lower unconformity, or both. Detailed stratigraphic or lithostratigraphic correlations to document thinning of individual units within the sequences bounded by unconformities are lacking, as are subsurface data to fully document areal isopach-structure relationships. Regional variations in interval thickness may be the result of localized intrabasin uplift and subsidence (see Chapter III), but the data are insufficient to systematically evaluate this possibility.

Known prethrust normal faults are of two types: soft-sediment growth faults restricted to the Mississippian Pride Mountain Shale-Hartselle

Sandstone contact, and growth faults affecting Silurian through Lower Mississippian (Fort Payne) strata. The former group of faults results from soft sediment flow of Pride Mountain shales, resulting in growth faulting of the overlying Hartselle Sandstone (Thomas, 1968). This type of faulting does not require a tectonic slope in order to develop, but is a sediment compaction phenomenon (Crans et al., 1980; Elliott and Ladipo, 1981).

A simple fault of the second type, located on the southeast flank of the Birmingham anticlinorium, disrupts Silurian strata, but was active only during the Devonian, as indicated by thickening of units on the downthrown side (Thomas et al., 1970; Thomas et al., 1979). A similar fault, located on the northwest flank, was discovered during this study. This fault disrupts the Silurian, but was active only during the earliest Mississippian; beds in the lower Fort Payne Chert thicken across the fault, but higher beds are unaffected. When bedding is restored to horizontal, the fault plane dips parallel to the strike of the anticlinorium. Displacement on both faults decreases downward into the shaly lower Red Mountain Formation, suggesting that they resulted from compaction of Silurian shales during deposition of Devonian and Mississippian strata.

The geometric relationship of both faults to the Birmingham anticlinorium demonstrates that they are distinct from normal faults associated with folding of the anticlinorium, and do not provide unequivocal evidence for early folding (Fig. V-11).

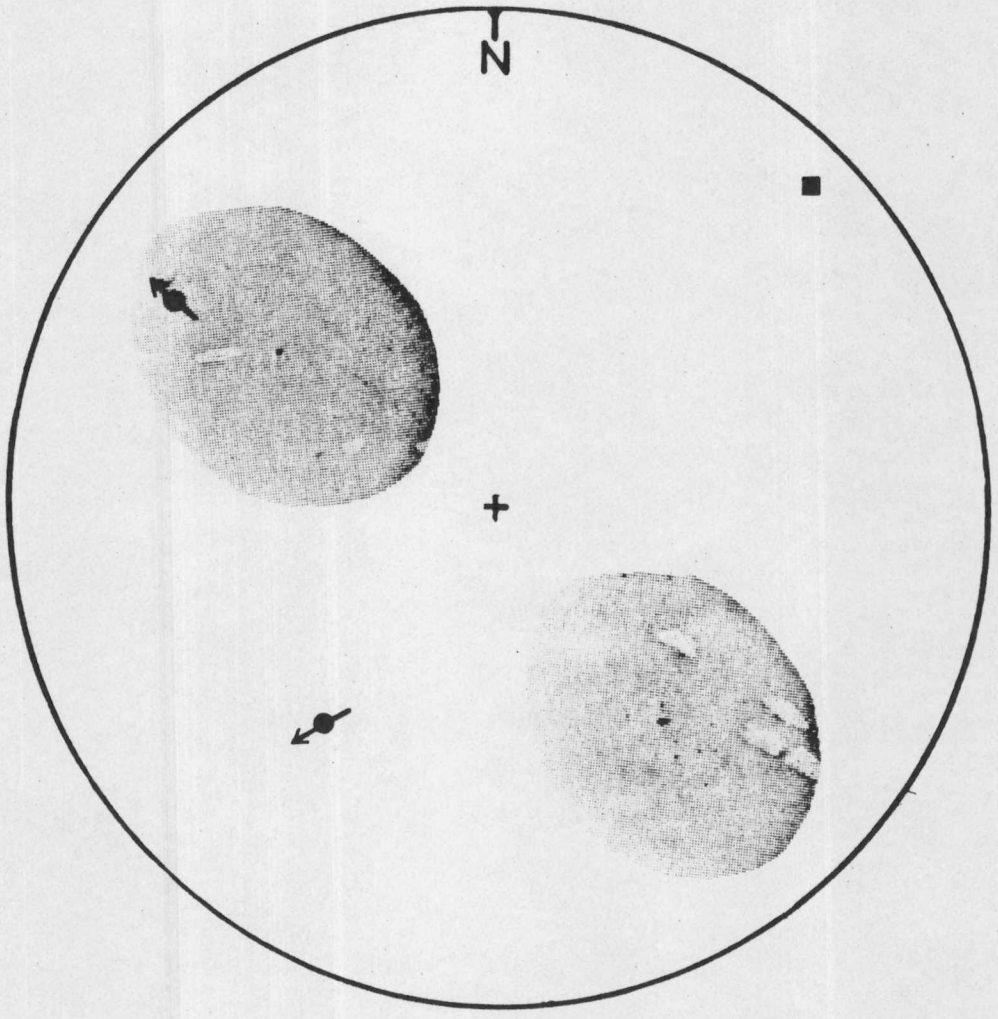

Figure V-11. Orientation of prethrust growth faults, Birmingham anticlinorium. Black discs are poles to fault surface, arrows represent motion of lower block. Shaded zones are fields expected for faults associated with flexure about axis of anticline (black square).

IV. STRUCTURAL EVOLUTION

The balanced cross-section constructed from data compiled during this study is presented as cross-section 7 in Plate II, along with a palinspastic restoration based on a minimum strain value determined by assuming minimum erosion from the leading edge of each thrust sheet. The total shortening determined for the thrust belt as a whole, ∿55%, is conservative, but compatible with that of other thrust belts.

Kinematic relationships based on mesoscopic fabrics and cross-cutting relationships of regional structures (Plate I) have been used to construct a series of stepwise cross-sections depicting the evolution of the thrust belt (Plate II). Upper case letters in parentheses in the text refer to localities shown in Plate II. Alternative interpretations are, of course, possible, based on differing interpretations of gross structure or kinematic sequence. Plate II also contains equal area stereographic plots of mesoscopic fabrics illustrating the development and relative timing of various structures, and the tectonic transport direction inferred from mesoscopic fabric analysis.

Fabrics and subfabrics were used to define strain axes from which movement in three dimensional space may be inferred. In this system the "a" axis is the direction of maximum elongation; "c," the axis of maximum shortening; and "b" the axis of minimum strain. The term transport direction is used to describe the azimuthal direction of the displacement of major rock masses. Because the zone of deformation is confined by the basement top and the rock-air interface, and because most strain is accommodated by thrusting, the transport direction provides a

simple but significant description of the strain history of the thrust belt.

The tectonic setting is that of a foredeep created by overthrusting of a major crystalline sheet (Roeder, Wielchowsky and Gilbert, 1978; Cook et al., 1979b; Sears et al., in press). In all sections, the hypothetical land surface is based either on probable slope of depositional surfaces in the foreland (Phases 1 through 4) or proportionate amounts of erosion implied by progression from Phase 3 to Phase 7 (present land surface). Estimates of maximum burial depth were cross-checked using data on color alteration indices of Middle Ordovician conodonts as an indicator of overburden thickness (Epstein et al., 1977). Maximum thickness of the foredeep fill was estimated from overburden thickness required to produce coal diagenesis at a low geothermal gradient of 2° to 3°C/100 m (Teichmuller and Teichmuller, 1979).

Phase 1, at approximately 325 mybp, represents the predeformational configuration of the foredeep, initiated by thrusting of a major crystalline nappe onto the shelf edge at a point beyond the southeast end of the cross-section. The margin of the stable foreland platform, marked by the easternmost extent of the shallow-water Hartselle, and Bangor facies, was near (A). The foredeep margin sloped gently eastward, and debris flows off the platform edge transported carbonate debris as far southeast as (B). Eastward slope of the basement and cover is hypothetical, based on the crustal loading model. Water depth and thickness of the foredeep sediments southeast of (B) are conjectural, and are based on several assumptions, including (1) a nearly flat basin floor, allowing transport of easterly-derived sediments by bottom currents; (2) a considerable

distance from the eastern basin margin, since mass flow deposits of terrigenous clastics, are absent; and (3) inferred basement slope. Stratigraphic control is lacking, and an alternative interpretation is that the easternmost basin (C) was already occupied by prodeltaic and deltaic clastics. Pinchout of the Fort Payne Chert at (D) marks the southeastern margin of the old epeiric sea.

During Phase 2 (∿320 mybp), thrusting above a décollément at the basement top resulted in imbrication of the cover. Transport of the Conasauga-Knox resulted in low-amplitude folding (E), not shown at the scale of the cross-section; those folds are in the upper block of the Pell City fault, and predate that fault (Fig. IV-4, page 139). Present orientation of these early structures in the upper block of the Pell City fault indicate a mean transport direction of 316° (Plate II). Ramping of the décollément into the lower foredeep fill caused superficial folding of the fill (F), indicated by systematic thinning of stratigraphic intervals over folds in the future Coosa synclinorium. At this time the foredeep was almost completely filled with sediment, and no deep-water (> 100 m) basins persisted west of (F). Complex ramping (G), which displaced lower Cambrian lithologies onto the Knox Group of the Pell City block, is assigned to this phase, as it postdates folding (E) but predates later thrusting of the Pell City block.

During Phase 3 (∿310 mybp), major deformation occurred in what is now the eastern Valley and Ridge. The décollément at the base of the foredeep fill developed into a large-scale fault duplex (H) of a type described by Dahlstrom (1970). Splays from the basal fault of this duplex plucked slices of variable stratigraphy off the underlying autochthon, and

tectonically emplaced them into the sheared foredeep fill. The carbonate slices within the Coosa deformed belt are the remnants of these slices, and distributive shearing (Fig. V-5, page 158) of the Coosa deformed belt is associated with this period of thrusting. Tectonic transport was in the direction 317° to 324°, as indicated by slickenside lineations on shear surfaces and axial surfaces of monoclinic folds (Plate II). During transport, tectonic slices of carbonate within the duplex underwent downdip lengthening in the direction of transport indicated by the elongation axes of deformed crinoid ossicles (Fig. V-5) and by conjugate fault systems restricted to the carbonate slices (Plate II).

Following thrusting, shear surfaces and transposed bedding were locally folded into upright monoclinic and orthorhombic folds with axial planar solution cleavage in calcareous rocks (Fig. V-6, page 160). The transition from shearing to folding may have resulted from a lessening of overburden pressure (Roeder, 1960) or loss of fluid over-pressure in shales of the décollément (Hubbert and Rubey, 1959). The transport direction during folding was the same as that which prevailed during thrusting (Plate II).

Locally, thrusting is postdated by shortening parallel to the b axis of thrusting. This shortening was accommodated by conjugate monoclinic folding of the shear surfaces about axes which plunge down the dip of the shear surfaces (Plate II). The two types of folds were not observed in combination, and their temporal relationships are therefore unknown.

By Phase 3 the entire foreland basin, west of (I), was occupied by the Pottsville fluvial system. The rapid influx of coarse-grained lower Paleozoic and crystalline debris (J) into the Pottsville was related to

erosion from the leading edges of thrust sheets involving rocks of both the foredeep and the orogenic core. Conglomerate beds in the upper Pottsville contain clasts of distinctive Knox Group and lower Pottsville lithologies, as well as clasts of vein quartz, quartzite, gneiss, phyllite, schist, and rhyodacite porphyry (Gilbert, 1976).

During Phase 4 Coosa-deformed belt structures associated with thrusting and folding above a décollément at the Floyd level were decapitated by the Pell City fault (K), which is discordant to structure in both the upper and lower blocks (Plate I, Plate II). The Pell City fault is unusual in that it does not cut up section toward the foreland. The leading edge of the upper block contains stratigraphic units as low as the Rome Formation (Fig. IV-1, page 129), but downdip the Fort McClellan and smaller windows (Fig. IV-1; Plate I) are framed entirely by the Knox Group. The upper block of the Pell City fault probably represents the upper levels of an older, internally deformed thrust sheet sheared off by later thrusting. In Plate II, the Pell City fault is depicted as a splay off the lower décollément which dissects an older allochthon.

Decapitation of Coosa-deformed belt structures by the Pell City fault produced the lower angle fold-discordant faults of the Coosa-deformed belt (T_2 of Figures V-6, page 160, and V-7, page 161). Transport direction along the Pell City fault was slightly more westerly (290° to 318°) than previous transport directions, as indicated by slickenside lineations in shales below the fault (Plate II).

Older faults which thrust Lower Cambrian clastics atop the Knox (G) were carried "piggyback" on the upper block of the Pell City fault.

The Opossum Valley and Helena faults postdate the Yellow Leaf, Coal City, Hog Pen Branch, and Straight Mountain-Rocky Row fault systems. However, the relative chronology in the latter group of faults cannot be determined. In the absence of any data from which a relative chronology might be determined, it has been assumed that active deformation migrated toward the foreland, producing the Yellow Leaf (L), Coal City (M), Hog Pen Branch (N), and Rocky Row (O) faults as shown in Phase 5.

The cross-section (Plate II) represents an area where displacement on the Yellow Leaf fault is relatively small, that on the Coal City fault greater. Relative displacement on the Coal City decreases southwestward in central Shelby County, while displacement on the Yellow Leaf and Dry Creek faults decreases northeastward in the same area (Plate I). The overlap on this pair of faults represents a simple transfer zone of the type described by Dahlstrom (1977) in which transport above a basal décollément is shared between two en échelon listric thrusts, and transport is accommodated by a single fault beyond the zone of overlap. As pointed out by Dahlstrom (1977), this would require that the Yellow Leaf and Coal City faults developed nearly simultaneously.

Transport direction on the Yellow Leaf and Coal City faults could not be determined from mesoscopic fabric data. The transport direction is presumed to have been normal to the strike of the faults, or about 314° to 319°.

The Hog Pen Branch fault is oblique to most Valley and Ridge structural trends (Plate I). Transport direction as inferred from mesoscopic fabric data is 340° (Plate II).

upper block), then ramped up-section to the northwest and into a décollément at the Pride Mountain-Floyd level (Plate II). The Birmingham anticlinorium, overlying the Opossum Valley fault, is a complex flat-topped fold similar in geometry to folds formed by ramping in the Cumberland Plateau (Harris, 1970). Space requirements in the subsurface and the suitability of the shales as a décollément both suggest that the fault flattens at the Pride Mountain-Floyd level. Mississippian shales have not been observed in windows through the Opossum Valley allochthon, but stratigraphically lower units do occur in such windows (Plate I).

Along most of the northwest flank of the anticlinorium the Opossum Valley fault again cuts up-section from the Mississippian décollément to the surface (Plate I). In southwestern Jefferson County, the surface trace of the Opossum Valley fault splays into a number of smaller faults bounding large fault slices of diverse stratigraphy. Southwest of this area shortening along the northwest margin of the anticlinorium is absorbed by folding of the Mississippian-Pennsylvanian sediments, with splays of the Opossum Valley fault dying out in the cores of anticlines (Plate I). The zone of complex faulting represents a complicated transverse step connecting the upward splay of the Opossum Valley fault with the segment in which strain is absorbed by superficial folding (Plate I).

Transport direction on the Opossum Valley fault is consistent at 296° to 303°. Early transport zone fabrics, primarily bedding telescopes, indicate a transport direction within this range (Plate II). Early transport zone fabrics on either flank of the Birmingham anticlinorium were folded about fold axes plunging 3° to 10° along an azimuth of 42° to 43°. Folding was contemporaneous with continued transport on the Opossum

Valley fault, as indicated by forelimb thrusts (R) which dissect frontal folds on the Opossum Valley allochthon.

The final period of thrusting, Phase 7, was development of the Helena fault (S), a major foreland discordant thrust. Transport direction of the Helena allochthon was more northerly, at 300° to 310°, as indicated by bedding telescopes, minor faults, and monoclinic folds near the fault (Plate II).

V. IMPLICATIONS FOR HYPOTHESES OF THRUST MECHANICS

At present, two hypotheses are generally advocated to explain the mechanical paradox of large-scale overthrusting. Elliot (1976) has proposed a modified gravity spreading model, in which foreland thrusting is a mass transfer mechanism by which excess topography, resulting from some other orogenic process, is reduced. Briefly summarized, the basic concept of Elliot's hypothesis is that topographic slope is the critical factor in initiation of thrusting; development of some minimum topographic slope results in stresses at the base of the sedimentary prism which exceed the yield strength of the rock, and the prism spreads down the topographic slope and toward the foreland (Fig. V-12). A result is that the slope is transferred toward the foreland, and the locus of a new detachment is progressively shifted toward the foreland, as in the Canadian Rockies.

Chapple (1978) hypothesized that lateral compressive forces from the hinterland are the dominant factor, with transport effected both by sliding over a weak basal layer, and internal collapse of the sedimentary prism by listric thrusting and folding. In this hypothesis, the

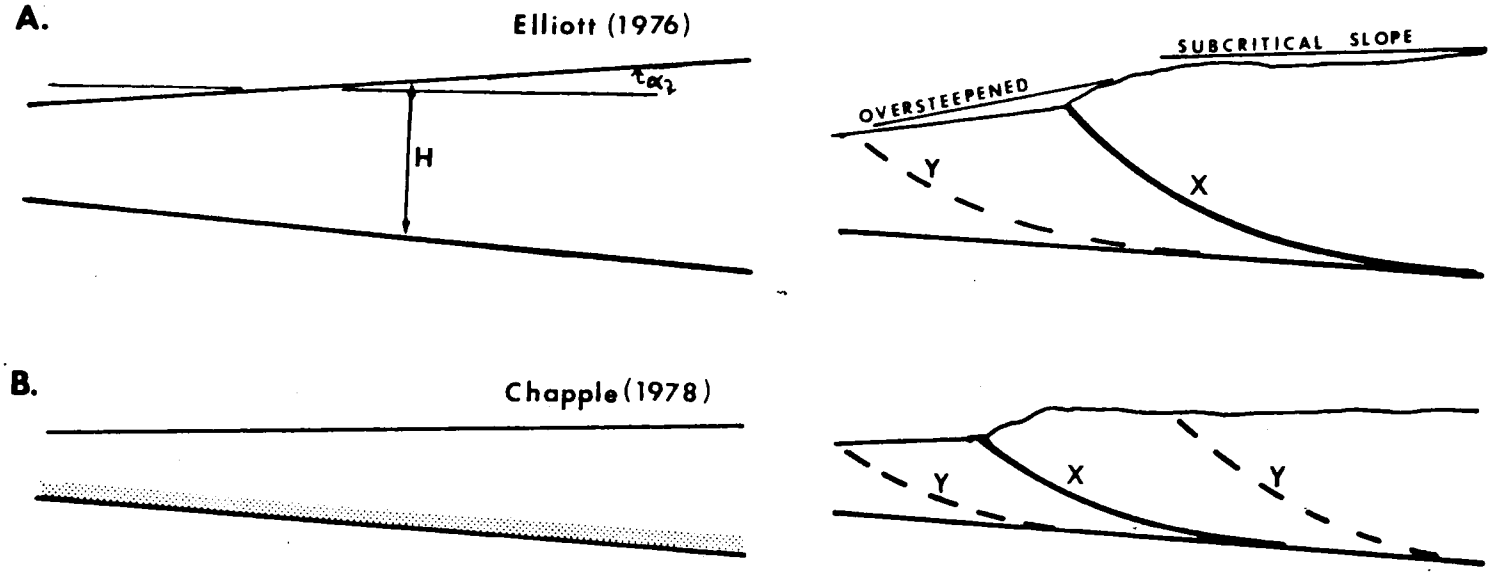

Figure V-12. Comparison of Elliot (1976) and Chapple (1978) hypotheses of thrust mechanics. A. In the Elliott hypothesis, the shear stress of (τ) at base of wedge is a function of wedge thickness thickness (H) and surface slope (α); as α or H approaches zero, τ approaches zero. Elevation of part of the mass by thrusting (X) results in steepening of foreland slopes, and loss of slope in hinterland regions, leading to forward progradation of faulting (Y). B. In the Chapple hypothesis, basal shearing is controlled by strengths of the basal layer and material of the wedge; surface slope facilitates thrusting but is not critical. Thus if surface slope is lost by faulting (X), subsequent faulting (Y) may occur toward either hinterland or foreland, depending upon material properties. Note similarity of very low surface slopes and hinterland migration of faulting to events in Plate II.

topographic slope only facilitates thrusting, and is likely to be a consequence rather than a cause of thrusting.

Foreland-discordant thrusts occur in many thrust belts (for example, Royse et al., 1975), but nowhere else do they appear to be a characteristic feature as in the southernmost Appalachians. As such, they represent an atypical, but not unique, feature of thrust belts which must be accounted for by any hypothesis. Putting aside consideration of the two hypotheses on the basis of theoretical merit, the relationships between thrust chronology and sedimentation depicted in Plate II may be used to evaluate the two hypotheses empirically.

According to Elliot's (1976) hypothesis, thrusting should work to maintain a forward (foreland) facing topographic slope, and thrusting should migrate toward the foreland (Plate II, L, M, and N). However, if uplift far into the foreland (Plate II, O) results in interruption of foreland-directed drainage and loss of topographic slope in the basin (Plate II, N-O), thrusting should continue to occur forward of the uplift, not in the area of subcritical slope behind the uplift (Fig. V-12). Thus, some difficulty is encountered in explaining foreland-discordant thrusts with this hypothesis. However, in Chapple's (1978) hypothesis, forward topographic slope is not a prerequisite for thrusting; the controlling factor is weakness of the basal layer. In special circumstances thrusting can occur under a rearward-facing slope (Chapple, 1978, p. 1192), and loss of topographic slope would not preclude shifting of thrusting toward the hinterland. Instead, shifting toward the hinterland would be required in order to reestablish a topographic slope and facilitate foreland vergent thrusting.

The occurrence of syndepositional thrusting in the belt also favors the Chapple hypothesis. The topographic slope (Plate II, Phases 2 and 3) alone is insufficient to provide enough shear stress to initiate thrusting in the Valley and Ridge, yet thrusting does occur. However, in the Chapple hypothesis, a sufficiently weak basal layer and lateral compressive thrust allows syndepositional thrusting under a very low topographic slope. In summary, although both hypotheses are approximations to the mechanics of thrusting, the existence of foreland discordant thrusts and low synorogenic surface slopes favor the Chapple (1978) hypothesis.

CHAPTER VI

SUMMARY AND CONCLUSIONS

The Paleozoic history of the southernmost Valley and Ridge thrust belt in Alabama consists of a sequence of events in the evolution of a rifted margin into a deformed orogenic foreland. This evolution is recorded in the sequence of sedimentary and structural features of the region, interpretation of which allows quantification of the regional history. Although complex, this history may be representative of orogenic forelands in general.

During the late Precambrian, the eastern margin of North America represented one side of a continental rift system, characterized by rapid subsidence and sedimentation (for example, Rankin, 1975). However, no record of this event has been recognized in the southernmost Appalachians of Alabama and western Georgia, in large part as a result of poorly known age relationships in the crystalline rocks.

During the Early Cambrian the proto-Atlantic Ocean began to encroach upon the subsiding cratonic margin, with deposition of linear clastic shoreline deposits. By Middle Cambrian time the proto-Atlantic covered the entire southernmost Appalachian foreland, and a broad Atlantic-type shelf developed which persisted through the Early Ordovician. Crustal subsidence during this period was atypical in that the rate did not decrease exponentially with time, but remained nearly constant, at ~2 cm/1000 yr. The tectonic cause of this linear subsidence is problematical, but may have been the result of an offshore island arc,

the increasing mass of the growing arc serving to depress the lithosphere. Alternatively, such subsidence behavior may be typical of some passive margins (Watts, 1981). During the Middle and Late Cambrian, the Birmingham anticlinorium underwent rapid localized subsidence, creating an intrashelf sedimentary basin (not a bathymetric basin). Such subsidence behavior is typical of rift cycles, and represented an aborted rift system within the shelf.

Following a major pre-Middle Ordovician sea level drop and development of the widespread unconformity, the proto-Atlantic once again encroached upon the craton from the southeast. In other parts of the southern Appalachians, the Middle Ordovician is characterized by rapid subsidence of the eastern Valley and Ridge, and an influx of easterly derived clastics from Taconic orogenic highlands. In this region, however, subsidence rates may have been low (~0.2 cm/1000 yr), coarse-grained and fine-grained turbidites are absent from the eastern basinal facies, and no conclusive evidence of Taconic tectonism is recognized in the interior crystalline belts (Wampler et al., 1970). These suggest at most a minor Taconic event in this region, and certainly no obduction of a major lithospheric plate onto the shelf edge; instead, the interval is characterized by downwarping of the eastern shelf, and slowing of shelf subsidence rates. These suggest an abortive arc-continent collision which terminated subsidence but did not result in large-scale deformation of the continental margin.

During the Silurian through earliest Mississippian, subsidence rates over the entire region were extremely low (~0.007 cm/1000 yr), and the region was occupied by an epeiric sea. The eastern part of the

region experienced differential uplift, so that eustatic changes resulted in major onlap/offlap cycles affecting a low-lying eastern land mass formed by broad uplift of older shelf sediments.

In the Early Mississippian the entire shelf began to subside, with greater subsidence occurring in the southeast. This subsidence continued to increase in rate, until by Early Pennsylvanian time rates had approached 100 cm/1000 yr (13 cm/1000 yr corrected for sediment loading) in the easternmost belts. Simultaneously, the foredeep thus created was filled by terrigenous clastics derived from a rising igneous/metamorphic terrane to the southeast, indicating deformation and imbrication of the lithosphere along the southeastern shelf margin.

Deformation prograded into the foreland as a thrust front which, in general, migrated rapidly toward the craton. However, the dominant structural elements of the region are foreland discordant thrusts which deform older structures in their own forelands.

Post-Paleozoic surface processes have resulted in a deeply eroded and weathered terrane in which exposure is poor. Thus, in reconnaissance or detailed studies the data base is poor, but can be augmented by remotely-sensed data.

The results of this study have significant implications for the study of regional geology and thrust belts in general. These are as follows:

(1) Middle Cambrian rifting of the North American craton, which produced the Rome Trough, and the southern continental margin, also affected the southern Appalachian foreland and may be the explanation for

the unusual subsidence behavior of the shelf and the mid-continent gravity anomalies in central Tennessee (Bryan, 1975);

(2) the southernmost Appalachians may have bordered on a backarc basin;

(3) Taconic tectonism did not affect the Alabama foreland, and probably not the crystalline terrane;

(4) the Silurian-Devonian was a period of relative quiescence and there was no recognizable "Acadian" orogeny in this region;

(5) Late Paleozoic (Alleghenian) deformation and foreland sedimentation were contemporaneous;

(6) the pronounced difference between finite subsidence rates induced by local sediment loading (~20 cm/1000 yr) and tectonically induced subsidence (~70 cm/1000 yr) suggests that tectonic loading was the major factor in foredeep subsidence;

(7) low synorogenic surface slopes suggest that the Chapple hypothesis provides a more accurate representation of thrust mechanisms than gravity-spreading hypotheses; and

(8) stratigraphic data can be used to generate quantitative data on nature and rates of ancient orogenic processes.

BIBLIOGRAPHY

BIBLIOGRAPHY

Bailey, E. B., 1936, Sedimentation and tectonics: Geol. Soc. America Bull., v. 47, pp. 1713-1726.

Bally, A. W., Gordy, P. L., and Stewart, G. A., 1966, Structure, seismic data, and orogenic evolution of southern Canadian Rocky Mountains: Bull. Canadian Petr. Geol., v. 14, pp. 337-381.

Barrell, Joseph, 1917, Rhythms and the measurements of geologic time: Geol. Soc. America Bull., v. 28, pp. 745-904.

Bathurst, R. G. C., 1966, Boring algae, micrite envelopes, and lithification of molluscan biosparites: Geol. Jour., v. 5, pp. 15-32.

Bathurst, R. G. C., 1976, Carbonate sediments and their diagenesis: Developments in Sedimentology 12, Elsevier, New York, N.Y., 632 pp.

Bearce, D. N., 1977, Stratigraphic problems of the eastern Coosa Valley, in Bearce, D. N. (ed.) Cambrian and Devonian stratigraphic problems of eastern Alabama: Alabama Geol. Soc. Guidebook, 15th Ann. Field Trip, pp. 37-53.

Bearce, D. N., 1978, Structure of the easternmost Coosa Valley, Alabama: Am. Jour. Sci., v. 278, pp. 461-476.

Bearce, D. N., and McKinney, F. K., 1977, Archeocyathids in east Alabama: Significance to the geologic interpretation of the Coosa deformed belt: Geology, v. 5, pp. 467-470.

Beavers, W. M., 1977, Depositional environments of the Hartselle Sandstone in Colbert and Franklin Counties, Alabama: Univ. of Alabama, M.S. thesis, 84 pp.

Bell, Gordon, 1978, Palentology of the Conasauga Formation in Jefferson County, in Kidd, J. T., and Shannon, S. W. (eds.), Stratigraphy and structure of the Birmingham area, Jefferson County, Alabama: Alabama Geol. Soc. Guidebook, 16th Ann. Field Trip, pp. 87-92.

Benedict, G. L. III, and Walker, K. R., 1978, Paleobathymetric analysis in Paleozoic sequences and its geodynamic significance: Am. Jour. Sci., v. 278, pp. 579-607.

Bensko, John, 1953, Ice crystal markings in the Red Mountain Formation near Birmingham, Alabama: Alabama Acad. Sci. Jour., v. 23, pp. 31-32.

Bergstrom, S. M., 1970, Conodont biostratigraphy of the Middle and Upper Ordovician of Europe and eastern North America, in Sweet, W. C., and Bergstrom, S. M. (eds.), Symposium on conodont biostratigraphy: Geol. Soc. America Mem. 127, pp. 83-162.

Bergstrom, Stig, and Drahovzal, J. A., 1972, Facies relationships in the Middle Ordovician of the Southern Appalachians in Alabama (abs.): Geol. Soc. America Abs. with Prog., v. 4, pp. 60-61.

Berry, W. B. N., 1960, Graptolite faunas of the Marathon region, west Texas: Texas Univ. Pub. 6005, 179 pp.

Berry, W. B. N., and Boucot, A. J. (eds.), 1970, Correlation of the North American Silurian rocks: Geol. Soc. America Spec. Paper 102, 289 pp.

Black, D. F. B., 1979, Structural evolution of central Kentucky (abs.): Symp. Kentucky Geol. Mapping Proj., Kentucky Geol. Survey, p. 5.

Bogel, H., and Closs, H., 1976, A geotraverse through the eastern and southern Alps, in Drake, C. D. (ed.), Geodynamics Progress and Prospects: Am. Geophys. Union, Wash., D.C., pp. 35-40.

Breland, F. C., 1972, A petrologic and paleocurrent analysis of Lower Pennsylvanian Pottsville Formation of the Warrior Basin in Alabama: Mississippi State Univ., M.S. thesis, 98 pp.

Briggs, Garrett, 1974, Carboniferous depositional environments in the Ouachita Mountains-Arkoma Basin area of southeastern Oklahoma, in Briggs, Garrett (ed.), Carboniferous of the southeastern United States: Geol. Soc. America Spec. Paper 148, pp. 225-240.

Briggs, Garrett, and Roeder, Dietrich, 1975, Sedimentation and plate tectonics, Ouachita Mountains and Arkoma Basin, in McBride, E. F., and Moiola, R. J. (eds.), Sedimentology of Paleozoic flysch and associated deposits, Ouachita Mountains-Arkoma Basin, Oklahoma: Dallas Geol. Soc. Guidebook, pp. 1-22.

Bryan, K. B., Jr., 1975, The Greenwood anomaly of the Cumberland Plateau: A test application of GRAVMAP, a system of computer programs for reducing and automatic contouring land gravity data: Univ. of Tennessee, M.S. thesis, 118 pp.

Burchard, F. F., and Andrews, T. G., 1947, Iron ore outcrops of the Red Mountain formation in northeast Alabama: Alabama Geol. Survey Spec. Report 19, 375 pp.

Butts, Charles, 1910, Birmingham Quadrangle, Alabama: U.S. Geol. Survey Atlas Series, Folio 175, 6 pp.

Butts, Charles, 1926, Paleozoic rocks, in Adams, G. I., Butts, Charles, Stephenson, L. W., and Cooke, W. J., Geology of Alabama: Alabama Geol. Survey Spec. Report 14, pp. 1-229.

Butts, Charles, 1927a, Bessemer-Vandiver Folio, Alabama: U.S. Geol. Survey Atlas Series, Folio 221, 22 pp.

Butts, Charles, 1927b, The Devonian of Alabama: Am. Jour. Sci., ser. 5, v. 14, no. 83, pp. 365-380.

Butts, Charles, 1940, Montevallo-Columbiana Folio, Alabama: U.S. Geol. Survey Atlas Series, Folio 226, 30 pp.

Causey, L. V., 1965, Geologic rock-type map of Talladega County, Alabama: Alabama Geol. Survey Map 38.

Chaiffetz, M. J., 1974, Ratios of larger palynomorphs, Red Mountain Formation, Alabama (abs.): Geol. Soc. America Abs. with Prog., v. 6, p. 392.

Chapple, W. M., 1978, Mechanics of thin-skinned fold and thrust belts: Geol. Soc. America Bull., v. 89, pp. 1189-1198.

Clark, H. B., Costain, J. K., and Glover, L. III, 1978, Structure and seismic reflection studies of the Brevard ductile deformation zone near Rosman, North Carolina: Am. Jour. Sci., v. 278, pp. 419-441.

Clarke, J. W., 1952, Geology and mineral resources of the Thornton Quadrangle, Georgia: Georgia Geol. Survey Bull. 59, 99 pp.

Cloud, P. E., Jr., 1967, Geology and bauxite deposits of the Rock Run and Goshen Valley areas, northeast Alabama: U.S. Geol. Survey Bull. 1199-N, 74 pp.

Coleman, J. M., 1976, Deltas: Processes of deposition and models for exploration: Cont. Educ. Pub. Co., Champaign, Ill., 102 pp.

Conant, L. C., and Swanson, V. E., 1961, Chattanooga Shale and related rocks of central Tennessee and nearby areas: U.S. Geol. Survey Prof. Paper 357, 91 pp.

Coogan, A. H., and Manus, R. W., 1975, Compaction and diagenesis of carbonate sands, in Chilingarian, G. V., and Wolf, K. H. (eds.), Compaction of coarse-grained sediments, I: Developments in Sedimentology 18A, Elsevier, New York, N.Y., pp. 79-166.

Cook, F. A., Albaugh, O. J., Brown, L. D., Kaufman, Sidney, Oliver, J. E., and Hatcher, R. D., Jr., 1979, Thin-skinned tectonics in the crystalline southern Appalachians; COCORP seismic reflection profiling of the Blue Ridge and Piedmont: Geology, v. 7, pp. 563-567.

Cooper, G. A., 1956, Chazyan and related brachiopods: Smithsonian Misc. Coll., v. 127, pt. 1, 1024 pp.

Crans, W., Mandl, G., and Haremboure, J., 1980, On the theory of gravity faulting; a geomechanical delta model based on gravity sliding: Jour. Petr. Geol., v. 2, pp. 265-307.

Culbertson, W. C., 1963, Correlation of the Parkwood Formation and the lower members of the Pottsville Formation in Alabama: U.S. Geol. Survey Prof. Paper 450E, pp. 47-50.

Cummings, D., 1960, The basal Chepultepec sandstone (Cambrian-Ordovician boundary) in the Ridge and Valley province of Tennessee: Jour. Sed. Petr., v. 30, pp. 228-240.

Dahlstrom, C. D. A., 1969, Balanced cross sections: Canadian Jour. Earth Sci., v. 6, pp. 743-757.

Dahlstrom, C. D. A., 1970, Structural geology in the eastern margin of the Canadian Rocky Mountains: Bull. Canadian Petr. Geol., v. 18, pp. 332-406.

Dahlstrom, C. D. A., 1977, Structural geology in the eastern margin of the Canadian Rocky Mountains, in Heisey, E. L., Norwood, E. R., and Wach, L. A. (eds.), Rocky Mountain thrust belt geology and resources: Wyoming Geol. Assoc. 29th Ann. Field Conf., pp. 407-440.

Dana, J. D., 1866, Observations on the origin of some of the earth's features: Am. Jour. Sci., 2nd Ser., v. 42, pp. 205-211, 252-253.

Davies, D. K., Ethridge, F. G., and Berg, R. R., 1971, Recognition of barrier environments: Am. Assoc. Petr. Geol. Bull., v. 55, pp. 550-565.

Decker, C. E., 1952, Stratigraphic significance of graptolites of Athens Shale: Am. Assoc. Petr. Geol. Bull., v. 36, pp. 1-145.

Dennison, J. M., 1976, Gravity tectonic removal of cover of Blue Ridge anticlinorium to form Valley and Ridge province: Geol. Soc. America Bull., v. 87, pp. 1470-1476.

Dennison, J. M., 1978, Stratigraphy and sedimentary tectonics of the Appalachian basin: Am. Assoc. Petr. Geol. Short Course Notes, Cleveland, OH, 96 pp.

Denson, N. M., and Waage, K. M., 1966, Some bauxite and clay deposits in northeastern Alabama: U.S. Geol. Survey Bull. 1198-P, pp. 1-27.

Dillon, W. P., Paull, C. K., Buffler, R. T., and Fail, J. P., 1978, Structure and development of the southeast Georgia Embayment and northern Blake Plateau: Preliminary analysis: Am. Assoc. Petr. Geol., Memoir 29, pp. 27-41.

Dinnean, R. F., 1974, Lower Carboniferous Bangor Limestone in Alabama: a multicycle clear water epeiric sea sequence: Louisiana State Univ. Ph.D. diss., 111 pp.

Doyle, L. J., Cleary, W. J., and Pilkey, O. H., 1968, Mica: its use in determining shelf-depositional regimes: Marine Geol., v. 6, pp. 381-391.

Drahovzal, J. A., 1967, Biostratigraphy of Mississippian rocks in the Tennessee Valley, in Smith, W. E. (ed.), Field Guide to Mississippian sediments in northern Alabama and south central Tennessee: Alabama Geol. Soc. Guidebook, 5th Ann. Field Trip, pp. 10-24.

Drahovzal, J. A., and Neathery, T. L., 1971, Middle and Upper Ordovician stratigraphy of the Alabama Appalachians, in Drahovzal, J. A., and Neathery, T. L. (eds.), Middle and Upper Ordovician of the Alabama Appalachians: Alabama Geol. Soc. Guidebook, 9th Ann. Field Trip, pp. 1-62.

Drahovzal, J. A., Neathery, T. L., and Wielchowsky, C. C., 1973, Significance of selected lineaments in Alabama: Third ERTS-1 Symposium, v. I-A, N.A.S.A. SP-351, pp. 897-910.

Drake, N. F., 1964, Economic geology of the Waynesboro quadrangle: Tennessee Geol. Survey, Res. of Tennessee, v. 7, no. 3, 22 pp.

Duff, N., 1975, Paleoecology of a bituminous shale in the Lower Oxford clay of Central England: Paleontology, v. 18, pp. 443.482.

Duncan, Helen, 1957, Bryozoans, in Ladd, H. J. (ed.), Treatise on marine ecology and paleoecology: Geol. Soc. America Memoir 67, v. 2, pp. 783-800.

Dunnington, H. V., 1967, Aspects of diagenesis and shape change in stylolitic limestone reservoirs: Proc. 7th World Petr. Cong., Mexico, v. 2, pp. 339-352.

Elliot, David, 1976, The motion of thrust sheets: Jour. Geophys. Res., v. 81, pp. 919-963.

Elliott, T., 1978, Clastic shorelines, in Reading, H. D. (ed.), Sedimentary environments and facies: Elsevier Press, New York, N.Y., pp. 143-177.

Elliott, T., and Ladipo, K. O., 1981, Syn-sedimentary gravity slides (growth faults) in the Coal Measures of South Wales: Nature, v. 291, pp. 220-222.

Epstein, A. G., Epstein, J. B., and Harris, L. D., 1977, Conodont color alteration-an index to organic metamorphism: U.S. Geol. Survey Prof. Paper 995, 27 pp.

von Eysinga, F. W. B., 1975, Geological time table: Elsevier Press, Amsterdam, Netherlands.

Faul, Henry, and Thomas, H. H., 1959, Argon ages of the great ash bed from the Ordovician of Alabama and the bentonite marker in the Chattanooga Shale from Tennessee (abs.): Geol. Soc. America Bull., v. 70, pp. 1600-1601.

Ferm, J. C., Ehrlich, R., and Neathery, T. L. (eds.), 1967, A field guide to Carboniferous detrital rocks in northern Alabama: Geol. Soc. America Geol. Div. Guidebook, 101 pp.

Fischer, A. G., 1964, Stratigraphic basis of paleoecology, in Imbrie, John, and Newell, N. O. (eds.), Approaches to Paleoecology: Wiley & Sons, New York, N.Y., pp. 32-42.

Fitch, T. J., 1970, Earthquake mechanisms in the Himalayan, Burmese, and Andaman regions and continental tectonics in central Asia: Jour. Geophys. Res., v. 75, pp. 2699-2709.

Foerste, A. F., 1905, The Silurian, Devonian and Irvine Formations of east central Kentucky: Kentucky Geol. Survey Bull. 7, 369 pp.

Gansser, A., 1964, The geology of the Himalayas: Wiley Interscience, New York, N.Y., 289 pp.

Gary, M., McAfee, R., and Wolf, C. L. (eds.), 1972, Glossary of geology: Am. Geol. Inst., Washington, D.C., 805 pp.

Gibson, A. M., 1893, Report on the geological structure of Murphrees Valley: Alabama Geol. Survey Spec. Rept. 4, 132 pp.

Gilbert, O. E., Jr., 1974, Stratigraphic and structural relationships of the Sylacauga unconformity in Alabama: Univ. Alabama, M.S. thesis, 98 pp.

Gilbert, O. E., Jr., 1976, Non-fossil fuel exploration in the Coosa Synclinorium, Shelby, St. Clair, Jefferson and Calhoun Counties, Alabama: U.S. Geol. Survey Branch Uranium and Thorium Res. open file report, 23 pp.

Gilbert, O. E., Jr., 1977a, Structural geology in the Winterboro area, Talladega County, Alabama, in Bearce, D. N. (ed.), Cambrian and Devonian stratigraphic problems of eastern Alabama: Alabama Geol. Soc. Guidebook, 15th Ann. Field Trip, pp. 20-28.

Gilbert, O. E., Jr., 1977b, Structural geology of the Coosa coal field and Coosa synclinorium, Alabama (abs.): Geol. Soc. America Abs. with Prog., v. 9, pp. 139-140.

Gilbert, O. E., Jr., and Nordstrom, H. E., 1976, Mechanism of thrust fault ramping in the eastern Valley and Ridge, Alabama: Alabama Geol. Survey unpublished ms., 16 pp.

Gilbert, O. E., Jr., Wielchowsky, C. C., and Warren, W. M., 1976, Thin-skinned tectonic origin of the Kelly Creek lineament, Alabama (abs.): Proc. Second Internat. Conf. on New Basement Tectonics, Denver, CO., p. 388.

Glover, Lynn, 1959, Stratigraphy and uranium content of the Chattanooga Shale in northeastern Alabama, northwestern Georgia, and eastern Tennessee: U.S. Geol. Survey Bull. 1087-E, pp. 133-168.

Gocht, H., 1973, Einbettunslage und Erhaltung von Ostracoden-Gehaüsen in Solnhofen Plattenkalk (Unter-Tithon, SW-Deutschland): Nues Jahrb, Geol. Palaontol. Monatsh., 4, pp. 189-206.

Graham, S. A., Dickinson, W. R., and Ingersoll, R. V., 1975, Himalayan-Bengal model for flysch dispersal in the Appalachian-Ouachita system: Geol. Soc. America Bull., v. 86, pp. 273-286.

Gunn, R., 1943, Quantitative evaluation of the influence of the lithosphere on anomalies of gravity: Jour. Franklin Inst., v. 236, pp. 47-65.

Hallam, A., 1977, Secular changes in marine innundation of USSR and North America through the Phanerozoic: Nature, v. 269, pp. 769-772.

Hallam, A., and Bradshaw, M. J., 1979, Bituminous shale, and oolitic ironstones as indicators of transgressions and regression: Jour. Geol. Soc. London, v. 136, pp. 157-164.

Hammes, R. R., 1965, Ouachita overthrusting-stratigraphic appraisal: Am. Assoc. Petr. Geol. Bull., v. 49, pp. 1666-1679.

Handford, C. R., 1977, Monteagle Limestone (Upper Mississippian) case for tidal bar sedimentation in the southern Cumberland Plateau (abs.): Am. Assoc. Petr. Geol. Bull., v. 61, p. 793.

Harris, L. D., and Bayer, R. C., 1979, Eastern projection of Valley and Ridge beneath metamorphic sequences of the Appalachian orogen (abs.): Am. Assoc. Petr. Geol. Bull., v. 63, p. 1579.

Harris, L. D., and Milici, R. C., 1977, Characteristics of thin-skinned style of deformation in the southern Appalachians, and potential hydrocarbon traps: U.S. Geol. Survey Prof. Paper 1018, 40 pp.

Hass, W. H., 1956, Age and correlation of the Chattanooga Shale and the Maury Formation: U.S. Geol. Survey Prof. Paper 286, 45 pp.

Hatcher, R. D., Jr., 1972, Developmental model for the southern Appalachians: Geol. Soc. America Bull., v. 83, pp. 2735-2760.

Hatcher, R. D., Jr., 1978, Tectonics of the western Piedmont and Blue Ridge, southern Appalachians; review and speculation: Am. Jour. Sci., v. 278, pp. 276-304.

Haxby, W. F., Turcotte, P. L., and Bird, J. M., 1976, Thermal and mechanical evolution of the Michigan basin: Tectonophysics, v. 36, pp. 57-75.

Hayes, C. W., 1891, Overthrust faults of the central Appalachians: Geol. Soc. America Bull., v. 2, pp. 141-152.

Hayes, C. W., 1894a, Description of the Kingston Sheet (Tenn.): U.S. Geol. Survey Atlas Series Folio 4, 4 pp.

Hayes, C. W., 1894b, Geology of a portion of the Coosa Valley in Georgia and Alabama: Geol. Soc. America Bull., v. 5, pp. 465-480.

Hayes, C. W., and Ulrich, E. O., 1903, Columbia, Tennessee folio: U.S. Geol. Survey Atlas Series Folio 95, 6 pp.

Hedberg, H. O., 1958, Stratigraphic classification and terminology: Am. Assoc. Petr. Geol. Bull., v. 42, pp. 1881-1896.

Hetenyi, M., 1946, Beams on elastic foundation: Univ. Michigan Press, Ann Arbor, Mich., 255 pp.

van Hinte, J. E., 1978, Geohistory analysis-application of micro-paleontology in exploration geology: Am. Assoc. Petr. Geol. Bull., v. 62, pp. 201-222.

Hinz, K., Beiersdorf, H., Exon, N. F., Roeser, H. A., Stagg, H. M. J., and von Stackelberg, U., 1978, Geoscientific investigations from Scott Plateau off northwest Australia to the Java trench: BMR Jour. Austral. Geol. and Geophysics, v. 3, pp. 319-340.

Hobday, D. K., 1974, Beach- and barrier-island facies in the upper Carboniferous of northern Alabama, in Briggs, Garret (ed.), Carboniferous of the southeastern United States: Geol. Soc. America Spec. Paper 148, pp. 209-223.

Horsey, C. A., 1979, Pottsville depositional environments in the western Black Warrior basin of Alabama (abs.): Geol. Soc. America Abs. with Prog., v. 11, p. 446.

Hossack, J. R., 1979, The use of balanced cross-sections in the calculation of orogenic contraction: a review: Jour. Geol. Soc. London, v. 136, pp. 705-711.

Howell, B. F., and Mason, J. F., 1938, Correlation of Middle Cambrian faunas of North America: Jour. Paleo., v. 12, pp. 295-297.

Howell, B. F. et al., 1944, Correlation of the Cambrian formations of North America (Chapt. 9): Geol. Soc. Bull., v. 55, pp. 993-1003.

Jacobeen, F., and Kanes, W. H., 1974, Structure of Broadtop synclinorium and its implications for Appalachian structural style: Am. Assoc. Petr. Geol. Bull., v. 58, pp. 362-375.

Jarvis, G. T., and McKenzie, D. P., 1980, Sedimentary basin formation with finite extension rates: Earth and Planetary Sci. Letters, v. 48, pp. 42-52.

Jewell, J. W., 1967, Upper Ordovician and Silurian stratigraphy and historical geology of northern Alabama and southern Tennessee, in Smith, W. E. (ed.), Field guide to Mississippian sediments in northern Alabama: Alabama Geol. Soc. Guidebook, 5th Ann. Field Trip, pp. 2-3.

Jonas, Anna, 1929, Structure of the metamorphic belts of the central Appalachians: Geol. Soc. Amer. Bull., v. 40, pp. 503-514.

Jones, W. B., 1929, Summary report on the Wattsville basin of the Coosa coal field: Alabama Geol. Survey, Circ. 6, 48 pp.

Karig, D. E., Caldwell, J. G., and Parmentier, E. M., 1976, Effects of accretion on geometry of the descending lithosphere: Jour. Geophys. Res., v. 81, pp. 6281-6291.

Kay, Marshall, 1955, Sediments and subsidence through time: Geol. Soc. America Spec. Paper 62, pp. 665-684.

Keen, M. J., and Keen, C. E., 1973, Subsidence and fracturing on the continental margin of eastern Canada: Canada Geol. Survey Paper 71-23, pp. 23-42.

Keith, A., 1903, Cranberry, North Carolina-Tennessee folio: U.S. Geol. Survey Atlas Ser. Folio 90, 9 pp.

Keller, F. B., 1977, Polyphase folding and thrusting along the western margin of the Blue Ridge, Tennessee-North Carolina (abs.): Geol. Soc. America Abs. with Prog., v. 9, pp. 152-153.

Kelley, J. C., 1969, Geologic study of the Chattanooga Shale of the Elkmont Quadrangle, Alabama: Univ. Alabama M.S. thesis, 43 pp.

Kidd, J. T., 1975, Pre-Mississippian stratigraphy of the Warrior Basin, Alabama: Gulf Coast Assoc. Geol. Soc. Trans., v. 25, pp. 20-39.

Kidd, J. T., and Neathery, T. L., 1976, Correlation between Cambrian rocks of the southern Appalachian geosyncline and the interior low plateaus: Geology, v. 4, no. 12, pp. 767-769.

Kidd, J. T., and Shannon, S. W., 1977, Preliminary geologic maps of the Valley and Ridge province, Jefferson County, Alabama: Alabama Geol. Survey Atlas Series 10, 41 pp.

Kiefer, J. D., 1970, Pre-Chattanooga Devonian stratigraphy of Alabama and northwest Georgia: Univ. Illinois (Urbana-Champaign) Ph.D. diss., 173 pp.

King, E. R., and Zietz, Isidore, 1978, The New York-Alabama lineament: geophysical evidence for a major crustal break in the basement beneath the Appalachian basin: Geology, v. 6, pp. 312-318.

King, P. B., 1959, Evolution of North America: Princeton Univ. Press, Princeton, N.J., 190 pp.

Klein, G. de V., 1967, Paleocurrent analysis in relation to modern marine sediment dispersal patterns: Am. Assoc. Petr. Geol. Bull., v. 51, pp. 366-382.

Kolter, J. E., and Vest, E. L., 1953, An Ordovician bioherm in Jefferson County, Alabama: Alabama Acad. Sci. Jour., v. 23, pp. 59-62.

Krumbein, W. C., Sloss, L. L., and Dapples, E. C., 1949, Sedimentary tectonics and sedimentary environments: Am. Assoc. Petr. Geol. Bull., v. 33, pp. 1859-1891.

Lecompte, Marius, 1956, Stromatoporoidea, in Moore, R. C. (ed.), Treatise on Invertebrate Paleontology: Geol. Soc. America, v. F., pp. F107-F144.

Lee, W., 1954, Thickness maps as criteria of regional structural movement: Geol. Survey Kansas Bull. 109, pp. 69-80.

Lesley, J. P., 1876, Historical sketch of geological exploration in Tennessee and other states: Pennsylvania Report of 2nd Geol. Survey, H3, pp. 217-237.

Lochman-Balk, Christina, 1971, Cambrian of the craton of the United States, in Holland, C. H. (ed.), Cambrian of the New World: Wiley Interscience, New York, N.Y., pp. 79-168.

Lochman-Balk, Christina, and Wilson, J. L., 1958, Cambrian biostratigraphy of North America: Jour. Paleo., v. 32, pp. 312-350.

Lougee, R. J., 1953, Chronology of postglacial time in eastern North America: Science Monthly, v. 76, pp. 259-276.

Lundin, R. F., and Newton, G. D., 1970, Ostracoda and the Silurian stratigraphy of northwest Alabama: Alabama Geol. Survey Bull. 95, 64 pp.

McCalley, Henry, 1896, Report on the valley regions of Alabama, part I, on the Tennessee Valley region: Alabama Geol. Survey, 476 pp.

McCalley, Henry, 1897, Report on the valley regions of Alabama, part II, on the Coosa Valley region: Alabama Geol. Survey, 862 pp.

McCalley, Henry, 1900, Report on the Warrior coal basin: Alabama Geol. Survey Spec. Rept. 10, 299 pp.

McKinney, F. K., 1977, Archaeocyatha of the Shady Formation, Sleeping Giants, Talladega County, Alabama, in Bearce, D. N. (ed.), Cambrian and Devonian stratigraphic problems of eastern Alabama: Alabama Geol. Soc. Guidebook, 15th Ann. Field Trip, pp. 16-19.

Mack, G. H., 1980, Stratigraphy and depositional environments of the Chilhowee Group (Cambrian) in Georgia and Alabama: Am. Jour. Sci., v. 280, pp. 487-517.

Markello, J. R., Tillman, C. G., and Read, J. F., 1979, Lithofacies and biostratigraphy of Cambrian and Ordovician platform and basin facies carbonates and clastics, southwestern Virginia, in Glover, L. III, and Read, J. F. (eds.), Guides to Field Trips 1-3: Geol. Soc. America Field Trip Guides, Southeastern Section, 1979, Blacksburg, VA., pp. 42-87.

Middleton, G. V., and Hampton, M. A., 1976, Subaqueous sediment transport and deposition by sediment gravity flows, in Stanley, D. J., and Swift, D. J. P. (eds.), Marine sediment transport and environmental management: John Wiley, New York, N.Y., pp. 197-218.

Milici, R. C., 1975, Structural patterns in the southern Appalachians-evidence for a gravity slide mechanism for Alleghanian deformation: Geol. Soc. America Bull., v. 86, pp. 1316-1320.

Milici, R. C., Brent, W. B., and Walker, K. R., 1973, Depositional environments in upper Conasauga lagoon-fill sequence, in Geology of Knox County, Tennessee: Tennessee Div. Geol. Bull. 70, pp. 138-148.

Molnar, P., Chen, W. P., Fitch, J. J., Tapponier, P., Warsi, W. E. K., and Wu, F. T., 1976, Structure and tectonics of the Himalayas: a brief summary of relevant geophysical observations: Collogues internationaux du C.N.R.S., No. 268, Ecologie et geologie de l'Himalaya, pp. 269-294.

Morris, R. C., 1974, Sedimentary and tectonic history of the Ouachita Mountains, in Dickinson, W. R. (ed.), Plate tectonics and sedimentation: Soc. Econ. Paleont. and Miner., Spec. Pub. 22, pp. 120-142.

Murrell, S. A. F., 1976, Rheology of the lithosphere-experimental indication: Tectonophysics, v. 36, pp. 5-24.

Murrie, G. W., Diamond, W. P., and Lambert, S. W., 1976, Geology of the Mary Lee Group of coal beds, Black Warrior coal basin, Alabama: U.S. Bur. Mines Rept. Inv. 8189, 49 pp.

Nadai, A., 1963, Theory of flow and fracture of solids, vol. 2: McGraw-Hill, Eng. Soc. Monographs, New York, N.Y., 705 pp.

Palmer, A. R., 1962, Glyptagnostus and associated trilobites in the United States: U.S. Geol. Survey Prof. Paper 374F, 45 pp.

Palmer, A. R., and Campbell, D. P., 1976, Biostratigraphic implications of trilobite facies; Albertella zone, Middle Cambrian, western United States: Brigham Young Univ. Geology Studies, v. 23, pp. 39-50.

Parsons, Barry, and Molnar, Peter, 1976, The origin of outer topographic rise associated with trenches: Geophys. Jour. Royal Astronom. Soc., v. 45, pp. 707-712.

Perrier, R., and Quiblier, J., 1974, Thickness changes in sedimentary layers during compaction history; methods for quantitative evaluation: Am. Assoc. Petr. Geol. Bull., v. 58, pp. 507-520.

Perry, W. J., Jr., 1978, Sequential deformation in the central Appalachians: Am. Jour. Sci., v. 278, pp. 518-542.

Pfeil, R. W., and Reed, J. F., 1980, Cambrian carbonate platform margin facies, Shady Dolomite, southwestern Virginia, U.S.A.: Jour. Sed. Petrology, v. 50, pp. 91-116.

Powell, W. J., Copeland, C. W., and Drahovzal, J. A., 1975, Delineation of linear features and application to reservoir engineering using Apollo 9 multispectral photography: Alabama Geol. Survey Inf. Ser. 41, 36 pp.

Price, R. A., 1967, Tectonic significance of mesoscopic subfabrics in the southern Rocky Mountains of Alberta and British Columbia: Canadian Jour. of Earth Sci., v. 4, pp. 39-70.

Prouty, W. F., 1916, The crystalline and other marbles of Alabama: Alabama Geol. Survey Bull. 18, 121 pp.

Ramsbottom, W. H. C., 1978, Carboniferous, in McKerrow, S. W. (ed.), The ecology of fossils: M.I.T. Press, Cambridge, Mass., pp. 146-183.

Rast, N., and Stringer, P., 1980, A geotraverse across a deformed Ordovician ophiolite and its Silurian cover, northern New Brunswick, Canada: Tectonophysics, v. 69, pp. 221-245.

Raymond, D. E., 1973, Upper Ordovician conodonts of Alabama: Univ. Alabama M.S. thesis, 159 pp.

Read, C. B., and Mamay, S. H., 1964, Upper Paleozoic floral zones and floral provinces in the U.S.: U.S. Geol. Survey Prof. Paper 454K, pp. K1-K35.

Reading, H. G. (ed.), 1978, Sedimentary environments and facies: Elsevier, New York, N.Y., 544 pp.

Reed, D. F., 1949, Investigation of Talladega grey iron ore, Talladega County, Alabama: U.S. Bur. Mines Rept. Inv. 4426, 29 pp.

Reineck, H. E., and Singh, C. B., 1973, Depositional sedimentary environments: Springer Verlag, New York, N.Y., 439 pp.

Reineck, H. E., and Wunderlich, F., 1968, Classification and origin of flaser and lenticular bedding: Sedimentology, v. 11, pp. 99-104.

Resser, C. E., 1938, Cambrian system (restricted) of the southern Appalachians: Geol. Soc. America Spec. Paper 15, 139 pp.

Rich, J. L., 1934, Mechanics of low-angle overthrust faulting as illustrated by Cumberland thrust block, Virginia, Kentucky, and Tennessee: Am. Assoc. Petr. Geol. Bull., v. 18, pp. 1643-1654.

Riding, Robert, 1975, Girvanella and other algae as depth indicators: Lethaia, v. 8, pp. 173-179.

Rodgers, John, 1949, Evolution of thought on structure of middle and southern Appalachians: Am. Assoc. Petr. Geol. Bull., v. 33, pp. 1643-1654.

Rodgers, John, 1953, Geological map of east Tennessee with explanatory text: Tennessee Div. Geol. Bull. 58, pt. 2, 168 pp.

Roeder, Dietrich, 1960, Der tektonische stil der Rocky Mountains in Alberta, Canada: Geol. Rundschau, v. 50, pp. 577-594.

Roeder, D. H., 1967, Rocky Mountains, der geologische Aufban des Kanadischen Felsengebirges: Borntrager, Berlin, 318 pp.

Roeder, Dietrich, Gilbert, O. E., Jr., and Witherspoon, W. D., 1978, Evolution and macroscopic structure of Valley and Ridge thrust belt, Tennessee and Virginia: Univ. of Tennessee, Studies in Geology No. 2, 25 pp.

Roeder, Dietrich, Wielchowsky, C. C., and Gilbert, O. E., Jr., 1978, Mechanics of thrusting and suture progradation in the southern Appalachians (abs.): Geol. Soc. America Abs. with Prog., v. 10, p. 196.

Roeder, Dietrich, and Witherspoon, W. D., 1977, Structure of Appalachian thrust belt between Roanoke and Birmingham (abs.): Geol. Soc. America Abs. with Prog., v. 9, p. 179.

Roeder, Dietrich, Yust, W. W., and Little, R. L., 1978, Folding in the Valley and Ridge province of Tennessee: Am. Jour. Sci., v. 278, pp. 477-496.

Rothrock, H. E., 1949, Geology and coal resources of the northeast part of the Coosa coal field, St. Clair County, Alabama: Alabama Geol. Survey Bull. 61, 163 pp.

Royse, F. J., Werner, M. A., and Reese, D. C., 1975, Thrust belt structural geometry and related stratigraphic problems, Wyoming-Idaho-northern Utah: Rocky Mtn. Assoc. Geol. Symp. on Deep Drilling Frontiers, Central Rocky Mountains, pp. 41-54.

Ruppel, S. C., 1979, Conodonts from the lower Mississippian Fort Payne and Tuscumbia formations of northern Alabama: Jour. Paleo., v. 53, pp. 55-70.

Safford, J. M., 1851, The Silurian basin of Middle Tennessee: Am. Jour. Sci., 2nd Ser., v. 12, pp. 352-361.

Safford, J. M., and Killebrew, J. M., 1876, Elements of geology of Tennessee: State of Tennessee, Nashville, Tenn., 255 pp.

Samman, N. F., 1975, Sedimentation and stratigraphy of the Rome Formation in Tennessee: Univ. of Tennessee Ph.D. diss., 337 pp.

Schlanger, S. O., 1964, Petrology of the limestones of Guam: U.S. Geol. Survey Prof. Paper 403-D, pp. 1-52.

Schlee, T. S., 1963, Early Pennsylvanian current directions in the southern Appalachian mountains: Geol. Soc. America Bull., v. 74, pp. 1439-1451.

Schuchert, C., 1955, Atlas of paleogeographic maps of North America: Wiley and Sons, New York, N.Y., 177 pp.

Sclater, J. G., Anderson, R. N., and Bell, M. L., 1971, Elevation of ridges and evolution of the central eastern Pacific: Jour. Geophys. Res., v. 76, pp. 7888-7915.

Sclater, J. G., and Christie, P. A. F., 1980, Continental stretching; an explanation of the post-Mid-Cretaceous subsidence of the central North Sea basin: Jour. Geophys. Res., v. 85, pp. 3711-3739.

Sears, J. W., Cook, R. B., Gilbert, O. E., Jr., Carrington, T. J., and Schamel, Steven, in press, Stratigraphy and structure of the Pine Mountain window in Georgia and Alabama: Georgia Geol. Survey Bull.

Self, D. M., Gilbert, O. E., Jr., and Wielchowsky, C. C., 1974, Quartz-pebble beds within the upper knox Group of Alabama (abs.): Geol. Soc. America Abs. with Prog., v. 6, pp. 797-798.

Self, D. M., Neathery, T. L., and Jacks, V. P., 1975, Structural lexicon of Alabama with map of structural features of Alabama: Alabama Geol. Survey, open file report.

Selley, R. C., 1978, Ancient Sedimentary environments: Cornell Univ. Press, Ithaca, N.Y., 2nd ed., 278 pp.

Settle, W. H., 1954, Mississippian formations of northern Alabama: Mississippi Geol. Soc. Guidebook, 11th Field Trip, 31 pp.

Shanmugan, Ganapathy, and Walker, K. R., 1978, Tectonic significance of distal turbidites in the Middle Ordovician Blockhouse and Lower Sevier Formations in east Tennessee: Am. Jour. Sci., v. 278, pp. 551-578.

Shanmugan, Ganapathy, and Walker, K. R., 1980, Sedimentation, subsidence, and evolution of a foredeep basin in the Middle Ordovician, southern Appalachians: Am. Jour. Sci., v. 280, pp. 479-496.

Shaw, C. E., Jr., 1970, Age and stratigraphic relations of the Talladega Slate: evidence of pre-Middle Ordovician tectonics in central Alabama: Southeastern Geol., v. 11, pp. 255-267.

Shaw, C. E., Jr., 1973, Stratigraphy, structure, and tectonics of rocks adjacent to the Piedmont physiographic front in Talladega County, Alabama, in Carrington, T. J. (ed.), Talladega metamorphic front: Alabama Geol. Soc. Guidebook, 11th Ann. Field Trip, pp. 56-65.

Shaw, C. E., Jr., 1974, Recumbent folds in the Valley and Ridge province in Alabama, in Thomas, W. A., and Drahovzal, J. A. (eds.), The Coosa deformed belt in the Alabama Appalachians: Alabama Geol. Soc. Guidebook, 12th Ann. Field Trip, pp. 87-98.

Shaw, C. E., Jr., 1976, Large-scale recumbent folding in the Valley and Ridge province of Alabama: Geol. Soc. America Bull., v. 69, pp. 1283-1296.

Sheldon, R. P., 1964, Iron deposits of the Birmingham district, Alabama: U.S. Geol. Survey, Prof. Paper 450A, p. A1.

Sheldon, R. P., 1970, Sedimentation of iron-rich rocks of Llanoverian age (Lower Silurian) in the southern Appalachian basin, in Berry, W. B., and Boucot, A. J. (eds.), Correlation of the North American Silurian rocks: Geol. Soc. America Spec. Paper 102, 289 pp.

Shepard, F. P., 1973, Submarine geology: Harper and Row, New York, N.Y., 517 pp.

Shinn, E. A., Halley, R. E., Hudson, J. H., and Lidz, B. H., 1977, Limestone compaction: an enigma: Geology, v. 5, pp. 21-24.

Simpson, T. A., 1963, Structural geology of the Birmingham red iron district: Alabama Geol. Survey Circ. 21, 17 pp.

Sleep, N. H., 1976, Platform subsidence mechanisms and eustatic sea level change: Tectonophysics, v. 36, pp. 45-56.

Sleep, N. H., and Snell, N. S., 1976, Thermal contraction and flexure of mid-continent and Atlantic marginal basins: Geophys. Jour. Royal Astron. Soc., v. 45, p. 125.

Sloss, L. L., and Weller, J. M., 1958, Stratigraphic facies differentiation and nomenclature: Am. Assoc. Petr. Geol. Bull., v. 42, pp. 609-639.

Smith, E. A., 1876, Report of progress for 1876: Alabama Geol. Survey Rept. Prog. 4, 99 pp.

Smith, E. A., 1893, Underthrust folds and faults: Am. Jour. Sci., 3rd Ser., v. 45, pp. 305-306.

Smith, E. A., McCalley, Henry, Squire, Joseph, Gibson, A. M., Langdon, D. W., and Johnson, L. C., 1894, Geological map of Alabama: Alabama Geol. Survey, Spec. Map 1.

Smith, W. E., 1967, Carbonate petrology of the Mississippian system in northern Alabama, in Smith, W. E. (ed.), Field guide to Mississippian sediments in northern Alabama and south-central Tennessee: Alabama Geol. Soc. Guidebook, 5th Ann. Field Trip, pp. 40-52.

Smith, W. E., Neathery, T. L., and Drahovzal, J. A., 1971, Ordovician K-bentonites in Alabama, in Drahovzal, J. A., and Neathery, T. L. (eds.), Middle and Upper Ordovician of the Alabama Appalachians: Alabama Geol. Soc. Guidebook, 9th Ann. Field Trip, pp. 125-136.

Squire, Joseph, 1890, Report on the Cahaba coal field: Alabama Geol. Survey, 180 pp.

Steinhart, J. S., and Meyer, R. P., 1961, Explosion studies of continental structure: Carnegie Inst. Pub. 622, Washington, D.C., 409 pp.

Stock, C. W., and Benson, D. J., 1981, Lithologies and organisms of a Chickamauga Limestone (Middle Ordovician) bioherm and associated strata in the Birmingham, Alabama, area (abs.): Geol. Soc. America Abs. with Prog., v. 13, p. 36.

Sweeney, J. F., 1976, Evolution of the Sverdrup Basin, Arctic Canada: Tectonophysics, v. 36, pp. 181-196.

Sweeney, J. F., 1977, Subsidence of the Sverdrup Basin, Canadian Arctic Islands: Geol. Soc. America Bull., v. 88, pp. 41-48.

Sweet, W. C., Ethington, R. L., and Barnes, C. R., 1970, North American conodont faunas, in Sweet, W. C., and Bergstrom, S. M. (eds.), Symposium on conodont biostratigraphy: Geol. Soc. America Mem. 127, pp. 163-194.

Taylor, R. S., 1971, Petrology and depositional history of Ordovician rocks of Cahaba Valley, Shelby County, in Drahovzal, J. A., and Neathery, T. L. (eds.), The Middle and Upper Ordovician of the Alabama Appalachians: Alabama Geol. Soc. Guidebook, 9th Ann. Field Trip, pp. 115-123.

Taylor, R. S., 1973, Basinal facies of the Middle Ordovician rocks of central Alabama (abs.): Geol. Soc. America Abs. with Prog., v. 5, p. 443.

Tegland, E. R., 1978, Seismic investigations in East Tennessee: Tenn. Div. Geol. Bull. 78, 68 pp.

Teichmuller, M., and Teichmuller, R., 1979, Digenesis of coal (lithification), in Larson, G., and Chilingar, G. V. (eds.), Diagenesis in sediments and sedimentary rocks: Developments in sedimentology, v. 25A, Elsevier Press, New York, N.Y., pp. 207-248.

Thomas, W. A., 1968, Contemporaneous normal faults on flanks of Birmingham anticlinorium, central Alabama: Am. Assoc. Petr. Geol. Bull., v. 52, pp. 2123-2136.

Thomas, W. A., 1972a, Mississippian stratigraphy of Alabama: Alabama Geol. Survey, Monograph 12, 121 pp. plus plates.

Thomas, W. A., 1972b, Regional Paleozoic stratigraphy in Mississippi between the Ouachita and Appalachian Mountains: Am. Assoc. Petr. Geol. Bull., v. 56, pp. 81-106.

Thomas, W. A., Bearce, D. N., and Drahovzal, J. A., 1970, Paleozoic folding of the Birmingham anticline, Alabama (abs.): Geol. Soc. America Abs. with Prog., v. 2, pp. 704-705.

Thomas, W. A., and Drahovzal, J. A., 1973, Regional Paleozoic stratigraphy of Alabama, in Carrington, T. J. (ed.), Talladega metamorphic front: Alabama Geol. Soc. Guidebook, 11th Ann. Field Trip, pp. 66-91.

Thomas, W. A., and Drahovzal, J. A., 1974, The Coosa deformed belt in the Alabama Appalachians: Alabama Geol. Soc. Guidebook, 12th Ann. Field Trip, 98 pp.

Thomas, W. A., Mack, G. H., and Waters, J. A., 1980, Depositional setting of the Mississippian Hartselle Sandstone and lower Bangor Limestone in northwest Alabama, in Tull, J. F. (ed.), Field trips for the southeastern section of the Geological Society of America, March 1980: Alabama Geol. Soc. special guidebook, pp. 29-68.

Thomas, W. A., Tull, J. F., Bearce, D. N., Russell, Gail, and Odom, A. L., 1979, Geologic synthesis of the southernmost Appalachians, Alabama and Georgia, in Wones, D. R. (ed.), Proceedings "The Caledonides in the U.S.A.": Va. Poly Inst. & State Univ. Dept. Geol. Soc. Mem. 2, pp. 91-98.

Thompson, A. M., 1971, Clastic-carbonate facies relationships and paleoenvironments in Upper Ordovician rocks of northeast Alabama, in Drahovzal, J. A., and Neathery, T. L. (eds.), The Middle and Upper Ordovician of the Alabama Appalachians: Alabama Geol. Soc. Guidebook, 9th Ann. Field Trip, pp. 63-78.

Ulrich, E. O., 1911, Revision of the Paleozoic systems: Geol. Soc. America Bull., v. 22, pp. 281-680.

Vail, P. R., Mitchum, R. M., Jr., and Thompson, S. III, 1977, Seismic stratigraphy and global changes of sea level, part 4: Global cycles of relative changes of sea level, in Payton, C. E. (ed.), Seismic stratigraphy-applications to hydrocarbon exploration: Am. Assoc. Petr. Geol. Mem. 26, pp. 83-97.

Vail, P. R., and Todd, R. G., in press, Northern North Sea Jurassic unconformities, chronostratigraphy and sea level changes from seismic stratigraphy: Proc. Petr. Geol. of the Continental Shelf of Northwest Europe Conf., London, 1980.

Viele, G. W., 1979, Cross-section of the eastern Ouachita Mountains, Arkansas: Geol. Soc. America Map MC-28F.

Walcott, R. I., 1972, Gravity, flexure, and the growth of sedimentary basins at the continental edge: Geol. Soc. America Bull., v. 83, pp. 1845-1848.

Wampler, J. M., Neathery, T. L., and Bentley, R. D., 1970, Age relations in the Alabama Piedmont, in Bentley, R. D., and Neathery, T. L. (eds.), Geology of the Brevard zone and related rocks in Alabama: Alabama Geol. Soc. Guidebook, 8th Ann. Field Trip, pp. 81-90.

Wanless, H. R., 1975, Appalachian Region, in McKee, E. D., and Crosby, E. J. (eds.), Paleotectonic investigations of the Pennsylvanian System in the U.S.: U.S. Geol. Survey Prof. Paper 853, pt. I, pp. 17-62.

Warman, J. C., and Causey, L. V., 1962, Geologic map of Calhoun County, Alabama: Alabama Geol. Survey Spec. Map 17.

Watts, A. B., 1981, The U.S. Atlantic continental margin: subsidence history, crustal structure, and thermal evolution, in Bally, A. W., Watts, A. B., Grow, J. A., Manspeizer, W., Bernoulli, O., Schreiber, C., and Hunt, J. M. (eds.), Geology of passive continental margins: Am. Assoc. Petr. Geol. Education Course Note Series 19, pp. 2-1 through 2-75.

Watts, A. B., and Ryan, W. B. F., 1976, Flexure of the lithosphere and continental margin basins: Tectonophysics, v. 36, pp. 25-44.

Watts, A. B., and Talwani, M., 1974, Gravity anomalies seaward of deep-sea trenches and their tectonic implications: Geophys. Jour. Royal Astronom. Soc., v. 36, pp. 57-90.

Welch, S. W., 1958, Stratigraphy of Upper Mississippian rocks above the Tuscumbia Limestone in northern Alabama and northeastern Mississippi: U.S. Geol. Survey Oil and Gas Inv. Chart OC-58.

Welch, S. W., 1959, Mississippian rocks of the northern part of the Black Warrior basin, Alabama and Mississippi: U.S. Geol. Survey Oil and Gas Inv. Chart OC-62.

White, J. R., Jr., 1976, Stratigraphy and depositional environments of the Carter Sand of Chester age in the subsurface of Lamar and Fayette Counties, Alabama: Univ. Alabama M.S. thesis, 78 pp.

Wickman, John, 1977, Interpretation of the Ouachita Mountains, Oklahoma, in Heisey, E. L., Lawson, D. E., Norwood, E. R., Wach, P. H., and Hale, L. A. (eds.), Rocky Mountain thrust belt geology and resources: Wyo. Geol. Assoc. Guidebook, 29th Ann. Field Conf., pp. 523-530.

Wielchowsky, C. C., 1976, Review and interpretations of available geophysical data from the Alabama Piedmont: Rice Univ. unpublished ms., 50 pp.

Wielchowsky, C. C., and Warren, W. M., unpublished ms., Application of remote sensing to reservoir engineering in a carbonate terrain at Logan Martin hydroelectric plant, Alabama: Alabama Geol. Survey open file report, 16 pp.

Wilson, A. O., 1971, Petrology of parts of Black River age strata of the Chickamauga limestones, Etowah and DeKalb Counties, Alabama, in Drahovzal, J. A., and Neathery, T. L. (eds.), The Middle and Upper Ordovician of the Alabama Appalachians: Alabama Geol. Soc. Guidebook, 9th Ann. Field Trip, pp. 79-114.

Wilson, C. W., 1949, Pre-Chattanooga stratigraphy in central Tennessee: Tenn. Dept. of Conservation, Division of Geology Bull. 56, 407 pp.

Woodward, H. P., 1961, Preliminary subsurface study of southeastern Appalachian interior plateau: Am. Assoc. Petr. Geol. Bull., v. 45, pp. 1639-1655.

Wunderlich, Friedrich, 1970, Genesis and environments of the "Nellen köpfchen schichten" (Lower Emsian, Rhenian Devonian) at locus typicus in comparison with modern coastal environments of the German Bay: Jour. Sed. Petr., v. 40, pp. 102-130.

Yeager, D. W., 1971, Petrography of the Newala Limestone in Northern Shelby County, Alabama: Alabama Acad. Sci. Jour., v. 42, pp. 3-9.

APPENDICES

APPENDIX A

SECTION RIM—Weisner Formation, in and near road across West Riser Mountain S of Riser Chapel, NE1/4 Sec. 17 and SE1/4 Sec. 8, T.20S., R.4E., Talladega County.

Note: Total preserved thickness above basal fault is 416 m; best exposures are the upper 114 m exposed in road ditches on SE side of mountain.

Unit	Thickness	Description
-	NA	Shady Dolomite residuum
56	3.72 m ±	very poorly sorted, fine- to coarse-grained, locally conglomeratic, ferruginous, pyritic sandstone; grains angular to subrounded, locally pyritic
55	0.79 m	laminated light- to dark-gray slate, local silty lenses < 1 mm thick, local soft sediment deformation
54	4.77 m	interbedded, laminated, light- to dark-gray slate, and medium-grained, thin-bedded, locally carbonaceous sandstone, and dark- to medium-gray silty slate; sand/slate contacts show ball and pillow structure; slates have inclined filter-feeder burrows filled by overlying sands
53	0.17 m	laminated, dark-brown to greenish-brown, fine-grained sandstone with thin laminae of black slate

Unit	Thickness	Description
52	0.95 m	very thinly- to thinly-laminated, fine-grained, dark- to medium-gray sandstone with laminae of black slate and silty slate
51	0.28 m	laminated fine-grained sandstone, badly weathered
50	0.98 m	badly weathered laminated sandstone and slate
49	2.07	thinly-laminated, dark-gray slate, with scattered laminae of fine-grained, medium-gray sandstone
48	0.05 m	medium-gray, fine-grained orthoquartzite, grades laterally into 30 cm dark-gray to black laminated slate
47	1.12 m	thinly-laminated, dark-gray to black slate and silty slate, with dark-gray, fine-grained sandstone lenticles
46	0.16 m	dark-gray to black slate
45	0.18 m	yellowish-brown, fine-grained sandstone
44	0.60 m	fine-grained, medium-gray sandstone, locally cross-bedded, with partings of black slate
43	0.25 m	black slate
42	0.63 m	fine-grained, medium-gray sandstone, rare partings of black slate
41	2.10 m	laminated dark-gray to black slate, with thin beds and lenses of fine-grained, medium-gray, glauconitic sandstone; sand bodies fewer and thinner toward base; ball and pillow structures of sand/slate contacts

Unit	Thickness	Description
40	4.33 m	very thin- to medium-bedded, fine-grained, medium-gray sandstone; local thin beds of laminated black slate
39	1.50 m	covered; black slate rubble
38	0.77 m	laminated black slate
37	1.89 m	covered
36	2.34 m	laminated, black slate with thin- to very-thin beds and lenses of medium- to dark-gray, fine-grained sandstone; sandier toward base
35	0.05 to 0.20 m	coarse-grained, poorly sorted, ferruginous orthoquartzite
34	0.69 m	irregularly laminated, light-gray silty slate
33	0.44 m	laminated to thinly-laminated, dark-gray to black slate, and light gray silty slate
32	0.93 m	dark-gray slate
31	0.20 m	laminated, dark-gray, silty slate
30	0.72 m	laminated, dark-gray to black slate; chaotically folded (soft sediment) with tops of folds scoured off
29	8.41 m	laminated, dark-gray slate; irregular beds and lenses of light- to medium-gray, fine-grained silty sandstone; locally flaser bedded, local scour and fill structure
28	0.76 m	poorly-sorted, medium-gray, fine-grained sandstone; thin lenses of dark-gray sandstone at base

Unit	Thickness	Description
27	3.21 m	interbedded, laminated to thin-bedded, black slate and medium-gray, silty slate; local very-thin beds and lenses of fine-grained, light- to very light-gray orthoquartzite
26	0.50 m	poorly sorted, medium-gray, fine-grained sandstone
25	0.43 m	laminated to thin-bedded, dark-gray to black, silty slate
24	0.02 to 0.08 m	dark-gray, medium-grained orthoquartzite
23	0.07 m	dark-gray slate
22	0.90 m	thin-bedded, light-brown siltstone
21	1.07 m	medium- to dark-gray slate
20	0.28 m	interbedded, very-thin to thin-bedded, coarse-grained subangular, ferruginous quartzite, and dark-gray slate
19	4.35 m	massive, fine-grained, medium-gray sandstone with local carbonaceous laminae; forms main crest of ridge
18	4.87 m	laminated to very thin-bedded, dark- to medium-gray, silty to sandy slate, locally micaceous; flaser bedded, local scour and fill structure
17	1.39 m	very thick-bedded, dark-gray slate
16	0.33 m	medium- to coarse-grained, poorly sorted, ferruginous quartzite
15	0.58 m	medium-bedded, dark-gray siltstone

Unit	Thickness	Description
14	0.23 m	dark-gray siltstone with intraclasts ripped from underlying bed; scoured base
13	2.24 m	laminated, dark-gray slate; locally silty
12	0.98 m	laminated, yellowish-orange siltstone with irregular lenses dark-gray slate; very-thin, irregular beds of light-gray to white, fine-grained sandstone
11	3.25 m	laminated dark-gray to black slate
10	10.40 m	covered; rubble of laminated black slate
9	0.74 m	pink to white weathered laminated slate
8	1.78 m	laminated dark-gray slate with thin- to medium-bedded lenses of fine-grained, light-gray sandstone
7	13.03 m	laminated dark-gray, locally silty, slate
6	5.49 m	same as above, with thin- to medium-interbeds of fine-grained, medium-gray sandstone
5	1.07 m	poorly sorted, coarse-grained, ferruginous quartzite with intraclasts of black slate up to 4 cm in diameter; ridge former
4	14.85 m	laminated dark-gray slate, some thin lenses light- to medium-gray, fine-grained sandstone
3	96.40 m	covered; rubble mostly black slate and fine-grained gray sandstone
2	6.00 m ±	laminated dark-gray slate and silty slate
1	200.00 m	covered

Unit	Thickness	Description
11	116 m	covered
10	3 ± m	massive, light-gray to white, finely-crystalline siliceous dolostone
9	158 m	covered
8	2 m	massive, light-gray, crystalline dolostone
7	223 m	covered
6	6 m	massive, light-gray, coarsely-crystalline dolostone; brecciated, possible fault
5	65 m	covered
4	3 m	massive, fine-grained, light gray dolostone
3	46 m	covered
2	10.5 m	thin- to very thin-bedded, light-gray dolostone; algal sediment laminae in lower 2 m
1	56 m	covered
-	NA	Weisner Formation

SECTION GRA—Conasauga Group, with Ketona Dolomite member, poorly exposed in creek beds on SE side of Birmingham Anticlinorium, SE1/4, Sec. 18, and Sec. 17, T.18S., R.3W., Jefferson County.

Notes: (1) base of Conasauga not exposed;
(2) units poorly exposed—Conasauga 28 percent exposure, Ketona 6 percent exposure;
(3) Kidd and Shannon (1978) put Ketona-Conasauga contact at unit 33-unit 34 boundary.

Unit	Thickness	Description
-	NA	Copper Ridge Dolomite
	KETONA DOLOMITE	
54	111 ± m	covered; sporadic exposures along strike suggest upper Ketona similar to lower units
53	2.0 m	massive, light-gray, crystalline replacement dolostone
52	16 ± m	covered
51	3 +	same as unit 53
50	3.5 m	very thinly interbedded, light-gray and dark-gray, replacement dolostone; remnant textures indicate protolith was a bioturbated biomicrite, with abundant branching burrows and trilobite fragments
49	24 ± m	covered
48	1.0 m	medium-bedded, light brownish-gray, replacement dolostone; remnant burrow texture as in unit 50
47	28 ±	covered

Unit	Thickness	Description
46	0.30 m	very thinly-interbedded, light- to dark-gray, locally bioclastic, fine-grained replacement dolostone; some beds bioturbated
45	65 ± m	covered
44	0.2 m	very thin-bedded, dark-gray coarsely crystalline replacement dolostone
43	2 + m	massive, medium dark-gray, crystalline replacement dolostone with intraclasts (up to 12 cm) of light-gray dolostone
42	21 ± m	covered
41	6.0 m	medium- to thick-bedded, light-gray, coarsely crystalline replacement dolostone with calcite
40	24 ± m	covered
39	1.0-2.0 m	very thick-bedded, light-gray, coarsely crystalline replacement dolostone with intraclasts as in unit 43; unreplaced matrix is micrite
38	17 ± m	covered
	CONASAUGA GROUP	
37	16 + m	very thin- to thin-bedded, light-gray micrite with patches of replacement spar
36	10 ± m	covered
35	3 + m	massive, medium-gray micrite, no textures or structure visible
34	15 ± m	covered
33	41 ± m	covered

Unit	Thickness	Description
32	1.5 m	very thin-bedded, medium-gray bioturbated biomicrite
31	4 m	covered
30	0.3 m	thin-bedded, medium-gray micrite, unevenly bedded
29	16 ± m	covered
28	1.55 m	thin-bedded, internally laminated, bioturbated biomicrite, intrasparite, and biointramicrite; fossil debris mostly trilobite; biomicrites show desiccation cracks and scoured surfaces overlain by intrasparite; sparsely dolomitic
27	2.8 m	thin-bedded, medium-gray dismicrite with horizontal trails
26	0.4 m	laminated lithology similar to unit 27
25	0.9 m	thin-bedded, dark-gray, evenly bedded micrite with desiccation cracks
24	2.7 m	very thin-bedded, medium-gray dismicrite
23	31 ± m	covered
22	0.6 m	very thin-bedded, medium-gray micrite with dolomitic mottling
21	140 ± m	covered
20	4 + m	very thin- to thick-bedded, medium-gray biomicrite and biointrasparite in uneven beds; biomicrite has desiccation cracks and scoured surfaces overlain by biointrasparite
19	32 ± m	covered

Unit	Thickness	Description
18	1.4 m	very thin- to thin-bedded, light-gray replacement dolostone
17	3 m	covered
16	1.5 m	thin-bedded, light- to medium-gray, bioturbated biomicrite and biointrasparite with patchy replacement dolomite; flat crenulated algal sediment laminae visible in outcrop
15	29 ± m	scattered exposures thin-bedded, dark-gray micrite and biomicrite
14	8.4 m	covered
13	3.0 m	very thin-to medium-bedded, dark-gray biomicrite, with trilobite and brachiopod fragments; locally pyritic
12	63 ± m	covered
11	34.4 m	thinly-laminated to thin-bedded, medium-gray biomicrite and calcareous shale; micrite dominant toward top of sequence, shale dominant toward base; irregular ripple bedding
10	17 ± m	covered
9	0.3 m	thin-bedded micrite and biomicrite
8	25 ± m	scattered exposures very thin- to thin-bedded, medium-gray micrite
7	1.0 m	very thin, lenticular beds of medium-gray biomicrite and biopelsparite
6	8 ± m	covered

Unit	Thickness	Description
5	28 ± m	thin-bedded, medium-gray, burrow mottled biomicrite, with encrusting bryozoan and trilobite fragments
4	41 ± m	covered
3	12 ± m	thin-bedded, light-gray biomicrite with trilobite fragments, interbedded, with scoured contacts, with biointrasparite; intraclasts poorly sorted and angular, some contain penecontemporaneous dolomite; mottle of replacement (?) dolomite
2	44 ± m	covered
1	10 m	very thin- to medium-bedded micrite, biomicrite, and biointrasparite; biointrasparite is very poorly sorted, with micrite intraclasts and trilobite, brachiopod, and ostracode fragments; horizontal trails and burrows (?); patchy replacement dolomite
		Base of exposures—crest of anticlinorium

SECTION LP— Knox Group (Copper Ridge Dolomite—Chepultepec Dolomite—Newala Limestone), Lenoir Limestone, and Little Oak Limestone; exposures in bed and shoreline of Little Cahaba River and Lake Purdy, Sec. 17, 20, 21, and 28, T.18S, R.1W., Shelby County.

Notes: (1) section accessible only at low water stage in reservoir;

(2) section partially duplicated by Cahaba Valley fault;

(3) Lenoir-Little Oak contact not picked;

(4) field examination suggests that nature of chert in residuum is related to lithotype with banded chert after laminated dolostone, wormy chert after bioturbated dolostone.

Unit	Thickness	Description
-	NA	Fort Payne Chert
	LITTLE OAK LIMESTONE (LENOIR LIMESTONE at base)	
83	3.1 m	massive, internally laminated biomicrite and intramicrite with rare algal oncolites; patchy replacement dolomite
82	170 ± m	very thin-bedded, dark-gray biomicrite, with varying proportions of algal grains, gastropods, algal oncolites, and finely divided skeletal debris; bioturbated with replacement dolomite concentrated in burrows and along fractures

Unit	Thickness	Description
81	55 ± m	covered
80	6.1 m	same as unit 82
79	20.7 ± m	covered
78	17.8 m	medium- to thick-bedded, light- to medium-gray biomicrite with desiccation birdseyes parallel to bedding
77	14 ± m	covered
76	14.6 m	massive, very dark-gray micrite and biomicrite, organic debris mostly broken and articulated ostracodes; desiccation fenestrae; internal lamination visible on weathered surfaces but not in broken surface or thin-section; sulfide nodules visible in outcrop
75	2.43 m	medium-bedded, medium-gray mottled micrite and very poorly sorted intrasparite, with rounded to sub-rounded micrite intraclasts; locally laminated
74	19.8 ± m	covered
73	6.1 m	thick- to very thick-bedded, internally laminated beds of light-gray mottled and dark-gray coarsely crystalline replacement dolostone
	NEWALA LIMESTONE	
72	27 ± m	covered
71	1+ m	thick-bedded, light-gray micrite and biomicrite
70	23.6 m	covered

Unit	Thickness	Description
69	3.66 m	thin-bedded, light- to dark-gray mottled poorly-sorted intrasparite; extensively recrystallized
68	24 ± m	covered
67	58 ± m	discontinuous exposures of thin-bedded to massive, light-gray micrite and biomicrite, locally scoured and cross-bedded
66	11 ± m	covered
65	3.66 m	very thin-bedded to massive, light-gray, fine-grained intrasparite, with biosparite lenses; locally cross-bedded, with intraclasts of intrasparite; scattered well-rounded, subspherical, detrital quartz grains
	CHEPULTEPEC DOLOMITE	
64	105 ± m	covered; residuum of stony chert
63	0.91 m	thick-bedded, medium-gray replacement dolostone; extensive burrows; weathering to "wormy" or "mealy" chert of Butts (1926)
62	56.5 ± m	covered
61	5.94 m	medium- to thick-bedded, medium-gray dolostone; internally laminated with alternating laminae silt + organic (?) + dolomite and finely crystalline dolomite; flat algal sediment laminae; irregular chert nodules parallel to bedding; weathering to banded chert

Unit	Thickness	Description
60	0.4 m	mealy chert as in unit 63
59	11.73 m	thick-bedded to massive, dark-gray, fetid smelling dolostone; 90 percent replacement dolomite, preserved protolith is micrite
58	0.56 m	medium-bedded, light-gray, finely crystalline replacement dolostone with preserved flat algal sediment laminae
57	9.6 m	thick-bedded, internally laminated, light- to dark-gray, fetid smelling, fine-grained replacement dolostone; locally contorted laminae are probable algal sediment laminae; lenticular chert in basal 3 m
43	1.5 m	thin- to very thin-bedded, dark-gray replacement dolostone and calcite; flat and flat-crenulated algal sediment laminae, gas fenestrae parallel to laminae; locally bioturbated with inclined burrows; original matrix micrite
42	22 ± m	covered
41	1.5 ± m	irregularly laminated, dark-gray intrabiosparite and banded micrite with flat crenulated algal sediment laminae, laminae locally ripped up with new laminae established above; extensive replacement dolomite
40	160 ± m	covered
39	8.5+ m	"wormy" chert residuum (see notes)

Unit	Thickness	Description
38	9.2 m	covered
37	7.5 m	poorly exposed massive, light-gray, finely crystalline replacement dolostone
36	19.5 ± m	covered
35	3.0 m	thin- to medium-bedded, light-gray, fetid smelling, finely-crystalline replacement dolostone, weathering to "wormy" and "banded" chert (see notes)
34	15.6 ± m	covered
33	18.3 m	medium-bedded, light- to medium-gray, finely crystalline replacement dolostone; weathering to "wormy" chert (see notes)
32	13.1 m	thick-bedded, alternating light- and dark-gray, fetid smelling dolostone with black chert nodules parallel to bedding; problematical algal sediment laminae; bioturbated, with some beds weathering to "wormy" chert (see notes)
31	60 ± m	covered
30	84 ± m	covered; mixed residuum with "wormy" chert, chert after algal stromatolites, "banded" chert, and bedded chert with branching horizontal trails or burrows (see notes)
29	17.6 ± m	covered
28	3.3 m	very thin-bedded, medium-gray, finely crystalline replacement dolostone; algal sediment laminae
27	10.7 ± m	covered

Unit	Thickness	Description
26	0.0-0.30 m	beds and lenses of fine-grained, well-rounded orthoquartzite, locally with voids from weathering of carbonate pebbles; calcareous cement
	COPPER RIDGE CHERT	
25	39 ± m	covered; residuum of blocky, yellowish-orange to gray, banded chert, and stromatolitic chert
24	93 ± m	covered
23	112 ± m	same as unit 25
22	21 ± m	covered; residuum of "wormy" chert, grading upward into light- to very light-gray banded chert and stromatolitic chert; rare laminated dolostone in rubble
21	1.83 m	boulders massive, internally laminated and cross-laminated, light-gray, siliceous, finely crystalline replacement dolostone
20	0.90 m	internally laminated, very dark-gray to black, poorly sorted, silty intrasparite, and micrite with flat algal sediment laminae; micrite has scour surfaces and desiccation cracks
19	4.57 m	same as unit 21
18	1.22 m	same as unit 21, but medium-gray
17	0.90 m	covered

Unit	Thickness	Description
16	1.52 m	thin- to medium-bedded, internally laminated, light-gray, finely crystalline dolostone; widely separated domal algal stromatolites weathering to banded chert
15	14 ± m	covered
14	2.6 m	thin- to thick-bedded, light- to medium-gray, internally laminated, crystalline dolostone; chert nodules parallel to bedding
13	3.05 m	thin-bedded to laminated, varicolored gray chert
12	2.01 m	massive, light-gray, finely crystalline replacement dolostone; original lithology biomicrite; locally pyritic, thin-bedded, internally laminated
11	0.97 m	light-gray replacement dolostone with chert nodules
10	0.66 m	medium-gray dolostone weathering to banded yellowish-orange chert
9	0.38 m	light-gray, replacement dolostone with chert nodules
8	1.73 m	thick-bedded, light-gray, finely crystalline replacement dolostone, grading upward into irregularly laminated, burrowed dolostone with angular chert fragments parallel to bedding
7	1.42 m	irregularly bedded, light-gray, siliceous replacement dolostone, with domal algal stromatolites about 1 m across

Unit	Thickness	Description
6	0.94 m	thick-bedded, light-gray replacement dolostone; flat and tufted algal sediment laminae with probable gas fenestrae
5	1.37 m	thick-bedded, light-gray, internally laminated replacement dolostone; distorted laminae with probable gas fenestrae
4	1.00 m	laminated, light-gray, siliceous, crystalline replacement dolostone, grading upward into thick-bedded unit of same lithology
3	0.30 m	covered
2	0.36 m	medium-gray replacement dolostone
1	36 ± m	covered
-	NA	Ketona Dolomite

SECTION CAL—Newala Limestone exposures in and near abandoned quarry, SE1/4 Sec. 28, T.18S., R.2E., Shelby County

Note: full section not exposed, fault at base.

Unit	Thickness	Description
-	NA	Fort Payne Chert
37	12.33 m	covered
36	2.5 m	light-gray, waxy textured micrite with desiccation fenestrae parallel to bedding
35	0.4 m	light-gray, fine-grained intrasparite
34	0.8 m	dark-gray, waxy micrite
33	0.9 m	medium-gray biomicrite, grading upward into very poorly-sorted, subangular to rounded intrasparite; penecontemporaneous dolomite
32	1.0 m	very dark-gray, waxy micrite
31	0.16 m	intrasparite with angular micrite clasts up to four cm
30	2.0 m	medium-gray, waxy intramicrite, grading upward into medium-gray, poorly-sorted intrasparite with clasts up to three cm
29	0.7 m	medium-gray, waxy micrite with dolomite mottling
28	1.5 m	medium-gray, waxy micrite
27	0.5 m	medium-gray intrasparite with replacement calcite mottling at base
26	0.45 m	dark-gray, waxy micrite with replacement calcite mottle

SECTION OA— Columbiana Formation and Lenoir Limestone, Southern Cement shale quarry, NW1/4, NE1/4, Sec. 5, T.24N., R.13E., Shelby County.

Note: measured by J. A. Drahovzal, R. S. Taylor, and K. Hudson—supplementary notes by O. E. Gilbert, Jr.

Unit	Thickness	Description
-	NA	Frog Mountain Sandstone
	COLUMBIANA FORMATION	
8	70.94 m	massive, internally laminated, dark-gray, calcareous shale, locally abundant graptolites; lamination apparently caused by alternation of organic-rich and organic-poor layers; microscopic layers of crystalline calcite and pyrite parallel to bedding
7	0.03 to 0.06 m	light gray-green bentonite
6	4.36 m	massive, internally laminated, dark-gray, calcareous shale; some thin interbeds locally graptolitic
5	0.03 m	highly calcareous, dark-gray shale, weathering to powder
4	2.44 m	massive, internally laminated, dark-gray, graptolitic shale
3	0.37 m	interbedded thin beds of dark-gray, calcareous shale and olive green, pyritic shale

Unit	Thickness	Description
	LENOIR LIMESTONE	
2	0.52 m	medium-bedded, dark-gray, argillaceous biomicrite, with ostracodes and graptolites
1	1.22 m	thin-bedded, dark-gray, argillaceous micrite
-	NA	BASE OF QUARRY

SECTION GP— Lenoir Limestone, Greensport Formation, Colvin Mountain Sandstone, Sequatchie Formation, Red Mountain Formation, Frog Mountain Sandstone, Fort Payne Chert, and Floyd Shale, road cuts SE1/4, NW1/4, and E1/2, SW1/4, Sec. 6, T.14S., R.6E., Etowah and Calhoun Counties

Note: measured by T. L. Neathery and J. A. Drahovzal, supplementary notes by O. E. Gilbert, Jr. (Lenoir not examined).

Unit	Thickness	Description
	FLOYD SHALE	
-	NA	top of section not exposed
49	2.83 m	massive, fine- to medium-grained, tan-weathering sandstone with cut and fill structure
48	3.35 m	laminated, mottled gray and reddish-gray shale; local thin sandstone beds as in unit 49
47	0.91 m	massive, tan-weathering, fine-grained sandstone, with local dark-gray shale partings
46	3.96 m	covered
	FORT PAYNE CHERT	
45	25.91 m	thin-bedded, white to gray or tan, fossiliferous chert with brachiopods and pelmatazoan columnals
44	27 ± m	covered
43	0.3 m	chert as in unit 45

Unit	Thickness	Description
	FROG MOUNTAIN SANDSTONE	
42	5.24 m	thick- to thin-bedded, maroon, fine- to coarse-grained, locally conglomeratic sandstone, and brown shale partings, with local lenses of shale up to 0.9 m near base; oscillation ripple marked, beds thin upward
	RED MOUNTAIN FORMATION	
41	3.38 m	medium beds and lenses of medium-gray, subgray-wacke sandstone; buff to olive and maroon variegated shale
40	5.33 m	medium-bedded, reddish-gray to reddish-brown sandstone, with interbedded thin-bedded, dark olive-gray shale
39	13.72 m	interbedded medium-bedded gray to reddish-gray, fine-grained, internally laminated and cross-bedded sandstone, and gray, fossiliferous shale and siltstone
	SEQUATCHIE FORMATION	
38	2.77 m	irregularly bedded, gray to greenish-gray, finely crystalline dolostone; grades into unit 37
37	0.85 m	medium-gray, coarsely crystalline sparite, with medium interbeds greenish-gray siltstone
36	3.35 m	thick-irregularly bedded, gray to bluish-gray dolostone, gradational downward into thickly-laminated siltstone

Unit	Thickness	Description
35	2.53 m	thin-irregularly bedded, red- and olive-variegated calcareous siltstone
34	12.5 m	medium-bedded, fine-grained, olive and red-mottled, dolomitic siltstone
33	4.9 m	covered; probably dolomitic siltstone
32	13.1 m	covered
	COLVIN MOUNTAIN SANDSTONE	
31	2.19 m	medium-bedded, buff, fine- to medium-grained, cross-bedded, subrounded orthoquartzite
30	2.68 m	thick-bedded, maroon to gray-green, fine- to medium-grained, subangular quartz sandstone; cut and fill structure, some bentonitic clay
29	1.52 m	medium-bedded, white to light-gray, medium-grained subrounded sandstone, locally cross-bedded; interbeds sandy bentonitic clay, locally a 24 cm bentonite bed
28	3.35 m	thin-bedded, white to yellowish-white, fine- to coarse-grained, rounded to subangular ortho-quartzite
27	3.14 m	thick-bedded, white to light-gray orthoquartzite; interbeds greenish-gray, bentonitic shale
26	2.20 m	thin-bedded, maroon to yellowish-green, fine-grained sandstone and silty shale

Unit	Thickness	Description
25	1.58 m	thick-bedded, internally thin-bedded, reddish-yellow to brown, coarse-grained, subrounded sandstone, with clay intraclasts up to 9 cm
24	1.31 m	very thick-bedded, tan to maroon, well-sorted, subrounded conglomeratic sandstone, with clay intraclasts
23	2.50 m	medium-bedded, white to light-gray, coarse-grained, well-rounded, well-sorted, conglomeratic, cross-bedded orthoquartzite; thin gray shale bed near top
GREENSPORT FORMATION		
22	0.49 m	thinly-laminated, maroon siltstone and shale, with thin, lenticular, maroon and olive-green sandstone
21	0.73 m	alternating very thin beds, maroon and olive-green sandstone and yellow siltstone
20	0.15 m	fine-grained, gray to pink sandstone
19	0.24 m	thin-bedded, alternating maroon and yellowish-green siltstone
18	0.21 m	thinly-laminated, fine-grained, tan to light-gray sandstone with maroon siltstone intraclasts derived from unit 17
17	1.34 m	thin alternating beds of maroon and yellowish-green siltstone
16	3.05 m	same as unit 17, but with thin interbeds tan to pinkish-white, fine-grained sandstone

Unit	Thickness	Description
	ANGULAR UNCONFORMITY	
15	5.94 m	thin- to medium-bedded, maroon and light olive-green, ocher-weathering, slightly dolomitic siltstone; vertical branching burrows, with silt infilling
14	3.2 m	medium-bedded, very fine-grained, cross-bedded, slightly calcareous siltstone
13	2.77 m	thin-bedded, maroon, cross-bedded, calcareous sandstone
12	0.3 m	gray to reddish-brown mottled calcareous sandstone
11	1.37 m	very thick-bedded, gray and maroon mottled, fine-grained sandstone, grading upward into siltstone
10	2.9 m	thinly-laminated, locally nodular, maroon and gray, calcareous siltstone and fine-grained sandstone; soft sediment deformation
9	0.91 m	thick-bedded, pink and olive-gray mottled, fine-grained sandstone
8	0.97 m	thin-bedded, cyclically alternating maroon to yellow siltstone-sandstone-shale sequence; brachiopods and oscillation ripple marks, ripple-bedded, bioturbated
7	4.63 m	thinly-laminated, maroon shale

Unit	Thickness	Description
6	1.1 m	thin-bedded, maroon shale, and yellowish-green sandstone; internally laminated
5	2.62 m	massive, maroon to reddish-gray, fine-grained, silty, calcareous sandstone
4	10.36 m	massive to medium-bedded, alternating sandstone and siltstone; vertical burrows common as in unit 15
3	2.59 m	covered
	LENOIR LIMESTONE	
2	72.85 m	massive, dark-gray, locally argillaceous micrite and biomicrite with replacement spar; locally cherty, locally intrasparite at top
1	8.84 m	covered
-	NA	Newala Limestone

Unit	Thickness	Description
73	3.35 m	interbedded, irregularly bedded, thin-bedded, dark medium-gray chert, and thin-bedded, internally laminated, brown, yellowish-brown, and green-gray clay
72	7.01 m	interbedded chert and clay as in unit 73, but chert is fossiliferous, with disarticulated pelmatazoan columnals and spiriferid brachiopods
	MAURY FORMATION	
71	0.07 m	light greenish-gray clay
70	0.10 m	dark-purple clay, with disc-shaped concretions of unidentified iron (phosphate?) mineral
	FROG MOUNTAIN SANDSTONE	
69	0.10 m	chocolate-brown clay, with lenses light-gray, silty clay
68	0.15 m	brown-yellow silt, grading downward into clayey sand
67	2.13 m	medium-bedded, light-gray and light-brown, fine-grained, cross-bedded sandstone with interbeds medium- to coarse-grained, conglomeratic sandstone; grains rounded to subangular, poorly-sorted, with hematite cement; some grains fractured, with hematite filling of fractures
66	2.74 m	irregular beds and thin- to medium-bedded lenses of dark-red sandstone, similar to unit 67; some soft sediment deformation

Unit	Thickness	Description
57	1.52 m	thin- to medium-bedded, light-gray, clay shale, interbeds of light-gray, very fine-grained, cross-laminated sandstone with vertical and subhorizontal burrows
56	2.44 m	very thin- to medium-bedded, light-gray, very fine-grained, fossiliferous, cross-laminated and cross-bedded, ripple-bedded sandstone; some very thin beds light-gray, silty shale; fauna includes cephalopods, gastropods, fenestellate bryozoa, ceratoid corals, colonial corals, all broken and probably transported
55	4.88 m	thin- to medium-bedded, medium-gray, silty shale with thin, irregular interbeds light medium-gray, very fine-grained, calcareous sandstone; sand grains rounded to subrounded, with superficial hematite coatings; sandier toward top of unit; fauna includes trilobites, pelmatazoans
54	0.30 m	thinly-laminated, medium dark-gray calcareous, fossiliferous shale; fenestellate bryozoa, pelmatazoans, brachiopod fragments; glauconite granules, superficial ooids of hematite
53	5.88 m	"Hickory Nut" ore bed; massive, dark-red, cross-bedded, fine- to coarse-grained, angular sandstone, with rare pebbles of rounded quartz, lenses of fossil debris, superficial hematite ooids, and

Unit	Thickness	Description
53 (cont'd.)		clay chips; fauna includes ceratoid corals, *Pentamerus oblongus*
52	1.52 m	thin-bedded, medium-gray, argillaceous, cross-laminated siltstone; trails on bedding surfaces; gradational into unit 51
51	0.30 m	ore bed; dark-red, medium- to coarse-grained, conglomeratic sandstone with superficial ooids of hematite
50	1.83 m	same as unit 52
49	2.74 m	"Ida" ore bed; massive, dark-red, fine-grained, cross-bedded, hematitic sandstone, with abundant superficial ooids of hematite at top; rare, very thin interbeds of dark-gray clay shale
48	2.13 m	ore bed; thin- to medium-bedded, dark-red, cross-bedded, internally laminated, fine-grained sandstone; rare clay shale interbeds as in unit 49
47	1.83 m	ore bed; massive, dark-red, fine- to coarse-grained, poorly sorted, rounded, cross-bedded, locally conglomeratic sandstone, with superficial ooids of hematite near top, grading downward to sand; intraclasts up to 5 cm near top
46	1.22 m	interbedded, medium-bedded, dark-red, fine- to coarse-grained, cross-bedded, poorly sorted, hematitic sandstone, and thinly laminated, gray

Unit	Thickness	Description
46 (cont'd.)		medium-gray, silty shale; sandstone-shale contacts scoured, with chips of shale in overlying sandstone
45	3.66 m	interbedded thin- to very thin-bedded, reddish-gray and reddish-brown, medium- to very coarse-grained sandstone with shale pebbles, and thin-bedded, dark medium-gray, silty shale with scattered lenses of sandstone; sandstones locally cross-bedded, with scour and fill structures at base; flame structure and soft sediment deformation of shales
44	1.83 m	interbedded laminated, dark gray, silty shale with interlaminated lenticles of cross-laminated, very fine-grained sandstone, and thin beds and lenses medium-gray coarse- to very coarse-grained, calcareous, locally conglomeratic sandstone; siltstone and shale dominant; disrupted by trails on bedding surfaces
43	6.10 m	"Big Seam" ore bed; massive, cross-bedded sandstone consisting of 10-15 percent fine-grained sand and silt, 10-12 percent broken brachiopod fragments, 8 percent ostracodes, 6-8 percent encrusting and ramose bryozoan, and 1-2 percent superficial hematite ooids, and 3 cm pebbles of sandy micrite and argillaceous micrite, with

Unit	Thickness	Description
43 (cont'd.)		calcite and hematite cement; fossils extensively coated and replaced by hematite; very thin beds gray shale near base, rare near top; shale interbeds pinch out rapidly over short lateral distances
42	1.52 m	"Kidney Seam" ore bed; intraformational conglomerate, with discoid pebbles up to 25 cm in a matrix of hematite ooids, medium- to very coarse-grained sand, with hematite and calcite cement; locally derived pebbles of dark-red hematite sandstone, biopelmicrite, and biomicrite; pebbles are imbricated and more abundant (40 percent) near top of unit, some with indented surfaces suggesting poor induration at time of deposition; local partings gray shale
41	1.83 m	"Irondale" ore bed; thin- to medium-beds and lenses of dark reddish-gray to dark-gray, fine-grained sandstone consisting of > 15 percent rounded polycrystalline quartz sand, 10-12 percent quartz silt, 10-15 percent superficial hematite ooids, 10 percent encrusting bryozoa, 10-15 percent ramose bryozoa, $\sim$ 8 percent brachiopod fragments, and < 1 percent Dasycladacean algal fragments with calcite cement; all grains coated with hematite; lenses of biosparite, thin discontinuous beds of

Unit	Thickness	Description
41 (cont'd.)		dark-gray shale, and intraformational conglomerate; base of conglomerate locally scoured, upper contact gradational
40	7.32 m	interbedded very thin-bedded, light medium-gray, very fine-grained, calcareous, ripple-bedded, micaceous sandstone with clay drapes, and dark-gray micaceous shale; vertical burrows in shale, trails on sand bed surfaces, in some cases extreme bioturbation has disrupted contacts; sand units consist of > 50 percent poorly sorted, rounded to subangular quartz sand, 1-2 percent fragmented bryozoa, 1 percent trilobite fragments, rare pelmatazoan fragments, and variable proportions of clay intraclasts in calcite cement; all grains hematite coated
39	0.30 m	dark-gray shale with very-thin interbeds and lenses of fine- to coarse-grained, calcareous sandstone and fossiliferous, silty sand; lenses consist of 5-40 percent silty matrix, with 40-60 percent trepostome and cryptostome bryozoa, < 10 percent rugose coral fragments, 5-10 percent encrusting bryozoa, < 5 percent each of trilobite and brachiopod fragments, and rare superficial hematite ooids

Unit	Thickness	Description
	NASHVILLE FORMATION	
31	0.30 m	very thin-bedded, medium-gray biomicrite with extensive replacement spar, thin clay partings; fauna includes 10-15 percent ramose and encrusting bryozoa, 5-10 percent encrusting algae, ∿ 5 percent solenoporoid algae
30	0.30 m	very thin-bedded, medium-gray, pyritic biosparite, with interbedded dark medium-gray, calcareous shale; limestone contains 30 percent ostracodes, ∿ 10 percent each of pelmatazoan grains and brachiopod fragments, ∿ 5 percent geopedal micrite; horizontal fragments impart poor lamination
29	0.30 m	medium-bedded, light medium-gray biointrasparite with discontinuous clay partings; contains ∿ 20 percent brachiopod fragments, ∿ 20 percent micrite intraclasts, 15 percent trilobite fragments, < 5 percent each of ostracodes, pelmatazoan grains, and encrusting bryozoa; scattered quartz sand grains
28	0.30 m	thin, interbedded limestone as in unit 29, and medium-gray micrite
27	0.61 m	same as unit 29

Unit	Thickness	Description
	STONES RIVER FORMATION (probable upper contact)	
26	3.66 m	very thin to thin interbeds of micrite, biomicrite, biosparite, and calcareous shale, locally with well-preserved brachiopods and trilobites; most fossil debris is Sowerbyella sp., locally up to 10 percent pelmatazoan grains, 1-2 percent ostracodes, 5 percent trilobite fragments; locally with quartz silt
25	0.08 m	waxy, gray-green, bentonitic clay with euhedral biotite (T-4 bentonite)
24	2.74 m	irregular beds of lithologies similar to unit 26, but with scattered bentonitic clay
23	0.15-0.30 m	bentonite similar to unit 25, but without biotite; locally chert at base
22	2.44 m	massive, interlaminated medium-gray micrite, biomicrite, biosparite, and intrasparite, some carbonaceous clay partings, one interbed black chert; beds micrite and biomicrite with up to 20 percent finely-divided fossil fragments, burrowed by deposit feeders, upper surfaces scoured and overlain by poorly sorted intrasparite and biosparite with micrite intraclasts up to 2 cm diameter, echinoid grains and spines (?) abundant near base, brachiopod fragments common near the top of unit, planispiral and conospiral gastropods

Unit	Thickness	Description
22 (cont'd.)		with geopedal micrite; algal oncolites near base of unit; Lingula sp. near top of unit
21	0.09 m	bentonite as in unit 23, very rare biotite, one interbed biointrasparite
20	0.91 m	medium-bedded, cross-bedded, medium-gray, bentonitic pelmicrite, with scattered intraclasts, some scattered biotite; one interbed bentonite with biotite; locally cherty at base (T-3 bentonite?)
19	14.93 m	very thin, irregular, beds of silty micrite and biomicrite, with lesser biosparite and biointrasparite; biomicrites contain up to 25 percent fossil debris, burrowed by deposit feeders, with dolomitization along burrows, penecontemporaneous dolomite parallel to bedding in lower part; biointrasparites contain up to 40 percent micrite intraclasts, fossil debris mainly abraded cryptostome bryozoa
18	2.13 m	massive, dark medium-gray, interlaminated biomicrite and intrasparite, locally with rugose corals near base; gradational into units 17 and 19
17	1.83 m	thin- to medium-bedded, interlaminated, medium-gray biomicrite and intrasparite, some calcareous clay laminae; intrasparites are fine-grained and

Unit	Thickness	Description
17 (cont'd.)		well-sorted, with ∿ 5 percent encrusting bryozoan fragments
16	3.66 m	irregular beds and lenses medium-bedded, dark medium-gray, cross-bedded biosparite, intrasparite, and dark-gray micrite; mostly poorly-sorted intrasparite and biosparite, with fragments of encrusting bryozoa and well-rounded biomicrite intraclasts; intraclasts are internally laminated by size
15	5.18	thin- to thick-bedded, medium dark-gray intramicrite and poorly-sorted intrasparite, with minor biomicrite, micrite, and calcareous shale; intraclasts very poorly sorted at base, better sorted near top of unit; intraclasts locally segregated into laminae by size; rare Dasycladacean algae
14	3.35 m	irregular, very thin-beds dark-gray, locally argillaceous micrite, biomicrite, and biosparite, with laminae of very dark-gray, calcareous shale; biomicrites contain finely divided trilobite, brachiopod, and ostracode fragments, with silt-size calcite and some quartz silt; biosparites contain encrusting bryozoan and brachiopod fragments, and intraclasts of micrite and intrasparite; desiccation cracks

Unit	Thickness	Description
13	4.58	thick-bedded to massive, internally laminated, medium dark-gray biomicrite and intrabiosparite; biomicrite desiccated, with pellet-filled vertical burrows and desiccation cracks; biosparite contains > 60 percent poorly-sorted intraclasts, ∿ 15 percent echinoid grains, ∿ 3 percent ostracodes, with ∿ 1 percent each algally bored ooids, bryozoa, algal oncolites, and Codiacean algal grains
12	5.79 m	similar to unit 13, with fragments in intrabiosparite coated with hematite; surfaces of micrite laminae scoured with partially detached intraclasts; near base of unit bands of penecontemporaneous dolomite parallel to bedding
11	5.18 m	thin-bedded, medium dark-gray biomicrite and intrasparite with algal oncolites and pelmatazoan columnals locally visible in outcrop; calcareous shale near top of unit; possible algal sediment laminae visible in outcrop; intrabiosparite consists of ∿ 40 percent biomicrite intraclasts, ∿ 4 percent bryozoa of encrusting and ramose habit, 15 percent pelmatazoan grains, 1 percent Dasycladacean algae, and < 1 percent superficial ooids (?) and asymmetric algal oncolites

Unit	Thickness	Description
10	0.03 m	gray-green shale with nodules of micrite and biosparite
9	7.32 m	thin, irregular beds of dark medium-gray micrite, biomicrite, and biointrasparite, locally argillaceous, with some very thin interbeds calcareous shale; more micritic toward base, biointrasparite more abundant toward top; biointrasparites near base are very poorly-sorted with abundant bryozoa, small gastropods and trilobites; units near top exhibit desiccation cracks, dolomitization, and abundant ostracodes
8	1.83 m	thin-bedded, dark medium-gray, poorly-sorted biointramicrite, with desiccation cracks; fossil remains include planispiral gastropods, Codiacean algal grains, brachiopod fragments, and ostracodes
7	0.91 m	similar to unit 8, but argillaceous, with shaly partings
6	2.74 m	similar to unit 8, with smaller and less abundant subrounded biomicrite intraclasts
5	3.96 ± m	thin-bedded, light-gray dismicrite with desiccation fenestrae; near base Tetradium, ostracodes, and low-spired gastropods comprise up to 3 percent; irregular bed surfaces with maroon to yellowish-olive clay drapes

Unit	Thickness	Description
	ATTALLA CHERT CONGLOMERATE MEMBER	
4	0.30-1.52 m	gray-green claystone, with nodules light-gray micrite; up to 1.5 m relief on base of unit; base is chert pebble breccia
3	0.0-1.52 m	medium-gray crystalline dolostone with chert sand and greenish-gray clay near base; locally cherty
2	0.0-1.22 m	structureless light-gray chert
	KNOX GROUP (COPPER RIDGE DOLOMITE?)	
1	10.97 + m	massive, light- to medium-gray, crystalline, cherty dolostone
-	NA	Covered

SECTION LOQ—Little Oak Limestone in and near old Pelham Quarry, NE1/4 Sec. 12, T.20S., R.3W., Shelby County.

Notes: (1) measured by W. A. Thomas, J. S. Ellard, V. M. Shamburger, C. W. Copeland, Jr., and revised by R. S. Taylor, O. E. Gilbert, Jr.; upper 36 percent of section exposed;

(2) "silt laminae" previously reported are stylocumulate layers which pervade all units.

Unit	Thickness	Description
-	NA	Frog Mountain Sandstone
7	16.76 m	massive, dark- to medium-gray micrite and biomicrite with brachiopods and pelmatazoan columnals; rare chert nodules and bedded chert
6	4.88 m	massive, dark-gray micrite; rare chert nodules
5	9.75 m	massive, dark-gray micrite and biomicrite; noncherty
4	6.1 m	same as unit 6, but with rare chert nodules and *Malcurites* sp. visible in outcrop
3	43.0 m	massive, dark- to medium-gray biomicrite, bioturbated; fossils include *Malcurites* sp., pelmatazoan columnals, whole ceratoid corals, ramose bryozoa, brachiopods
2	0.7 m	dark gray dismicrite units with finely-divided fossil debris; Codeacian algal debris abundant, rare superficial algal oncolites

Unit	Thickness	Description
1	144 m	covered
-	NA	Lenior Limestone

SECTION WOLF CREEK—Frog Mountain Sandstone, bed of Wolf Creek through gap in ridge 0.24 km south of Wolf Ranch Lake, NW1/4, SW1/4, Sec. 10, T.12S., R.3E., St. Clair County.
Note: measured by Kiefer (1970), supplementary notes by O. E. Gilbert, Jr.

Unit	Thickness	Description
-	NA	Fort Payne Chert
3	5.3 m	medium- to thick-bedded, coarse-grained, light-gray orthoquartzite with rare fragmentary brachiopods and ceratoid corals
2	0.9 m	medium- to thick-bedded, coarse-grained, light-gray, calcareous sandstone
1	6.5+ m	medium-bedded, dark-gray limestone, replacement spar with fragmentary brachiopods

SECTION PIN—Tuscumbia Limestone and Pride Mountain Formation, old Vann Quarry, NE1/4, Sec. 14, T.16S., R.1W., Jefferson County.

Unit	Thickness	Description
-	NA	Hartselle Sandstone
	PRIDE MOUNTAIN FORMATION	
26	19.51 m	laminated, dark-gray to very dark-gray calcareous shale, beds and nodules of siderite, scattered horizontal burrows; locally fossiliferous in lower meter, with small brachiopods, gastropods, Goniatites sp., and orthocone cephalopods
	TUSCUMBIA LIMESTONE	
25	1.78 m	oopelsparite grading upward into bio-oosparite; superficial ooids decrease from 50 percent near base to 3 percent near top, abundant pelmatazoan grains, brachiopod fragments, ostracodes, algal fragments
24	0.05 m	dark-gray calcareous shale
23	0.25 m	coarse-grained oobiosparite; brachiopod fragments up to three cm
22	0.15 m	dark-gray, argillaceous micrite
21	1.37 m	thick-bedded biosparite; rugose corals and pelmatazoan columnals, locally micritic
20	0.10 m	light-gray, fine-grained biosparite; poorly sorted pelmatazoan grains, bryozoan fragments, algal fragments, and micrite intraclasts

Unit	Thickness	Description
19	0.01 m	dark-gray calcareous shale
18	2.79 m	thick-bedded lenses of poorly-sorted, light-gray biosparite, primarily pelmatazoan grains, and fenestelloid bryozoan fragments with asymmetric algal oncolite overgrowths
17	4.0 m	massive, light-gray biosparite with fossil fenestelloid bryozoa up to 13 cm, locally cross-bedded, local partings of siliceous calcareous shale
16	0.25 m	light-gray, poorly-sorted biosparite; primarily brachiopod, pelmatazoan, and ramose bryozoan fragments
15	1.32 m	thick- to very thick-bedded, light-gray biosparite; primarily pelmatazoan grains, finely-divided fenestelloid bryozoan fragments with micrite envelopes and algal oncolites
14	0.84 m	same as unit 15, but fewer pelmatazoan grains
13	0.01 m	dark-gray calcareous shale
12	1.3 m	light-gray, very poorly-sorted biosparite, badly broken pelmatazoan grains, ramose bryozoa, and algal grains; large scale cross-bedding
11	1.92 m	massive, medium-gray biomicrite, local replacement spar

Unit	Thickness	Description
10	3.75 m	massive, light-gray biosparite, with whole pelmatazoan columnals, grading upward into biosparite with abraded pelmatazoans, algal grains, ramose bryozoa, with rare superficial ooids and grapestone
9	1.58 m	thick-bedded, light-gray micrite with mottle of replacement spar and scattered chert nodules
8	4.51 m	massive, lenticular, light-gray biosparite, grading upward into biosparite and biomicrite; dominantly abraded pelmatazoan grains and ramose bryozoa, with rare algal oncolites
7	2.5 m	similar to unit 8, but with algal grains, fenestelloid bryozoan fragments; grades upward and laterally into unit 8
6	1.58 m	very thick-bedded, light-gray biosparite, with scattered micrite intraclasts
5	1.46 m	thick-bedded, poorly-sorted biosparite, primarily abraded pelmatazoan grains and encrusting bryozoa
4	1.22 m	poorly-sorted biomicrite, with very thin chert interbeds
3	3.66 m	poorly-sorted biosparite similar to unit 6, with abundant fragments of brachiopods with micrite envelopes
2	1.83 m	thick-bedded, poorly-sorted, silty biomicrite; ramose bryozoa and pelmatazoan grains

Unit	Thickness	Description
1	25 ± m	covered
-	NA	Fort Payne Chert

SECTION MB— Bangor Limestone in and near abandoned quarry, NE1/4, SW1/4, Sec. 26, T.16S., R.1W., Jefferson County.

Note: Lower half of formation covered by residuum and alluvium, and is only intermittently exposed.

Unit	Thickness	Description
-	NA	Parkwood Formation
18	6 ± m	covered
17	0.20 m	thin-bedded, medium-gray biosparite, primarily abraded pelmatazoan grains
16	4.5 m	covered
15	0.6 m	medium-bedded, medium-gray biosparite, similar to unit 17
14	0.02 m	light-gray, argillaceous micrite
13	3.9 m	massive, light-gray biosparite, similar to unit 17
12	1.1 m	thick-bedded, light-gray, poorly-sorted biosparite, primarily abraded grains of pelmatazoans and fenestellate bryozoa
11	2.98 m	massive, medium-dark-gray biosparite, grading upward into light gray oosparite containing 80 ± percent superficial ooids; upper contact irregular and marked by conical pits
10	2.04 m	massive biosparite, dominantly abraded pelmatazoan fragments with minor ramose cryptostome bryozoa and foraminifera

Unit	Thickness	Description
9	0.0-0.01 m	reddish-gray, crystalline "crust" with encrusting bryozoa
8	2.37 m	massive, medium-gray biomicrite; some rugose corals up to two cm diameter
7	0.77 m	thick-bedded, light-gray, fine-grained biosparite, similar to unit 10, but with rare superficial ooids, aggregate grains, and fenestellate bryozoa (Archimedes)
6	0.58 m	medium-bedded, dark-gray biomicrite with pelmatazoans and Archimedes
5	1.0 m	thick-bedded, dark-gray biosparite, similar to unit 10
4	6 ± m	inaccessible in flooded quarry; apparently similar to unit 5
3	25 ± m	covered
2	3 ± m	massive, dark-gray biomicrite with gastropods and algal oncolites visible in outcrop
1	3 ± m	covered
-	NA	Hartselle Sandstone

SECTION CAH—Floyd Shale and Parkwood Formation, exposures in bed and banks of Little Cahaba River, Sec. 19 and 20, T.16S., R.1E., Jefferson County.

Unit	Thickness	Description
-	NA	Pottsville Formation
	PARKWOOD FORMATION	
27	77 m	covered; wooded slopes at base of Black Jack Ridge covered by colluvial material
26	7.3 m	thin- to medium-bedded, fine- to medium-grained, well-sorted, quartzose sandstone; zones of tabular cross-bedding
25	37.0 ± m	intermittent exposures of thin- to medium-bedded, fine-grained, brownish-weathering subgraywacke sandstone; local zones of angular clay intraclasts or cross-laminated, medium-grained orthoquartzite
24	16.0 ± m	intermittent exposures of laminated, dark- to very dark-gray shale, with scattered lenses (up to two m thick) of fine-grained, light-gray, micaceous, carbonaceous, internally laminated sandstone; abundant trails on bedding surfaces, ball and pillow structure at shale/sandstone contacts, oscillation and current ripples, and problematical rain imprints

23	129 ± m	semicontinuous outcrop of thin- to medium-bedded, orthoquartzite and fine-grained sandstone; locally irregularly bedded and cross-bedded, with local current and oscillation ripple marks
22	8 m	covered; few outcrops of thin planar beds of very fine-grained subgraywacke sandstone, interbedded with irregularly laminated, olive brown, micaceous siltstone; oscillation ripple marks in sandstone beds
21	104 ± m	thin- to very thick-bedded, medium- to fine-grained, well sorted quartzose sandstone and orthoquartzite, locally conglomeratic, with quartz pebbles and clay intraclasts
20	14.5 m	covered
19	0.7 m	very thin-bedded, light brownish-gray, fine-grained, carbonaceous subgraywacke sandstone, with oscillation ripple marks
18	2.6 m	covered
17	1.16 m	thinly-bedded, unevenly bedded, fine-grained sandstone as unit 19
16	0.33 m	medium-gray, calcareous, sandy siltstone
15	0.30 m	thin-bedded sandstone similar to unit 19, but with cut and fill sandstone
14	0.25 m	unevenly laminated, dark-grayish-brown, calcareous, micaceous siltstone, with plant debris and brachiopods

Unit	Thickness	Description
13	1.6 m	thin-bedded, dark-gray, fine-grained, subgraywacke sandstone, internally laminated, with plant debris and cut and fill structures
12	3.0 m	thin- to medium-bedded, reddish-gray, fine-grained sandstone, locally cross-bedded and with oscillation ripple marks
11	1.0 m	very thin-bedded, olive-brown, fine-grained, silty, micaceous sandstone, locally carbonaceous, internally cross-laminated, oscillation ripples
10	4.6 m	covered
9	3.0 m	laminated, very dark-gray, micaceous shale with plant debris, silty toward base, with thin beds of ripple-bedded siltstone and silty sandstone
8	1.5 m	thin- to medium-bedded, fine-grained, very dark-gray, carbonaceous, micaceous sandstone, with sole marks and flaser bedding
	FLOYD SHALE	
7	47 ± m	covered
6	1.5 m	medium-bedded, internally laminated, highly calcareous, medium- to dark-gray shale; intensely bioturbated
5	20 ± m	covered
4	10 m	very thin to thin planar beds of fine-grained, silty, medium- to dark-gray subgraywacke sandstone
3	14.5 ± m	covered

Unit	Thickness	Description
2	3.0 m	interbedded very thin bedded, very fine-grained, silty sandstone, and very dark-gray, thinly laminated, calcareous shale; ripple bedded
1	52 ± m	covered; rubble mostly weathered laminated shale and siltstone
-	NA	Bangor Limestone

Notes: (1) Selection of Floyd-Parkwood boundary is arbitrary due to gradational natures, but this pick agrees with Thomas (1972a) and Kidd and Shannon (1978);

(2) Floyd grades laterally into Bangor to SW;

(3) unit 6 may represent a tongue of highly argillaceous Bangor.

APPENDIX B

Figure B-1. Sedimentary and diagenetic features of the Weisner Formation and Shady Dolomite. A. Cross-bedded orthoquartzites of Weisner-beach facies, Choccolocco Mountain, Calhoun County. B. Interbedded and interlaminated sandstones and slates of upper Weisner, Riser Mountain, Talladega County. Note bioturbation and soft-sediment deformation. Scale bar 5 cm. C. Intramicrite with flat crenulated algal sediment laminae, producing laminated weathering surface; irregular surfaces are stylolites. Shady Dolomite, Weaver, Calhoun County. D. Replacement dolomite typical of Shady, Wewoka Creek, Talladega County. 16 X, unpolarized light. Stratigraphic top toward top of page.

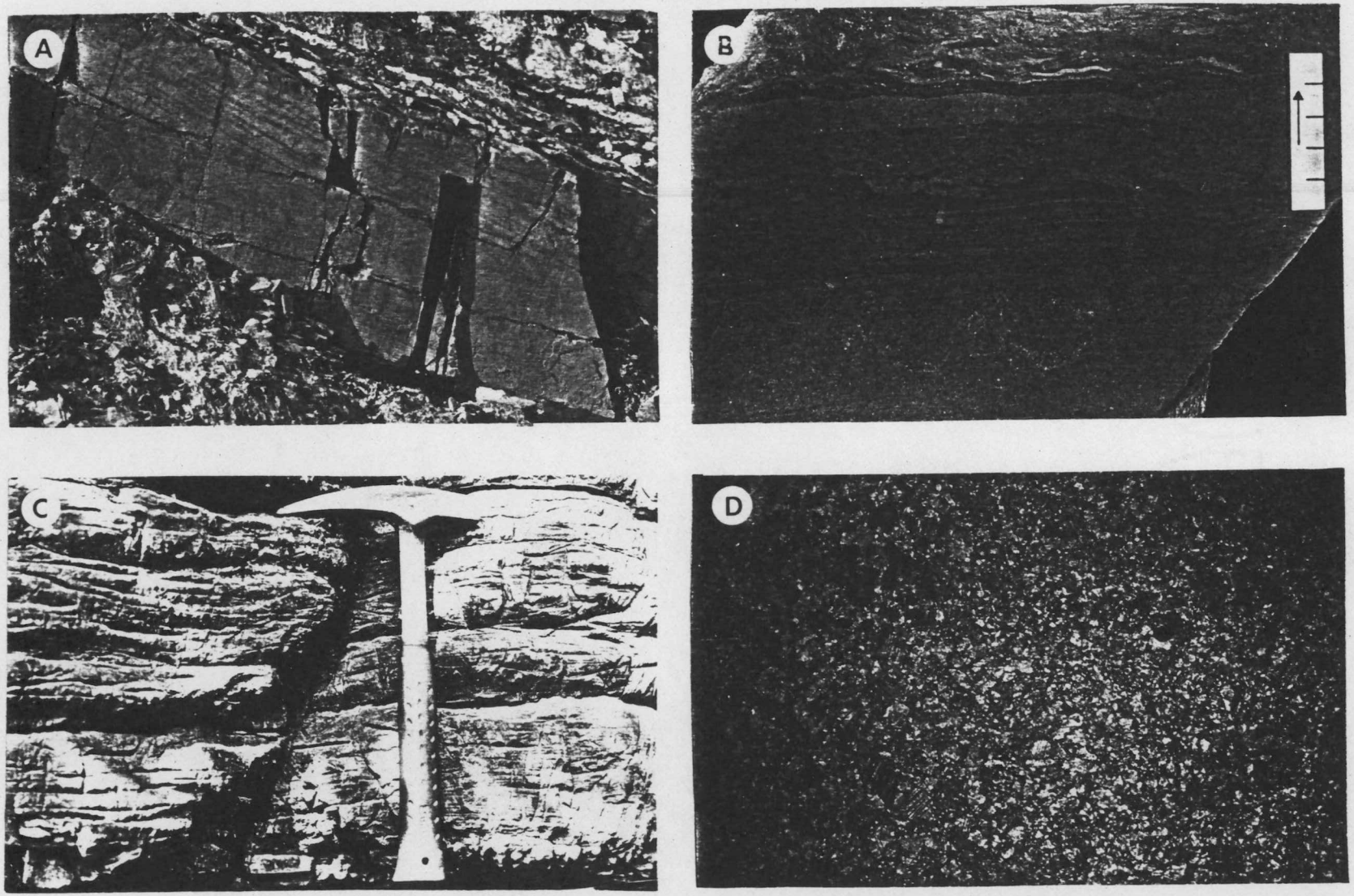

Figure B-1.

Figure B-2. Sedimentary features of the Rome Formation and Conasauga Group. A. Selectively dolomitized dismicrite; burrows are dolomitized, and stand out in relief on weathered surface. Rome Formation, Fourmile, Calhoun County. B. Maroon Rome shale with oscillation ripple marks and sand-filled desiccation cracks. Fourmile. Scale bar 5 cm. C. Scoured surface of micrite, with vertical burrows, overlain by intrabiosparite. Conasauga Group, Powderly, Jefferson County. 16 X, unpolarized light.

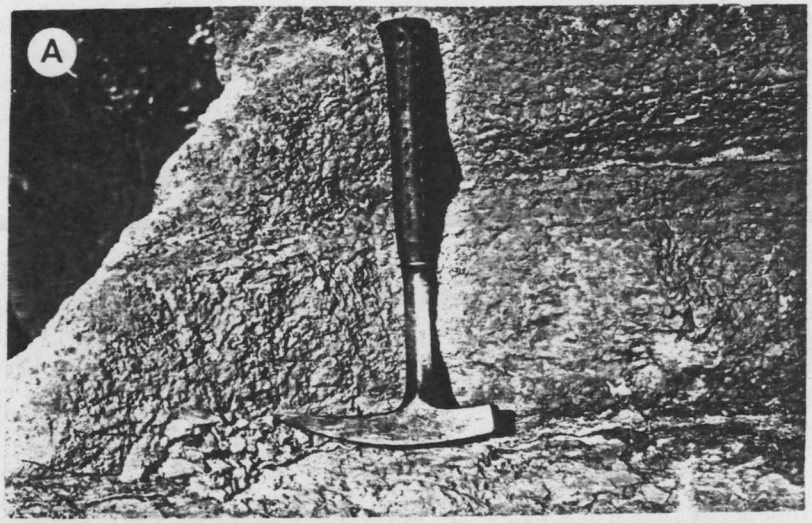

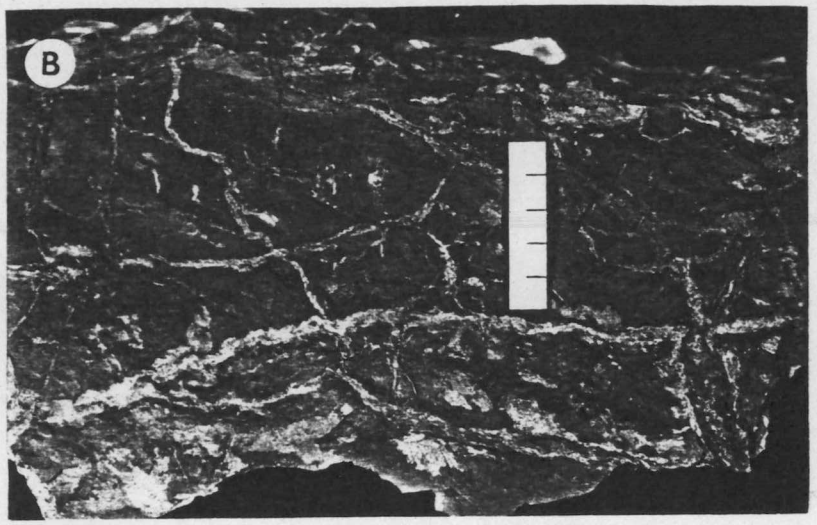

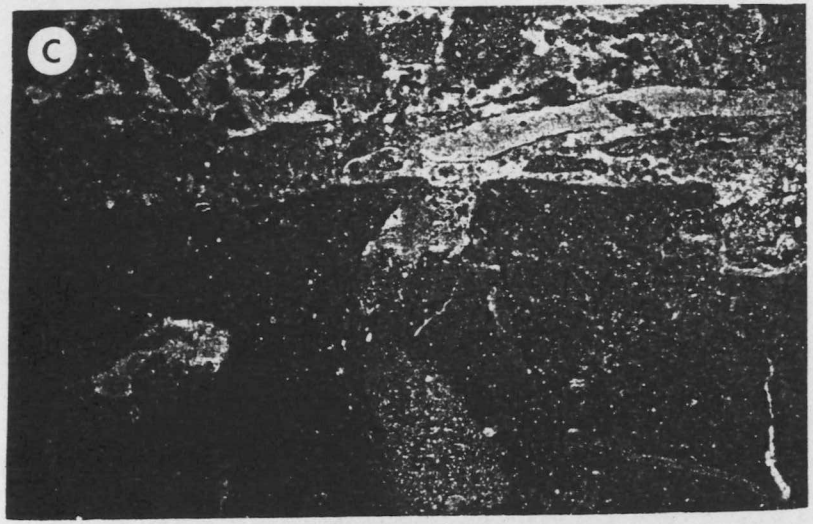

Figure B-2.

Figure B-3. Sedimentary features of the Copper Ridge Dolomite. A. Scoured surface of deformed, laminated dolostone. Basal Copper Ridge, Lake Purdy, Jefferson County. 16 X, unpolarized light. B. Algal stromatolites, middle Copper Ridge, Talladega, Talladega County. C. Flat algal sediment laminae with gas (?) fenestrae. Middle Copper Ridge, Lake Purdy, Jefferson County. 16 X, unpolarized light

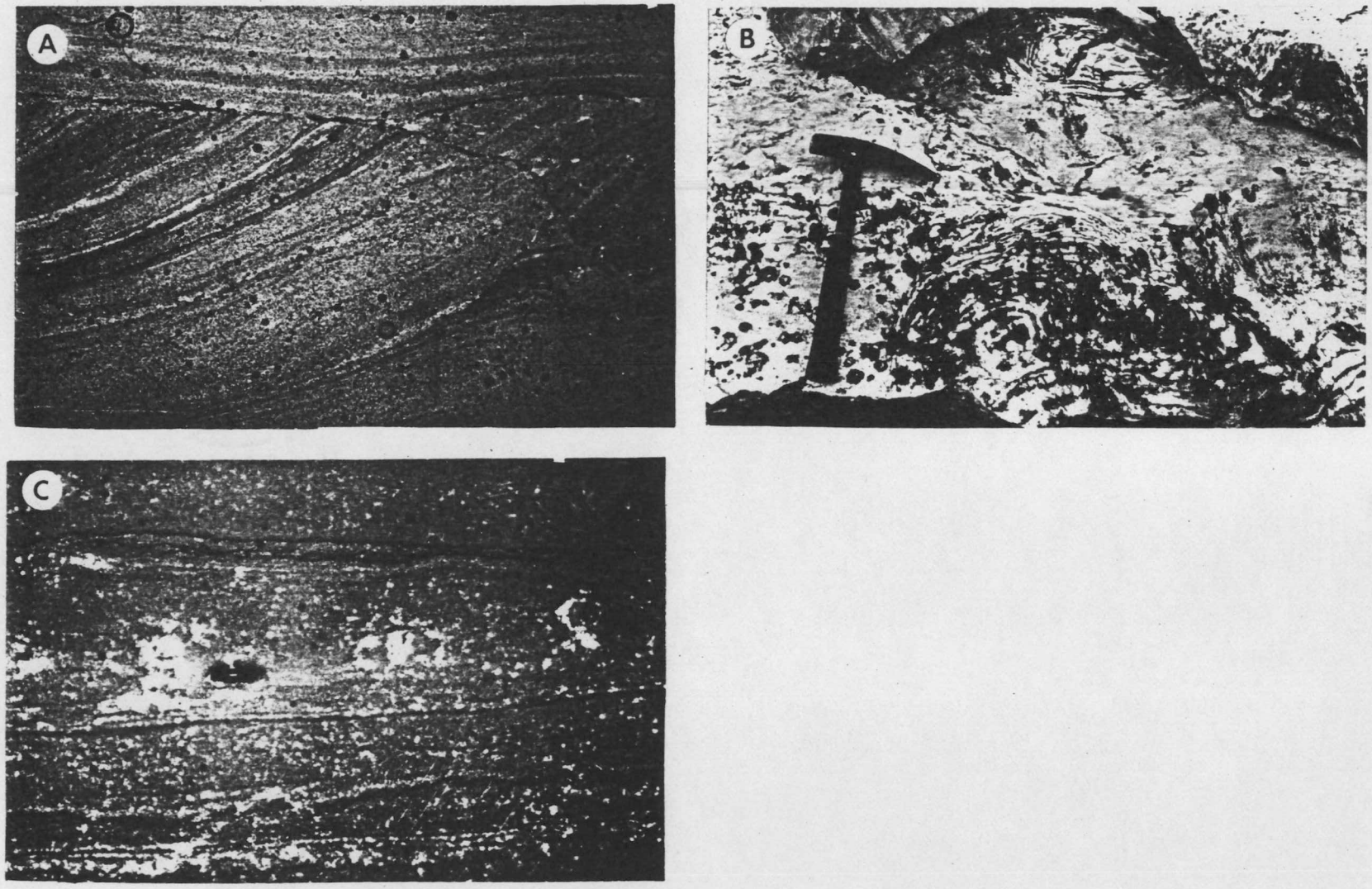

Figure B-3.

Figure B-4. Sedimentary and diagenetic features of the Chepultepec Dolomite and Newala Limestone. A. Orthoquartzites of basal Chepultepec, voids formed by weathering of carbonate clasts. Bedding vertical, black disc 5.5 cm diameter. Birmingham, Jefferson County. B. Crenulated algal sediment laminae in replacement dolostone of Chepultepec. Lake Purdy, Jefferson County. 16 X, unpolarized light. C. Interbedded "birdseye" micrite (dark) with desiccation cracks and intrasparite (light). Newala Limestone, Calcis, Shelby County. Stratigraphic top toward top of page. D. Bedding-parallel laminae of penecontemporaneous (?) dolomite. Newala Limestone, Calcis. Stratigraphic top toward top of page. 16X, unpolarized light.

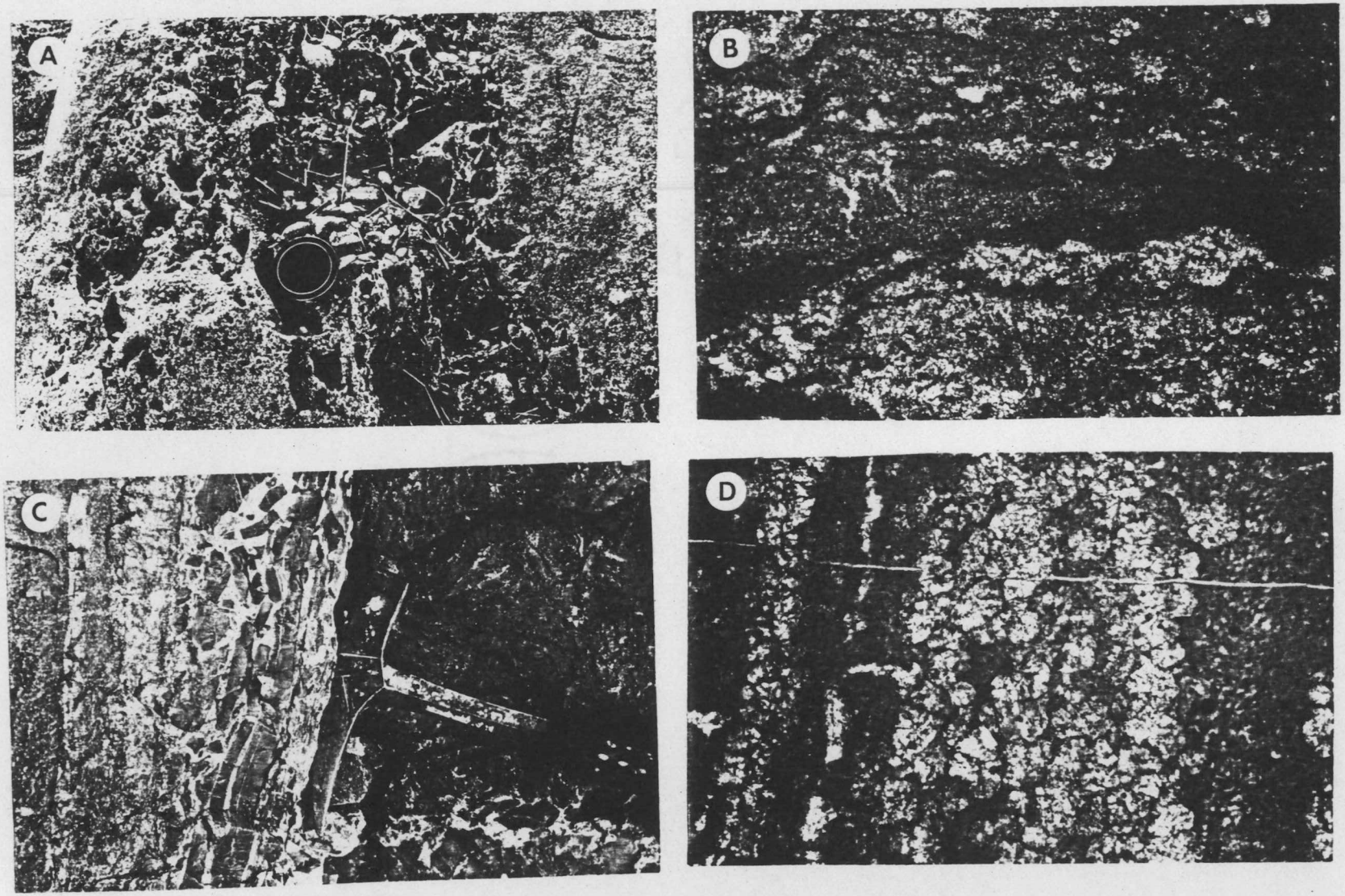

Figure B-4.

Figure B-5. Sedimentary features of the Columbiana Formation and Little Oak Limestone. A. Alternating silt-rich and organic-rich laminae of Columbiana; round white objects are calcite spheres of unknown origin, possibly tintinnines. Newala, Shelby County. Stratigraphic top toward top of page. 16 X, unpolarized light. B. Discontinuous laminae of crystalline calcite in black Columbiana shale. Stratigraphic top toward top of page. 16 X, unpolarized light. C. Dismicrite with finely-divided fossil debris and replacement dolomite. Codeacian algal grain visible at left center. Shady Dolomite at Pelham, Shelby County. 16 X, unpolarized light.

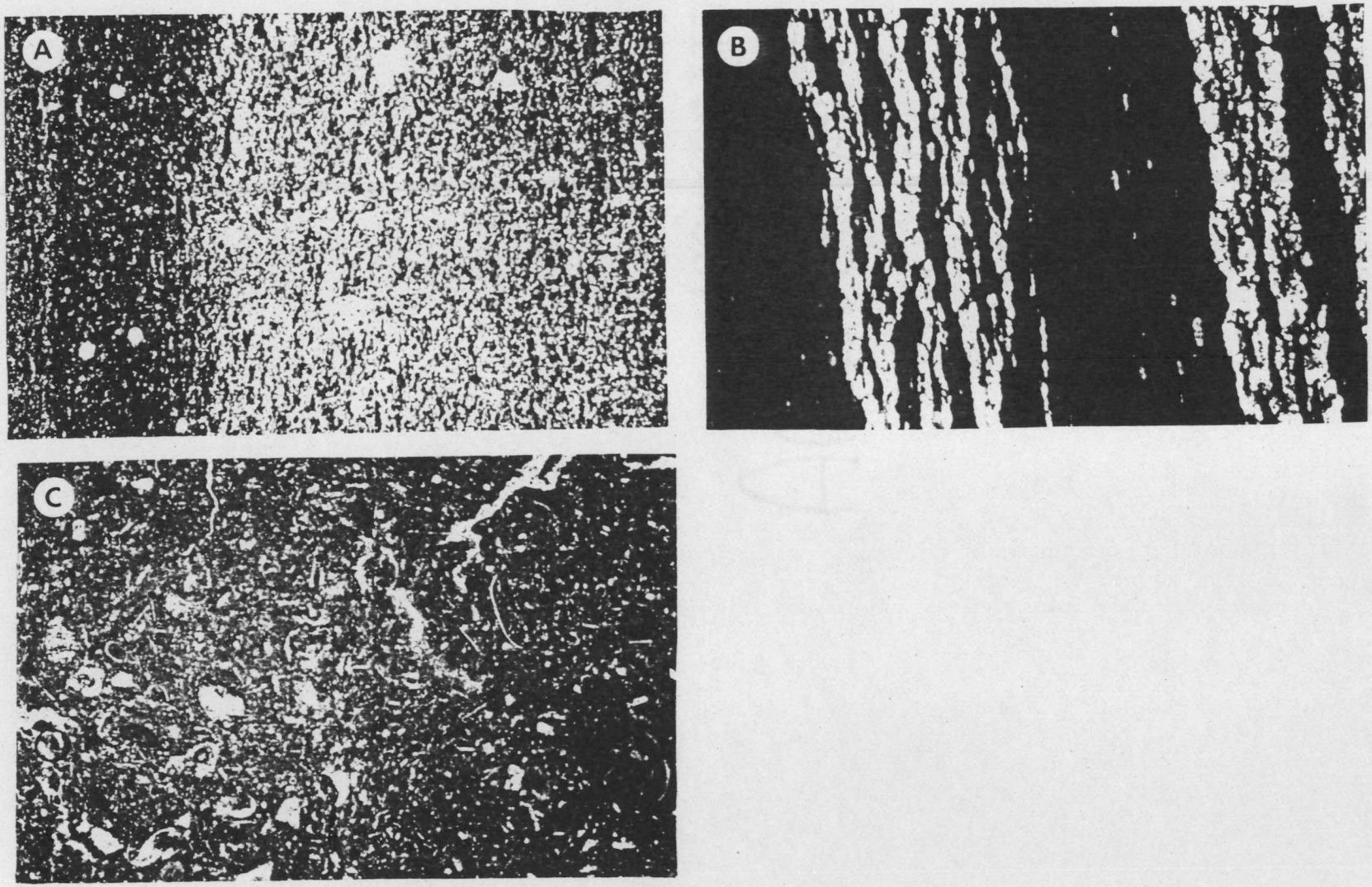

Figure B-5.

Figure B-6. Sedimentary features of the Greensport Formation and Colvin Mountain Sandstone. A. Maroon siltstone (dark) with vertical branching burrows which are filled with olive-green siltstone (light); upper Greensport, Greensport, Etowah County. B. Cross-bedded, locally conglomeratic Colvin Mountain (upper) overlying Greensport siltstones. Note erosional channels in sandstone. Hammer near center gives scale. Greensport, Etowah County.

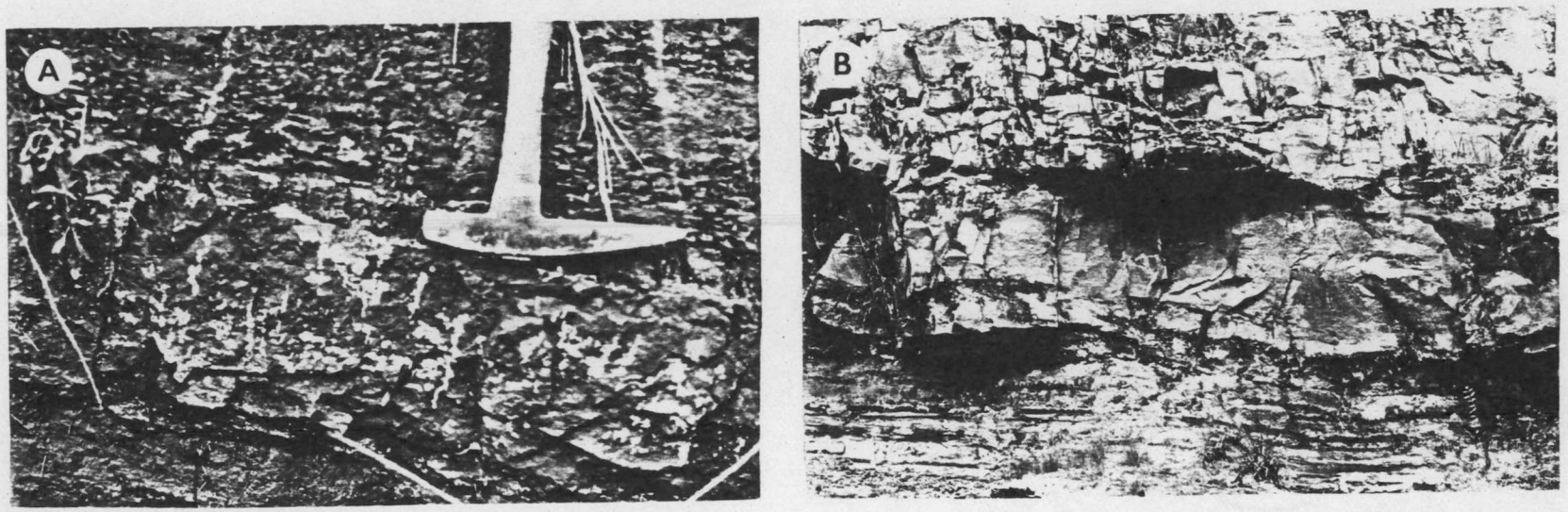

Figure B-6.

Figure B-7. Sedimentary features of the Stones River, Nashville, and Sequatchie Formations, Birmingham, Jefferson County. A. Desiccation fenestrae in biomicrite, basal Stones River. Stratigraphic top toward top of page. 16 X, unpolarized light. B. Small bryozoan colonies in growth position (left and right of coin) indicative of subtidal environment, upper Stones River. Bryozoans also act as binding agents in bioherms up to 1.5 m high.

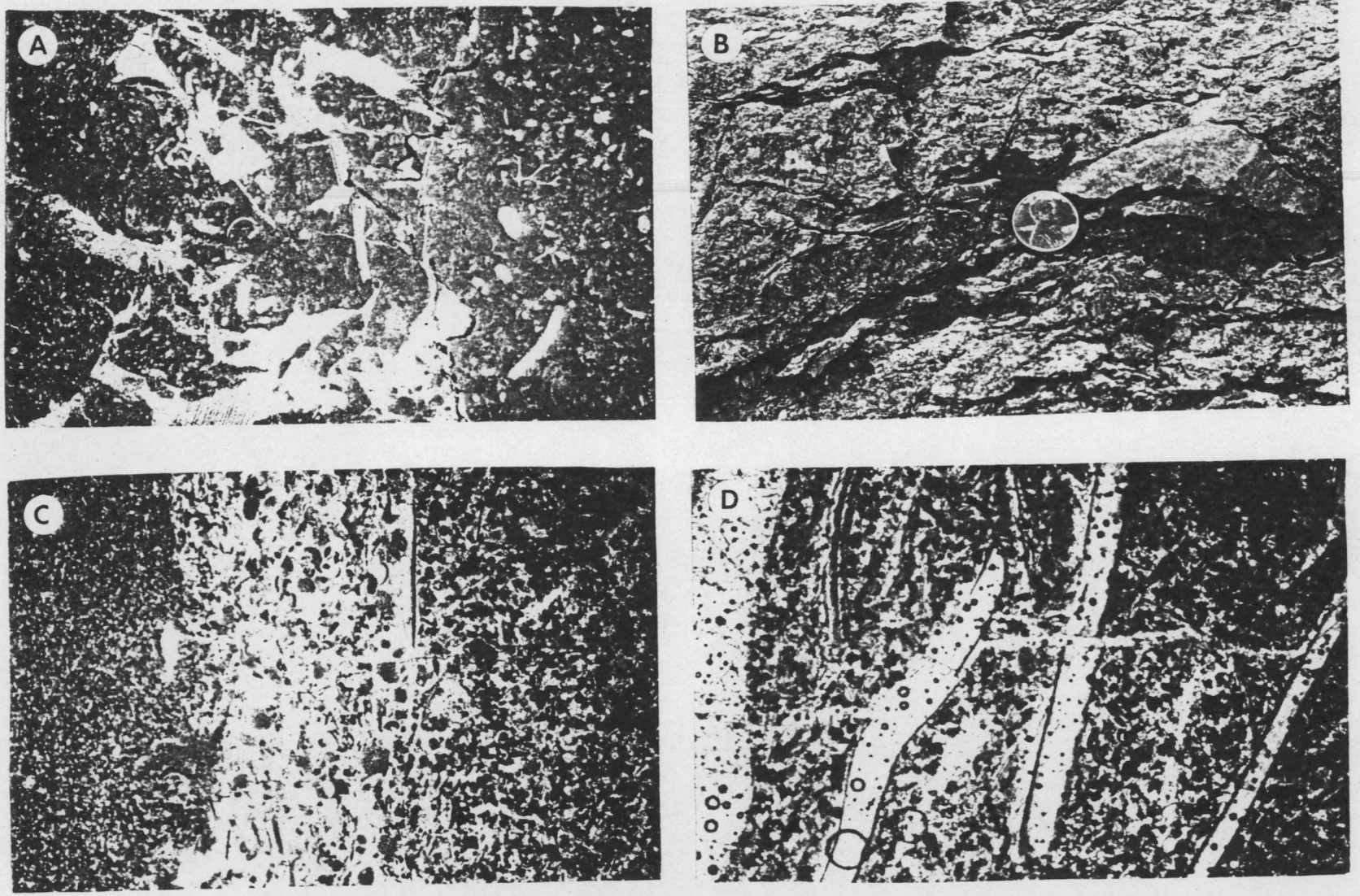

Figure B-7.

Figure B-8. Sedimentary features of the Red Mountain Formation, Frog Mountain Sandstone and Chattanooga Shale. A. Intraformational conglomerate in the sand/shale facies of the Red Mountain, Birmingham, Jefferson County. Pebbles exhibit slight imbrication. B. Cross-bedded oolitic sandstone. Lighter bands are calcite skeletal debris. Birmingham, Jefferson County. C. Filter-feeder burrows in fine-grained Frog Mountain sandstone, Birmingham, Jefferson County. Mounds around burrow mouths are cone-shaped, suggesting low current energy. D. Alternating quartz silt-rich and organic-rich laminae in Chattanooga Shale, Big Ridge, DeKalb County. Stratigraphic top toward top of page. 16 X, unpolarized light.

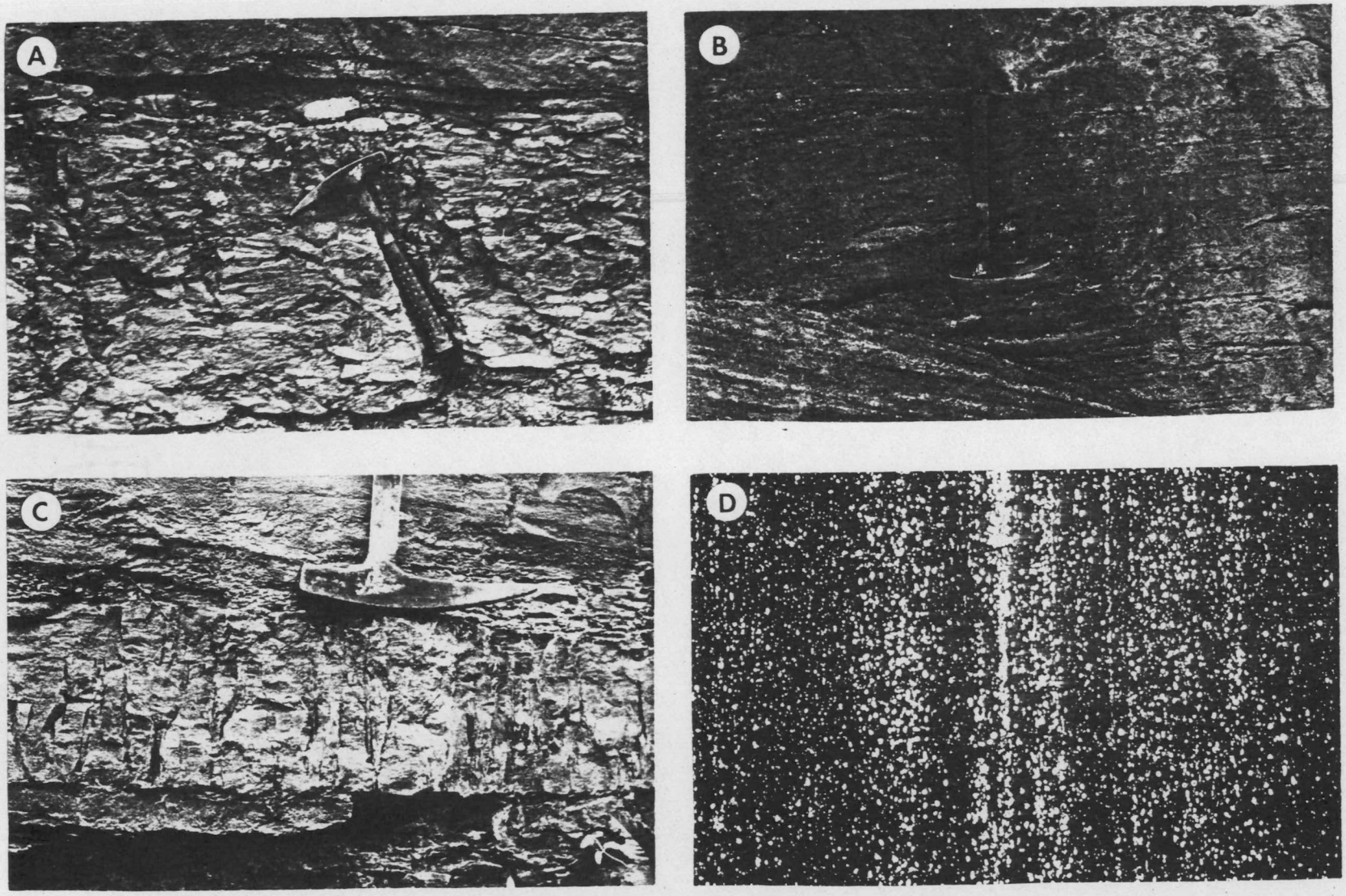

Figure B-8.

Figure B-9. Sedimentary and diagenetic features of the Fort Payne Chert and Tuscumbia Limestone. A. Replacement chert with ooids and rounded intraclasts, Fort Payne Chert, NE St. Clair County. Scale bar 5 cm. B. Typical nodular bedded biomicrite and clay of Fort Payne, Walker County, Georgia. C. Pelmatazoan grainstone of Tuscumbia, Trussville, Jefferson County. 16 X, unpolarized light. D. Oosparite (superficial ooids) of uppermost Tuscumbia, Trussville, Jefferson County. 16 X, unpolarized light.

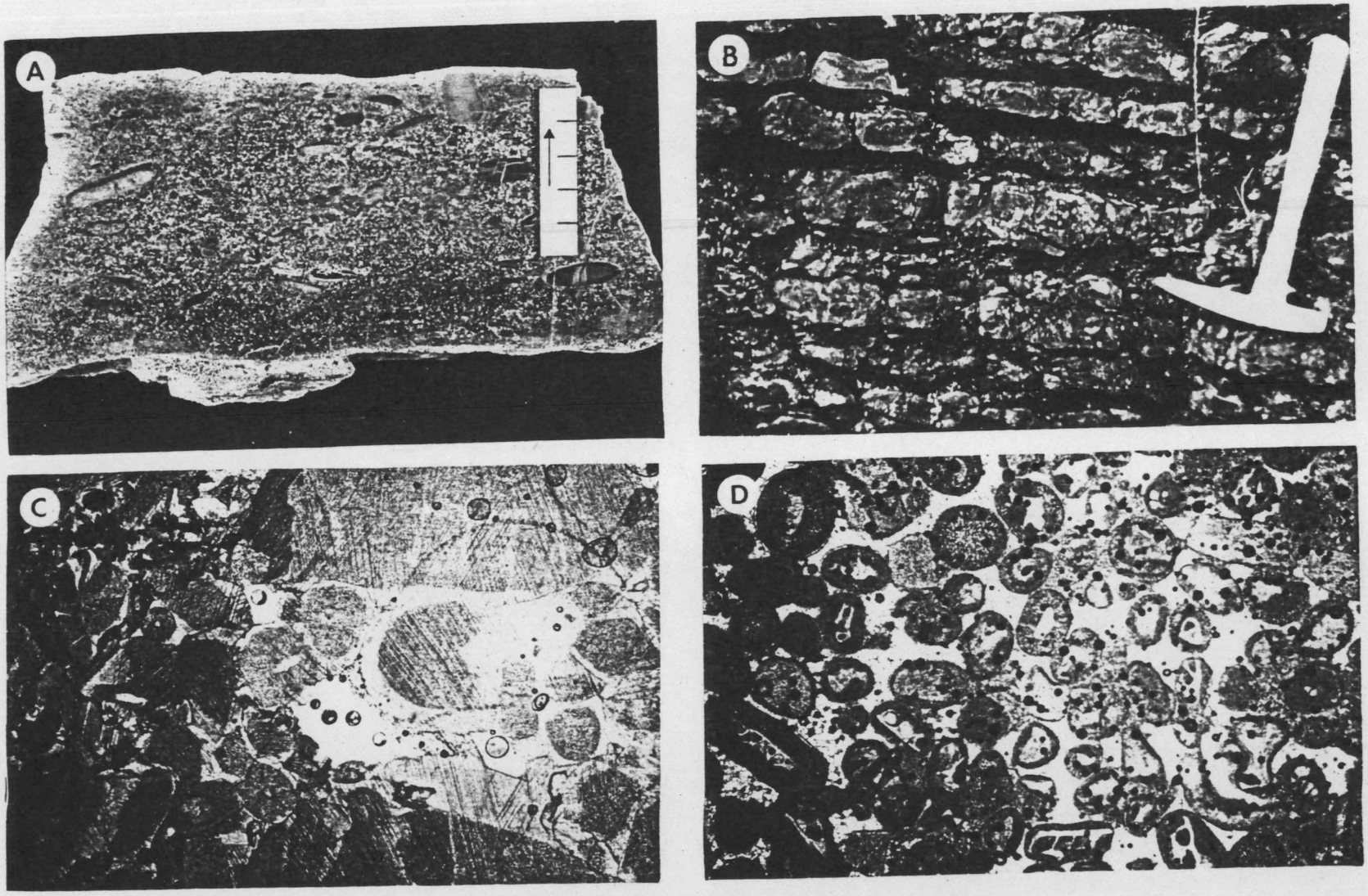

Figure B-9.

Figure B-10. Sedimentary features of the Pride Mountain Formation and Hartselle Sandstone, Jefferson County. A. Laminated shales and siderite bands and nodules of the Pride Mountain Formation, Trussville. B. Thick-bedded to massive orthoquartzites of the Hartselle conformably overlying Pride Mountain (right). Irondale. C. Tabular cross-bedding in locally conglomeratic orthoquartzites. Cross-beds dip SE, away from Warrior platform. Irondale.

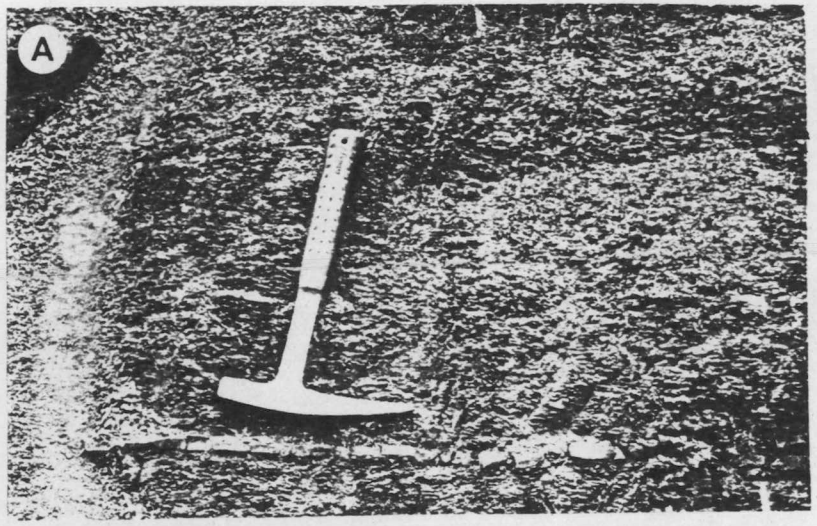



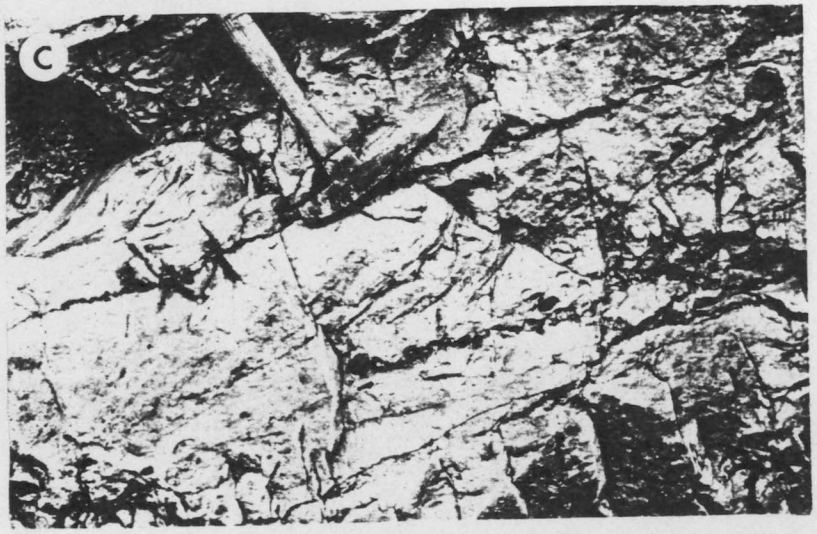

Figure B-10.

Figure B-11. Sedimentary features of the Floyd Shale, Leeds, Jefferson County. A. Penecontemporaneous microfault in silty Floyd Shale. 16 X, unpolarized light. B. Deposit feeder burrow in silty Floyd Shale; note alighment of plant fragments (black) parallel to bedding. 16 X, unpolarized light. C. Basal contact of limestone bed, shale removed by weathering. Contact is abrupt, with shale clasts (below coin), algal oncolites, and shell debris indenting surface of underlying laminated shale. Coin 2.4 cm diameter. D. Upper contact of limestones with laminated shale. Contact is sharply defined, with protruding carbonate grains.

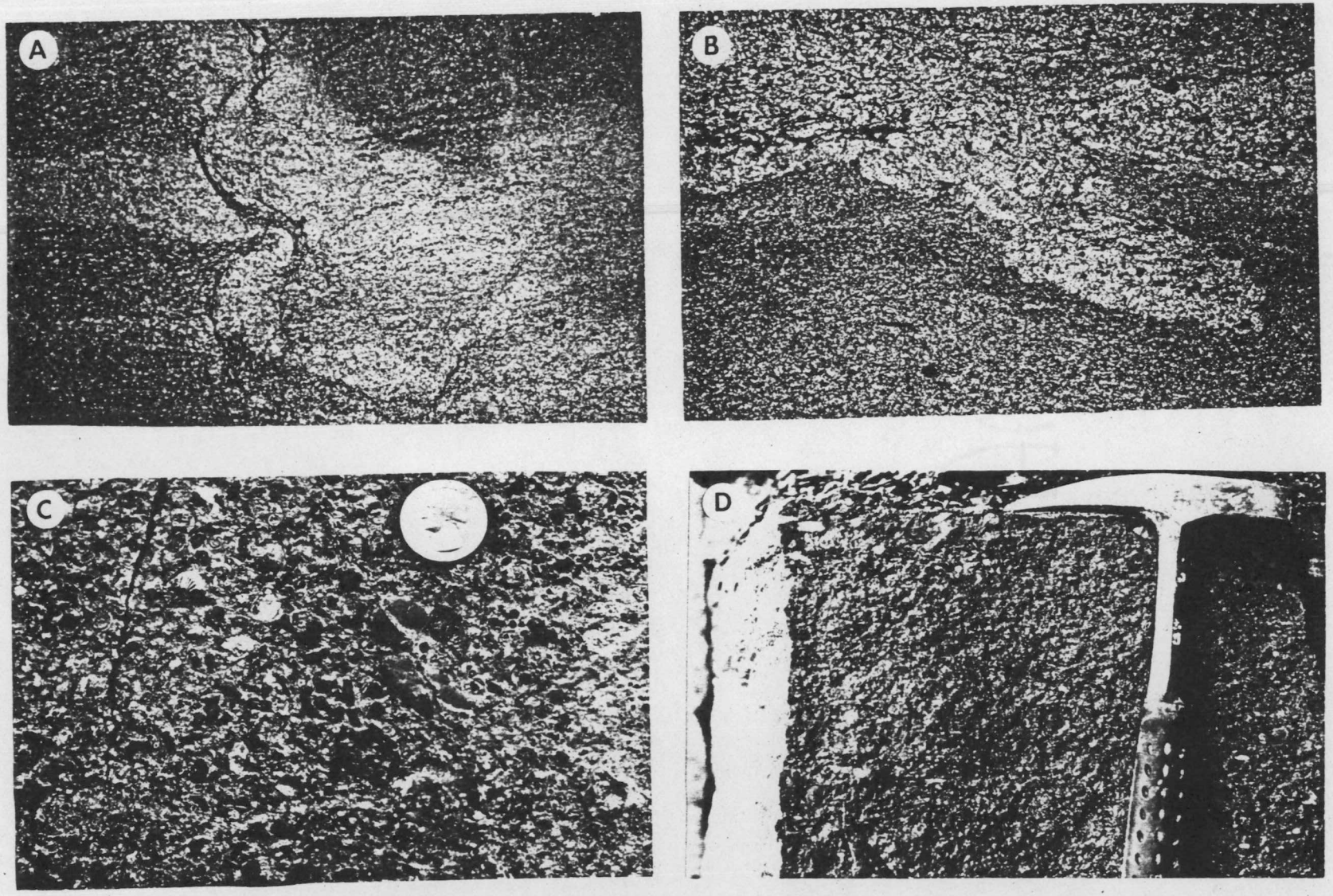

Figure B-11.

Figure B-12. Sedimentary features of the Floyd Shale and Parkwood Formation. A. Polished and etched slab of exotic carbonate, Floyd Shale, Leeds, Jefferson County. Basal contact indents, but does not scour, laminated shale. Large gray objects are shale clasts, concentrically banded objects are algal oncolites; remainder is bryozoan, coral, and pelmatazoan grains in a clay matrix. Note poorly developed graded bedding. Stratigraphic top toward top of page. Scale bar 5 cm. B. Interbedded shales and sandstones of the basal Parkwood. Light colored unit near center is a sandstone bed of probable storm origin. Homewood, Jefferson County. C. Detail from (B) showing clay drapes, ripple bedding, bipolar crossbeds and reactivation surfaces typical of tidally-influenced deposition. Coin 1.8 cm diameter. D. Sand shoal facies of Parkwood, Cahaba River, Jefferson County. Note tabular crossbeds in orthoquartzite. Height of outcrop $\sim$ 7.5 m. Stratigraphic top toward right of page.

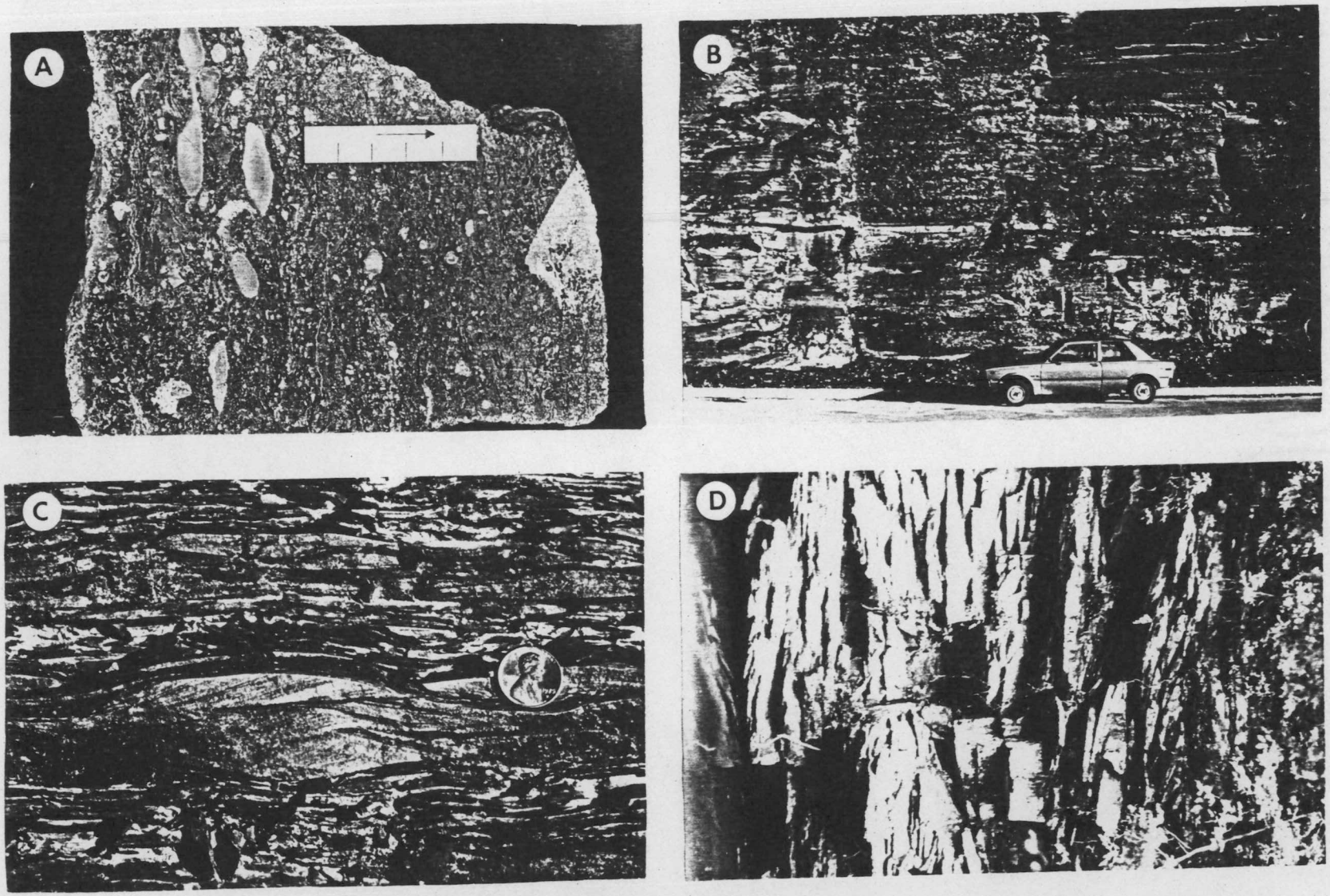

Figure B-12.

Figure B-13. Sedimentary features of the Pottsville Formation. A. Lagoonal deposits of the interconglomerate measures (lower), shoreline deposits of Pine Ridge Sandstone (middle) and fluvial deposits of the Straight Ridge sequence (upper). Leeds, St. Clair County. B. Soft-sediment slump in tabular shore face laminae of Shades Sandstone member. Compass case (center) 7 cm diameter. Nichols Gap, St. Clair County. C. Tidal channel of Shades eroded into underlying Parkwood. Channel is ∿ 1.5 m in depth. Leeds, St. Clair County. D. Fluvial deposits of the Yellowleaf sequence. Cross-bedded channel sands (light) deposited in channel eroded into interdistributary redbeds (dark). Chelsea, Shelby County.

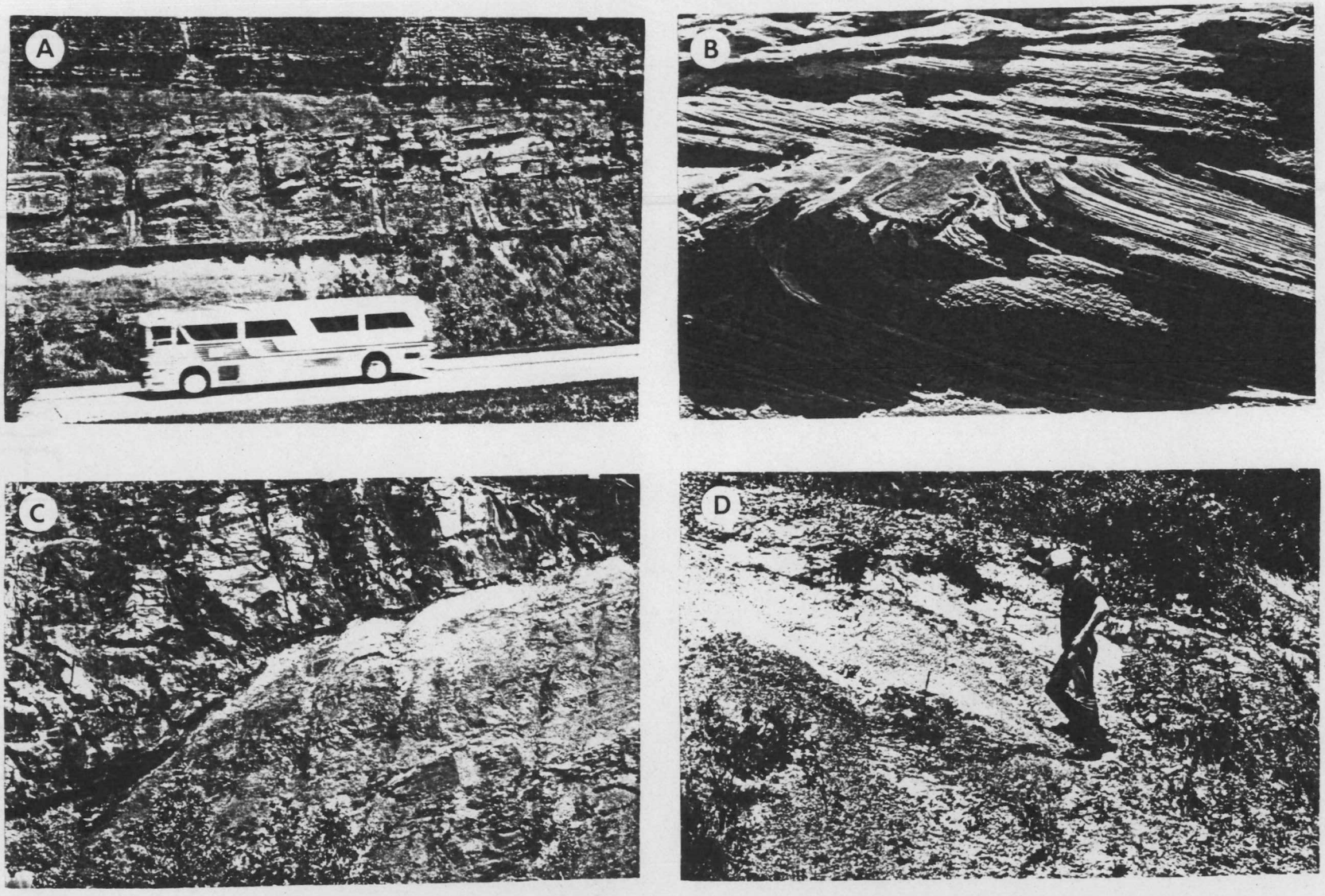

Figure B-13.

VITA

Oscar Edward Gilbert, Jr., was born in Birmingham, Alabama, on December 10, 1946. He attended primary and secondary schools in that city, and was graduated from Jones Valley High School in 1964. He attended both the University of Alabama in Birmingham and the University of Alabama, and received the Bachelor of Science in Geology degree from the latter institution in 1969.

After active duty in the United States Marine Corps Reserve, he entered the Graduate School of the University of Alabama, and received the Master of Science degree in 1974. During the period 1970 until 1976, he was employed by the Geological Survey of Alabama in Tuscaloosa.

In the fall of 1976, he entered the Graduate School of The University of Tennessee, completing course work in the summer of 1978. From 1978 until 1980 he was employed by Geology Department, Auburn University, and is currently employed by the Exxon Production Research Company, Houston, Texas. He received the Doctor of Philosophy degree with a major in geology in December 1981.

Mr. Gilbert is a member of Sigma Xi, Sigma Gamma Epsilon, and the Geological Society of London. He is married to the former Catherine Rittmann; they have two children, Elizabeth Jordan Gilbert and Oscar Edward Gilbert III.